Applications and Developments in the Effective Field Theory Approach to Forward Scattering in Gauge Theories and Gravity

by

Michael Saavedra

Submitted in partial fulfillment of the
requirements for the degree of
Doctor of Philosophy
at
Carnegie Mellon University
Department of Physics
Pittsburgh, Pennsylvania

Advised by Professor Ira Z. Rothstein

May 13, 2025

Abstract

In this thesis, we study the forward limit in gauge theories and gravity using the tools of Soft Collinear Effective Theory (SCET) with Glauber operators. For gauge theories, we derive relations for the anomalous dimensions of hard scattering operators in terms of diagrams with Glauber gluon exchanges from unitarity and analyticity considerations. Similar arguments can be applied to the forward scattering amplitude and Glauber operators, leading to new relations, constraints, and calculation techniques for these operators. We then generalize the Glauber SCET approach to the problem of gravitational scattering, and we use this to study classical gravitational scattering. We find an infinite tower of large logarithms in the classical phase, and we describe how they may be calculated at any desired order in perturbation theory.

Acknowledgments

I would like to thank my advisor Ira Rothstein for his patience and insight with research questions, and for giving me interesting problems to work on and for introducing me to an an exciting area of research. It has truly been an fulling experience working with Ira over the past six years.

I am grateful to Ryan Plestid, who has been a wonderful mentor and collaborator over the past year. I am also grateful for his invitation to give a talk at Cal Tech, without which the next stage of my career would not have been possible.

I am especially thankful for my parents, Pablo and Suzanne, and my siblings, Alex, Sara, and Sophia, who have provided me with endless love, support, and enthusiasm, since long before the start of my PhD. I would also like to thank the many friends who have been with me over the past six years.

Lastly, I would like to thank my thesis committee members, Ian Moult, Riccardo Penco, and Rachel Rosen, for their time and energy in evaluating this thesis.

Contents

List of Figures

Chapter 1

Introduction

The last two decades have seen a remarkable development in techniques for perturbative calculations in quantum field theory. With tools such BCFW recursion relations for tree amplitudes [42, 43], generalize unitarity [32], and double copy [112, 25], and a deeper understanding of Feynman integrals[173], calculations at higher loop and higher multiplicity are becoming increasingly common, with many results in the literature available up to three or four loops[122, 141, 79, 90]. The study of scattering amplitudes has long been central in collider physics. More recently, it has been realized that scattering may be applied in a seemingly distinct problem, that of the classical two-body problem in General Relativity (GR). Through a careful analysis of loop integrands, one is able to extract the classical contributions to the amplitude, leaving the quantum terms behind. Due to the detection of gravitational waves by LIGO [2, 3] and the subsequent need for high precision theoretical predictions, the field has seen explosive progress in the past several years, with partial results being available at fourth order in perturbation theory for the scattering potential[30, 77].

Despite the advances in perturbative calculations, the all-orders structure of scattering amplitudes is not always well understood. In asymptotic kinematic limits however, the problem greatly simplifies, and one can learn a great deal. A particularly rich limit is the near forward, or high energy limit of 2 to 2 scattering. This limit is characterized by a large center of mass (CoM) energy $\sqrt{s}$ and a small momentum transfer $\sqrt{-t}$, leading to a scenario in which the two incoming high-energy projectiles interact over large distances and are lightly deflected. Historically, this limit has long been of theoretical interest, where it was applied in early pre-QCD studies in relativistic scattering theory[62], as the high-energy limit is highly constrained by unitarity and analyticity. In the 90s, this work was turned towards QCD, where a number of structures in the amplitude were described, notably gluon Reggeization[120], in which the gluon exchanged between the two projectiles becomes dressed with a power scaling in s, and the BFKL equation [121, 14], which describes the

leading s-dependence of the total cross-section in QCD. More recent studies have reframed the problem as the scattering of Wilson lines[46, 47], and identified an infinite tower of such structures, leading to a messy and unclear picture of amplitudes in the high-energy limit.

Somewhat orthogonally, the high-energy limit happens to overlap with the classical limit in gravitational scattering. Given the large distance between the scattering projectiles $b \sim 1/\sqrt{-t}$, the classical angular momentum of the system is $J \sim \sqrt{s}b \gg 1$, which dominates over the quantum angular momentum scale $\hbar = 1$. Despite the classical nature of the problem, Ref. [9] was able to apply techniques from the QCD literature to calculate the classical contribution to the gravitational amplitude for the case of massless scattering at two loops. While not directly relevant to the binary black hole inspiral problem, this calculation has served as an important theoretical cross-check for explicit calculations[72], as well as useful input to constrain phenomenological models of black hole mergers[64]. More generally, the high energy limit is formally interesting, as it is a regime where one can probe transplankian scattering. As long as the momentum transfer t is sufficiently small, s can be much larger than the Planck mass, as we can reliably calculate in the case of two stars or black holes scattering off of each other. The high energy limit has also been used to explore the approach towards black hole formation in perturbative GR.

In recent years, an effective field theory (EFT) approach to this problem in QCD has been developed within the framework of Soft Collinear Effective Theory [16, 19, 18, 20]. Here, the problem of forward scattering is reframed as the exchange of the so-called "Glauber modes". These Glauber modes are are analogous to potential modes in non-relativist settings, as they mediate the forward scattering between highly boosted projectiles. Similarly to potential modes in non-relativistic EFTs (i.e. NRQCD [128]), these modes get integrated out of the EFT into a set of potential Glauber operators. These Glauber operators then are used to organize the calculation of amplitudes and observables in the forward limit, and the renormalization group (RG) running of these operators generate the structures found in the 2-to-2 forward amplitude in QCD. The goal of this thesis is to further develop this Glauber SCET approach to forward scattering. In particular, we show how there is interesting interplay between unitarity and the EFT, which leads to interesting constraints and new calculational techniques for the RG properties of both Glauber operators as well as hard scattering operators. We also generalize the Glauber operators to the case of gravity, where we use the RG properties to show how one can characterize and calculate certain terms in the classical amplitude to high loop orders.

This thesis is organized as follows. Chapter 2 will review the salient details of SCET and Glauber operators which are built off of in the rest of this thesis, with a particular focus on Glauber SCET for QCD. In Chapter 3, we discuss a formalism which allows one to use Glauber operators to calculate the anomalous dimensions of hard scattering operators.

Chapter 4 extends this formalism to include the Glauber operators themselves and further studies the formal implications of the methodology. In Chapter 5, we take a step back from QCD and discuss the construction and matching of Glauber operators in gravity SCET, and in chapter 6 we apply this EFT to the problem of classical gravitational scattering.

Chapter 2

The $\mathcal{ABC}(DFGJk\mathcal{L}m^2n\bar{n}\mathcal{OP}Q^2\mathcal{S}twxZ)$'s of SCET

In a typical scattering process, contributions to scattering amplitudes or cross-sections are dominated by low-energy, or soft, modes and by high-energy modes which are (nearly) collinear to the scattering states. These regions of phase space dominate as they set internal propagators (close to) on-shell. Soft Collinear Effective Theory (SCET) [16, 19, 18, 20] then provides a framework for describing the interactions of these modes and their contributions to physical observables.

One of the major benefits of working with SCET is that it provides a systematic method of resumming large logarithms which can cause a breakdown of perturbation theory. In particular, one encounters (Sudakov) logarithms of the form $\alpha_s \log^2 Q^2/m^2$, where Q^2 is the typical hard or UV scale in the problem, and m^2 is the low-energy scale. In phenomenologically relevant cases, the two scales are widely separated, such that the ratio $Q^2/m^2 \gg 1$, and then numerically $\alpha_s \log^2 Q^2/m^2 \gtrsim 1$. At the *nth* order in perturbation theory, we generically expect a contribution of the form $(\alpha_s \log^2 Q^2/m^2)^n$, and so we have lost calculational control of the problem. SCET solves this issue through the separation of scales. The EFT allows us to calculate the $\log(m^2)$, while the hard $\log(Q^2)$ appears as a Wilson coefficient from integrating out the hard physics. Renormalization group techniques then allow us to resum the tower of large logs, often into an exponential, restoring calculational control.

SCET has been successfully applied to calculate for a number of scattering processes relevant for QCD collider physics. More recently, SCET has been generalized to the case of gravitational scattering. There, the focus has so far been to provide a new perspective on the origin of gravitational soft theorems [24, 23, 22].

In this section we provide an overview of the relevant features of SCET. In particular, we describe an EFT called SCET_{II}, which is used throughout the remainder of this work. In this chapter, we will provide a description of SCET for QCD. We will return to the case of gravity in Chapters 5 and 6.

2.1 Modes and Lagrangian

SCET describes the physics of states moving with (nearly) light-like momenta; it is therefore useful to introduce a set of lightcone coordinates for each set of collinear states. We may do so by choosing a lightcone vector n^μ and corresponding conjugate lightcone vector $\bar{n}^\mu$, which satisfy

$$n^2 = \bar{n}^2 = 0, \qquad n\cdot\bar{n} = 2; \tag{2.1}$$

a convenient choice is

$$n^\mu = (1,0,0,1), \qquad \bar{n}^\mu = (1,0,0,-1). \tag{2.2}$$

These vectors define a coordinate system, and we may decompose any momentum p^μ as

$$p^\mu = \frac{n^\mu}{2}\bar{n}\cdot p + \frac{\bar{n}^\mu}{2} n\cdot p + p_\perp^\mu \equiv (\bar{n}\cdot p,\, n\cdot p, p_\perp), \tag{2.3}$$

where $p_\perp$ is the component of the momentum transverse to n and $\bar{n}$,

$$n\cdot p_\perp = \bar{n}\cdot p_\perp = 0. \tag{2.4}$$

Often, we will also use the alternate notation, $p^+ \equiv \bar{n}\cdot p$ and $p^- \equiv n\cdot p$. It will also be useful to give the product of two vectors in lightcone coordinates, which is given as

$$p\cdot k = \frac{1}{2}p^+k^- + \frac{1}{2}p^-k^+ + p_\perp\cdot k_\perp, \qquad p^2 = p^+p^- + p_\perp^2. \tag{2.5}$$

Lastly, we note that the $\perp$-components of momenta are always space-like. This is most obvious in the parametrization of n and $\bar{n}$ given above, where the $\perp$-momenta space the x-y plane. It is then often appropriate to Euclideanize the $\perp$-components, which is denoted as

$$p_\perp^2 = -\vec{p}_\perp^{\,2}, \qquad \vec{p}_\perp^{\,2} > 0. \tag{2.6}$$

Now that the notation is in place, we may describe the EFT. SCET is modal theory: each field is then decomposed into *n-collinear* modes with momenta that scale as

$$k_n \sim (1,\, \lambda^2,\, \lambda), \tag{2.7}$$

soft modes, with momenta that scale as

$$k_s^\mu \sim (\lambda,\, \lambda,\, \lambda), \tag{2.8}$$

and $\bar{n}$-*collinear* modes with momenta that scale as

$$k_n \sim (\lambda^2,\, 1,\, \lambda). \tag{2.9}$$

These are the low-energy modes which makeup the EFT. Collinear momenta have large $k^\pm$, but they are still "low-energy" modes in the sense that they have small invariant masses, $k_n^2 \sim \lambda^2$, which is the same as the soft modes, $k_s^2 \sim \lambda^2$. Often, one also finds that the *hard* modes are relevant to a scattering process. For our purposes, hard modes are any which have a virtuality of $k_H^2 \sim \lambda^a$, $a < 2$. The modes get integrated out of the EFT, and they generate hard-scattering operators and Wilson coefficients. Soft and collinear modes are sometimes referred to as being "on-shell" modes, in the sense that they have $k^+k^- \sim k_\perp^2 \sim \lambda^2$. Any modes which do not satisfy this, i.e. has $k^+k^- \nsim k_\perp^2$, are likewise called "off-shell". Off-shell modes are also integrated out of the EFT, and doing so builds up Wilson lines or Glauber operators.

The fact that the various modes have different λ-scalings for different components leads to some complications when attempting to write down the EFT. To deal with this, we introduce the multipole expansion: we decompose momenta p into a "label component" p_ℓ and a "residual component" p_r, $p^\mu = p_\ell^\mu + p_r^\mu$ The label component p_ℓ contains the large components p; for n-collinear momentum p, we have

$$p_\ell^\mu = \frac{\bar{n}^\mu}{2} p_\ell^+ + p_{\ell\perp}^\mu \sim (1, 0, \lambda). \tag{2.10}$$

The residual momenta then contain just the small $O(\lambda^2)$ terms; this includes the $-$ component of the momentum, but also additional $O(\lambda^2)$ components of the $+$ and $\perp$ components, as adding a small λ^2 piece to the $O(\lambda^0)$ p_ℓ^+ and $O(\lambda)$ $p_{\ell\perp}$ will no change their scalings. At leading power in the λ, the $+$ and $\perp$ components of the residual momenta will not appear in collinear propagators, as these components are dominated by the labels.

To implement the multipole expansion at the level of the action, we Fourier transform the collinear fields over the label momenta. Using the n-collinear quark field ξ_n (which we define below) as an example, we write

$$\hat{\xi}_n(x) = \sum_{p_\ell \neq 0} e^{-ix\cdot p_\ell} \xi_{n,p_\ell}(x). \tag{2.11}$$

At this point, we introduce the "label operator" $\mathcal{P}^\mu$, which picks out the label momenta of

a given field:

$$\mathcal{P}^\mu \xi_{n,p_\ell} = p_\ell^\mu \xi_{n,p_\ell}. \tag{2.12}$$

We may then rewrite Eq. (2.11) as

$$\begin{aligned}\hat{\xi}_n(x) &= \sum_{p_\ell \neq 0} e^{-ix\cdot\mathcal{P}} \xi_{n,p_\ell}(x) = e^{-ix\cdot\mathcal{P}} \sum_{p_\ell \neq 0} \xi_{n,p_\ell}(x), \\ &\equiv e^{-ix\cdot\mathcal{P}} \xi_n(x).\end{aligned} \tag{2.13}$$

This is just a rephasing of the collinear fields, but this reorganizes the power-counting so that the large $O(1)$ and $O(\lambda)$ components of the momenta are encoded into the labels, while all spacial dependence contains the residual momenta. As a result, we have $\partial \xi_n \sim \lambda^2 \xi_n$. For soft fields, we introduce "soft labels" $k^\pm \sim \lambda$ for the lightcone components, and corresponding $in\cdot\partial_S$ and $i\bar{n}\cdot\partial_S$, with the $\perp$-component being picked out by $\mathcal{P}_\perp^\mu$ still. We can also combine these into a "soft label operator"

$$\mathcal{P}_S^\mu = \frac{\bar{n}^\mu}{2} n\cdot i\partial_S + \frac{n^\mu}{2} \bar{n}\cdot i\partial_S + \mathcal{P}_\perp^\mu. \tag{2.14}$$

Integration over a momentum now involves both a sum over labels, both large and soft, as well as integrals over the residual components. We formally write

$$\int [d^4k] = \sum_{k_\ell} \sum_{k_s^+, k_s^-} \int [d^4 k_r]. \tag{2.15}$$

Likewise, we break up delta functions into label (Kronecker) deltas and residual deltas:

$$(2\pi)^4 \delta^4(p-k) = \int d^4x\, e^{ix\cdot(p_\ell - k_\ell)} e^{ix\cdot(p_s - k_s)} e^{ix\cdot(p_r - k_r)} = \delta_{p_\ell,k_\ell} \delta_{p_s,k_s} (2\pi)^4 \delta^4(p_r - k_r). \tag{2.16}$$

Here we must be careful though, as having label and residual momenta in the same coordinate will lead to the residual momenta dropping out. For example, for p, k collinear with no soft labels for simplicity, we have

$$\begin{aligned}\int d^4x\, e^{ix\cdot(p_\ell - k_\ell)} e^{ix\cdot(p_r - k_r)} &= \int d^4x\, e^{\frac{i}{2}x^-(p_\ell^+ - k_\ell^+)} e^{\frac{i}{2}x^+(p_r^- - k_r^-)} e^{ix_\perp\cdot(p_{\ell\perp} - k_{\ell\perp})}, \\ &= \delta_{p_\ell^+,k_\ell^+} \delta_{p_{\ell\perp},k_{\ell\perp}} (2\pi)^4 \delta(p_r^- - k_r^-) \delta^3(0) + O(\lambda^2), \\ &= (2\pi)^4 \delta^4(p-k) + O(\lambda^2),\end{aligned} \tag{2.17}$$

where the $+O(\lambda^2)$ comes from the residual p_r^+ and k_r^+ that were dropped relative to the large labels. The $\delta(0)$'s that appear are there formally, and recombine with the label deltas

to given

$$\delta_{p_\ell^+,k_\ell^+}(2\pi)\delta(0) = (2\pi)\delta(p_\ell^+ - k_\ell^+), \qquad \delta_{p_{\ell\perp},k_{\ell\perp}}(2\pi)^2\delta^2(0) = (2\pi)^2\delta(p_{\ell\perp} - k_{\ell\perp}). \tag{2.18}$$

In $\mathrm{SCET_{II}}$ problems, one never encounters residual $\perp$-momenta, and therefore it is conventional to go ahead and combine deltas as above for the $\perp$ components. In general, one does not typically need to be too careful about label vs residual momentum in calculations once factorization theorems have been established, but the formal manipulations needed to establish factorization do require a careful treatment. We will see an example of this when dealing with Glauber operators.

The action for the effective field theory[1] at leading power in λ is given by

$$S_{SCET} = \sum_{n,\bar{n}} S_n(\{A_n,\, \xi_n\}) + S_S(\{A_S,\, \psi_S\}) + S_{\mathrm{HS}}(\{A_n,\, \xi_n\}; A_S,\, \psi_S) + S_{\mathrm{Glauber}}(\{A_n,\, \xi_n\}; A_S,\, \psi_S). \tag{2.19}$$

S_n and S_S are the actions for the soft and collinear fields. A_n and A_S are the collinear and soft gluon fields and ξ_n and ψ_S are the collinear and soft quark fields. Each term in the action is equivalent to the full QCD, although in the collinear sectors it is typical to use the equations of motion to rewrite the Lagrangian into a more convenient form. S_{HS} and S_{Glauber} are the action for hard scattering and Glauber operators, which generate interactions between the separate sectors.

The leading collinear Lagrangian is then given by

$$\mathcal{L}_n^{(0)} = \mathcal{L}_{n\xi}^{(0)}(\xi_n,\, A_n) + \mathcal{L}_{nA}(A_n), \tag{2.20}$$

with the leading quark action given by

$$\mathcal{L}_{n\xi}^{(0)} = e^{-ix\cdot\mathcal{P}}\bar{\xi}_n \left(in\cdot D_n + i\not{D}_{n\perp}\frac{1}{i\bar{n}\cdot D_n} i\not{D}_{n\perp} \right) \frac{\not{\bar{n}}}{2}\xi_n. \tag{2.21}$$

Here, g is the usual QCD coupling constant. The various derivative terms are

$$\begin{aligned} iD_n^\mu &= i\mathcal{D}_n^\mu + gA_n^\mu, \\ i\mathcal{D}_n^\mu &= \frac{n^\mu}{2}\bar{n}\cdot\mathcal{P} + \mathcal{P}_\perp^\mu + \frac{\bar{n}^\mu}{2} in\cdot\partial. \end{aligned} \tag{2.22}$$

The overall exponential comes from the multipole expansion, and it simply functions to enforce the conservation of label momenta, and lead to a momentum conserving delta func-

[1] The EFT we are describing here is known as $\mathrm{SCET_{II}}$. There is a similar EFT called $\mathrm{SCET_I}$, which also includes ultrasoft modes with virtuality $k_{\mathrm{us}}^2 \sim \lambda^4$. In the problems at hand, ultrasoft modes do not appear, and so we use $\mathrm{SCET_{II}}$.

tion which drops out of the Feynman rules. The fields in the actions satisfy the relation $\not{n}\xi_n = 0$, and are related to the full quark fields ψ_n via

$$\psi_n = \left(1 + \frac{1}{i\bar{n}\cdot D_n} i\not{D}_{n\perp} \frac{\not{\bar{n}}}{2}\right) \xi_n. \tag{2.23}$$

The collinear gluon action is given by the full-theory gluon action, with all derivatives replaced by $\mathcal{D}_n$. It is then straightforward to power-count the collinear fields, and we have

$$\xi_n \sim \lambda, \qquad A_n^\mu \sim (1, \lambda^2, \lambda) \sim k_n^\mu. \tag{2.24}$$

The soft actions are obtained from the standard QCD action with derivatives replaced by $\mathcal{P}_S$, and is given by

$$\mathcal{L}_{S\psi}^{(0)} = \bar{\psi}_S (i\not{D}_S)\psi_S, \tag{2.25}$$

with the soft covariant derivative given by

$$iD_S^\mu = \mathcal{P}_S^\mu + g\, A_S^\mu. \tag{2.26}$$

Power-counting the soft fields, we find

$$\psi_S \sim \lambda^{3/2}, \qquad A_S^\mu \sim (\lambda, \lambda, \lambda) \sim k_s^\mu. \tag{2.27}$$

SCET possesses some important symmetries. Firstly, we note that since each soft and collinear actions are equivalent to full QCD in the absence of hard scattering or Glaubers, each is separately invariant under gauge transformations. This places an important constraint that the hard scattering and Glauber operators must also be invariant under separate gauge transformations on the soft and collinear operators. Next we note that, as described so far, there is some ambiguity in the construction of the EFT. Notably, we have some freedom in choosing the lightcone vectors n and $\bar{n}$, as these are not physical quantities. This additional freedom is called reparamiterization invariance (RPI) [134]. Most relevant here is RPI_{III}[2] transformations, which is the invariance of the EFT under simultaneous rescalings of n and $\bar{n}$,

$$n \to e^{-\alpha} n, \quad \bar{n} \to e^{\alpha} \bar{n}. \tag{2.28}$$

Physically, this is a manifestation of the fact that any observable we calculate must be Lorentz invariant due to the Lorentz invariance of full QCD, which we have broken in the EFT by introducing the vectors n and $\bar{n}$. This symmetry places important constraints on

[2]There are also RPI_{I} and RPI_{II} transformations, but in SCET_{II} these only constrain subleading operators, which we are mostly not interested in here.

how lightcone vectors can appear in hard scattering and Glauber operators, and in Chapter 3 we will show how this can be exploited to further constrain hard scattering operators and the forward scattering amplitude through unitarity. Lastly, we note that the labels n and $\bar{n}$ are arbitrary, so the theory should be invariant under swapping n and $\bar{n}$.

2.2 Operator Building Blocks, Hard Scattering, and Factorization

To construct hard scattering operators in SCET, one may follow the usual EFT matching procedure of expanding out full theory diagrams for the process of interest and matching to the appropriate EFT operator. The requirement that the operator be separately gauge invariant under soft and collinear gauge transformations greatly restricts what may be written down, and one may use the equations of motion to simply this further. It turns out these two constraints are enough to reduce the allowed objects for n-collinear fields down to three "building blocks" [135]:

$$\chi_n, \qquad \mathcal{B}^{\mu}_{n\perp}, \qquad \mathcal{P}^{\mu}_{\perp}, \tag{2.29}$$

corresponding to a gauge-invariant quark field, a gauge-invariant gluon field, and a label derivative. For the soft fields, it is also useful to introduce similar building blocks, but we add an additional quark and gluon building block for each collinear sector, as the soft fields have no preferred direction, unlike the collinear fields:

$$\psi_S^{n/\bar{n}}, \qquad \mathcal{B}_{S\perp}^{n/\bar{n}\mu}. \tag{2.30}$$

The quark building blocks are defined as

$$\begin{aligned} \chi_n &= W_n^\dagger \xi_n, \\ \psi_S^n &= S_n^\dagger \psi_S, \end{aligned} \tag{2.31}$$

where W_n and S_n are semi-infinite Wilson lines in the fundamental $\mathrm{SU}(N_c)$ representation with collinear and soft gluons in the $\bar{n}$ and n directions respectively:

$$\begin{aligned} W_n &= \sum_{\text{perms}} \exp\left(\frac{-g}{\bar{n}\cdot\mathcal{P}}\bar{n}\cdot A_n\right) = \mathrm{FT}\,\mathrm{P}\exp\left(ig\int_{-\infty}^{0} ds\,\bar{n}\cdot A_n(x+\bar{n}s)\right), \\ S_n &= \sum_{\text{perms}} \exp\left(\frac{-g}{n\cdot\mathcal{P}_S}n\cdot A_S\right) = \mathrm{FT}\,\mathrm{P}\exp\left(ig\int_{-\infty}^{0} ds\,n\cdot A_S(x+ns)\right), \end{aligned} \tag{2.32}$$

where P is the path ordering symbol, and FT means Fourier Transform. One generically will also encounter Wilson lines which run from 0 to $+\infty$ in hard scattering operators, and whether one uses the $(-\infty, 0)$ Wilson lines or $(0, +\infty)$ Wilson lines depends on the process and scattering states being considered. The gluon building blocks may be defined as

$$\mathcal{B}^{\mu}_{n\perp} = \frac{1}{g}\left[W_n^\dagger i D^\mu_{n\perp} W_n\right] = \frac{1}{g}\frac{1}{\bar{n}\cdot\mathcal{P}} W_n^\dagger [i\bar{n}\cdot D_n, iD^\mu_{n\perp}] W_n, \tag{2.33}$$
$$\mathcal{B}^{n\mu}_{S\perp} = \frac{1}{g}\left[S_n^\dagger i D^\mu_{S\perp} S_n\right] = \frac{1}{g}\frac{1}{n\cdot\mathcal{P}_S} S_n^\dagger [in\cdot D_S, iD^\mu_{S\perp}] S_n.$$

These building blocks are SU(N) matrices in the fundamental representation. It also turns out to be useful to write down soft gluon building blocks and field strength tensors which are matrices in the adjoint representation. These may be written as

$$\tilde{\mathcal{B}}^{AB\mu}_{Sn\perp} = \frac{-if^{ABC}}{\bar{n}\cdot\mathcal{P}_S} iG_S^{-\mu_\perp\, D} \mathcal{S}_n^{DC}, \qquad \tilde{G}_S^{\mu\nu\, AB} = -if^{ABC} G_S^{\mu\nu\, C}, \tag{2.34}$$

with $igG_S^{\mu\nu\, C} T^C = [iD_S^\mu, iD_S^\nu]$ being the soft gluon field strength tensor and $\mathcal{S}_n$ being the soft Wilson line in adjoint representation.

The gauge-invariance of these building blocks follows from the configuration of the Wilson lines. In general, a Wilson running along some path from points x to y transforms as

$$W[x, y] \to U(x) W[x, y] U^\dagger(y), \tag{2.35}$$

where $U(x)$ is the local SU(N) matrix at point x. Under the so-called "small" gauge transformations, the gauge parameter goes to 0 at infinity, and so one has

$$U(x) \xrightarrow{x\to\infty} 1. \tag{2.36}$$

Since all the Wilson lines in the building blocks run out to infinity, this guarantees that the building blocks are gauge invariant. It should be mentioned, however, that these building blocks are *not* invariant under the "large" gauge transformations, which are those which do not die off at infinity. Unlike the small gauge transformations, which are redundancies in the theory, large gauge transformations are a genuine symmetry of the theory. Historically, it has been assumed that the gauge field vanishes at infinity, and so large gauge transformations have been ignored. It would be interesting to see if requiring invariance under large gauge transformations in SCET leads to any new constraints on operator construction.

Given the importance of the operator building blocks to the construction of the EFT, it is worth asking how we should interpret them. One way to do this is by first fixing lightcone gauge, $\bar{n}\cdot A = 0$, say for the n-collinear fields. Doing so trivializes the Wilson lines, setting

$W_n = 1$. The building blocks then reduce to

$$\chi_n \xrightarrow{\bar{n}\cdot A_n = 0} \xi_n, \qquad \mathcal{B}_n^\mu \xrightarrow{\bar{n}\cdot A_n = 0} A_n^\mu. \tag{2.37}$$

The operator building blocks are then nothing but the quark and gluon fields in lightcone gauge. If we look at the definitions of the building blocks, we can see that they are equivalent to performing a gauge transformation with $U(x) = W_n(x)$. This is obvious for the quark building block, and for the gluon building block we just have to expand the definition.

$$\frac{1}{g}\left[W_n^\dagger i D_n^\mu W_n\right] = W_n^\dagger A_n^\mu W_n + \frac{i}{g} W_n^\dagger \partial^\mu W_n. \tag{2.38}$$

One way to derive the building blocks is then to perform a gauge transformation which takes the gluon field from a general gauge to lightcone gauge. This also implies that we could attempt to quantize the theory in lightcone gauge to make the operator building blocks to interpolating fields in the theory. While this has been considered previously[106, 94, 82], it is generally avoided in most SCET applications. Lightcone gauge QCD introduces several complications, including new degrees of freedom which live at infinity[3]. These complications generally make it preferable to work in a covariant gauge (usually Feynman gauge).

We are now ready to discuss the application of SCET to hard scattering. As a first example of a hard scattering operator, we consider the matching for the process of $e^+e^- \to$ 2 jets. The calculation may be reduced to the problem of computing matrix elements of a quark current,

$$F(Q^2/m^2) = \langle p_1, p_2 | \, J_\Gamma \, | 0 \rangle = \langle p_1, p_2 | \, \bar{\psi}\, \Gamma \, \psi \, | 0 \rangle \, . \tag{2.39}$$

In this process, the electrons annihilate into either a photon or a Z-boson, with either a vector or an axial coupling to the current; we have accounted for this through the unspecified Dirac structure Γ in the current. Here, $Q^2 = (p_1, p_2)$, and m^2 is some IR scale that depends on the details of the calculation. F is known as the Sudakov Form Factor, and due to its simplicity it serves as a particularly useful playground for both understanding SCET, as well as for exploring some of the tools developed here. In particular, we note that F is only a function of the ratio Q^2/m^2, as it does not renormalize.

We are interested in the case of small or negligible quark masses relative to Q^2, so that the quarks may be treated as collinear. We also need p_1 and p_2 to live in different collinear sectors so that Q^2 is large, $Q^2 \sim p_1^+ p_2^-$. The IR scale m may be either a gluon mass we use to regulate IR divergences, or mass for the quarks. The latter case is sometimes called the massive Sudakov form factor, and it is closely related to the case of electroweak corrections.

[3]These degrees of freedom turn out to be distinct from the ones introduced when studying large gauge transformations; see [130] for details.

The latter is the massive quark form factor, and it is commonly used for top quark physics. In either case, the tree level matching is the same, and the two form factors only differ at loop level.

At leading order, it is straightforward to match the operator in SCET, as we have

$$J_{\rm SCET} = \bar{\chi}_n \Gamma \chi_{\bar{n}}. \tag{2.40}$$

This fixes both the collinear quark and collinear gluon contributions through the Wilson lines in the quark building blocks. The Wilson lines then are fixed entirely by the requirement of n-collinear and $\bar{n}$-collinear gauge-invariance. We may also consider the emission of soft gluons off of the operator. Scanning through the soft gluon building blocks, listed above we note that since all building blocks scale as $\sim \lambda$, which would add additional power-suppression to the operator. There is however an additional set of soft-gauge invariant operators we may construct, through pairs of Wilson lines $S_n^\dagger S_{\bar{n}}$ or $S_{\bar{n}}^\dagger S_n$. These scale as λ^0, and so we are free to include these in the operator. A quick comparison to full QCD shows that only $S_n^\dagger S_{\bar{n}}$ appears, and so the full SCET current is given by

$$J_{\rm SCET} = \bar{\chi}_n S_n^\dagger \Gamma S_{\bar{n}} \chi_{\bar{n}}. \tag{2.41}$$

In principle we could have added arbitrarily many powers of $S_{\bar{n}}^\dagger S_n$ and $S_n^\dagger S_{\bar{n}}$, which is not ruled out by matching at one soft gluon. A careful analysis at arbitrary soft gluon multiplicity is required to fully rule this out. There are alternative methods of matching circumvent the need for such calculations[20].

Now we come to the matrix element. In the leading order action for SCET, the soft and collinear modes all have separate Lagrangians, and there is no cross-talk between the different modes, outside of Glauber and hard-scattering operators. Therefore, when we quantize the theory, the Hilbert space itself factorizes, i.e. soft and collinear fields live in different Hilbert spaces. We therefore find that matrix elements of hard scattering operators must then factorize into separate soft n-collinear, and $\bar{n}$-collinear matrix elements. For the Sudakov form factor, we write

$$\left\langle p_1^n p_2^{\bar{n}} \right| J_{\rm SCET} \left| 0 \right\rangle = \left\langle p_1^n \right| \bar{\chi}_n \left| 0 \right\rangle \Gamma \left\langle 0 \right| S_n^\dagger S_{\bar{n}} \left| 0 \right\rangle \left\langle p_2^{\bar{n}} \right| \chi_{\bar{n}} \left| 0 \right\rangle, \tag{2.42}$$

$$= J_n \Gamma S J_{\bar{n}}, \tag{2.43}$$

where in the last line we have packaged the matrix elements as

$$\begin{aligned} J_n &= \langle p_1^n | \, \bar{\chi}_n \, |0\rangle \,, \\ S &= \langle 0 | \, S_n^\dagger S_{\bar{n}} \, |0\rangle \,, \\ J_{\bar{n}} &= \left\langle p_2^{\bar{n}} \right| \chi_{\bar{n}} \, |0\rangle \,. \end{aligned} \tag{2.44}$$

This is an all orders in α_s statement. Each individual matrix element may be computed by expanding the Wilson lines and through time-ordered products of Lagrangian interactions from the appropriate soft or collinear actions. Each matrix element also gets separately renormalized, as we write

$$J_n^{\text{Bare}} = Z_n \, J_n^{\text{Renorm}}, \qquad S^{\text{Bare}} = Z_s \, S^{\text{Renorm}}. \tag{2.45}$$

Letting the renormalization scale be μ, each matrix element then satisfies a renormalization group equation

$$\mu \frac{d}{d\mu} J_n = \gamma_\mu^n J_n, \qquad \mu \frac{d}{d\mu} S = \gamma_\mu^S S, \tag{2.46}$$

with the anomalous dimensions defined as

$$\gamma_\mu^{n,S} = -Z_{n,S}^{-1} \, \mu \frac{d}{d\mu} Z_{n,S}. \tag{2.47}$$

One may use these to resum large logs of Q^2/m^2 by solving these and running from m to Q.

It is important to mention that we have been a bit blithe with the discussion of factorization, as we have not mentioned Glauber operators. The action for Glaubers is leading order in λ, and so in principle it causes a breakdown of the picture of factorization painted above. For some operators, it is known that despite this, Glauber modes either do not contribute or otherwise may be absorbed into the soft contributions. The Sudakov form factor is one such case, and so the above factorization is safe to use. When we discuss forward scattering, we will see an example of how Glauber modes can cause this simplified factorization to fail.

In a generic hard scattering process, the UV scale Q^2 is typically some large momentum invariant, with $Q^2 \sim (p_1 + p_2)^2 = p_1^+ p_2^-$ for the Sudakov example. Hard scattering operators then encode the UV dependence on Q^2 through a Wilson coefficient, as per standard EFT expectations. Note this means that the hard coefficient depends on the large labels of the momenta flowing through the operator. However, we must be careful here, as collinear interactions can change the large labels. To account for this, we must then sum over all

configurations of large labels. This may be implemented by specifying the large momentum component in each building block:

$$\chi_{n,\omega} = \delta(\omega - \bar{n}\cdot\mathcal{P})\chi_n, \qquad \mathcal{B}^{\mu}_{n\perp,\omega} = \delta(\omega - \bar{n}\cdot\mathcal{P})\mathcal{B}^{\mu}_{n\perp}. \tag{2.48}$$

The sum over labels then looks like a convolution between the Wilson coefficient and the SCET operator:

$$\int \{d\omega_i d\omega_{i'} d\bar{\omega}_j d\bar{\omega}_{j'}\} C(\{\omega_i;\bar{\omega}_j)\mathcal{O}(\{\chi_{n,\omega_i}, \mathcal{B}_{n,\omega_{i'}}; \chi_{\bar{n},\bar{\omega}_j}, \mathcal{B}_{\bar{n},\bar{\omega}_{j'}}\}), \tag{2.49}$$

where the dependence on the soft fields has been suppressed to ease the notation. Of course, there are also the soft labels in addition to the large collinear labels; these may also induce convolutions. It is typical to condense all these convolutions using the symbol $\otimes$, where the precise meaning is usually specified on a case-by-case basis. Using this notation, we may then write a general factorized matrix element of a hard scattering operator as

$$C \otimes J_n \otimes J_{\bar{n}} \otimes S. \tag{2.50}$$

In cases where there are convolutions present, the SCET matrix elements (or equivalently the Wilson coefficient) are convolutionally renormalized. Using the collinear function as an example, we have

$$J_n^{\mathrm{B}} = Z_n \otimes J_n^{\mathrm{R}}, \qquad \mu\frac{d}{d\mu}J_n^{\mathrm{R}} = \gamma_\mu^n \otimes J_n^{\mathrm{R}}, \qquad \gamma_\mu^n = -Z_{n,S}^{-1} \otimes \mu\frac{d}{d\mu}Z_{n,S}. \tag{2.51}$$

Such convolutional RGE's are typically much more difficult to solve, and are generally only possible when there exist transformations on the labels that take the convolution to a product, most commonly Fourier or Mellin transforms.

Returning to the case of the Sudakov form factor, we are thankfully spared from having convolutions, as momentum conservation forces the label to be fixed by the states being scattered. Including the Wilson coefficient, the SCET form factor is given by

$$F(Q^2/m^2) = C(Q^2/\mu^2)J_n(\mu^2/m^2)\Gamma S(\mu^2/m^2)J_{\bar{n}}(\mu^2/m^2) + O(\lambda). \tag{2.52}$$

Here we have reintroduced the scale dependence of the matrix elements. As previously discussed, the Wilson coefficient only depends on the hard scale Q^2, while the EFT matrix elements only depend on the low-energy scale m^2. The resummation of large logs of Q^2/m^2 may then be achieved by running the soft and collinear matrix elements from the scale m to the scale Q, or alternatively by running C from Q down to m. This equivalence may be

seen through the μ-independence of F. Using this, we find the relation

$$\gamma^H + \gamma^n_\mu + \gamma^{\bar{n}}_\mu + \gamma^S_\mu = 0, \tag{2.53}$$

where γ^H is the anomalous dimension of the hard coefficient. Similar relations may be derived for other hard scattering operators.

2.3 Rapidity Divergences and the Rapidity RGE

There is one final wrinkle in the factorization formula for the Sudakov form factor in Eq. (2.52) which we now address. Let us reconsider the soft and collinear modes. Both have the same virtualites, $k_n^2 \sim k_s^2 \sim \lambda^2$, which is to say both modes live at the same invariant mass at the scale m^2. These modes are then only distinguished by the size of their rapidities, k^+/k^-. Obviously this is not a Lorentz-invariant statement; we could perform a boost in the z-direction which takes a collinear mode to a soft mode, and vice-versa. We already know that the EFT breaks Lorentz invariance though, through the two preferred vectors n and $\bar{n}$ built into the theory. In principle, we could add a cutoff on integrals over the rapidities to separate the modes, but by the principles of EFT we must take said cutoffs to infinity or zero. This leads to additional divergences which are *not* regulated by dimensional regularization, as they occur at fixed invariant mass. The prototypical example of such divergent integrals is

$$I_\pm = \int \frac{dk^\pm}{k^\pm} f(k), \tag{2.54}$$

where $f(k)$ approaches some finite value as $k^\pm \to 0$ or ∞. Such integrals can arise from diagrams with Wilson line contributions. If we look at the one gluon term in the definition of a Wilson line in Eq. (2.33), for example, we find it generates a Feynman rule

$$W_n^{(1)} = \frac{-g}{\bar{n}\cdot k} \bar{n}\cdot A_n(k), \tag{2.55}$$

which provides the eikonal $1/k^+$ propagator for the rapidity divergent integral.

In addition to the appearance of rapidity divergences, there are also associated "rapidity logarithms" which are large for the processes we can apply SCET to and thus need to be resummed. Like the hard logs we encountered in the previous section, rapidity logs also take an argument of Q^2/m^2, but rather than being a ratio of scales, this may be thought of as a measure of how boosted the collinear states are relative to each other. This is a statement about the IR physics, which is why it appears in the low-energy theory. If we

break up the log, we can write it as

$$\log \frac{Q^2}{m^2} = \log \frac{p_1^+}{\nu} + \log \frac{p_2^-}{\nu} + \log \frac{\nu^2}{m^2}, \tag{2.56}$$

where ν is some arbitrary rapidity scale. As we have written this, we can clearly identify an n-collinear, $\bar{n}$-collinear, and soft contribution. Resumming rapidity logarithms then amounts to regulating and renormalizing rapidity divergences, and then running the soft (or collinear) matrix elements in ν to the appropriate rapidity scale[54].

There are a number of rapidity regulators available for use in the literature, but we choose to use the η-regulator[57]. This is implemented in the action by modifying the Wilson line definitions:

$$W_n = \sum_{\text{perms}} \exp\left(\frac{-gw^2}{\bar{n}\cdot\mathcal{P}} \frac{|\bar{n}\cdot\mathcal{P}|^{-\eta}}{\nu^\eta} \bar{n}\cdot A_n\right), \tag{2.57}$$

$$S_n = \sum_{\text{perms}} \exp\left(\frac{-gw}{n\cdot\mathcal{P}_S} \frac{|2\mathcal{P}_{Sz}|^{-\eta/2}}{\nu^{\eta/2}} n\cdot A_S\right),$$

with $2\mathcal{P}_{Sz} = \bar{n}\cdot\mathcal{P}_S - n\cdot\mathcal{P}_S$. This regulator is functionally quite similar to dimensional regularization, with η playing the role of ϵ, and ν being the new scale which acts as a cutoff in rapidity space, analogous to how μ is the momentum cutoff scale. $w = w(\nu)$ is a dummy coupling needed to derive the rapidity renormalization group equations, which gets set to 1 after renormalization.

Practically, the procedure for working with rapidity divergences is almost identical to dealing with UV divergences. When computing a diagram with the η regulator, we first expand in η, followed by expanding in ϵ. In particular, this means that all terms of the form $\eta/\epsilon^n \to 0$. All η and ϵ poles get absorbed into the appropriate counter terms. We may then calculate anomalous dimensions for both μ and ν running by taking derivatives of the counter terms with respect to μ or ν, as in Eq. (2.51). The order in which we choose to run μ and ν does not matter, as μ and ν are independent parameters, and we have

$$\left[\mu\frac{d}{d\mu}, \nu\frac{d}{d\nu}\right] = 0. \tag{2.58}$$

This is closely related to the fact that the generators for scale transformations D and Lorentz boosts $M_{\mu\nu}$ commute:

$$[D, M_{\mu\nu}] = 0. \tag{2.59}$$

Just as the μ-RG controls the scale dependence of matrix elements, the ν-RG controls the rapidity dependence. In fact, we will see later that the above generators may be exactly

related to the (R)RG of form factors and amplitudes.

If we return now to the example of the Sudakov form factor, we may write the complete renormalized factorization with all scale dependence as

$$F(Q^2/m^2) = C(Q^2/\mu^2)J_n(\mu^2/m^2; p_1^+/\nu)\Gamma S(\mu^2/m^2; \nu^2/m^2)J_{\bar{n}}(\mu^2/m^2; p_2^-/\nu). \tag{2.60}$$

Given that the form factor is independent of ν, it must be the case that the ν-dependence cancels between the soft and collinear matrix elements. In fact this cancellation is guaranteed by the boost invariance of the full theory form factor. The running of ν cause a flow from the soft to the collinear region (or vice-versa); this may equivalently be achieved by performing boost. Thus boost invariance inevitably leads to the conclusion that the total form factor must be independent of ν. Note that this also implies that the (unrenormalized) form factor must be independent of η as well, since the ν-dependence is tied to the η poles through the counter terms. Practically, this means that all $1/\eta$ poles must cancel when one sums over all soft and collinear contributions at any given order in α_s.

Each factorized matrix element J_n, S, and $J_{\bar{n}}$ satisfy an RG for ν, just as they do for μ. Generically, these rapidity RG equations may be convolutional as well, and we have

$$(J_n^{\rm B}, S^{\rm B}) = Z_n \otimes (J_n^{\rm R}, S^{\rm R}), \qquad \nu\frac{d}{d\nu}(J_n^{\rm R}, S^{\rm R}) = \gamma_\nu^{n/S} \otimes (J_n^{\rm R}, S^{\rm R}), \qquad \gamma_\nu^{n/S} = -Z_{n,S}^{-1} \otimes \nu\frac{d}{d\nu}Z_{n,S}. \tag{2.61}$$

For the case of the Sudakov form factor, these convolutions reduce to being multiplicative. The ν-independence of the form-factors places a consistency constraint on the ν-anomalous dimensions:

$$\gamma_\nu^n + \gamma_\nu^{\bar{n}} + \gamma_\nu^S = 0. \tag{2.62}$$

This is equivalent to the relation between μ-anomalous dimensions in Eq. (2.53), without γ_H as the hard coefficient is already boost invariant. The commutivaty of μ and ν evolution places one final constraint on the anomalous dimension,

$$\nu\frac{d}{d\nu}\gamma_\mu = \mu\frac{d}{d\mu}\gamma_\nu = \left(\mu\frac{\partial}{\partial\mu} + \beta\frac{\partial}{\partial g}\right)\gamma_\nu = z\,\Gamma_{\rm Cusp}, \tag{2.63}$$

where z is some integer that depends on the process and the anomalous dimension of interest. β is the QCD beta function, and $\Gamma_{\rm Cusp}$ is known as the cusp anomalous dimension, which is related to the anomalous dimensions of Wilson line pairs.

Let us make the above discussions concrete by returning to the Sudakov form factor once more. We now perform explicit calculations to demonstrate how the (rapidity) renormalization procedure works. For loops, we use Feynman gauge for the gluon propagator,

adding a gluon mass m to regulate the IR. At tree level, we may write the form factor as

$$\begin{aligned} F^{(0)} =& \bar{u}_n \Gamma v_{\bar{n}}, \\ J_n^{(0)} = \bar{u}_n, \qquad & S^{(0)} = 1, \qquad J_{\bar{n}}^{(0)} = v_{\bar{n}}. \end{aligned} \tag{2.64}$$

The one-loop contribution to the collinear matrix element is straightforward to compute. Using the one-gluon term in the rapidity-regulated Wilson line and the collinear quark-collinear gluon Feynman rule listed in Appendix B, we have

$$\begin{aligned} &= ig^2 w^2 C_F \int \frac{[d^d k]}{|\bar{n}\cdot k|^{1+\eta}} \frac{\mu^{2\epsilon}\nu^\eta \, 2\bar{n}\cdot(k+p_1)}{(k^2 - m^2 + i0)((k+p_1)^2 + i0)}, \\ &= \frac{g^2 w^2 C_F}{8\pi^2} \left(\frac{\Gamma(\epsilon) e^{\epsilon\gamma_E}}{\eta} \left(\frac{\mu^2}{m^2}\right)^\epsilon + \frac{1}{\epsilon}\left(1 - \log\frac{p_1^+}{\nu}\right) + \log\frac{\mu^2}{m^2}\left(1 - \log\frac{p_1^+}{\nu}\right) - \frac{\pi^2}{6} + 1 \right). \end{aligned} \tag{2.65}$$

To compute this, we have performed the $n\cdot k$ integral by contours, and performed the $k_\perp$ and $\bar{n}\cdot k$ integrals using standard dim. reg. techniques. We also have expanded the result in $\eta \to 0$ first before $\epsilon \to 0$. Notice also that the $1/\eta$ term is left unexpanded in ϵ; formally this term is at finte η, and so it must be kept to all orders in ϵ. The $\bar{n}$-collinear matrix element is identical under the replacement $p_1^+ \to p_2^-$. Next we have the soft matrix element. Starting at one loop, we must be careful about direction of the Wilson lines in S. For the case of pair production that we are considering, the Wilson lines both run from $(0, \infty)$. This may be determined from matching at tree level with one soft gluon emission and keeping track of the $i0$ prescriptions. With this, the one loop soft matrix element is

$$\begin{aligned} &= -2ig^2 w^2 C_F \int [d^d k] \frac{\mu^{2\epsilon} |2k_z|^{-\eta} \nu^\eta}{(k^2 - m^2 + i0)(n\cdot k + i0)(\bar{n}\cdot k - i0)}, \\ &= \frac{g^2 w^2 C_F}{4\pi^2} \left(-\frac{\Gamma(\epsilon) e^{\epsilon\gamma_E}}{\eta} \left(\frac{\mu^2}{m^2}\right)^\epsilon + \frac{1}{2\epsilon^2} + \left(\frac{1}{2\epsilon} + \frac{1}{2}\log\frac{\mu^2}{m^2}\right)\log\frac{\mu^2}{-\nu^2 - i0} - \frac{1}{4}\log^2\frac{\mu^2}{m^2} - \frac{\pi^2}{24} \right). \end{aligned} \tag{2.66}$$

To obtain this result, we have first computed the k_0 integral by contours, closing over the lower half plane. There are two poles, one at $k_0 = \sqrt{k_z^2 - k_\perp^2 + m^2 - i0}$, and one at $k_0 = k_z - i0$. The former residue may be calculated using standard integration techniques. To deal with the latter term, one uses the integral

$$\int [dk_z] \frac{|2k_z|^{-\eta}\nu^\eta}{-2k_z + \Delta + i\epsilon} = -\frac{i}{4} + O(\eta). \tag{2.67}$$

Details on the calculation may be found in Appendix B.2 of [159]. Lastly, the remaining $k_\perp$ integral is straightforward. This generates an overall factor of $i\pi$, which may be combined with the $\log\nu^2$ from the first term to give the $\log(-\nu^2 - i0)$ which appears in the final result. We will discuss this $i\pi$ term in more detail after introducing Glauber operators.

The full one-loop result for the form factor in the EFT is then given by summing over the soft and collinear contributions. Doing so gives the result

$$[J_n \Gamma S J_{\bar{n}}]^{(1)} = \bar{u}_n \Gamma v_{\bar{n}} \frac{g^2 C_F}{4\pi^2} \left[\frac{1}{2\epsilon^2} + \frac{1}{\epsilon} \left(\frac{1}{2} \log \frac{\mu^2}{-Q^2} + 1 \right) + \left(\frac{1}{2} \log \frac{\mu^2}{m^2} + 1 \right)^2 + \frac{1}{4} \log \frac{\mu^2}{m^2} \log \frac{-Q^2}{m^2} - \frac{5\pi^2}{24} \right]. \tag{2.68}$$

Here we have used $Q^2 = p_1^+ p_2^-$, and the shorthand $-Q^2 \equiv -Q^2 - i0$, as well as setting $w = 1$. As claimed, all η- and ν-dependence has canceled from the EFT form factor, and boost-invariance has been restored.

We may now renormalize the form factors. We first account for wave-function renormalization for the collinear quarks, which is the same as for full QCD quarks, as the collinear quark Lagrangian is identical to the full QCD Lagrangian. This adds a factor of $Z_\psi^{1/2}$ to each collinear matrix element, with

$$Z_\psi = 1 + \frac{g^2 C_F}{16\pi^2} \left(-\frac{1}{\epsilon} - \log \frac{\mu^2}{m^2} + \frac{1}{2} \right). \tag{2.69}$$

Renormalizing as in Eq. (2.126),we then find the counter terms to be

$$Z_n = 1 + \frac{g^2 w^2 C_F}{8\pi^2} \left(\frac{\Gamma(\epsilon) e^{\epsilon \gamma_E}}{\eta} \left(\frac{\mu^2}{m^2} \right)^\epsilon + \frac{1}{\epsilon} \left(1 - \log \frac{p_1^+}{\nu} \right) \right), \tag{2.70}$$

$$Z_s = 1 + \frac{g^2 w^2 C_F}{4\pi^2} \left(-\frac{\Gamma(\epsilon) e^{\epsilon \gamma_E}}{\eta} \left(\frac{\mu^2}{m^2} \right)^\epsilon + \frac{1}{2\epsilon^2} + \frac{1}{2\epsilon} \log \frac{\mu^2}{-\nu^2 - i0} \right).$$

Here, we see that the counter terms depend explicitly on the IR scale m! This is fine as long as the m-dependence sticks to the rapidity-divergent terms. This is because from the perspective of the regulator, m^2 is the scale of the invariant mass hyperbola we have integrated along to obtain the $1/\eta$ divergence, and so m is not an IR parameter from the perspective of the RRG. It had better be the case though that when we compute the μ-anomalous dimension, the mass dependence drops out.

The μ anomalous dimensions are given by

$$\gamma_\mu^n = \frac{g^2 C_F}{4\pi^2} \left(-\log \frac{p_1^+}{\nu} + \frac{3}{4} \right), \qquad \gamma_\mu^S = \frac{g^2 C_F}{4\pi^2} \log \frac{\mu^2}{\nu^2}. \tag{2.71}$$

$\gamma_\mu^{\bar{n}}$ is obtained through replacing p_1^+ with p_2^- in γ_μ^n. To obtain the ν anomalous dimensions, we use the fact that the dummy coupling w obeys the RG

$$\nu \frac{d}{d\nu} w(\nu)^2 = -\eta\, w(\nu)^2, \tag{2.72}$$

which is analogous to the lowest order beta function for α_s in dim. reg., $\beta = -\epsilon\alpha_s + O(\alpha_s^2)$. With this, the ν anomalous dimensions are found to be

$$\gamma_\nu^n = \frac{g^2 C_F}{8\pi^2} \log \frac{\mu^2}{m^2}, \qquad \gamma_\nu^S = -\frac{g^2 C_F}{4\pi^2} \log \frac{\mu^2}{m^2}. \tag{2.73}$$

These obey the expected consistency condition of Eq. (2.62), as we have $\gamma_\nu^S = -2\gamma_\nu^n$. Moreover, we can check that μ-ν commutivity of Eq. (2.63) is also satisfied, as we have

$$\mu \frac{d}{d\mu} \gamma_n^\nu = \nu \frac{d}{d\nu} \gamma_n^\mu = \frac{g^2 C_F}{4\pi^2}, \tag{2.74}$$

with similar results for the soft anomalous dimensions. As expected, the dependence on m in γ_ν has dropped out in the μ-derivative. This result also gives us the correct cusp anomalous dimension, which at one loop is given as

$$\Gamma_{\text{Cusp}}^{(1)} = \frac{g^2 C_F}{4\pi^2}. \tag{2.75}$$

2.4 Glaubers and Forward Scattering

In the previous section, we have introduced SCET and discussed several features of the EFT, with a particular focus on applying the EFT to wide angle, or hard, scattering. However, this is not the only class of problems for which SCET will apply. The other interesting limit is that of small angle, or near-forward scattering. This limit is characterized by a large center of mass energy s and a small momentum transfer t.

For massive particles, there are several regimes of forward scattering, which include potential scattering in the case where the states are moving non-relativistically. The forward limit is also the regime of classical scattering. This can be seen from the total angular momentum L of the system. For non-relativistic particles $L \sim mvr$, with r being the spacial separation between the scattering states. Since $1/r \ \sqrt{-t} \ll mv$, it follows that $L \gg 1 = \hbar$. Similar considerations lead to the same conclusion in relativistic settings. For ultra-relativistic or massless particles, which we are interested in here, this limit is known as the high energy, or the Regge, limit. Rather than potentials, scattering is mediated by the Glauber mode, a relativistic analogue of potential modes. As we will see, integrating out Glauber modes gives rise to a set of "potential" operators, which are similar to the potential operators that arise in nonrelativistic EFTs, such as NRQCD [128]and NRGR [98].

The high energy limit is also theoretically interesting in its own right. The behavior of scattering amplitudes and cross-sections is heavily constrained by unitarity, and a number of interesting structures appear. The most familiar of these is that of "Reggeization", in which

the t-channel pole of the exchanged particle becomes dressed with a power-law scaling:

$$\frac{1}{t} \to \frac{1}{t}\left(\frac{s}{-t}\right)^{\alpha_R(t)}, \tag{2.76}$$

where $\alpha_R(t)$ is known as the Regge trajectory. For example, it has been known since the 80s that amplitudes with fermions or gluons exchanged in the t-channel are dominated by Regge scaling up to next-to-leading log (NLL) order[120, 136]. This power-law scaling is sometimes called a "Regge pole". A second important structure is that of the "Regge cut" [4]. The prototypical example of a Regge cut in QCD is the BFKL equation [121, 14], which governs the s-scaling of the imaginary part of the amplitude, or by the optical theorem the forward cross-section. In perturbative QCD, these structures arise from summing large logs of s/t; for example, leading order Reggeization is found by summing the series

$$\sum_n \left(\alpha_s \alpha_R^{(1)} \log \frac{s}{-t}\right)^n. \tag{2.77}$$

Glauber modes provide a very different perspective on the physics. By organizing the physics into operators with a distinct number of Glauber exchanges, the EFT provides a natural translation of Regge theory behaviors into statements about the rapidity renormalization group properties of these operators. Moreover, gauge-invariance in automatically obtained from the gauge-invariance of the Glauber Lagrangian, allowing for the power to make very precise statements about the amplitude.

Glauber modes are also known to be closely linked to the violation of the factorization of hard scattering operators we saw in the previous section. This is clear from the action, as Glauber modes generate interactions between soft and collinear modes at leading power in λ, and thus they muddy the argument that soft and collinear modes live in orthogonal Hilbert spaces. However, in many hard scattering problems it can be shown that either Glaubers do not contribute, as their contributions cancel when summed over, or their contributions may be entirely absorbed into the soft function. The Sudakov form factor is an example of

[4] These terms come from studies on the high energy limit in the 50s, predating QCD. Schematically, one can perform a partial wave decomposition on the amplitude $A(s,t) \sim \sum_\ell P_\ell(\cos(\theta_t))A_\ell(t)$, with P_ℓ being the Legendre polynomials and θ_t being the t-channel scattering angle. One then analytically continued A_ℓ to be a continuous function of ℓ, on the so-called "complex angular momentum plane" [62]. Using unitarity, crossing symmetry, and the analyticity of the amplitude in the high energy limit one could constrain the amplitude. Regge poles then correspond to poles in ℓ, while Regge cuts are likewise cuts of the amplitude in ℓ-space. For example, Reggeization comes from $A_\ell(t) \sim 1/(\ell - \alpha_R(t))$. The fact that poles in the scattering amplitude correspond with states in the theory then leads to the interpretation of a Regge trajectory as the exchange of a particle with angular momentum $\alpha_R(t)$ and propagator (2.76), called a Reggeon. Regge cuts then take on the interpretation of a bound state of Reggeons. The most famous case in QCD is that of the Pomeron, claimed to be a bound state of two Reggeized gluons. Such an interpretation has lead to a search for an underlying field theory which describes these degrees of freedom, the "Reggeon field theory", with mixed success[46, 47, 89]

the latter case, as we will explore. There is a class of observables for which this has been proven, but the general conditions for which factorization violation occur are still mostly unknown.

In this section, we discuss the aspects of Glaubers and Glauber operators needed for the rest of this work, summarizing the formalism developed in [159, 93]. We first introduce the Glauber Lagrangian in QCD and some of its useful properties. Following this, we show how to write down the $2\to 2$ forward scattering amplitude within the EFT, and how it may be organized in terms of Glauber operators. Finally, we look at the RRGs of the EFT operators, and how they corresponds to more traditional Regge theory notions.

2.4.1 Forward Scattering and Glauber Operators

To describe Glauber operators, we first discuss the kinematics of forward scattering. We consider the two-to-two scattering of massless states, $p_1\, p_2 \to p_3\, p_4$. For physical onshell scattering, this sets $s = (p_1 + p_2)^2 > 0$ and $t = (p_3 - p_2)^2 < 0$. Forward scattering is characterized as the limit of small $-t \ll s$, with the obvious choice in power-counting parameter being $\lambda^2 = s/|t|$. Taking p_1 to be $\bar{n}$-collinear and p_2 to be n-collinear, we have $s = p_1^- p_2^+$ at leading order in λ. The requirement of small t then forces p_3 to be n-collinear and p_4 to be $\bar{n}$-collinear. The momentum exchanged in the t-channel is often denoted as $q = p_3 - p_2 = p_1 - p_4$. Keeping the collinear momenta onshell (i.e. preserving the scalings in Eqs. (2.7) and (2.9)) fixes q to scale as

$$q \sim (\lambda^2, \lambda^2, \lambda). \tag{2.78}$$

This is the promised Glauber scaling. We can also consider the forward scattering of collinear and soft particles. This leads to modes with slightly different scalings,

$$q_{ns} \sim (\lambda, \lambda^2, \lambda), \qquad q_{\bar{n}s} \sim (\lambda^2, \lambda, \lambda). \tag{2.79}$$

All three scalings are referred to as Glauber modes, although the latter two are sometimes called n- or $\bar{n}$-Glaubers. For collinear-collinear forward scattering, the large labels are conserved in the scattering, that is $p_1^- = p_4^-$, and $p_2^+ = p_3^+$. It is then convenient to work in a frame with $q = q_\perp$, i.e. $n\cdot q = \bar{n}\cdot q = 0$. We can then parameterize the $\perp$-components of the momenta as

$$p_1^\perp = -p_4^\perp = q_\perp/2, \qquad p_2^\perp = -p_3^\perp = -q_\perp/2. \tag{2.80}$$

The on-shell condition $p_i^2 = 0$ then fixes the remaining residual component of the momenta.

q is offshell in the sense of $q^+q^- \ll q_\perp^2$, and so it cannot be a dynamical mode in the EFT. Glauber modes must then be integrated out of the EFT, but since they are infrared

modes ($q^2 \sim \lambda^2$), the resulting operator will be non-local[5], in contrast to the local operators of hard scattering. To see how this works, let us first consider collinear quark-antiquark forward scattering. At tree level, the leading order contribution is given by a t-channel exchange of a gluon,

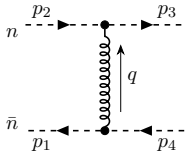

$$= \left[\bar{u}_n \frac{\bar{n}\!\!\!/}{2} T^A u_n\right] \frac{8i\pi\alpha_s}{q_\perp^2} \left[\bar{v}_{\bar{n}} \frac{n\!\!\!/}{2} \bar{T}^A v_{\bar{n}}\right]. \tag{2.81}$$

This is then matched onto an operator of the form

$$O_{n\bar{n}} = \bar{\xi}_n \frac{\bar{n}\!\!\!/}{2} T^A \xi_n \frac{8\pi\alpha_s}{\mathcal{P}_\perp^2} \bar{\xi}_{\bar{n}} \frac{n\!\!\!/}{2} \bar{T}^A \xi_{\bar{n}}, \tag{2.82}$$

where we can see the nonlocality built into the operator from the inverse label operators. This operator is not gauge invariant, but the replacement of ξ_n with the appropriate building block χ_n fixes this. We also find that one is allowed the emission of a soft gluon off of the Glauber, through diagrams such as

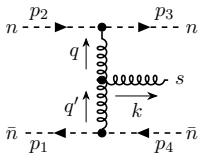

(2.83)

Here, q has n-Glauber scaling, while q' has $\bar{n}$-Glauber scaling. The soft gluon then carries away the $O(\lambda)$ components of the momenta so that the Glaubers have the correct scalings. The full set of Glauber operators is found by integrating out all such diagrams.

For collinear-collinear ($n\bar{n}$) scattering, the leading power Glauber operators are

$$\begin{aligned} O_{ns\bar{n}}^{qq} &= \mathcal{O}_n^{qA} \frac{1}{\mathcal{P}_\perp^2} \mathcal{O}_S^{AB} \frac{1}{\mathcal{P}_\perp^2} \mathcal{O}_{\bar{n}}^{qB}, & O_{ns\bar{n}}^{gq} &= \mathcal{O}_n^{gA} \frac{1}{\mathcal{P}_\perp^2} \mathcal{O}_S^{AB} \frac{1}{\mathcal{P}_\perp^2} \mathcal{O}_{\bar{n}}^{qB}, \\ O_{ns\bar{n}}^{qg} &= \mathcal{O}_n^{qA} \frac{1}{\mathcal{P}_\perp^2} \mathcal{O}_S^{AB} \frac{1}{\mathcal{P}_\perp^2} \mathcal{O}_{\bar{n}}^{gB}, & O_{ns\bar{n}}^{gg} &= \mathcal{O}_n^{gA} \frac{1}{\mathcal{P}_\perp^2} \mathcal{O}_S^{AB} \frac{1}{\mathcal{P}_\perp^2} \mathcal{O}_{\bar{n}}^{gB}. \end{aligned} \tag{2.84}$$

On the left-hand side the subscripts indicate that these operators involve three sectors $\{n, s, \bar{n}\}$, while the first and second superscript determine whether we take a quark or gluon

[5]Note that this is neither unexpected, since low-energy modes propagate over long distances, nor is it unquie, as several other EFTs also have non-locality built into them, such as potential NRQCD[39]. SCET$_{\rm II}$ already has nonlocality built into it from the soft Wilson lines, which are nonlocal at distances of order $1/\lambda$. It is also worth mentioning that the EFT is still local on the largest distance scales, those at $1/\lambda^2$, as the Glauber mode propagates only over distances of $\sim 1/\lambda$.

operator in the n-collinear or $\bar{n}$-collinear sectors. The collinear operators are defined as

$$\mathcal{O}_n^{qA} = \bar{\chi}_n \frac{\bar{n}\!\!\!/}{2} T^A \chi_n, \qquad \mathcal{O}_n^{gA} = \left[\frac{i}{2} f^{ABC} \mathcal{B}^B_{n\perp\mu} \frac{\bar{n}}{2} \cdot (\mathcal{P} + \mathcal{P}^\dagger) \mathcal{B}^{C\mu}_{n\perp} \right]. \tag{2.85}$$

The soft operator is universal (i.e. independent of the scattering states), and is given as

$$\begin{aligned} \mathcal{O}_S^{AB} = 8\pi\alpha_s \Big\{ & \mathcal{P}_\perp^\mu \mathcal{S}_n^T \mathcal{S}_{\bar{n}} \mathcal{P}_{\perp\mu} - g \mathcal{P}_\mu^\perp \tilde{\mathcal{B}}^{n\mu}_{S\perp} \mathcal{S}_n^T \mathcal{S}_{\bar{n}} - g \mathcal{S}_n^T \mathcal{S}_{\bar{n}} \tilde{\mathcal{B}}^{\bar{n}\mu}_{S\perp} \mathcal{P}_\mu^\perp - g^2 \tilde{\mathcal{B}}^{n\mu}_{S\perp} \mathcal{S}_n^T \mathcal{S}_{\bar{n}} \tilde{\mathcal{B}}^{\bar{n}}_{S\perp\mu} \\ & - g \frac{n_\mu \bar{n}_\nu}{2} \mathcal{S}_n^T i\tilde{G}_S^{\mu\nu} \mathcal{S}_{\bar{n}} \Big\}^{AB}. \end{aligned} \tag{2.86}$$

Collinear-soft (ns) scattering only involves two of the three modes, and the operators are

$$O_{ns}^{qq} = \mathcal{O}_n^{qA} \frac{1}{\mathcal{P}_\perp^2} \mathcal{O}_s^{q_n A}, \quad O_{ns}^{qg} = \mathcal{O}_n^{qA} \frac{1}{\mathcal{P}_\perp^2} \mathcal{O}_s^{g_n A}, \quad O_{ns}^{gq} = \mathcal{O}_n^{gA} \frac{1}{\mathcal{P}_\perp^2} \mathcal{O}_s^{q_n A}, \quad O_{ns}^{gg} = \mathcal{O}_n^{gA} \frac{1}{\mathcal{P}_\perp^2} \mathcal{O}_s^{g_n A}, \tag{2.87}$$

with

$$\begin{aligned} \mathcal{O}_s^{q_n A} &= 8\pi\alpha_s \left(\bar{\psi}_S^n T^A \frac{\bar{n}\!\!\!/}{2} \psi_S^n \right), \\ \mathcal{O}_s^{g_n A} &= 8\pi\alpha_s \left(\frac{i}{2} f^{ABC} \mathcal{B}^{nB}_{S\perp\mu} \frac{n}{2} \cdot (\mathcal{P} + \mathcal{P}^\dagger) \mathcal{B}^{nC\mu}_{S\perp} \right). \end{aligned} \tag{2.88}$$

The Glauber Lagrangian may then be written as

$$\mathcal{L}_{\rm G} = e^{-ix\cdot\mathcal{P}} \sum_{i,j=q,g} \mathcal{O}_n^{iA} \frac{1}{\mathcal{P}_\perp^2} \mathcal{O}_S^{AB} \frac{1}{\mathcal{P}_\perp^2} \mathcal{O}_{\bar{n}}^{jB} + e^{-ix\cdot\mathcal{P}} \sum_{\{n,\bar{n}\}} \sum_{i,j=q,g} \mathcal{O}_n^{iA} \frac{1}{\mathcal{P}_\perp^2} \mathcal{O}_s^{j_n A}. \tag{2.89}$$

This is the complete Glauber Lagrangian from tree-level matching. It is manifestly gauge invariant, being constructed out of gauge-invariant SCET operator building blocks, and as such it contains interactions at all orders in α_s due to the presence of Wilson lines. Notice that this form of the Lagrangian implies the collinear operators always come together as a sum over particle species, specifically in the combination

$$\mathcal{O}_n^{qA} + \mathcal{O}_n^{gA}. \tag{2.90}$$

This will have important implications for the RG properties of the operators.

An particularly important property of the Lagrangian is that loops do not generate any corrections to the Lagrangian (at leading power in λ), either non-trivial Wilson coefficients or new operators.

It is particularly convenient for formal manipulations to write the Glauber Lagrangian

in transverse momentum space rather than in position space. To start, we first notice that all soft and collinear operators are evaluated at $x_\perp = 0$, as we have already pulled out all $x_\perp$ dependence into the overall exponential, and since there are no residual $\perp$-momentum scales of $O(\lambda^2)$, this is the only $x_\perp$-dependence. In the action, we may then perform the $x_\perp$-integration, which leads to an overall label-conserving delta function. We may make the labels explicit by writing

$$\mathcal{O}_n^{iA}(q_\perp) = \left[\delta^2(q_\perp - \mathcal{P}_\perp)\mathcal{O}_n^{iA}\right], \qquad \mathcal{O}_{\bar{n}}^{iA}(-q'_\perp) = p\left[\delta^2(q'_\perp - \mathcal{P}_\perp)\mathcal{O}_{\bar{n}}^{iA}\right], \tag{2.91}$$

so that we have

$$\mathcal{O}_n^{iA} = \int d^2q_\perp \mathcal{O}_n^{iA}(q_\perp), \qquad \mathcal{O}_{\bar{n}}^{iA} = \int d^2q'_\perp \mathcal{O}_{\bar{n}}^{iA}(-q'_\perp). \tag{2.92}$$

If we include the overall $\perp$-label conserving delta function into the soft operator, we write

$$\int d^4x \mathcal{L}_G = \sum_{i,j=q,g} \int [d^2\tilde{x}] \int \frac{d^2q_\perp d^2q'_\perp}{q_\perp^2\, q_\perp'^2} \mathcal{O}_n^{iA}(q_\perp)\mathcal{O}_S^{AB}(q_\perp, -q'_\perp)\mathcal{O}_{\bar{n}}^{iB}(-q'_\perp) \tag{2.93}$$

$$+ \sum_{n,\bar{n}} \sum_{i,j=q,g} \int [d^2\tilde{x}] \int \frac{d^2q_\perp}{q_\perp^2} \mathcal{O}_n^{iA}(q_\perp)\mathcal{O}_s^{j_nA}(-q_\perp). \tag{2.94}$$

Here, $[d^2\tilde{x}] = 1/2dx^+dx^-e^{i/2(x^+\mathcal{P}^- + x^-\mathcal{P}^+)}$ is the measure for the lightcone positions, with the overall label exponentials. The soft operator in transverse momentum space is then given as

$$\begin{aligned}\mathcal{O}_S(q_\perp, -q'_\perp) =& (8\pi\alpha_s)(2\pi)^2\delta^2(q_\perp + q'_\perp - \mathcal{P})\Big\{ q_\perp \cdot q'_\perp \mathcal{S}_n^T\mathcal{S}_{\bar{n}} - g q_\mu^\perp \tilde{\mathcal{B}}_{S\perp}^{n\mu}\mathcal{S}_n^T\mathcal{S}_{\bar{n}} - g\mathcal{S}_n^T\mathcal{S}_{\bar{n}}\tilde{\mathcal{B}}_{S\perp}^{\bar{n}\mu}q'^\perp_\mu \\ & - g^2\tilde{\mathcal{B}}_{S\perp}^{n\mu}\mathcal{S}_n^T\mathcal{S}_{\bar{n}}\tilde{\mathcal{B}}_{S\perp\mu}^{\bar{n}} - g\frac{n_\mu\bar{n}_\nu}{2}\mathcal{S}_n^T i\tilde{G}_S^{\mu\nu}\mathcal{S}_{\bar{n}}\Big\}^{AB}. \end{aligned} \tag{2.95}$$

It is also useful to add a second integral over the lightcone positions in $\mathcal{O}_{ns\bar{n}}$, via

$$\int d^4x \mathcal{O}_{ns\bar{n}}(x) = \int [d^2\tilde{x}][d^2\tilde{x'}] \int \frac{d^2q_\perp d^2q'_\perp}{q_\perp^2\, q_\perp'^2} \mathcal{O}_n^{iA}(q_\perp, \tilde{x})\mathcal{O}_S^{AB}(q_\perp, -q'_\perp; \tilde{x}, \tilde{x}')\mathcal{O}_{\bar{n}}^{iB}(-q'_\perp, \tilde{x}'), \tag{2.96}$$

with

$$\mathcal{O}_S^{AB}(q, -q'_\perp; \tilde{x}, \tilde{x}') = \delta^2(\tilde{x} - \tilde{x}')\mathcal{O}_S^{AB}(q, -q'_\perp, \tilde{x}). \tag{2.97}$$

This final modification will see use when discussion the factorization of the amplitude.

Lastly, we mention that Glauber operators have been found for fermionic Glauber exchanges, relevant for quark-gluon back scattering. This process is, however, λ-suppressed

relative to forward scattering, and so it is not relevant to the discussions here.

2.4.2 Glauber Loops and Amplitude Factorization

When calculating in the EFT, we encounter loops with Glauber momentum running through them, from time-ordered products (T-products) of Glauber operators. The prototypical cases of are the box and cross-box diagrams that appear at one loop. These diagrams are straightforward to write down, and they are

$$\begin{aligned} &= I_2(q_\perp) \int \frac{[d^2k^\pm]}{(k^- + \Delta_n + i0)(-k^+ + \Delta_{\bar{n}} + i0)}, \\ &= I_2(q_\perp) \int \frac{[d^2k^\pm]}{(k^- + \Delta_n + i0)(k^+ + \Delta_{\bar{n}} + i0)}, \end{aligned} \tag{2.98}$$

with $\Delta_n = p_3^- + (k_\perp + q_\perp/2)^2/p_2^+$ and $\Delta_{\bar{n}} = p_4^- + (k_\perp + q_\perp/2)^2/p_1^-$. $I_2(q_\perp)$ contains the integrals over the Glauber $1/k_\perp^2$ propagators, and is identical for both diagrams. It is fairly clear that the integrations over $k^\pm$ are logarithmically divergent in both k^+ and k^-, reminiscent of rapidity divergent integrals. However, the η-regulator for the soft and collinear sectors does not regulate the divergences, as they only see the large and soft labels, while Glauber $k^\pm$ are residual. Moreover, these divergences are not regulated by dim. reg. These divergences require a new regulator, which is called the η' regulator. It may be implemented at the level of the action by writing

$$\begin{aligned} S_G = &\sum_{i,j=q,g} \int [d^2\tilde{x}] \int \frac{d^2q_\perp d^2q'_\perp}{q_\perp^2\, q_\perp'^2} \mathcal{O}_S^{AB}(q_\perp, -q'_\perp) \left[\mathcal{O}_n^{iA}(q_\perp) w'^2 \frac{|i\bar{n}\cdot\vec{\partial} + in\cdot\overleftarrow{\partial}|^{-\eta'}}{\nu'^{-\eta'}} \mathcal{O}_{\bar{n}}^{iB}(-q'_\perp) \right] \\ &+ \sum_{n,\bar{n}} \sum_{i,j=q,g} \int [d^2\tilde{x}] \int \frac{d^2q_\perp}{q_\perp^2} \mathcal{O}_n^{iA}(q_\perp) w'^2 \frac{|\beta_{ns} i\bar{n}\cdot\vec{\partial}_S + in\cdot\overleftarrow{\partial}|^{-\eta'}}{\nu'^{-\eta'}} \mathcal{O}_s^{j_n A}(-q_\perp). \end{aligned} \tag{2.99}$$

Just as with the η-regulator, w' is a dummy parameter that gets set to 1 at the end of the calculation, and ν' is the scale that gets introduced with the regulator. β_{ns} is a formal boost parameter with $\beta_{ns} \sim \lambda$, as is needed to maintain homogeneity in the power-counting, since $\partial_S \sim \lambda$ while $\partial \sim \lambda^2$. For the box and cross-box diagrams, this regulator has the effect of adding a factor of $|2k_z|^{-\eta'}$ to the integrands, with $2k_z = k^+ - k^-$. The lightcone integrals may now be performed by changing variables from (k^+, k^-) to (k_0, k_z), with $2k_0 = (k^+ + k^-)$, and we have

$$\begin{aligned} &= I_2(q_\perp) \int \frac{[dk_0 dk_z]\, |2k_z|^{-\eta'}}{(k_0 - k_z + \Delta_n + i0)(-k_0 - k_z + \Delta_{\bar{n}} + i0)}, \\ &= I_2(q_\perp) \int \frac{[dk_0 dk_z]\, |2k_z|^{-\eta'}}{(k_0 - k_z + \Delta_n + i0)(k_0 + k_z + \Delta_{\bar{n}} + i0)}. \end{aligned} \tag{2.100}$$

The k_0 integrals may be performed by contours. For the cross-box diagram, the poles both sit below the reals axis, and we may close the contour on the upper half-plane which sets the integral to zero. For the box diagram, we perform the k_0 integral, and use Eq. 2.67 to obtain the final result,

$$= I_2(q_\perp)\left(-\frac{1}{4} + O(\eta')\right). \tag{2.101}$$

This result is finite in the $\eta' \to 0$ limit, and so despite the rapidity divergence, Glauber loops do not induce any new RGs.

It is also useful to look at the N-loop Glauber box diagrams, with $N+1$ Glauber exchanges. Without going into the details (see Section 9.1 of [159] for the full calculation), the result may be found to be

$$= 2I_{N+1}(q_\perp)\frac{(-ig^2)^{N+1}}{(N+1)!}. \tag{2.102}$$

Morally, we may interpret this result as teaching us that a diagram with N Glauber exchanges gives a $1/N!$ combinatorial factor, as well as a factor of $i\pi$ for every Glauber loop. These observations continue to hold in the presence of soft and collinear loops, including with more complicated, nonplanar graph topologies. The latter fact is of particular note, since it tells us that Glaubers build up the imaginary part of the amplitude, and hence are closely linked with unitarity cuts. The $1/N!$ meanwhile allows us to exponentiate the sum of the box diagrams. If we look at the $\perp$-integrals, we find they are given as

$$\begin{aligned} I_N(q_\perp) &= \int \left(\prod_{i=1}^{N} \frac{[d^{d-2}k_{i\perp}]}{k_{i\perp}^2}\right) \delta\left(\sum_i k_{i\perp} - q_\perp\right), \\ &= \int d^{d-2}b_\perp e^{ib_\perp\cdot q_\perp}(i\chi(b_\perp))^N, \end{aligned} \tag{2.103}$$

where χ is the Fourier transform of a Glauber potential,

$$\chi(b_\perp) = \int \frac{[d^{d-2}q_\perp]}{q_\perp^2} e^{-ib_\perp\cdot q_\perp}. \tag{2.104}$$

Combining this with Eq.(2.102), we find the sum of boxes to be

$$= 2\int d^{d-2}b_\perp e^{ib_\perp\cdot q_\perp}\left(e^{ig^2\chi(b_\perp)} - 1\right). \tag{2.105}$$

Therefore the sum of the Glauber box diagrams reproduces classical eikonal exponentiation at leading order.

We may understand this result physically as follows. Since Glauber modes only prop-

agate in transverse space, they are instantaneous in time and longitudinal position. The η' regulator breaks the instantaneity in the longitudinal direction. This then mandates an ordering of the Glauber exchanges along longitudinal space, as dictated by the collinear propagators moving in the x^- or x^+ directions. This ordering is what leads to the $1/N!$, since it picks out exactly one of the $N!$ configurations of Glauber exchanges. Taking $\eta' \to 0$ at the end of the calculation restores the instantaneous nature of the Glauber potential.

As can be seen in the above discussions, each Glauber loop will generate a power of $i\pi$. In fact, we can expect that all factors of $i\pi$ in SCET matrix elements to come from Glauber loops[6]. As an example, let us revisit the Sudakov form factor calculation of Eq. (2.107). Written explicitly, the result contains an $i\pi$ through the rapidity log, $\log\left(-\nu^2 - i\epsilon\right) = \log\left(\nu^2\right) - i\pi$. Although the calculation is performed for a soft loop, the origin of this $i\pi$ term is still Glauber. To see this, we can calculate the diagram with a Glauber exchange between the collinear legs:

$$\begin{aligned} =&F^{(0)}(2ig^2C_F)\int[d^dk]\frac{\mu^{2\epsilon}|2k_z|^{-\eta'}\nu'^{\eta'}}{(k_\perp^2-m^2)(n\cdot k+\Delta_n+i\epsilon)(-\bar{n}\cdot k+\Delta_{\bar{n}}+i\epsilon)}, \\ &= F^{(0)}\frac{C_F\,g^2}{8\pi^2}(i\pi)\left(\frac{1}{\epsilon}+\log\frac{\mu^2}{m^2}\right), \end{aligned} \tag{2.106}$$

which is exactly the $i\pi$ term in Eq. (2.107). However, it now sees as though we have doubled the $i\pi$ term, coming from both the Glauber and the soft graphs. Indeed, we have double-counted the Glauber region, as part of the soft integration region overlaps with the Glauber region, when $k^\pm \to 0$. This can be resolved by expanding the soft integrand in the Glauber region, and subtracting this integral from the full soft loop. This Glauber sub-region of the soft loop is sometimes referred to as the zero-bin, or Glauber-bin, and the procedure of subtracting out these overlapping regions is known as zero-bin subtractions[7]. For the calculation at hand, the zero-bin for the soft loop is given as

$$S^{(G)} = -2ig^2w^2C_F\int[d^dk]\frac{\mu^{2\epsilon}|2k_z|^{-\eta}\nu^\eta}{(k_\perp^2-m^2+i0)(n\cdot k+i0)(\bar{n}\cdot k-i0)}, \tag{2.107}$$

$$= \frac{C_F\,g^2}{8\pi^2}(i\pi)\left(\frac{1}{\epsilon}+\log\frac{\mu^2}{m^2}\right). \tag{2.108}$$

The complete result for the soft diagram is then given by $\tilde{S} = S - S^{(G)}$, which simply cancels the $i\pi$ term in Eq. (2.107). Essentially, the Glauber graph and Glauber-bin subtraction

[6]Note that the claim here is for factors of $i\pi$, and not π. Loop calculations rather generically will lead to terms that depend on even zeta values $\zeta(2n)$, which are proportional to π^{2n}. Additional factors of $i\pi$ can also appear in Wilson coefficients as well.

[7]In other SCET applications, one can also encounter soft- or Glauber-bin subtractions for collinear loops.

cancel, leaving the unsubtracted soft graph behind as the final result[8]. This correspondence between Glauber loops and $i\pi$'s turns out to be a very useful tool for exploring the implications of unitarity on the EFT, as we will see in the following chapters.

This brings us to the "factorization" of the forward amplitude for collinear-collinear scattering. Glaubers break factorization since they couple soft and collinear modes together. If we treat Glauber exchanges as small perturbations, we may still "factorize" in the sense of factorization of matrix elements. However, we lose the stronger meaning of factorization, whereby the amplitude may be written as a single factorized matrix element. Instead, the forward amplitude turns out to be a sum of soft-collinear factorized matrix elements, which each occur at a distinct number of Glauber exchanges. We start with the time evolution operator in SCET, which is given as

$$U(a,b) = \lim_{T\to(1-i0)\infty} \int [\mathcal{D}\phi] \exp\left[i \int_{-T}^{T} d^4x \left(\mathcal{L}_{ns\bar{n}}(x) + \mathcal{L}_G(x) \right) \right]. \tag{2.109}$$

Here, a and b are the field boundary conditions at $-T$ and T respectively, and $\mathcal{L}_{ns\bar{n}}(x)$ are the soft and collinear Lagrangians. The Glauber part of U may be written as a time-ordered exponential, which we then write in a series expansion as

$$\begin{aligned} T\exp\left[i\int d^4x \mathcal{L}_G(x) \right] &= \left[1 + i\int d^4x \mathcal{L}_G(x) + i^2 \int d^4x d^4y\, T\left\{ \mathcal{L}_G(x)\mathcal{L}_G(y) \right\} + ... \right], \\ &= 1 + T\sum_{k=1}^{\infty}\sum_{k'=1}^{\infty} \left[\prod_{i=1}^{k} \int [d^2\tilde{x}] \frac{d^2q_{i\perp}}{q_{i\perp}^2} [\mathcal{O}_n^{qA_i} + \mathcal{O}_n^{gA_i}](q_{i\perp}, \tilde{x}_i) \right] \\ &\qquad \times \left[\prod_{j=1}^{k'} \int [d^2\tilde{x}'_j] \frac{d^2q'_{j\perp}}{q_{j\perp}^2} [\mathcal{O}_n^{qB_j} + \mathcal{O}_n^{gb_i}](q'_{j\perp}, \tilde{x}'_j) \right] \\ &\qquad \times \mathcal{O}_{S(k,k')}^{\{A_i\}\{B_j\}}(\{q_{i\perp}\}, \{q'_{i\perp}\}, \{\tilde{x}_i\}, \{\tilde{x}'_j\}), \\ &= 1 + \sum_{k=1}^{\infty}\sum_{k'=1}^{\infty} U_{(k,k')}. \end{aligned} \tag{2.110}$$

In the second line, we have not written out the soft operator explicitly, as it is quite complicated in general, and it involves a sum over all possible products of $\mathcal{O}_S^{AB}$ and $\mathcal{O}_{sn/\bar{n}}^{i_{n/\bar{n}}A}$. For example, at $k = k' = 1$, we have

$$\mathcal{O}_{S(1,1)}^{AB}(q_\perp, q'_\perp, \tilde{x}, \tilde{x}') = \mathcal{O}_S^{AB}(q_\perp, q'_\perp, \tilde{x}, \tilde{x}') + \sum_{i,j=q,g} \mathcal{O}_{sn}^{i_nA}(q_\perp, \tilde{x}) \mathcal{O}_{s\bar{n}}^{j_{\bar{n}}B}(q'_\perp, \tilde{x}'). \tag{2.111}$$

[8]This matching between the soft zero-bin subtraction and the Glauber contributions is sometimes known as the soft-Glauber correspondence [159]. Not every observable in SCET obeys this correspondence, with the forward scattering amplitude being a notable counter example.

If we consider the scattering of projectiles κ and κ', we then can write the scattering amplitude as

$$i\mathcal{M}^{\kappa\kappa'} = \sum_{k=1}^{\infty}\sum_{k'=1}^{\infty}\left\langle p_3^{\kappa}p_4^{\kappa'}\right| U_{(k,k')}\left|p_1^{\kappa'}p_2^{\kappa}\right\rangle_{\text{connected}}. \tag{2.112}$$

We can see from the second line of Eq. (2.110) that each matrix element in the sum will naturally factorize into a convolution of an n-collinear, soft, and $\bar{n}$-collinear matrix element. Foregoing a careful analysis for the moment, this may be written as

$$i\mathcal{M}^{\kappa\kappa'} = \sum_{MN}\iint_{\perp(N,M)} J_{\kappa(N)}^{\{A_N\}}(\{l_{\perp i}\},\epsilon,\eta)S_{(N,M)}^{\{A_N\}\{B_M\}}(\{l_{\perp i}\};\{l'_{\perp i}\},\epsilon,\eta)\bar{J}_{\kappa'(M)}^{\{B_M\}}(\{l'_{\perp i}\},\epsilon,\eta). \tag{2.113}$$

Here, we have introduce notation for the Glauber convolutions,

$$\iint_{\perp(N,M)} = \frac{i^{N+M}}{N!M!}\int\prod_{i=1}^{N}\prod_{j=1}^{M}\frac{[d^{d'}l_{i\perp}]}{l_{i\perp}^2}\frac{[d^{d'}l'_{j\perp}]}{l'^2_{j\perp}}\bar{\delta}^{d'}(\sum l_{i\perp}-q_\perp)\bar{\delta}^{d'}(\sum l'_{j\perp}-q_\perp). \tag{2.114}$$

These convolutions have the effects of Glauber loops built into them, as can be seen from the factor $(-i)^{N+M}/N!M!$.

At tree level[9], the collinear functions for quarks and gluons are given by

$$\begin{aligned} J_{n(M)}^{qA_1\ldots A_M(0)} &= g^M\bar{u}_n T^{A_1}\ldots T^{A_M}\frac{\bar{n}\!\!\!/}{2}u_n, \\ J_{n(M)}^{qA_1\ldots A_M(0)} &= g^M\epsilon^\star_{n\mu}\mathcal{T}^{A_1}\ldots\mathcal{T}^{A_M}b^{\mu\nu}\epsilon_{n\nu}, \end{aligned} \tag{2.115}$$

where $b^{\mu\nu}$ is the product of two momentum space field strength tensors at one gluon,

$$\epsilon^\star_{n\mu}b^{\mu\nu}\epsilon_{n\nu} = \frac{1}{\bar{n}\cdot p_2}G^n_{+\mu}(\epsilon_n,p_2)G_n^{+\mu}(\epsilon^\star_n,p_3), \tag{2.116}$$

$$= \epsilon^\star_{n\mu}\left[\bar{n}\cdot p_2 g_\perp^{\mu\nu} - \bar{n}^\mu p_{2\perp}^\nu - p_{3\perp}^\mu\bar{n}^\nu + \frac{p_2^\perp\cdot p_3^\perp\bar{n}^\mu\bar{n}^\nu}{\bar{n}\cdot p_2}\right]\epsilon_{n\nu}, \tag{2.117}$$

where in the first line the collinear momentum space field strength is $G^n_{\mu\nu}(\epsilon,p) = p_\mu\epsilon_\nu - p_\nu\epsilon_\mu$. $\mathcal{T}^A$ is the $SU(N)$ generator in the adjoint representation, $\mathcal{T}^A = if^{\cdot A\cdot}$. The collinear function for antiquarks may be found by replacing $u_n \to v_n$ and $T^A \to \bar{T}^A$ in the quark function. The tree level soft function is only non-zero for diagonal elements, i.e. $N = M$ in Eq. (6.13):

$$S_{N,M}^{\{A_N\}\{B_M\}(0)}(\{\ell_{N\perp}\},\{\ell'_{M\perp}\}) = 2\delta_{N,M}M!(-i)^M\prod_{j=1}^{M}\ell_{j\perp}^2\prod_{k=1}^{M-1}\bar{\delta}^{d'}(\ell_{j\perp}-\ell'_{j\perp}). \tag{2.118}$$

[9]Tree level here means the absence of soft or collinear loops.

This is essentially the identity operator for the Glauber convolutions, which suggests the compact notation,

$$S_{N,M}^{\{A_N\}\{B_M\}(0)} = 2\delta_{N,M}\mathbb{1}_{\perp(M)}, \qquad \mathbb{1}_{\perp(M)} = \prod_{j=1}^{M} \ell_{j\perp}^2 \prod_{k=1}^{M-1} \delta^{d'}(\ell_{j\perp} - \ell'_{j\perp}). \tag{2.119}$$

Placing all the tree-level functions into the factorization formula then reproduces the sum of Glauber box diagrams:

$$\sum_{M,N} \left[\iint_{\perp(M,N)} J_{\kappa(N)} S_{(N,M)} \bar{J}_{\kappa'(M)} \right]^{(0)} = \sum_{N} J_{\kappa(N)} \left(2I_N(q_\perp) \frac{(-i)^N}{N!} \right) \bar{J}_{\kappa'(M)}, \tag{2.120}$$

which matches Eq. (2.102) up to the collinear tree factors. We have suppressed the color indices for ease of notation.

The physical picture of this factorization is that when collinear projectiles forward scatter, they emit a burst of Glauber exchanges, which may scatter with virtual soft fluctuations. The soft fluctuations then emit their own Glauber burst which interacts with the second collinear projectile. The number of Glauber exchanges in this second burst is allowed to be different from the first burst, and the soft sector is *necessary* for transitions between different numbers of Glauber exchanges, as Glaubers do not self interact or otherwise split. An important and useful fact is that transitions of $1 \to N$ or $M \to 1$ are kinematically forbidden for $M, N \neq 1$, and so $S_{(1,N)} = S_{(M,1)} = 0$. This provides some nice simplifications for the rapidity RGEs and analyses of Reggeization.

2.4.3 Rapidity RGE

The Glauber operators match onto the full QCD amplitude, which, other than the usual coupling and wave-function renormalization, does not get renormalized. Moreover, as discussed, Glauber operators do not get corrected by loop-level effects. Therefore the UV RGE is trivial, and the Glauber soft and collinear functions have vanishing μ-anomalous dimensions[10]. However, the collinear and soft matrix elements are rapidity divergent, which leads to a very non-trivial rapidity RGE. In addition to the expected convolutions in transverse momentum space, we can also expect mixing between operators with different numbers of Glauber exchanges.

The collinear functions are renormalized as

$$J^{\mathrm{B}}_{\kappa(M)}(\{\ell_{M\perp}\}; \epsilon, \eta) = \sum_{N} \int_{\perp(N)} J^{\mathrm{R}}_{\kappa(N)}(\{k_{N\perp}\}; \epsilon, \nu) Z_{n(N,M)}(\{k_{N\perp}\}, \{\ell_{M\perp}\}; \epsilon, \eta, \nu). \tag{2.121}$$

[10]The ϵ-dependence in Eq. (6.13) comes from infrared-divergences.

We have introduced the notation for a single Glauber convolution

$$\int_{\perp(N)} = \frac{i^N}{N!} \int \prod_{j=1}^{N} \frac{[d^{d'} k_{j\perp}]}{k_{j\perp}^2} \delta^{d'}(\sum k_{j\perp} - q_\perp). \tag{2.122}$$

Similarly the soft function is renormalized as

$$\begin{aligned} S^{\mathrm{B}}_{(N,M)}(\{\ell_{M\perp}\}, \{\ell'_{M\perp}\}; \epsilon, \eta) = \sum_{I,J} \iint_{\perp(I,J)} & Z_{S(N,I)}(\{\ell_{M\perp}\}, \{k_{M\perp}\}; \epsilon, \eta, \nu) \\ & \times S^{\mathrm{R}}_{(I,J)}(\{k_{M\perp}\}, \{k'_{M\perp}\}; \epsilon, \nu) Z_{S(J,M)}(\{k'_{M\perp}\}, \{\ell'_{M\perp}\}; \epsilon, \eta, \nu). \end{aligned} \tag{2.123}$$

Given that this is rather cumbersome to write out (and read) explicitly, we often just use the convolution symbol instead. With this, the bare functions may be compactly written as

$$\begin{aligned} J^{\mathrm{B}}_{\kappa(M)} &= \sum_{N} J^{\mathrm{R}}_{\kappa(N)} \otimes Z_{n(N,M)}, \\ S^{\mathrm{B}}_{(N,M)} &= \sum_{I,J} Z_{S(N,I)} \otimes S^{\mathrm{R}}_{(I,J)} \otimes Z_{S(J,M)}. \end{aligned} \tag{2.124}$$

By the consistency of the rapidity RGE, we have the following relation between the soft and collinear counterterms:

$$Z_{n(I,J)} = Z^{-1}_{S(I,J)}, \tag{2.125}$$

where the inverse is both on the convolutional space, as well as a matrix inverse on indices (I, J). Given the above relation, we will generally drop the n and S labels on the counterterms altogether. The RGEs straightforwardly follow, and we have

$$\begin{aligned} \nu \frac{\partial}{\partial \nu} J_{\kappa(i)} &= \sum_{j=1}^{\infty} J_{\kappa(j)} \otimes \gamma_{(j,i)}, \\ \nu \frac{\partial}{\partial \nu} S_{(i,j)} &= -\sum_{k=1}^{\infty} \gamma_{(i,k)} \otimes S_{(k,j)} - \sum_{k=1}^{\infty} S_{(i,k)} \otimes \gamma_{(k,j)}, \\ \nu \frac{\partial}{\partial \nu} \bar{J}_{\kappa'(i)} &= \sum_{j=1}^{\infty} \gamma_{(i,j)} \otimes \bar{J}_{\kappa'(j)}, \end{aligned} \tag{2.126}$$

where the anomalous dimension is defined as

$$\gamma_{i,j} = -\sum_{k} \left(\nu \frac{d}{d\nu} Z_{n(i,k)} \right) \otimes Z^{-1}_{n(k,j)}. \tag{2.127}$$

The fact that the same anomalous dimension appears in both the soft and the collinear

RGEs follows from the consistency condition in Eq. (2.62). Symmetry of the EFT under $n \to \bar{n}$ also further implies that the anomalous dimensions matrices are symmetric, i.e. $\gamma_{(i,j)} = \gamma_{(j,i)}$.

A consequence of the vanishing of $S_{(1,N)}$ and $S_{(N,1)}$ is that the counterterms $Z_{(1,N)}$ and $Z_{(N,1)}$, as well as the anomalous dimensions $\gamma_{(1,N)}$ are also zero. This immediately implies that the RGE for the one-Glauber operator does not mix with any other operators in the EFT. Moreover, from definition of the Glauber convolution Eq. (2.122), we can see that this RGE is actually multiplicative, since the one momentum integral gets eaten up by the delta function: $\int_{\perp(1)} = i/q_\perp^2$. It is conventional to absorb these overall factors into the definitions of the soft function $S_{(1,1)}$ and the anomalous dimension, and the rapidity RGE becomes

$$\nu \frac{\partial}{\partial \nu} J_{\kappa(1)} = \gamma_{(1,1)} J_{\kappa(1)}. \tag{2.128}$$

We can easily solve this, since rapidity divergences are only ever singly logarithmic. Running from the collinear rapidity scale at $\nu = p_2^+ = \sqrt{s}$ down to the soft rapidity scale at $\nu = \sqrt{-t}$, we have

$$J_{\kappa(1)}(\nu = \sqrt{-t}) = \left(\frac{s}{-t}\right)^{-\gamma_{(1,1)}/2} J_{\kappa(1)}(\nu = \sqrt{-s}). \tag{2.129}$$

This is precisely the statement of Reggeization. In the absence of soft radiation, the one Glauber operator generates a single t-channel pole, which gets dressed with the exponentials from the ν-running. Comparing Eq. (2.76) with Eq. (2.129) (and including the $\bar{n}$-collinear running as well), we can make the identification of the Regge trajectory with $\gamma_{(1,1)}$

$$\alpha_R(t) = -\gamma_{(1,1)}. \tag{2.130}$$

Although the naive definition of gluon Reggeization in Eq. (2.76) breaks down at NNLL, Eq. (6.33) provides a very clean and natural definition for gluon Reggeization at all orders in perturbation theory. More importantly, this definition is manifestly gauge-invariant, as the Regge trajectory is shown to be a anomalous dimension of a gauge-invariant operator.

Chapter 3

Unitarity, Anomalous Dimensions, and All That Part I

3.1 Introduction

Canonical perturbation theory inadequately describes field theories when dimensionful parameters form large hierarchies that lead to numerically large logarithms. Typically, perturbation theory can be salvaged by re-summing these logs using the renormalization group (RG) which takes advantage of the invariance of physical quantities under the change in subtraction scales. There exists another class of logs, which may be with associated with IR divergences, that are not immediately summable by naive RG methods. For instance, often we run into logs whose argument involves a mass(es), e.g. $\ln(p^2/M^2)$. These logs *may* be summable using the RG if the masses are acting as "intermediate" scales, in the sense that there is some physical IR scale below the scale of the mass. In such cases one can work within an EFT and integrate out the mass. Below the mass scale the IR divergences get converted to a UV divergence and the logs become amenable to canonical RG methods. Effectively what this process amounts to is encapsulated in the following relation

$$\ln(p^2/M^2) = \ln(p^2/\mu^2) - \ln(M^2/\mu^2) \tag{3.1}$$

where the *RG* scale μ, is taking on double duty as both the invariant mass factorization and RG scales. Any log which is summable by RG can be considered an invariant mass log, as the RG flow corresponds to a Wilsonian flow in the invariant mass [1]. Notice that the RG is a manifestation of factorization. That is, the RG scales distinguishes between low

[1] It is important to emphasize here that the logs of interest in this paper are only large when working in Minkowskian signature.

and high virtuality modes such that an amplitude can be written as a product

$$\mathcal{M} = H(Q,\mu)S(p_i,\mu) \tag{3.2}$$

where Q is the short distance (hard) scale and p_i are the small momenta. The log of the mass in Eq. (3.1) goes into the hard function while the other log is part of the soft. This is nothing more than an operator product expansion. The key point we are reviewing here is that the logs are summable because amplitudes factorize in invariant mass.

The RG anomalous dimension is determined by calculating the UV poles arising from operator insertions and following the Feynman rules from a given Lagrangian. Reference [49] noted that the RG anomalous dimensions could be calculated using unitarity/on-shell methods that have facilitated modern higher order radiative corrections. They showed that the RG anomalous dimensions are intimately related to the phase of the S-matrix, essentially as a consequence of the fact that the imaginary part of the amplitude is the discontinuity in logarithms. A general log in an amplitude relates the large log to the phase via

$$A\ln\left(-q^2/m^2 - i\epsilon\right) = A\ln\left(q^2/m^2\right) - iA\pi. \tag{3.3}$$

This fact is, not only formally interesting, but also leads to technical simplifications as unitarity methods can be used to effectively "gain a loop" in the sense that one can calculate using cut diagrams [49]. This method was used to simplify two loop SMEFT anomalous dimensions in [29, 84]. This relation between cuts and logs in scattering amplitudes was used in the past by the Russian school to calculate fixed order logs, see e.g. [87].

However, the method in [49] does not address the issue of rapidity logs since it utilizes the variation of matrix elements under scale transformations and, in the full theory, rapidity logs (such as in Eq. (6.21)) are independent of μ. In this paper we show that one can extract the rapidity logs and their associated anomalous dimensions by generalizing the ideas in [49] and replacing the dilatations utilized in their derivation by an special type of complex boosts, once the amplitude is properly factorized into soft and collinear sectors.

At first sight it might seem strange to relate the phase of the S-matrix to the anomalous dimensions, as surely such a relation cannot hold for a general process. If we consider a semi-classical approximation, for instance, the phase will correspond to the classical action

$$\mathcal{M}_{SC} \sim e^{iS_{cl}}, \tag{3.4}$$

which is not related to any RG anomalous dimension [2]. However, for the canonical semi-classical scattering process of near forward, or eikonal scattering, the amplitude is charac-

[2]The RG anomalous dimensions is associated with the hard quantum contribution, as discussed below.

terized by large rapidity logs of the form $\log(s/t)$, which are controlled by the RAD, which in this case, is called the "Regge trajectory" and is related to the phase. In fact, it has been known for a long time that the Regge trajectory can be calculated from the phase of the S-matrix in planar Yang-Mills theory[120], and moreover, can be calculated exactly within the BDS ansatz [28] of $N = 4$ SUSY [147]. The phase contains both classical as well as quantum mechanical contributions, the latter of which is related to the RAD. In this paper we will not be discussing the case of Regge Logs as they necessitate a slightly different formalism that the one introduced here. Here will discuss the Regge trajectory calculation in a forthcoming publication [154].

In this chapter we will be focusing processes for which there is a hard scattering. We show how unitary can be used to extract RAD at the two loop level in two distinct cases. The simplifications which arise using this phase/RAD relation are two-fold, as we will demonstrate: It simplifies the integrals as the phase arises due to the contribution from gluons whose momentum resides in the Glauber region where $k^\mu \sim (0, 0, k_\perp)$ in light cone-coordinates. Expanding around this region trivializes many of the integrals. Moreover, after expanding around the Glauber region, the integrals are all finite in dimensional regularization, as no rapidity divergences arise, since the anomalous dimensions are rapidity finite. Thus, there is *no need to introduce a rapidity regulator* that can complicate higher loop calculations[3].

This chapter is structured as follows. First, we review the results in [49] showing how the phase of the (hard part) of the S-matrix can be used to extract the RG anomalous dimensions for observables. The generalization of these results to the case of rapidity anomalous dimensions follows once the factorization is proven, which is accomplished by invoking the Soft Collinear Effective Theory (SCET)[18, 17, 20]. Once we have established a relationship between the phase and the RAD, we illustrate the use of the formalism in two examples. First for a local operator, the Sudakov form factor and then for a non-local operator, the two parton transverse momentum soft function. This chapter is based on the paper [156].

[3]It should be mentioned that this statement is true only after summing over all contributions to a given process; individual Feynman diagrams can still be rapidity divergent as will be seen in the explicit calculations. Moreover, the form factor itself can be rapidity divergent, but it is straightforward to account for iterative terms which build up the form factor. Alternatively, one may work entirely in the full theory, where no rapidity divergences ever appear.

3.2 The Master Formulae

3.2.1 The RG Master Formula

Reference [49] derives a relation between the S-matrix phase and the RG anomalous dimension. One starts by considering a generic form factor [4]

$$\mathcal{F}(p_1...p_n) = \int d^d x e^{-iq\cdot x} \ {}_{out}\langle p_1...p_n \mid F(x) \mid 0\rangle_{in} \tag{3.5}$$

where we will take all states outgoing in this way all of the invariants will be postive. This choice ensures that all the invariants are positive. Consider the action of the following complex dilatation (D) on this form factor

$$e^{iD\pi}\mathcal{F}(p_1...p_n) = \mathcal{F}(-p_1... - p_n) = \int d^d x e^{-iq\cdot x} \ {}_{out}\langle 0 \mid F(x) \mid \bar{p}_1...\bar{p}_n\rangle_{in} \tag{3.6}$$

where in the last line we utilized crossing symmetry and bar denotes the anti-particle. It follows that

$$e^{iD\pi}\mathcal{F}(p_1...p_n) = \int d^d x e^{-iq\cdot x} \ {}_{in}\langle \bar{p}_1...\bar{p}_n \mid F^\star(x) \mid 0\rangle^\star_{out}. \tag{3.7}$$

Mechanically this transformation returns invariants back to their original form but now on the other side of the cut.

Then inserting $CPT(CPT)^{-1}$ appropriately into the matrix element we have

$$e^{iD\pi}\mathcal{F}(p_1...p_n) = \mathcal{F}(p_1...p_n)^\star. \tag{3.8}$$

Next one treats F as a perturbation to the S-matrix

$$S = S_0 + iF \tag{3.9}$$

such that the unitarity relation $SS^\dagger = 1$ gives

$$S_0F^\dagger - FS_0^\dagger = 0, \tag{3.10}$$

where F^2 terms wont contribute to our matrix elements. Then we have

$$F = S_0F^\dagger S_0. \tag{3.11}$$

Restricting ourselves to the subset of matrix elements with no incoming particles we can

[4] Following the notation in [49], any calligraphic character corresponds to a matrix element and not an operator.

effectively write

$$F = S_0 F^\dagger, \tag{3.12}$$

and using (3.8)

$$e^{-i\pi D}\mathcal{F}^\star = \mathcal{S}\mathcal{F}^\star. \tag{3.13}$$

Or in words: the anomalous dimensions equals the phase of the S-matrix. Now to make this result more user friendly one writes the S-matrix element as $\mathcal{S} = 1 + i\mathcal{M}$. Expanding (3.13) to first order in perturbation theory

$$-\pi\gamma_\mu^{(1)}\mathcal{F}^{(0)\star} = \mathcal{M}^{(0)}\mathcal{F}^{\star(1)} + \mathcal{M}^{(1)}\mathcal{F}^{\star(0)}, \tag{3.14}$$

where γ_μ is the anomalous dimensions of F. Since the RHS corresponds to a matrix equation, we can consider any set of intermediate states between $\mathcal{M}$ and $\mathcal{F}^\star$. As emphasized in [49], this result needs to be refined due to the existence of "IR anomalous dimensions" ($\gamma_{\rm IR}$), which corresponds to μ dependence introduced when regulating IR divergences. So to extract γ one must mod out by the appropriate matrix elements which capture the IR divergences. It is important to emphasize that $\gamma_{\rm IR}$ is not related in any way to the rapidity anomalous dimensions. In the language of EFT, the relation (3.14) applies to the hard matching coefficients.

3.2.2 The Rapidity Anomalous Dimensions Master Formula

We now wish to generalize the RG formalism to the RRG case which follows once one uses the intuition gained from the work in [54] on the RRG. In the case of RAD, the relevant generator becomes K_z, the boost generator in the $\hat{z}$ direction, instead of dilatations, D. However, it **is not** the canonical boost in the following sense. We notice from (6.21) that if we want to move the singularity in the rapidity logs to the other side of the cut, as in the case of the invariant mass logs, we will need to boost the large $\pm$ light-cone momenta separately and independently, which is obviously not a symmetry of the action. This can be implemented by boosting each collinear sector separately:

$$\begin{aligned} p_n^\mu &= (p_n^+,\, p_n^-,\, p_\perp^\mu) \to (e^\gamma p_n^+,\, e^{-\gamma} p_n^-,\, p_{n\perp}^\mu) \\ p_{\bar{n}}^\mu &= (p_{\bar{n}}^+,\, p_{\bar{n}}^-,\, p_{\bar{n}\perp}^\mu) \to (e^{-\gamma} p_{\bar{n}}^+,\, e^{\gamma} p_{\bar{n}}^-,\, p_{\bar{n}\perp}^\mu). \end{aligned} \tag{3.15}$$

Using this operation we are able to transform $p_\mu \to -p_\mu$ by choosing $\gamma = i\pi$, and by furthermore rotating by π around the $\perp$ direction. For each sector this rotation will act trivially on the amplitude since each sector is invariant under rotations along the jet axis

[5]. This modified transformation, whose generator we denote as $\bar{K}_z$, acts as follows

$$e^{i\pi\bar{K}_z}\mathcal{F}(p_1,...,p_n) = \mathcal{F}(-p_1,...,-p_n) = \mathcal{F}^\star(p_1,...,p_n), \tag{3.16}$$

The modified boost generator acts only on the collinear sectors' momenta along the lightcone directions, so we may make the identification

$$\bar{K}_z \equiv \sum_{i=n,\bar{n}} K_z^i, \tag{3.17}$$

where K_z^i is the boost in the ith collinear sector's z-direction,

$$\begin{aligned} K_z^n &= \sum_{\{p_j\in n\}} \left(p_j^+ \frac{\partial}{\partial p_j^+} - p_j^- \frac{\partial}{\partial p_j^-} \right), \\ K_z^{\bar{n}} &= \sum_{\{p_j\in \bar{n}\}} \left(p_j^- \frac{\partial}{\partial p_j^-} - p_j^+ \frac{\partial}{\partial p_j^+} \right). \end{aligned} \tag{3.18}$$

Dependence on $p_\pm$ only appears in rapidity logarithms $\ln \mid p_i^\pm \mid /\nu$ in the collinear functions, where the absolute value follows from the definition of the regulator. Therefore, when operating on the these functions we may make the replacement

$$\bar{K}_z \simeq -\nu\frac{\partial}{\partial\nu}. \tag{3.19}$$

Using the rapidity RGE equation

$$\nu\frac{\partial}{\partial\nu}O_{n/\bar{n}} = \gamma_\nu^{n/\bar{n}} J_{n/\bar{n}}, \tag{3.20}$$

we have

$$\bar{K}_z\, J_{n/\bar{n}} = -\gamma_\nu^{n/\bar{n}} \otimes J_{n/\bar{n}}. \tag{3.21}$$

Thus we can write

$$\begin{aligned} e^{i\pi\bar{K}_z}\mathcal{F} &= \left(e^{i\pi\bar{K}_z} J_n\right) \otimes \mathcal{S} \otimes \left(e^{i\pi\bar{K}_z} J_{\bar{n}}\right), \\ &= e^{-i\pi(\gamma_\nu^n+\gamma_\nu^{\bar{n}})\otimes} J_n \otimes \mathcal{S} \otimes J_{\bar{n}}, \\ &= e^{i\pi\gamma_\nu^s\otimes}\mathcal{F}., \end{aligned} \tag{3.22}$$

[5]We are not considering observables which may be sensitive to the angle between transverse momenta in differing jet directions, when there are more than two.

where we have introduced the notation

$$e^{a\otimes}b = b + a\otimes b + \frac{1}{2!}a\otimes a\otimes b + ... \tag{3.23}$$

Now we use unitarity just as in the RG case to write

$$e^{-i\pi(\gamma_\nu^n+\gamma_\nu^{\bar{n}})\otimes}\mathcal{F}^\star = \mathcal{S}\mathcal{F}^\star = (1+i\mathcal{M})\mathcal{F}^\star. \tag{3.24}$$

From here on out, we will drop the convolution as all further discussion and example do not rely on its (non)presence, but it is to be understood that it is present as necessary.

It is worth going into the details of this result in the context of the effective theory. The rapidity regulator is defined such that the arguments of the logs involve $\mid p_\pm \mid$, and given that $p_\pm$ are defined to be large, the action of $-p_\pm\frac{\partial}{\partial p_\pm}$ will simply yield $- \mid p_\pm \mid$. Thus the action of the exponentiated generator will yield the phase, as shown in the previous equation, and thus $J(-p) \neq J^\star(p)$. On the other hand, we know that the action on the entire form factor should result in a conjugation, implying that the soft function contains a phase such that

$$J_n(-p)J_{\bar{n}}(-p)S = e^{i\pi\gamma_\nu^s}J_n(p)J_{\bar{n}}(p)S = (J_n(p)J_{\bar{n}}(p)S)^\star = (J_n(p)J_{\bar{n}}(p)S^\star), \tag{3.25}$$

since J is real. We may conclude that

$$S^\star = e^{i\pi\gamma_\nu^s}S. \tag{3.26}$$

This is a useful result since it means that we can calculate γ_ν using the master formula Eq. (3.24) by only considering soft graphs, via the replacement of $\mathcal{F}$ with S. Physically this result is a result of the fact that the phase of the amplitude comes from the soft region (determined by the direction of the Wilson line).

An obvious question which arises is, is it the RG anomalous dimension or the RAD which is related to the phase of the S-matrix? The answer is that the phase of the hard scattering piece gives the RG while the phase of the IR piece gives the RAD [6]. As previously emphasized since when we calculate we include all of the modes, we could just as well calculate in the full theory, but if we do so we must still subtract out the hard piece, which is typically a simpler calculation since it involves integrals with fewer scales.

Another important distinction from the RG case is the fact that in SCET the imaginary part is divergent, as phase space is unbounded due to the use of the multipole expansion which is necessitated by the power counting [100], and we must amend Eq.(3.13) to account

[6] Since IR divergences are independent of ν they will not pose any obstruction.

for this fact. Defining the renormalized operator

$$F^R = Z_F^{-1} F^B, \tag{3.27}$$

we have to revisit the result (3.12)

$$F = S_0 F^\dagger, \tag{3.28}$$

which leads to [7]

$$\mathcal{F}_B = \mathcal{S}_0 \frac{Z_F}{Z_F^\star} \mathcal{F}_\mathcal{B}{}^\star. \tag{3.29}$$

Then writing $S_0 = 1 + iM$ we have

$$e^{i\pi\gamma_\nu^s} \mathcal{F}^{\star B} = \frac{(Z_F^\star)^{-1}}{Z_F^{-1}} \mathcal{F}^{\star B} + i\mathcal{M}\mathcal{F}^{\star B} \frac{(Z_F^\star)^{-1}}{Z_F^{-1}}. \tag{3.30}$$

Expanded to one loop order, this gives

$$\gamma_\nu^{s(1)} \mathcal{F}^{\star(0)} = \frac{1}{\pi} \left((\mathcal{M}\mathcal{F}^\star)^{(1)} - 2\mathrm{Im}[Z_F^{-1}]^{(1)} \mathcal{F}^{\star(0)} \right). \tag{3.31}$$

3.2.3 Calculating in the Full Theory Versus the Effective Theory

The result (3.30) was derived within the EFT where the hard part (H) had already be removed. To work in the full theory we must repristinate H and allow for it to be complex. This is a trivial exercise with the result being that the new master formula is

$$e^{-i\pi\gamma_\nu^s} F^{R*} = \frac{H^\star}{H} S \otimes F^{R*}, \tag{3.32}$$

leaving

$$\gamma_\nu^s = \frac{i}{\pi} \log \left[\frac{H^\star}{H} \left(1 + i \sum_X \frac{\langle \psi_f \mid X \rangle \langle X \mid F^{R*} \mid 0 \rangle}{\langle \psi_f \mid F^{R*} \mid 0 \rangle} \right) \right]. \tag{3.33}$$

This amendment to the EFT formula acts to remove any phase that might be generated by the hard part and is not relevant to the RAD. It is important to note that in this paper we will be doing all of our calculations in the effective theory. We have included the result (3.33) for those who would prefer to work in the full theory.

There are several advantages to working in the full theory. One can use the amplitudes tool box to skip having to write down Feynman diagrams. Furthermore, and perhaps more importantly, there may be no need to introduce a rapidity regulator which can lead to both nettlesome integrals as well as calculational subtleties. At the same time it is also true

[7] The distinction between F and $\mathcal{F}$ become murky in the EFT as the operators are tailored to the states in a very specific way.

that the effective theory one need not regulate the rapidity divergences since we know that the RAD is finite. However, to remove the rapidity regulator we would need to combine integrands coming from various diagrams. The EFT calculation is also simplified by the fact that we only need to calculate soft graphs.

On the flip side, in the full theory integrals are in general more difficult, though given the library of known integrals this may be an irrelevant fact. In the EFT one draws all possible Feynman diagrams, of which, there can be many since the theory is modal, i.e. split into regions. However, as we have discussed above, one need only concern oneself with the soft sector. In cases where the rapidity anomalous dimension is IR finite, we may simply ignore scaleless integrals. This is not the case when calculating RG anomalous dimensions where typically we would need to split such integrals into UV and IR pieces. Thus whether one chooses to work in the full or effective theory is a matter of convenience/taste.

3.2.4 The structure of iterations

Formula Eq.(3.12) has some interesting properties when we consider its expansion in the coupling as it contains redundant information. Consider the expansion of Eq.(3.12)

$$e^{i\gamma_s^\nu \pi} S^{R*(2)} = S^{R*(2)} + i\pi \left(\gamma_s^{\nu(1)} S^{R*(1)} + \gamma_s^{\nu(2)} S^{R*(0)}\right) - \frac{\pi^2}{2}(\gamma_s^{\nu(1)})^2 S^{R*(0)} + ... \qquad (3.34)$$

where here, for the sake of illustration we focus only on the terms which are second order in the coupling. $S^{R*(n)}$ is the $n'th$ order contribution to the soft function. All of the terms aside from the one proportional to the target $\gamma_s^{\nu(2)}$ are Abelian in the sense that they are scale as C_F^2 and can be considered redundant information that need not be calculated. That these terms cancel in the extraction of $\gamma_s^{\nu(2)}$ is a manifestation of non-Abelian exponentiation [139, 96], which states, effectively, that the sum of the graphs for the product of any number of Wilson lines will exponentiate [95] at the level of diagrams where the only diagrams that contribute are those that are within a "web" at a given order in the coupling. In the case of two Wilson lines, as for the Sudakov form factor, a web consists of diagrams which are two particle eikonally irreducible in that they can not be disconnected by cutting the two Wilson lines. At the order we are working webs will always have color weights which are linear in C_F which is sometimes called"maximally-non-Abelian". Anomalous dimensions for Wilson line operators will always consist solely of webs, given that the coupling is independent of the rapidity scale ν and thus the solution to the RRG is always a simple exponential.

It is worthwhile to understand how the non-web pieces cancel in the result for $\gamma_s^{\nu(2)}$.

The RHS of the Eq. (3.12) has a second order contribution of the form

$$(\frac{Z_S^\star}{Z_S}\mathcal{S}\otimes S^{R*})_{(2)} = (\frac{Z_S^\star}{Z_S}(1+iM)\otimes S^{R*})_{(2)} = S^{R*(2)}+(\frac{Z_S^\star}{Z_S})_{(1)}\, S^{R*(1)}+iM_{(1)}\otimes S^{R*(1)}+iM_{(2)}S^{R*(0)}. \tag{3.35}$$

Equating Eq.(3.34) and Eq.(3.35) we find

$$i(\gamma_s^{\nu(1)}(S^{R*(1)})+\gamma_s^{\nu(2)}S^{R*(0)})\pi-\frac{\pi^2}{2}(\gamma_s^{\nu(1)})^2S^{R*(0)} = iM_{(1)}\otimes S^{R*(1)}+i(M_{(2)}S^{R*(0)})_{sub}, \tag{3.36}$$

where the counter-terms have been used to subtract the UV divergences from the final term on the RHS. Once we accept that $\gamma_s^{\nu(2)}$ has a maximally non-Abelian structure, and we utilize the fact that all of the other terms on the LHS are NOT maximally non-Abelian, we may simply discard all of the C_F^2 pieces of the RHS to extract $\gamma_s^{\nu(2)}$.

An obvious question arises when one consider that the unitarity method, originally designed to calculate RG logs, leads to an equation of the exact same form as Eq. (3.33). Why are the RG logs not also strictly given by webs? The answer is that when one applies (3.33) in the RG case it is applied to the hard piece only, whereas as we are actually excising the hard piece from the full theory result. Furthermore, non-Abelian exponentiation has only been proven to apply to Wilson line observables, but our methods are more general than that. In the next chapter we will apply these techniques to the case of forward scattering where the collinear lines do not eikonalize.

3.3 The Sudakov Form Factor

As our first example we consider Sudakov form factor which involves one IR (a mass) and one UV scale (Q) and has the interesting property of containing double logarithms at each loop order which dominate its asymptotic behavior. As usual to extract that anomalous dimensions we consider all out-going particles, i.e. we will be considering this form factor in the time-like $Q^2 > 0$ region. The double logs arise from overlapping soft and collinear divergences, and since the virtuality of the relevant modes (soft and collinear) are the same the result includes a rapidity divergence. The resummation of these logs is an ancient subject (see for instance [58]) upon which we hope to shed some new light as using our methodology can greatly simplify higher order computations. We will be considering two distinct ways of representing the IR scale, by giving the gluon or quarks a mass. The massive gluon is in some sense the simpler case since the mass cuts off all IR divergences, but is not terribly useful beyond one loop, since beyond that order we lose gauge invariance unless we are willing to Higgs the theory. It would in fact be interesting to use the techniques introduced here to calculate higher order corrections to the electroweak Sudakov form factor

[56, 55], but this goes beyond the scope of this paper. On the other hand, using a quark mass has the advantage of maintaining gauge invariance at all orders but needs dimensional regularization to handle the soft IR divergences. This form factor is not physical, since it is not IR safe, but in the case of the massive quark it is possible to generate a physical result by introducing a theory below the scale of the mass which will absorb the IR divergences into long distance matrix elements [92].

3.3.1 The Massive Gluon Sudakov Form Factor (MGFF)

Let us now calculate the one loop value for γ_ν^S using our master formula Eq.(3.31). We are interested in the matrix element of the soft function that appears in the Sudakov form factor which is given by the product of two soft Wilson lines

$$S \equiv S_n S_{\bar{n}}^\dagger \tag{3.37}$$

where in position space we have

$$S_n = P e^{ig\int_0^\infty d\lambda A(\lambda n)\cdot n d\lambda}. \tag{3.38}$$

Using our master formula we are interested in the matrix element

$$\langle p_1^n p_2^{\bar{n}} \mid (\mathcal{M}S^\star)^{(1)} \mid 0\rangle = \sum_X \langle p_1^n p_2^{\bar{n}} \mid \mathcal{M} \mid X\rangle\langle X \mid S^{\star(1)} \mid 0\rangle, \tag{3.39}$$

where, as previously discussed we need only concern ourselves with the soft piece to extract the RAD. The intermediate state must involve both n and $\bar{n}$ (eikonlized) partons, i.e.

$$\sum_X \to \sum_x \mid p_3^n p_4^{\bar{n}} + x\rangle\langle p_3^n p_4^{\bar{n}} + x \mid . \tag{3.40}$$

As we have emphasized it is the Glauber region of the softs that generates the phase. So we include the Glauber operator in our action [8] . The soft contribution will not contribute to the phase once we perform the zero-bin subtraction. Returning to Eq.(3.31), we see that

[8]The reader might be bothered by the fact that the Glauber operator includes fermionic fields and the soft function has not such field with which to contract (i.e. its a pure Wilson line). But this is just a technical misdirection as it is simple to just replace soft exchanges by Glauber exchanges.

there is only one diagram with a non-vanishing cut and it is given by

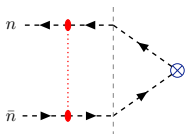

$$= 2i\frac{\alpha_s}{\pi}C_F\,\bar{\mu}^{2\epsilon}\int[d^dk]\frac{(\bar{n}\cdot p')\,n\cdot p}{k_\perp^2+M^2}$$

$$\times\,\delta_+(n\cdot p\bar{n}\cdot k-k_\perp^2)\delta_+(\bar{n}\cdot p' n\cdot k+k_\perp^2). \tag{3.41}$$

We can also see that the $k_\perp$ integral is UV divergent. This is not too surprising, since as previously mentioned, the phase-space integrals in the effective theory are often divergent due to the multipole expansion. Performing the integral, we find

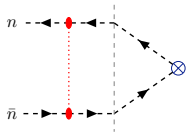

$$= iC_F\alpha_s\,\bar{\mu}^{2\epsilon}(4\pi)^\epsilon\Gamma(\epsilon)M^{-2\epsilon},$$

$$= iC_F\alpha_s\left[\frac{1}{\epsilon_{\rm UV}}+\ln\frac{\mu^2}{M^2}\right]. \tag{3.42}$$

We must also include the counter-term piece in Eq. (3.31), but, by construction, the imaginary part of the counter-term is nothing more than the negative of the divergent part of Eq.(3.39), so there is no need to perform any calculation, one may simply drop the divergent part of Eq.(3.39). Nonetheless as a check we may extract the counter-term from the full SCET (all sectors) one loop correction to the current. The imaginary part of the Sudakov form factor soft function one-loop counter-term is given by

$$\mathrm{Im}\left[Z_F^{-1}\right] = -\frac{\alpha_s C_F}{2\epsilon_{\rm UV}}. \tag{3.43}$$

Using the master formula (3.31) in conjunction with (3.42), we obtain a finite result, and we deter- mine the RAD to be

$$\gamma_\nu^s = \frac{C_F\alpha_s}{\pi}\ln\frac{M^2}{\mu^2}. \tag{3.44}$$

Which agrees with the standard result for the soft RAD [54] for the massive gluon Sudakov form factor.

3.3.2 The Massive Quark Sudakov Form Factor (MQFF)

The inclusion of a quark mass avoids the gauge invariance issue, however at one loop the relevant integral is scaleless and technically vanishes. However after separating and UV and

IR divergences we can write

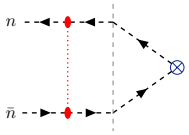

$$= iC_F\alpha_s\,\bar{\mu}^{2\epsilon}\int_0^\infty \frac{d^{2-2\epsilon}k_\perp}{k_\perp^2}$$

$$= iC_F\alpha_s(\frac{1}{\epsilon_{\rm UV}} - \frac{1}{\epsilon_{\rm IR}}). \tag{3.45}$$

including the counter-term piece we find

$$\gamma_\nu^s = \frac{\alpha_s C_F}{\pi}\frac{1}{\epsilon_{\rm IR}}, \tag{3.46}$$

which agrees with result derived using the canonical method. As a check we can see that integrating the equation for the soft function

$$dS = \gamma_\nu^s S(d\ln\nu) \tag{3.47}$$

by taking $S = 1$ on the RHS we reproduce the term $\frac{\alpha_s C_F}{\pi}\frac{1}{\epsilon_{\rm IR}}\ln(Q/m)$ in the full theory result[104].

3.3.3 Massive Quark Form-Factor at Two Loops

The RAD of the Sudakov form factor with massive matter lines has two incarnations. If there is no IR scales below the quark mass then the form factor is an IR divergent quantity, as is its RAD. This is the case discussed in the previous section. In more physical cases, there is an IR scale below the mass (typically the QCD scale) and all IR divergences get absorbed into a non-perturbative low energy matrix element. This latter version, which we will focus on in this paper, is relevant e.g., for resummations in boosted top quark production and was first calculated in [104], where a dispersive techniques was utilized to circumvent the need to regulate the IR using a gluon mass which breaks gauge invariance beyond one loop. Here we demonstrate that we can extract the RAD by direct calculation by use of Eq. (3.33) without any reference to a gluon mass. The one loop contribution shown in figure (1) is scaleless and given by

$$(1) = -i\alpha_s C_F\left(\frac{1}{\epsilon_{UV}} - \frac{1}{\epsilon_{IR}}\right). \tag{3.48}$$

The UV divergence will be killed by the counter-term for the current and the IR divergence will be dropped since it will be factorized into a low energy matrix element. Thus ($\gamma_s^{(1)\nu} = 0$). As a consequence of this fact, all of the iterative terms in (3.36) vanish.

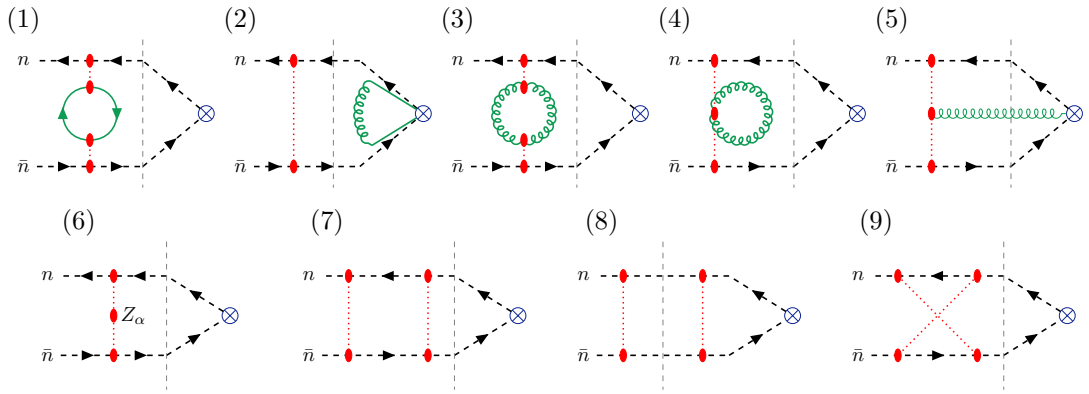

Figure 3.1: Cut diagrams contributing to the 2-loop Sudakov RAD. Greens lines are soft (zero-bin subtracted) while dotted are Glauber. All of the diagrams are scaleless except for the first.

Figure one shows all the diagrams that arise at $O(\alpha^2)$. All of the diagrams are are scaleless save for figure (1) where the massive quark is running through the loop. We conclude that we can read off the anomalous dimension at two loops from diagram,

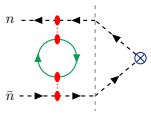

$$= 64\pi^2 C_F\, T_F\, S_\Gamma \int \frac{\bar{\mu}^{4\varepsilon}\, đ^{d-2}k_\perp\, đ^d q}{(q^2-m^2)\left((q+k_\perp)^2-m^2\right)(k_\perp^2)^2} \mathrm{tr}\left[(\not{q}+\not{k}_\perp+m)\frac{\not{n}}{2}(\not{q}-m)\frac{\not{\bar{n}}}{2}\right],$$

$$= i\frac{C_F\, T_F\, \alpha_s^2}{\pi}\frac{\Gamma(2\varepsilon)\Gamma(2+2\varepsilon)^2}{\varepsilon\,\Gamma(4+2\varepsilon)}\left(\frac{\mu^2}{m^2}\right)^{2\varepsilon}, \tag{3.49}$$

$$= i\pi\, C_F\, T_F\, \frac{\alpha_s^2}{\pi}\left(-\frac{1}{6\varepsilon^2}-\frac{1}{3\varepsilon}\log\frac{\mu^2}{m^2}+\frac{5}{18\varepsilon}-\frac{1}{3}\log^2\frac{\mu^2}{m^2}+\frac{5}{9}\log\frac{\mu^2}{m^2}-\frac{\pi^2}{36}-\frac{14}{27}\right).$$

This integral can be evaluated by evaluating the q-integral first before the $k_\perp$-integral; this is recursively one-loop and can be handled by, e.g. Feynman parameters.

We can extract that RAD by dropping all the poles, since the counter-term contribution assures us of a UV finite result, and the previous argument above permits us to drop the IR divergent pieces. Thus we are left with

$$\gamma_\nu^s = C_F\, T_F\, \frac{\alpha_s^2}{\pi^2}\left(-\frac{1}{3}\log^2\frac{\mu^2}{m^2}+\frac{5}{9}\log\frac{\mu^2}{m^2}-\frac{\pi^2}{36}-\frac{14}{27}\right). \tag{3.50}$$

By keeping the quark masses in the loops and using $\overline{MS}$ we are inherently working in a non-decoupling (ND) scheme. It is therefore prudent to change back to the usual EFT/$\overline{MS}$ scheme where the quarks are taken to be massless. The relation between these schemes is

[51]

$$\alpha_s^{ND} = \alpha_s(1 + (\Pi(m^2, 0) - \frac{\alpha_s}{3\pi}\frac{T_F}{\epsilon})). \tag{3.51}$$

where Π is the scalar part of the vacuum polarization at $k = 0$. We must make this replacement in the one loop IR divergent result and subsequently drop all the IR divergent terms. Thus the results will only be sensitive to the $O(\epsilon)$ piece of Π

$$\Pi(m^2, 0)_\epsilon = \frac{\alpha T_F}{3\pi}\epsilon\left(\frac{1}{2}\log^2\frac{\mu^2}{m^2} + \frac{\pi^2}{12}\right), \tag{3.52}$$

The net sum gives for the RAD

$$\gamma_\nu^s = -C_F\, T_F\, \frac{\alpha_s^2}{3\pi^2}\left(\frac{1}{2}\log^2\frac{m^2}{\mu^2} + \frac{5}{3}\log\frac{m^2}{\mu^2} + \frac{14}{9}\right) \tag{3.53}$$

which agrees with the result given in [104]. Note that had we worked with the full IR divergent Sudakov form factor, we would have seen a $C_F C_A$ term as well, with contributions from figures (2-6). Given that these diagrams are scaleless, the $C_F C_A$ term would be pure IR divergence. In the above result, the IR divergences have been absorbed into a low energy matrix element as described in the set-up of this section, leading to only the $C_F T_F n_f$ color structure appearing in the anomalous dimension.

3.4 Form Factors of non-Local Operators: The Soft Function

Next we will apply the unitarity technique to calculate the RAD of a non-local operator. In particular we will consider the soft function that arises in the factorization of a class of hard scattering observables. We will choose one particular operator but the method can be applied more generally. We are interested in operators whose matrix elements include rapidity divergences/logs. As such, we will choose observables whose diagrams include soft and collinear modes of the same virtuality, the classic example of which are differential cross sections where one measures the transverse momentum ($p_\perp$) of some set of particles, with $p_\perp \ll Q$, where Q is the hard scattering scale. Schematically the cross section takes the form

$$\frac{d\sigma}{dp_\perp} = H(Q, \mu)C_n(p_\perp/\mu, n\cdot p/\nu) \otimes C_{\bar{n}}(p_\perp/\mu, \bar{n}\cdot p'/\nu) \otimes S(\mu/\nu, p_\perp/\mu), \tag{3.54}$$

where $\otimes$ denotes a convolution in the momentum variables. $n\cdot p$ and $\bar{n}\cdot p'$ are the incoming light-cone momenta, which are integrated over weighted by PDF's. The collinear pieces are transverse momentum parton distribution functions (TMPDFs) while the soft function is

the vacuum expectation value of Soft Wilson lines in the fundamental representation

$$S(b_\perp) = \frac{1}{N_c}\langle 0 \mid S_n^{ce}(b_\perp;0,\infty)S_{\bar{n}}^{\dagger ed}(b_\perp;0,-\infty)S_{\bar{n}}^{de}(0;0,-\infty)S_n^{\dagger ec}(0;0,\infty) \mid 0\rangle, \tag{3.55}$$

where for convenience we have Fourier transformed to impact parameter space. One can also consider double, or higher, order n-parton scattering in which case the soft function becomes the non-local product of n pairs of Wilson lines with each in a different light cone-direction. The arguments below are easily generalizable beyond the two parton scattering we consider here. In trying to use our unitarity methods however, we are immediately met with the fact that S is a real valued function. We can circumvent this problem by looking at a different matrix element which shares the same RAD. In analogy with what we did for the Sudakov form factor we will consider particle production with four outgoing states. Recall that this step was also necessary to eliminate the factor of S on the left-hand side of Eq.(3.11). A similar calculation was done for the RG anomalous dimensions for parton distributions in [49].

We will consider the matrix element with all out going partons

$$M(b_\perp) = \sum_X \langle p_n \bar{p}_{\bar{n}} q_n \bar{q}_{\bar{n}} \mid X\rangle\langle X \mid \bar{S}(b) \mid 0\rangle. \tag{3.56}$$

The "crossed" Wilson line is then

$$\bar{S}(b_\perp) = \frac{1}{N_c}\langle 0 \mid S_n^{ce}(b_\perp;\infty,0)S_{\bar{n}}^{\dagger ed}(b_\perp;0,-\infty)S_n^{df}(0;\infty,0)S_{\bar{n}}^{\dagger fc}(0;0,-\infty). \mid 0\rangle, \tag{3.57}$$

We have dropped the dependence on $x_\pm$ since the RAD cannot depend upon the parton light-cone momentum fraction. At one loop there are only two diagrams. The diagrams where the Glauber connects partons with the same impact parameter will be scaleless and can be dropped. Furthermore, there are no soft exchanges since they have no cut piece (recall the phase comes from the Glauber piece of the soft) except for self-energy diagrams which vanish. Thus at one loop we have two diagrams which give the identical result:

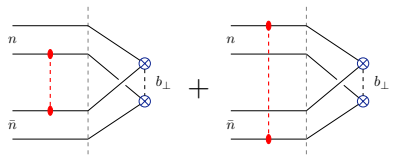

$$\begin{aligned} &= 2i\,g^2 C_F \int \frac{d^{d-2}k_\perp}{k_\perp^2} e^{-ik_\perp\cdot b_\perp} \\ &= 2i\,g^2 C_F \frac{\Gamma(-\epsilon)}{4\pi}(\tilde{b}^2\mu^2)^\epsilon \\ &= -C_F \frac{i\,g^2}{2\pi}\left(\frac{1}{\epsilon} + \ln\left(\tilde{b}^2\mu^2\right) + O(\epsilon)\right), \end{aligned} \tag{3.58}$$

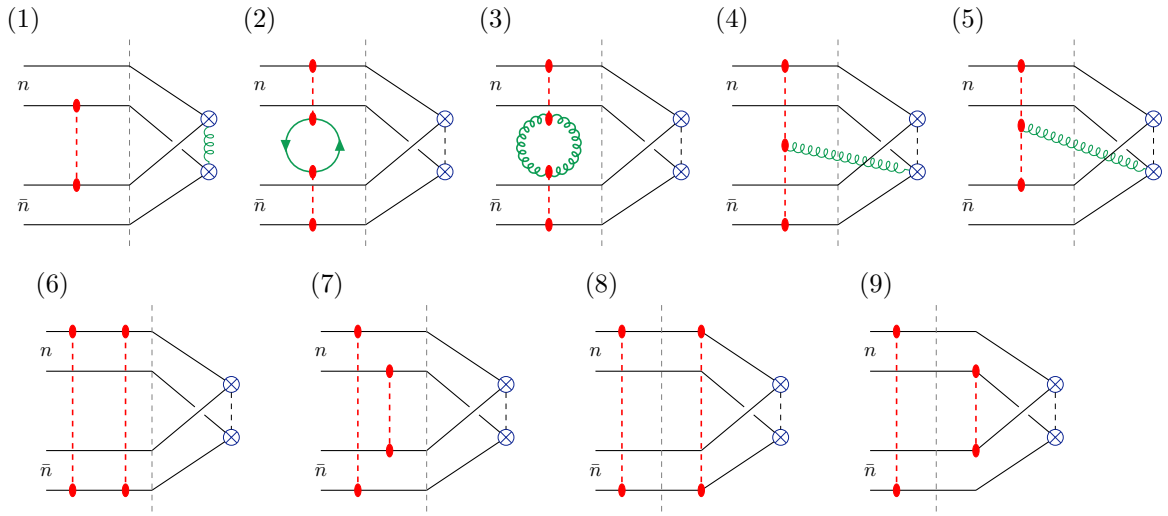

Figure 3.2: 2-loop cut diagrams with soft loops. Diagram (1) is the iterative soft-Glauber graph, diagrams (2) and (3) come from the one-loop amplitude, and diagrams (4) and (5) are the real-emission contributions. Diagrams (7-10) involve two Glauber exchanges, and cancel when summed over. Not shown are the graphs given by taking $n \leftrightarrow \bar{n}$.

with $\tilde{b}^2 = b_\perp^2 e^{\gamma_E}/4$. Dropping the UV divergence, we have exactly the one-loop RAD

$$\gamma_\nu^{s(1)} = \frac{\alpha_s}{\pi}(2C_F)\ln\Big(\tilde{b}^2\mu^2\Big). \tag{3.59}$$

3.4.1 TMD Two-Loop Rapidity Anomalous Dimension

The graphs which contribute at two loops are shown in figure (2). Graph (1) factors into the product of the one-loop soft-graph and the one loop cut:

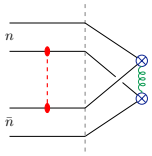

$$= -4g^4 C_F(2C_F - C_A)\int \frac{đ^d k_1 đ^{d-2} k_{2\perp}\left|\frac{2k_1^z}{\nu}\right|^{-\eta}}{k_1^2\,(k_1^+ + i\epsilon)(k_1^- - i\epsilon)\vec{k}_{2\perp}^2} e^{-i\vec{b}_\perp\cdot(\vec{k}_{1\perp}-\vec{k}_{2\perp})},$$

$$= \frac{ig^4\,(C_F^2 - 2C_F C_A)}{16\pi^2}\frac{\Gamma(1/2-\eta/2)\Gamma(\eta/2)\Gamma(-\varepsilon-\eta/2)\Gamma(-\varepsilon)}{2^\eta\pi^{3/2}\Gamma(1+\eta/2)}\frac{(\tilde{b}^2\mu^2)^{2\varepsilon+\eta}}{e^{(2\varepsilon+\eta)\gamma_E}}, \tag{3.60}$$

$$= i(2C_F^2 - C_F C_A)\frac{\alpha_s^2}{\pi}\left[\frac{2\Gamma(-\varepsilon)^2 e^{-\varepsilon\gamma_E}}{\eta}(\tilde{b}^2\mu^2)^\varepsilon - \frac{1}{\varepsilon^3} + \frac{1}{\varepsilon^2}(L_\nu - L_b)\right.$$
$$\left. + \frac{2}{\varepsilon}L_b L_\nu + \frac{2}{3}L_b^3 + 2L_b^2 L_\nu + \zeta(2)(L_b + L_\nu) + \frac{\zeta(3)}{3}\right],$$

with $L_\nu = \log \mu^2/\nu^2$. The C_F^2 term cancels the iteration terms $\gamma_s^{\nu(1)} F^{\dagger(1)} - i\pi/2(\gamma_s^{\nu(1)})^2 F^{\dagger(0)}$ when added to the cut-renormalization $2\mathrm{Im}[Z_F^{-1}]F^{\dagger(0)}$, while the $C_F C_A$ term contributes to the 2-loop rapidity anomalous dimension.

We next consider the diagrams which contain one-loop corrections to the amplitude, which are the soft "eye" and the fermion vacuum polarization graphs. For the fermion vacuum polarization we have

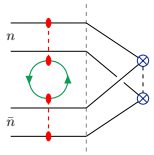

$$= 2g^2 C_F T_F n_f \int \frac{đ^d k_1 đ^{d-2} k_{2\perp}}{\vec{k}_{2\perp}^2 k_1^2 (k_1 + k_{2\perp})^2} \mathrm{Tr}[\not{k}_1 \frac{\not{\bar{n}}}{2} (\not{k}_1 + \not{k}_{2\perp}) \frac{\not{n}}{2}] e^{-i\vec{b}_\perp \cdot \vec{k}_{2\perp}},$$

$$= \frac{-ig^4}{4\pi^3} C_F T_F n_f \frac{\Gamma(\varepsilon)\Gamma(2-\varepsilon)^2\Gamma(-2\varepsilon)}{\Gamma(4-2\varepsilon)\Gamma(1+\varepsilon)} \frac{(\tilde{b}^2\mu^2)^{2\varepsilon}}{e^{-2\varepsilon\gamma_E}}, \tag{3.61}$$

$$= i\frac{\alpha_s^2}{\pi} C_F T_F n_f \left[\frac{1}{3\varepsilon^2} + \frac{1}{\varepsilon}(\frac{5}{9} + \frac{2}{3}L_b) + \frac{2}{3}L_b^2 + \frac{10}{9}L_b + \frac{1}{3}\zeta(2) + \frac{28}{27}\right]. \tag{3.62}$$

There is only one other term with the color structure $C_f T_F n_f$, which comes from the two-loop renormalized coupling. This comes from multiplying the one-loop diagram in Eq. (**??**) by Z_α, and gives

$$-iC_F\beta_0 \frac{\alpha_s^2}{2\pi} \frac{\Gamma(-\varepsilon)}{\varepsilon} (\tilde{b}^2\mu^2)^\varepsilon = i\frac{\alpha_s^2}{\pi} C_F \left(\frac{11C_A}{3} - \frac{4T_F n_f}{3}\right) \left[\frac{1}{2\varepsilon^2} + \frac{1}{2\varepsilon}L_b + \frac{1}{4}L_b^2 + \frac{1}{4}\zeta(2)\right], \tag{3.63}$$

with β_0 being the 1-loop beta-function coefficient, $\beta_0 = 11/3C_A - 4/3T_F n_f$. Adding the $T_F n_f$-terms, we obtain

$$\text{quark terms} = C_F T_F n_F \frac{\alpha_s^2}{4\pi} \left[\frac{-1}{3\varepsilon^2} + \frac{5}{9\varepsilon} - \frac{2}{3}L_b^2 + \frac{10}{9}L_b + \frac{28}{27}\right], \tag{3.64}$$

which, after dropping the UV poles and dividing by $-\pi$, is exactly the $T_F n_f$ terms in the two-loop TMD rapidity anomalous dimension.

For the soft-eye graph, we find

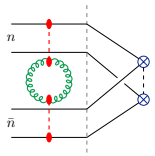

$$
\begin{aligned}
&= 2g^4 C_F C_A \int \frac{\bar{d}^{d-2}k_{2\perp}\bar{d}^d k_1 \left|\frac{2k_1^z}{\nu}\right|^{-\eta}}{\vec{k}_{2\perp}^2 (k_1+k_{2\perp})k_1^2}\left[\frac{4[k_1\cdot(k_{2\perp}+k_1)]^2}{n\cdot k_1\,\bar{n}\cdot k_1}\right. \\
&\qquad \left. + \left\{(d-2)n\cdot k_1\,\bar{n}\cdot k_1 + 4k_{2\perp}^2 - 2(k_1+k_{2\perp})^2 - 2k_1^2\right\}\right] e^{-i\vec{b}_\perp\cdot\vec{k}_{2\perp}}, \\
&= -i\frac{g^4 C_F C_A}{8\pi^3}\left[\frac{\Gamma(1/2-\eta/2)\Gamma(-\varepsilon-\eta/2)\Gamma(-2\varepsilon-\eta/2)}{4^{-\varepsilon}\eta\,\Gamma(1/2-\varepsilon-\eta/2)}\frac{(\tilde{b}^2\mu^2)^{2\varepsilon+\eta/2}}{e^{(2\varepsilon+\eta/2)\gamma_E}}\left(\frac{\mu^2}{\nu^2}\right)^{-\eta/2}\right. \\
&\qquad \left. + \frac{\Gamma(\varepsilon)\Gamma(-2\varepsilon)}{2\Gamma(1+\varepsilon)}\left(\frac{\Gamma(2-\varepsilon)^2}{\Gamma(4-2\varepsilon)} - 2\frac{\Gamma(1-\varepsilon)^2}{\Gamma(2-2\varepsilon)}\right)\frac{(\tilde{b}^2\mu^2)^{2\varepsilon+\eta/2}}{e^{-(2\varepsilon+\eta/2)\gamma_E}}\right], \qquad (3.65) \\
&= -i\frac{C_F C_A \alpha_s^2}{4\pi}\left[\left\{\frac{4\Gamma(-\varepsilon)^2 e^{-2\varepsilon\gamma_E}}{\eta} + \frac{3}{\varepsilon^3} + \frac{2}{\varepsilon^2}(2L_b - L_\nu) + \frac{1}{\varepsilon}\left(2L_b^2 - 4L_bL_\nu + 3\zeta(2)\right)\right.\right. \\
&\qquad \left.\left. - 4L_b^2 L_\nu + 4\zeta(2)L_b - 2\zeta(2)L_\nu + 6\zeta(3)\right\} - \left\{\frac{11}{3\varepsilon^2} + \frac{1}{3\varepsilon}\left(\frac{67}{3} + 22L_b\right)\right. \\
&\qquad \left. + \frac{22}{3}L_b^2 + \frac{134}{9}L_b + \frac{11}{3}\zeta(2) + \frac{404}{27}\right\}\Bigg].
\end{aligned}
$$

On the final line we have written the η- and ε-expansions such that the terms in the first set of curly brackets come from the rapidity divergent term the line above, and the terms in the second set of square brackets all come from the second set of curly brackets.

In principle, we should also take into account the flower graph, which is given by contracting the two soft gluon emission vertex off a Glauber with itself (see [160] for the appropriate Feynman rule), however this diagram is scaleless and thus can be ignored .

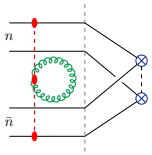

$$
= 4g^4 C_F C_A \int \frac{\bar{d}^{d-2}k_{2\perp}\bar{d}^d k_1 \left|\frac{2k_1^z}{\nu}\right|^{-\eta}}{k_1^2\,\vec{k}_{2\perp}^2\, n\cdot k_1\,\bar{n}\cdot k_2} e^{-i\vec{b}_\perp\cdot\vec{k}_{2\perp}}. \qquad (3.66)
$$

There are two different real emission graphs which involve the Lipatov vertex (the cou-

pling of a soft gluon to the Glauber). The first of these is given by

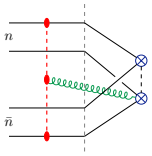

$$= -2g^4 C_F C_A \int \frac{đ\bar{n}\cdot k_1 đn\cdot k_2 đ^{d-2}k_{1\perp} đ^{d-2}k_{2\perp} \left|\frac{\bar{n}\cdot k_1 + n\cdot k_2}{\nu}\right|^{-\eta}}{\vec{k}_{1\perp}^2 \vec{k}_{2\perp}^2 \, \bar{n}\cdot k_1 n\cdot k_2} e^{-i\vec{b}_\perp\cdot\vec{k}_{1\perp}}$$
$$\times \left(-2\bar{n}\cdot k_1 n\cdot k_2 - 2\vec{k}_{1\perp}^2 - 2\vec{k}_{2\perp}^2\right) \delta^{(+)}(-\bar{n}\cdot k_1 n\cdot k_2 - (\vec{k}_{1\perp} - \vec{k}_{2\perp})^2),$$

$$= i\frac{C_F C_A g^4}{4\pi^3} \frac{\Gamma(\eta/2)\Gamma(1-\varepsilon)\Gamma(-\varepsilon-\eta/2)}{(\eta+4\varepsilon)\Gamma(1+\eta)} \frac{(\tilde{b}^2\mu^2)^{2\varepsilon+\eta/2}}{e^{(2\varepsilon+\eta/2)\gamma_E}} \left(\frac{\mu^2}{\nu^2}\right)^{-\eta/2}, \tag{3.67}$$

$$= -iC_F C_A \frac{\alpha_s^2}{2\pi}\left[\frac{4\Gamma(-\varepsilon)^2 e^{-2\varepsilon\gamma_E}}{\eta} + \frac{3}{\varepsilon^3} + \frac{2}{\varepsilon^2}(2L_b - L_\nu) + \frac{1}{\varepsilon}(2L_b^2 - 4L_b L_\nu + \zeta(2))\right.$$
$$\left. - 4L_b^2 L_\nu - 2\zeta(2)L_\nu\right]. \tag{3.68}$$

The second single real emission vertex is given by

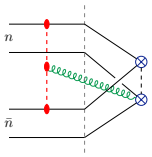

$$= -g^4 C_F C_A \int \frac{đ\bar{n}\cdot k_1 đn\cdot k_2 đ^{d-2}k_{1\perp} đ^{d-2}k_{2\perp} \left|\frac{\bar{n}\cdot k_1 + n\cdot k_2}{\nu}\right|^{-\eta}}{\vec{k}_{1\perp}^2 \vec{k}_{2\perp}^2 \, \bar{n}\cdot k_1 n\cdot k_2} e^{-i\vec{b}_\perp\cdot(\vec{k}_{1\perp}-\vec{k}_{2\perp})}$$
$$\times \left(-2\bar{n}\cdot k_1 n\cdot k_2 - 2\vec{k}_{1\perp}^2 - 2\vec{k}_{2\perp}^2\right) \delta^{(+)}(-\bar{n}\cdot k_1 n\cdot k_2 - (\vec{k}_{1\perp} - \vec{k}_{2\perp})^2),$$

$$= -2ig^4 C_F C_A \frac{\Gamma(\eta/2)\Gamma(-\varepsilon)^2\Gamma(1+\varepsilon)\Gamma(-2\varepsilon-\eta/2)}{2^{6+\eta}\pi^{5/2}\Gamma(1/2+\eta/2)\Gamma(-2\varepsilon)\Gamma(1+\varepsilon+\eta/2)} \frac{(\tilde{b}^2\mu^2)^{2\varepsilon+\eta/2}}{e^{(2\varepsilon+\eta/2)\gamma_E}} \left(\frac{\mu^2}{\nu^2}\right)^{-\eta/2}, \tag{3.69}$$

$$= iC_F C_A \frac{\alpha_s^2}{4\pi}\left[\frac{4\Gamma(-\varepsilon)^2 e^{-2\varepsilon\gamma_E}}{\eta} - \frac{1}{\varepsilon^3} + \frac{2}{\varepsilon^2}L_\nu + \frac{1}{\varepsilon}\left(2L_b^2 + 4L_b L_\nu + \zeta(2)\right)\right.$$
$$\left. + \frac{8}{3}L_b^3 + 4L_b^2 L_\nu + 4\zeta(2)L_b + 2\zeta(2)L_\nu + \frac{28}{3}\zeta(3)\right]. \tag{3.70}$$

Adding up all the (non-abelian) terms gives the final result

$$C_F C_A + C_F T_F n_f \text{ terms}$$
$$= iC_F C_A \frac{\alpha_s^2}{4\pi}\left[\frac{11}{3\varepsilon^2} - \frac{67}{9\varepsilon} + \frac{2\zeta(2)}{\varepsilon} - \frac{11}{3}L_b^2 + 4\zeta(2)L_b - \frac{134}{9}L_b + 14\zeta(3) - \frac{404}{27}\right]$$
$$+ iC_F T_F n_f \frac{\alpha_s^2}{4\pi}\left[-\frac{4}{3\varepsilon^2} + \frac{20}{9\varepsilon} + \frac{4}{3}L_b^2 + \frac{40}{9}L_b + \frac{112}{27}\right]. \tag{3.71}$$

We see that all the $1/\eta$ poles, $\log\nu$ terms, $1/\varepsilon^3$ UV divergences, and non-local divergence terms have all cancelled in the sum over diagrams, as expected. Dropping the $1/\varepsilon$ poles

gives exactly $-i\pi$ times the two-loop TMD rapidity anomalous dimension:

$$\gamma_\nu^s = -C_F C_A \frac{\alpha_s^2}{4\pi^2}\left[-\frac{11}{3}L_b^2 + 4\zeta(2)L_b - \frac{134}{9}L_b + 14\zeta(3) - \frac{404}{27}\right] - C_F T_F n_f \frac{\alpha_s^2}{4\pi^2}\left[\frac{4}{3}L_b^2 + \frac{40}{9}L_b + \frac{112}{27}\right] \tag{3.72}$$

This agrees with the known result [83].

Lastly, we note that the rapidity anomalous dimension for the TMD soft function has been calculated to four loops in [80, 142]. This calculation was accomplished by using the correspondence between soft and rapidity anomalous dimensions [172]. It would certainly be interesting to explore any implications this has in the context of the work presented here.

3.5 Discussion

In this chapter we have shown that all the large logs that show up in a certain class of S matrix element are controlled by the phase. This includes RG logs of invariant mass ratios, as was first shown [49], as well as large logs of rapidity ratios. We have demonstrated how one can calculate the rapidity anomalous dimensions for both local and non-local operators at two loops. By focusing on the S-matrix phase we are able to extract these anomalous dimensions by calculating the much simpler set of cut diagrams. Furthermore, since we are calculating the rapidity finite anomalous dimensions directly, instead of having to calculate counter-terms, the integrals do not need a rapidity regulator, which, in general, makes integrating more challenging. If one chooses to calculate using Feynman diagrams, as opposed to using on-shell methods, then individual diagrams will in general need to be regulated, whereas finite integrals will only arise once one combines diagrams. In the case of the massive Sudakov form factor there was no need to a rapidity regulator even at the diagramatic level. In the next chapter, we will show how the ideas presented here may be extended to the case of forward scattering and Glauber operators.

Chapter 4

Unitarity, Anomalous Dimensions, and All That Part II

4.1 Introduction

Despite the remarkable progress made in our understanding of resummed perturbative field theory, it is fair to say that when it comes to the near forward scattering (Regge) limit, $s \gg t$ there are still many open questions. Gribov's original approach [99] to the problem has led to a number of perspectives including the classic work of Balitsky, Fadin, Kuraev and Lipatov [88], Lipatov's effective action [124], and more modern approaches in terms of Wilson lines[13, 46, 47, 171, 90].

What complicates the perturbative series in the Regge limit is the existence of large logs of the ratio s/t that appear at each order in perturbation theory. The resummation of large logs is not an exotic phenomena as logs of the ratios of invariant masses are summed via a canonical renormalization group analysis which follows from factorization of mass scales, or equivalently decoupling. However, Regge logs grow as a ratio of rapidities and are not summable in this way.

The resummations of rapidity logs has a long history. In the context of hard scattering, the Collins-Soper equation [59] resums logs in hard scattering transverse momentum distributions, while the BFKL [121, 14] and its generalization the BJIMWLK equation [110, 105] resum rapidity logs[1] in near forward scattering processes. A universal formalism which allows for the resummation of rapidity logs for both hard scattering and in the Regge limit was developed in [57, 54]. The universality of this approach stems from fact that it is based upon an operator formalism within the confines of an effective field theory, which in the case of hard scattering, corresponds to SCET [16, 17, 18] and its' generalization in the

[1] We will use the acronym RRG to refer to the rapidity renormalization group equation.

near forward scattering limit (GSCET) [159] [2] . The EFT approach to forward scattering systematizes the problem in the sense that the resummation of rapidity logs is reduced to finding the anomalous dimensions for a set of well defined gauge invariant operators in the effective theory[3].

What makes the Regge problem more complex than the case of hard scattering is that at each order of perturbation theory, there are new operators, broken up into irreducible representations of color of various dimensions, that appear at the same (leading) order in t/s which leads to a complex mixing matrix for non-local operators. However, it has been known for a long time that the perturbative series in the Regge limit has a very rich structure that can serve to greatly simplify the system. This structure is manifested in the results found [120] for the gluon near forward amplitude in the anti-symmetric octet (8_A) channel. In particular, it was shown that at NLL the glue-glue scattering amplitude in this channel takes the form

$$\begin{aligned}\mathcal{M}_{2\to 2}^{8_A} &= [g_s T^c_{aa'} C_g(p_a, p_{a'})]\frac{s}{t}\left[\left(\frac{s+i\epsilon}{-t}\right)^{\alpha(t)} + \left(\frac{-s+i\epsilon}{-t}\right)^{\alpha(t)}\right][g_a T^c_{bb'} C_g(p_b, p_{b'})] \\ &= [g_s T^c_{aa'} C_g(p_a, p_{a'})]\frac{s}{t}\left[\left(\frac{s+i\epsilon}{-t}\right)^{\alpha(t)}(1+e^{-i\pi\alpha(t)})\right][g_a T^c_{bb'} C_g(p_b, p_{b'})] \qquad (4.1)\end{aligned}$$

with $C_g(t)$ being the so-called "impact factor" and $\alpha(t)$ is the gluon Regge trajectory. Note that the result is anti-symmetric under crossing in the kinematic variable and Bose symmetry follows since the color factor is crossing odd. Similar results holds for the case of the non-crossing symmetric quark scattering amplitude[120], albeit with different impact factors C_q and representations of the color generators. For details on the structure at two loops and the breakdown of the result beyond NLL see [78]. This result is valid to next to leading log (NLL) and is exact in the planar limit. It is fair to say that this result seems unexpected as it implies several remarkable facts. The power law in s/t has the form of a solution to a simple differential equation which arises when running local operators, whereas non-local operators obey integro-differential equations whose solutions are in general not simple power laws. Such power laws correspond to "Regge poles" as opposed to "Regge cuts" that arise in the complex angular momentum plane (see e.g. [119]). Furthermore, there seems to be only one quantity associated with an "anomalous dimension", $\alpha(t)$,while

[2]The Glauber mode breaks factorization in the case of hard scattering. In all SCET proofs to date [20] utilized the version of SCET which did not include Glaubers[16], it was simply assumed (given the proofs of Collins, Soper and Sterman ([60]) in the full theory) that the Glauber mode cancelled in the relevant observables.

[3]The EFT approach is related to but quite distinct from the Reggeon field theory approach. For instance, Reggeon exchange should not be equated with Glauber exchange. For a discussion of these distinctions see [93].

we would expect at least two such anomalous dimensions at two loops, and more beyond. Other hints of underlying structure were pointed out in [65] where it was shown that the constants appearing in the one-loop quark and gluon impact factors involve the finite part of the two-loop Regge trajectory, though the impact factors are polluted by additional constants that are not related to the Regge trajectory. Intuitively this iterative structure would seem to be a consequence of unitarity as forward scattering is a semi-classical process which leads to the exponentiation of the classical (shock wave) action. On the other hand the anomalous dimensions and the associated logs are a quantum effect so there is no a priori reason to expect any natural relation between the iterative (phase) structure and the aforementioned anomalous dimensions relation. The are other interesting relations between the lower loop results and higher order contributions to the cusp anomalous dimensions [116, 117, 67, 68], which will not be relevant to our discussion.

In [143] it was shown that the iterative structure is elegantly exposed within the EFT formalism [159]. In particular, the authors used the EFT approach to show that, given the form of the amplitude (4.1), the finite part of the two-loop Regge trajectory must be encoded in the order ϵ piece of a one loop correction (with no contamination) while the divergent pieces arise from a simplified (in a manner to made clear below) two loop calculation which, at the technical level, is effectively one loop. Their results also shows that in the EFT one reduces the calculation of the two loop Regge trajectory to three diagrams. Finally, the authors were able to derive the maximally matter dependent contributions to the Regge trajectory to all loop orders.

In this chapter, we will generalize the result in [143] in several ways. Firstly due to the reliance of [143] on the use of the form of the amplitude (4.1) their results can only used in the 8_A channel and only to NLL, away from the planar limit, whereas our relations will be valid in all channels and to all orders. In allowing for more general processes we will also uncover additional relations among various anomalous dimensions which will contribute to Regge cuts. Furthermore, our results show that simplifications in calculating the Regge trajectory, in the case of anti-symmetric octet are universal and, moreover, the Regge trajectory as well as other anomalous dimensions, can be calculated directly via cut diagrams in the EFT. That Regge logs can be extracted by cut diagrams in the full theory was shown in [87], though working in the EFT systematizes the methodology, and streamlines the calculations, especially at higher orders.

4.2 Implications of Eq.(4.1)

The form of the amplitude (4.1) implies that the form rapidity RG equations (6.21) in the EFT must be strongly constrained at least up to NLL and to all orders in the planar limit.

At NLL, where we keep all terms which scale as $\alpha^2 \log(s/t)$, with $\alpha \log(s/t) \sim 1$, we need to run the one Glauber operator at two loops and the octet of the two Glauber operator at one.

The form of (4.1) implies that the RRG equation (in the 8_A channel) has a power law solution $(s/t)^\alpha$. This is prima facia consistent with the one Glauber exchange where the factorized form will reduce to a product (Regge Pole) since the exchanged momentum is fixed to be $q_\perp = \sqrt{-t}$. However, once we allow for two Glauber exchange we expect a convolution (Regge cut). Moreover, in principle, we can have mixing between one and two Glauber exchanges, i.e. $\gamma^{8_A}_{1,2} \neq 0$[4]. Finally, even if the two Glauber exchange RRG had a power law solution, the form of (4.1) implies that integral of $\gamma_{(2,2)}$ has to be fixed by $\gamma_{(1,1)}$. This also implies that there can be no mixing between the one and two Glauber sectors of the theory, e.g. $\gamma_{(1,2)} = 0$. Calculating in the EFT it has been found that [93], not only is $\gamma_{(1,2)} = 0$, but *all transitions* between one and multi-Glauber exchanges vanishes. i.e. beyond the one and two Glauber sector.

If we go to the planar limit this leads to an infinite number of constraints since the solution to the RG have a pole structure, i.e no convolutions, such that the RRG has a simple exponential solution as in Eq. (4.1). Moreover, there is no mixing between the different Glauber sectors to all order in perturbation theory. From here on out we would like to keep things as general as possible and will not assume planarity.

We gain further control of the RRG structure in the planar limit where Eq.(4.1) is valid to all orders, which implies that the full RRG system is multiplicative, i.e. its a pure pole. Moreover all of the anomalous dimensions $\gamma_{n,n}$ are fixed in terms of $\gamma_{(1,1)}$. It has been known for a long time that the planar limit leads to pure Regge poles [120], and how this phenomena occurs in the EFT was explained in [93]. Here we briefly summarize the arguments. In the EFT the basic reason for the all-order pole structure is remarkably simple and it has to do with the so-called "collapse rule" put forth in [159] which states that a Glauber burst can not be interrupted. In figure (1.1) a collinear interruption between Glauber bursts (meaning multiple Glauber exchange with possible soft interactions) leading to a vanishing contribution. Figure (1.3) is planar and non-vanishing and leads to pole behavior, while figure (1.2) is non-planar and leads to cut behavior. Thus we conclude that, in accordance with Eq.(4.1), the collapse rule implies there can be no convolution, when considering the RRG for J or $\bar{J}$, since all the Glauber loop momenta can be run through a single collinear line.

[4]There is no reason in general why non-planar diagrams could not generate cut structures either in the next to leading order two Glauber anomalous dimension or the leading order three Glauber anomalous dimension.

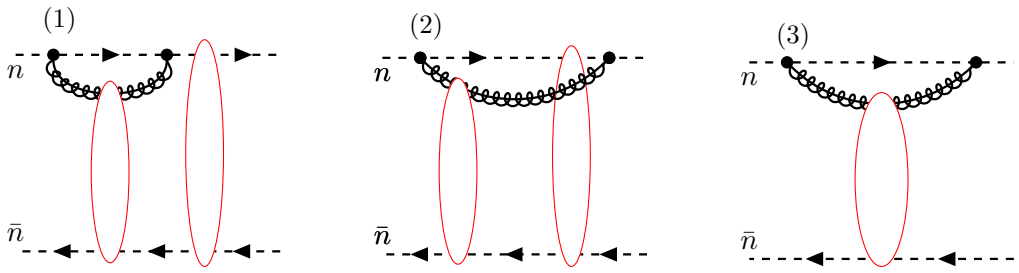

Figure 4.1: Different configurations of Glauber bursts. Here the bubble outlined in red represents an arbitrary number of Glauber exchanges. The first diagram presents a planar configuration of two Glauber bursts, which are interrupted by the collinear gluon-quark vertex. This class of diagrams all vanish by the collapse rule. Diagram (2.) represents a non-planar set of Glauber exchanges which are in general non-vanishing and will generate non-pole solutions. Lastly Diagram (3.) is a planar Glauber burst which is not interrupted.

4.3 Explaining the Iterative Structure

As mentioned in the introduction an interesting piece of data regarding the perturbative series is that the finite part of the two loop anomalous dimensions can be extracted from the $O(\epsilon)$ piece of the one loop calculations. By comparing this form to Eq.(4.1) the authors of [143] were able to derive a relation between the two loop Regge trajectory and the constant pieces of the one and two Glauber exchange graphs: $S^{(1)}_{2,2}$, $S^{(0)}_{2,2}$, $S^{(1)}_{1,1}$, in the color octet channel, where the superscript denotes the order of the correction beyond the Glauber exchange. In particular, they derived the relation

$$\begin{aligned} \alpha^{(1)} &= -2S_2^{(0)} && (4.2)\\ \alpha^{(2)} &= -2\left(S_1^{(1)} - S_1^{(1)}S_2^{(0)}\right), && (4.3) \end{aligned}$$

where the $S_i^{(n)}$ are defined via

$$\begin{aligned} S^{8_A}_{(1,1)} &= S_1^{(0)}(1+\tilde{\alpha}S_1^{(1)} + \tilde{\alpha}^2 S_1^{(2)} + ...)\\ S^{8_A}_{(2,2)} &= i\pi S_1^{(0)}(\tilde{\alpha}S_2^{(0)} + \tilde{\alpha}^2 S_2^{(1)} + ...)\\ S_1^{(0)} &= \frac{8\pi i\alpha_s}{t} && (4.4) \end{aligned}$$

and

$$\alpha(t) = \sum_i \alpha^{(i)}\left(\frac{\tilde{\alpha}}{4\pi}\right)^i, \qquad (4.5)$$

where $\tilde{\alpha}$ is the rescaled coupling constant (see [143]). Not only is this useful to explain why the two loop Regge trajectory shows up in a one loop calculation, but it also simplifies the

calculation of the two loop trajectory itself, as it drastically reduces the number of diagrams one needed to calculate, since we don't need to consider two loop soft corrections to one Glauber exchange ($S^{(2)}_{1,1}$), and only need to calculate three diagrams [143]. Moreover, these three two loop diagrams all involve a Glauber loop which reduces the relativistic loop order by one.

In this paper we will utilize the recently developed formalism [156] to generalize the results in [143] to all orders and in any color channel. Moreover, the formalism will also generate relations between anomalous dimensions of operators with differing number of Glaubers.

4.4 Unitarity Methods

4.4.1 Application to Regge Kinematics

In the previous chapter, we introduced a method for analyzing rapidity anomalous of hard scattering form factors. We would now like to apply this methodology to the present case of interest, near forward scattering. The use of unitarity in this regime is certainly not new, and goes back to, at least, [120]. However, here we will exploit unitary in a systematic fashion within the confines of an EFT to generate relations for anomalous dimensions to all order in pertrubation theory. If we try to apply the same arguments as we did above, regarding correlations between the logs and the phase, to this case, it becomes clear that a straight forward application will fail. To understand this we recall that the near forward scattering process is semi-classical and as such the amplitude comes with a phase $e^{iS_{cl}}$ which is not directly associated with the quantum rapidity logs. This can be most straightforwardly seen in QED, where the photon does not Reggeize, but there is certainly a phase which arises from the semi-classical solution. In QCD there is a quantum rapidity log that Reggeizes the gluon, but its' relationship to the $i\pi$ that arises do to the Glauber loop, at face value, is unclear. Consider quark-antiquark scattering, with a gluon mass regulator m, we have

$$\begin{aligned}
\text{1-loop} &= \frac{i\alpha_s^2}{t} S^{(1)}_{n\bar{n}} \left[8i\pi \ln\left(\frac{-t}{m^2}\right)\right] + \frac{i\alpha_s^2}{t} S^{(2)}_{n\bar{n}} \left[-4\ln^2\left(\frac{m^2}{-t}\right) - 12\ln\left(\frac{m^2}{-t}\right) - 14\right] \\
&+ \frac{i\alpha_s^2}{t} S^{(3)}_{n\bar{n}} \left[-4\ln\left(\frac{s}{-t}\right)\ln\left(\frac{-t}{m^2}\right) + \frac{22}{3}\ln\left(\frac{\mu^2}{-t}\right) + \frac{170}{9} + \frac{2\pi^2}{3}\right] \\
&+ \frac{i\alpha_s^2}{t} S^{(4)}_{n\bar{n}} \left[-\frac{8}{3}\ln\left(\frac{\mu^2}{-t}\right) - \frac{40}{9}\right],
\end{aligned} \tag{4.6}$$

where the various color and spinor prefactors are given by

$$\begin{aligned} S_{n\bar{n}}^{(1)} &= -\left[\bar{u}_n T^A T^B \frac{\not{n}}{2} u_n\right]\left[\bar{v}_{\bar{n}} \overline{T}^A \overline{T}^B \frac{\not{\bar{n}}}{2} v_{\bar{n}}\right], \quad S_{n\bar{n}}^{(2)} = C_F \left[\bar{u}_n T^A \frac{\not{n}}{2} u_n\right]\left[\bar{v}_{\bar{n}} \bar{T}^A \frac{\not{\bar{n}}}{2} v_{\bar{n}}\right], \\ S_{n\bar{n}}^{(3)} &= C_A \left[\bar{u}_n T^A \frac{\not{n}}{2} u_n\right]\left[\bar{v}_{\bar{n}} \bar{T}^A \frac{\not{\bar{n}}}{2} v_{\bar{n}}\right], \quad S_{n\bar{n}}^{(4)} = T_F n_f \left[\bar{u}_n T^A \frac{\not{n}}{2} u_n\right]\left[\bar{v}_{\bar{n}} \bar{T}^A \frac{\not{\bar{n}}}{2} v_{\bar{n}}\right]. \end{aligned} \tag{4.7}$$

We see that the $i\pi$ does not come with the same color structure as the rapidity $\log(s)$, which is inherently non-Abelian and thus we must consider an object which directly ties the phase to the rapidity logs.

4.4.2 Amplitudes of definite signature

We can get hint as to the proper direction by first recalling that the $i\pi$ in Eq. (4.6) arises from the box Glauber diagram. Moreover, the cross-boxed diagram, which would carry a non-Abelian color factor and could correlate with the rapidity log, vanishes in the effective theory (see Section 5 of [159]). However, if we consider the crossed-amplitude ($s \to u = -s + O(t/s)$), the box will come with a non-Abelian color factor. In fact, if we consider the linear combination $M_s - M_u$ the Glauber contribution will generate exactly the C_A color factor that must appear with the rapidity log. This combination is what is known as a "negative signature amplitude" and it (along with the positive signature case) have been an object of study in the forward scattering amplitude for many decades (see e.g. [66]).

Much can be gleaned about the definite signature amplitudes from dispersion relations. In particular, it has been pointed out [48] that these objects have exactly the reality properties needed to fully control the phase from the logarithms. Generally, this is used to simplify calculations by allowing one to drop/ignore $i\pi$ terms that might complicate the calculation. Here we are able to exploit this connection by combining signature with the factorization of the amplitude into multi-Glauber operators. One can decompose the 2-to-2 amplitude as

$$\begin{aligned} \mathcal{M}_{2\to 2} &= \mathcal{M}^{(-)} + \mathcal{M}^{(+)}, \\ \mathcal{M}^{(\pm)} &= \frac{1}{2}\left(\mathcal{M}_{2\to 2}(s,t) \pm \mathcal{M}_{2\to 2}(u,t)\right), \end{aligned} \tag{4.8}$$

where $\mathcal{M}_{2\to 2}(s,t)$ is the s-channel amplitude and $\mathcal{M}_{2\to 2}(u,t)$ is the u-channel amplitude. Therefore the $(+)$ and $(-)$ signature amplitudes are even or odd under $(s \leftrightarrow u)$ crossing. Both are functions of the crossing symmetric combination of logarithms[48],

$$L = \frac{1}{2}\left(\log\frac{-s - i\epsilon}{-t} + \log\frac{-u - i\epsilon}{-t}\right) = \log\frac{|s|}{|t|} - \frac{i\pi}{2}, \tag{4.9}$$

where we have used $u = -s$ in the high-energy limit. It was further shown in [48] that the coefficients of L are either purely real for the odd-signature amplitude or purely imaginary for the even-signature amplitude. These reality properties then allow us to exactly relate the logarithms to the phase.

4.4.3 Signature Symmetry and the Complex Boost

In order to make use of the connection between the rapidity logs and the $i\pi$'s, we now utilize the boost operator $\bar{K}_z$, defined in section (3.2.2). Then, by acting on L with $e^{i\pi\bar{K}_z}$, we have

$$e^{i\pi\bar{K}_z} L = \frac{1}{2}\left(\log\frac{-se^{2\pi i} - i\epsilon}{-t} + \log\frac{-u - i\epsilon}{-t}\right) = \log\frac{|s|}{|t|} + \frac{i\pi}{2} = L^\star. \tag{4.10}$$

The boost only acts non-trivially on the $\log(-s)$ the log is evaluated right below the branch cut, while the $\log(-u)$ is evaluated away from the branch cut and a rotation by $2\pi i$ has no effect. The definite signature amplitudes then transform as

$$e^{i\pi\bar{K}_z}\mathcal{M}^{(\pm)}(L) = \mathcal{M}^{(\pm)}(L^\star) = \mp\mathcal{M}^{(\pm)}(L)^\star. \tag{4.11}$$

The last equality follows from the reality properties of the amplitudes and the Schwartz reflection principle.

4.4.4 The Master Formulae

We now use the factorization to write the definite-signature amplitudes as

$$\mathcal{M}^{(\pm)} = i\sum_{i,j=1}^{\infty}\left[J^{(s)}_{\kappa(i)}\otimes S^{(s)}_{(i,j)}\otimes \bar{J}^{(s)}_{\kappa'(j)} \pm J^{(u)}_{\kappa(i)}\otimes S^{(u)}_{(i,j)}\otimes \bar{J}^{(u)}_{\kappa'(j)}\right], \tag{4.12}$$

where the (s/u) superscripts denote whether the matrix element is computed in the s- or u-channels. Each component, J, S etc, is decomposed in terms of color irreps, whose indices we have suppressed. Since the amplitude may only depend on p_n^+ and $p_{\bar{n}}^-$ through the rapidity logs in the collinear functions, we may write

$$\begin{aligned}\bar{K}_z\mathcal{M}^{(\pm)} = {} & i\sum_{i,j=1}^{\infty}\left[\left(-\frac{1}{2}\nu\frac{\partial}{\partial\nu}J^{(s)}_{\kappa(i)}\right)\otimes S^{(s)}_{(i,j)}\otimes\bar{J}^{(s)}_{\kappa'(j)} \pm \left(-\frac{1}{2}\nu\frac{\partial}{\partial\nu}J^{(u)}_{\kappa(i)}\right)\otimes S^{(u)}_{(i,j)}\otimes\bar{J}^{(u)}_{\kappa'(j)}\right] \\ & + i\sum_{i,j=1}^{\infty}\left[J^{(s)}_{\kappa(i)}\otimes S^{(s)}_{(i,j)}\otimes\left(-\frac{1}{2}\nu\frac{\partial}{\partial\nu}\bar{J}^{(s)}_{\kappa'(j)}\right) \pm J^{(u)}_{\kappa(i)}\otimes S^{(u)}_{(i,j)}\otimes\left(-\frac{1}{2}\nu\frac{\partial}{\partial\nu}\bar{J}^{(u)}_{\kappa'(j)}\right)\right].\end{aligned} \tag{4.13}$$

Using the rapidity RRG equation we have

$$\begin{aligned}\mp\mathcal{M}^{(\pm)\star} &= e^{i\pi\bar{K}_z}\mathcal{M}^{(\pm)} \\ &= i\sum_{i,j,k,l=1}^{\infty}\Bigg[\left(J^{(s)}_{\kappa(i)}e^{-\otimes\frac{i}{2}\pi\gamma_{(i,j)}}\right)\otimes S^{(s)}_{(j,k)}\otimes\left(e^{-\frac{i}{2}\pi\gamma_{(k,l)}\otimes}\bar{J}^{(s)}_{\kappa'(l)}\right) \\ &\quad\pm\left(J^{(u)}_{\kappa(i)}e^{-\otimes\frac{i}{2}\pi\gamma_{(i,j)}}\right)\otimes S^{(u)}_{(j,k)}\otimes\left(e^{-\frac{i}{2}\pi\gamma_{(k,l)}\otimes}\bar{J}^{(u)}_{\kappa'(l)}\right)\Bigg].\end{aligned} \tag{4.14}$$

Note that the action of $\bar{K}_z$ generates a factor of $1/2$, as compared to the action of $\bar{K}_z$ when acting on an amplitude [156]. This comes from the fact that we are looking at the signatured amplitude and the action of the generator on the difference/sum of the two channels naturally leads to twice the anomalous dimension.

To extract the Regge trajectory, we focus on the odd-signature amplitude. Using the vanishing of $1\to j$ transitions, we can rewrite Eq.(4.11) as

$$\mathcal{M}^{(-)}_1 e^{-i\pi\gamma_{(1,1)}} = \mathcal{M}^{(-)\star} - e^{i\pi\bar{K}_z}\mathcal{M}^{(-)}_{\geq 2}, \tag{4.15}$$

where we have used the fact that the one Glauber exchange is multiplicative (Regge pole).

We now use that the action of the boost is to transform L to $L^\star$, or shift $\log(s)\to\log(s)+i\pi$. With this, we can write the master formula for the Regge trajectory as

$$\mathcal{M}^{(-)}_1 e^{-i\pi\gamma_{(1,1)}} = \mathcal{M}^{(-)\star} - \mathcal{M}^{(-)}_{\geq 2}\Big|_{s\to e^{2\pi i}s}. \tag{4.16}$$

Notice that in the second term the action of the boost generator $e^{i\pi\bar{K}_z}$ does not conjugate $\mathcal{M}^{(-)}_{\geq 2}$, since L is formed from one Glauber (the log) and two Glauber (the $i\pi$) exchange graphs.

As a last step, we apply the unitarity relation $(\mathcal{M}^{(-)}-\mathcal{M}^{(-)\star}) = i(\mathcal{M}\mathcal{M}^\star)^{(-)}$ where $(\mathcal{M}\mathcal{M}^\star)^{(-)} = 1/2(\mathcal{M}_s\mathcal{M}^\star_s - \mathcal{M}_u\mathcal{M}^\star_u)$, we arrive at the master formula

$$\boxed{\mathcal{M}^{(-)}_1\left(e^{-i\pi\gamma_{(1,1)}}-1\right) = -i(\mathcal{M}\mathcal{M}^\star)^{(-)} + \left[\mathcal{M}^{(-)}_{\geq 2} - \mathcal{M}^{(-)}_{\geq 2}\Big|_{s\to e^{2\pi i}s}\right].} \tag{4.17}$$

A few comments are in order. First, we note that while this formula does involve more terms than just unitarity cuts (first term on the RHS), there are two major simplifications that it provides. The first is that the terms in the square brackets always come from graphs with at least two Glauber insertions, and so must have at least one Glauber loop. This provides many of the same technical simplifications as only working with cut graphs, as Glauber loops are easier to perform than soft or collinear loops. The second simplification is that only terms proportional to rapidity logarithms contribute to the terms in the square

brackets, as all other contributions vanish in the subtraction. The coefficients of the rapidity logarithms are generally easier to compute than the rapidity-finite terms. Moreover, one can also combine the two integrands (with the appropriate changes in sign in the second) to yield a rapidity finite integral that needs no regulator which can complicate the evaluation at higher loops.

Lastly, we give the equivalent formula for the even-signature sector. Due to an extra sign in Eq. (4.14), we find

$$\boxed{\left(e^{i\pi\bar{K}_z}-1\right)\mathcal{M}^{(+)}=-2\mathrm{Re}[\mathcal{M}^{(+)}].} \tag{4.18}$$

Unlike with the odd signature formula, the even signature relation cannot be simplified further using unitarity. Note that $\mathcal{M}_1^{(+)}=0$ to all orders so to extract information from this equation we will need to go to higher orders.

4.5 Calculating the Regge Trajectory through Two Loops

4.5.1 Leading order one Glauber anomalous dimension: $\gamma^{(1)}_{(1,1)}$

We now verify the master formula in Eq. (4.17). At one loop, it simplifies to

$$\mathcal{M}_1^{(-)(0)}\gamma^{(1)}_{(1,1)}=\frac{1}{\pi}\left(\mathcal{M}^{\dagger}\mathcal{M}^{(-)}\right)^{(1)}. \tag{4.19}$$

The tree-level odd signature amplitude for quark-antiquark scattering is given by

$$\mathcal{M}_1^{(-)(0)}=\frac{1}{2}\left(\begin{array}{ccc}p_2 & & p_3\\ n & & \\ & & \\ \bar{n} & & \\ p_1 & & p_4\end{array}\right.\quad-\quad\left.\begin{array}{ccc}\bar{p}_3 & & \bar{p}_2\\ n & & \\ & & \\ \bar{n} & & \\ p_1 & & p_4\end{array}\right)\equiv\left(\begin{array}{ccc}n & & \\ & & \\ \bar{n} & &\end{array}\right)^{(-)},$$

$$=\left[\bar{u}_nT^A\frac{\bar{\not{n}}}{2}u_n\right]\frac{8\pi\alpha_s}{t}\left[\bar{v}_{\bar{n}}\bar{T}^A\frac{\not{n}}{2}v_{\bar{n}}\right]. \tag{4.20}$$

In the first line we have introduced the notation of taking the odd-signature piece of the diagram, which can be computed by subtracting the crossed u-channel diagram from the s-channel diagrams. Note that we do not need to include the contributions of the terms in the square brackets of Eq. (4.17) at this order, as only the tree-level matrix elements of $J_{\kappa(2)}$, $S_{(2,2)}$, and $\bar{J}_{\kappa'(2)}$ contribute, and these contain no rapidity logarithms[93]. If we

compute the cut, we then find

$$\left(\mathcal{M}^\dagger\mathcal{M}^{(-)}\right)^{(1)} = \left(\right)^{(-)}$$

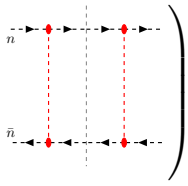

$$= \frac{-4\pi\alpha_s^2}{t}\left[\bar{u}_n\left(T^A T^B - T^B T^A\right)\frac{\bar{n}\!\!\!/}{2}u_n\right]\left[\bar{v}_{\bar{n}}\bar{T}^A\bar{T}^B\frac{n\!\!\!/}{2}v_{\bar{n}}\right]\frac{\Gamma(1+\varepsilon)\Gamma(-\varepsilon)^2}{\Gamma(-2\varepsilon)}\left(\frac{\bar{\mu}^2}{-t}\right)^{\varepsilon},$$
$$= \frac{C_A\alpha_s}{4}\frac{\Gamma(1+\varepsilon)\Gamma(-\varepsilon)^2}{\Gamma(-2\varepsilon)}\left(\frac{\bar{\mu}^2}{-t}\right)^{\varepsilon}\left[\bar{u}_n T^A\frac{\bar{n}\!\!\!/}{2}u_n\right]\frac{8\pi\alpha_s}{t}\left[\bar{v}_{\bar{n}}\bar{T}^A\frac{n\!\!\!/}{2}v_{\bar{n}}\right],$$
$$= \pi\gamma^{(1)}_{(1,1)}\mathcal{M}^{(-),(0)}. \tag{4.21}$$

Which yields the standard result for the leading order Regge trajectory

$$\gamma^{(1)}_{(1,1)} = \frac{C_A\alpha_s}{4\pi}\frac{\Gamma(-\epsilon)^2\Gamma(\epsilon+1)\left(\frac{\bar{\mu}^2}{-t}\right)^{\epsilon}}{\Gamma(-2\epsilon)} = -\frac{C_A\alpha_s}{2\pi}\left(\frac{1}{\epsilon}+\log\left(\frac{\mu^2}{-t}\right)\right)+O(\epsilon). \tag{4.22}$$

Through one loop this relation is almost trivial since the amplitude is linear in $\log|s/t|$ at this order. On the other hand, this calculation is significantly simpler than the direct calculation of the anomalous dimension (see [159]).

4.5.2 Next to leading order anomalous dimension for one Glauber operator: $\gamma^{(2)}_{(1,1)}$

Now we move onto the two-loop Regge trajectory, i.e. $\gamma^{(2)}_{(1,1)}$, which is still pure octet since we are focussing on the one Glauber operator. At this order Eq. (4.17) becomes

$$\mathcal{M}_1^{(-)(0)}\gamma^{(2)}_{(1,1)} + \mathcal{M}_1^{(-)(1)}\gamma^{(1)}_{(1,1)} - \frac{i\pi}{2!}\left(\gamma^{(1)}_{(1,1)}\right)^2\mathcal{M}_1^{(-)(0)} = \frac{1}{\pi}\left(\mathcal{M}^\dagger\mathcal{M}^{(-)}\right)^{(2)} + \frac{i}{\pi}\left[\mathcal{M}_{\geq 2}^{(-)(2)} - \mathcal{M}_{\geq 2}^{(-)(2)}\Big|_{s\to e^{2\pi i}}\right]. \tag{4.23}$$

Since $\gamma_{(1,1)}$, $\mathcal{M}_1^{(-)(1)}$, and the two-loop cut are all real, the only imaginary parts of this formula come from the iterative $\gamma^2_{(1,1)}$ term and the difference term. In particular, the difference term must be entirely imaginary, as at this order, only $J_{\kappa(2)}$, $S_{(2,2)}$, and $\bar{J}_{\kappa'(2)}$ can generate a $\log(s)$, the coefficient of which is purely imaginary. Then by looking at the real

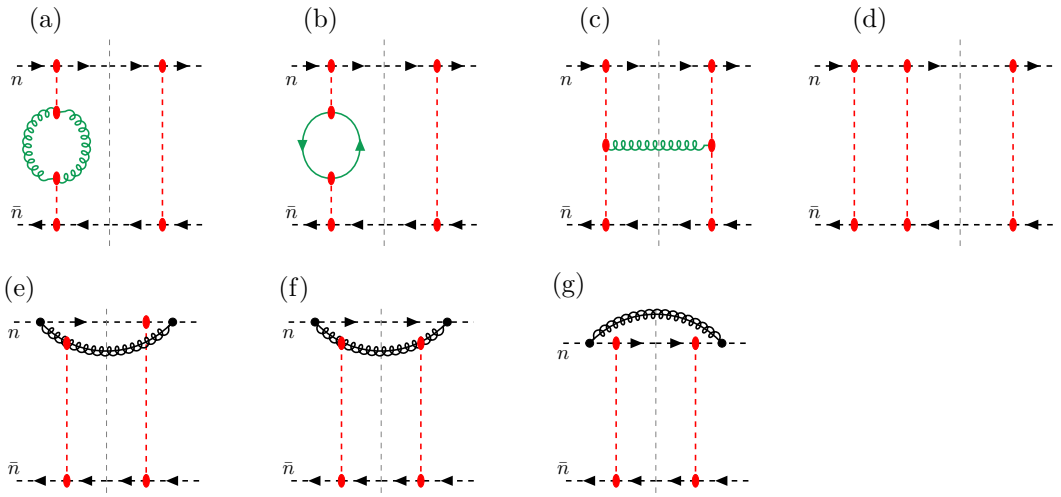

Figure 4.2: Two-loop cut diagrams contributing to the two loop Regge trajectory. Diagrams (a), (b), and (c) build up the Regge trajectory and the iterative soft contributions in the single Glauber operator, while the collinear loops (f) and (g) only build up the collinear iterative terms. Diagrams (d) and (e) vanish when summing over their mirror images and taking the odd-signature piece.

and imaginary parts separately, we obtain the following set of formulas:

$$\mathcal{M}_1^{(-)(0)}\gamma_{(1,1)}^{(2)} + \mathcal{M}_1^{(-)(1)}\gamma_{(1,1)}^{(1)} = \frac{1}{\pi}\left(\mathcal{M}^\dagger\mathcal{M}^{(-)}\right)^{(2)}, \tag{4.24}$$

$$\left(\gamma_{(1,1)}^{(1)}\right)^2 \mathcal{M}_1^{(-)(0)} = -\frac{2}{\pi^2}\left[\mathcal{M}_{\geq 2}^{(-)(2)} - \mathcal{M}_{\geq 2}^{(-)(2)}\Big|_{s\to e^{2\pi i}}\right]. \tag{4.25}$$

The reality of the term in the brackets follows from the fact that the Glauber loop gives an $i\pi$ as does the difference between the logs in the two amplitudes.

We first use Eq. (4.24) to obtain the two loop anomalous dimension starting with the diagrams needed for the one-loop single Glauber term $\mathcal{M}_1^{(-)(1)}$, of which there are two soft contributions:

$$\left(\quad\right)^{(-)} = -i\mathcal{M}^{(-)(0)}\frac{2\,T_F n_f \alpha_s}{\pi}\,\frac{\Gamma(2-\epsilon)^2}{\Gamma(4-2\epsilon)}\Gamma(\epsilon)\left(\frac{\bar{\mu}^2}{-t}\right)^{\epsilon}. \tag{4.26}$$

The soft eye graph is given by

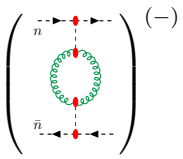

$$= -i\mathcal{M}^{(-)(0)}\frac{C_A\alpha_s}{2\pi}\left(\frac{\bar{\mu}^2}{-t}\right)^{\epsilon}\left\{\frac{\Gamma(2-\epsilon)^2}{\Gamma(4-2\epsilon)}\Gamma(\epsilon)-2\frac{\Gamma(1-\epsilon)^2}{\Gamma(2-2\epsilon)}\Gamma(\epsilon)\right.$$
$$\left.+\frac{\Gamma(\eta/2)\Gamma(1/2-\eta/2)\Gamma(1+\epsilon+\eta/2)\Gamma(-\epsilon-\eta/2)}{\Gamma(1+\eta/2)\Gamma(1/2-\epsilon-\eta/2)4^{-\epsilon}}\left(\frac{\nu^2}{-t}\right)^{\eta/2}\right\}. \quad (4.27)$$

Adding these together, we find

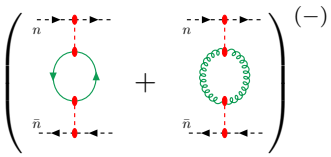

$$=i\mathcal{M}^{(-)(0)}\left(\frac{\alpha_s}{4\pi}\right)\left(\frac{\mu^2}{-t}\right)^{\epsilon}\left[-2C_A\frac{\Gamma(1+\epsilon)\Gamma(-\epsilon)^2}{\Gamma(-2\epsilon)}\left(\frac{1}{\eta}+\frac{1}{2}L_\nu\right)\right.$$
$$-\frac{2C_A}{\epsilon^2}+\frac{11C_A}{3\epsilon}-\frac{4T_Fn_f}{3\epsilon}+\frac{67C_A}{9}-\zeta(2)C_A-\frac{20T_Fn_f}{9} \quad (4.28)$$
$$\left.+\epsilon\left(-\frac{28C_A}{3}\zeta(3)-\frac{11C_A}{6}\zeta(2)+\frac{404C_A}{27}+\frac{2T_Fn_f}{3}\zeta(2)-\frac{112n_fT_F}{27}\right)+O(\epsilon^2)\right],$$

where we have introduced $L_\nu = \log\left(\nu^2/-t\right)$.

We have only three classes of cut diagrams to compute. There are two diagrams involving the soft eye graph on either side of the cut. These are just the soft eye graph convoluted with the Glauber box diagram, and they evaluate to

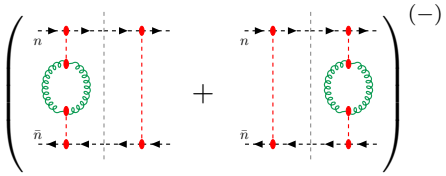

$$= -\mathcal{M}^{(-)(0)}\frac{C_A^2\alpha_s^2}{4\pi}\left(\frac{\bar{\mu}^2}{-t}\right)^{2\epsilon}\left\{\left(\frac{\Gamma(2-\epsilon)^2}{\Gamma(4-2\epsilon)}\Gamma(\epsilon)-2\frac{\Gamma(1-\epsilon)^2}{\Gamma(2-2\epsilon)}\Gamma(\epsilon)\right)B(1,1+\epsilon)\right. \quad (4.29)$$
$$\left.+\frac{\Gamma(\eta/2)\Gamma(1/2-\eta/2)\Gamma(1+\epsilon+\eta/2)\Gamma(-\epsilon-\eta/2)}{\Gamma(1+\eta/2)\Gamma(1/2-\epsilon-\eta/2)4^{-\epsilon}}B(1,1+\epsilon+\eta/2)\left(\frac{\nu^2}{-t}\right)^{\eta/2}\right\}.$$

Similarly, there are 2 cut diagrams with soft fermion loops:

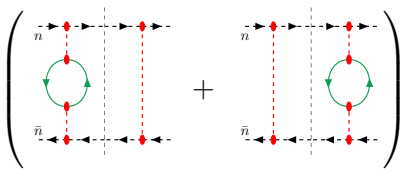

$$= -\mathcal{M}^{(-)(0)} \frac{C_A\, T_F n_f \alpha_s^2}{\pi} \frac{\Gamma(2-\epsilon)^2}{\Gamma(4-2\epsilon)} \Gamma(\epsilon) B(1,1+\epsilon) \left(\frac{\bar{\mu}^2}{-t}\right)^{2\epsilon}. \tag{4.30}$$

Here, $B(a,b)$ is the coefficient of the one-loop bubble integral in $2-2\epsilon$ dimensions:

$$(4\pi)^{-\epsilon} \int \frac{[d^{2-\epsilon}k_\perp]}{[\vec{k}_\perp^2]^a [(\vec{k}_\perp + \vec{q}_\perp)^2]^b} = \frac{B(a,b)}{4\pi} (\vec{q}_\perp^2)^{1-\epsilon-a-b}, \tag{4.31}$$

with

$$B(a,b) = \frac{\Gamma(1-a-\epsilon)\Gamma(1-b-\epsilon)\Gamma(-1+a+b+\epsilon)}{\Gamma(a)\Gamma(b)\Gamma(2-a-b-2\epsilon)}. \tag{4.32}$$

Lastly, we move onto the cut H-graph. The uncut H-graph was computed in [143], and the cut graph is almost identical. We have

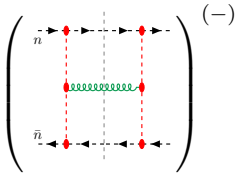

$$= -\mathcal{M}^{(-)(0)} \frac{C_A^2 \alpha_s^2}{16\pi} \frac{\Gamma(\eta/2)\Gamma(1/2-\eta/2)}{\sqrt{\pi} 2^\eta} \left(\frac{\bar{\mu}^2}{-t}\right)^{2\epsilon} \left(\frac{\nu^2}{-t}\right)^{\eta/2} \tag{4.33}$$

$$\times \left[B_2(\eta/2) e^{-2\gamma_E \epsilon} - 2B(1,1)B(1+\eta/2, 1+\epsilon)\right].$$

B_2 is the coefficient of a two-loop bubble integral:

$$e^{2\gamma_E \epsilon} \int \frac{[d^{d'}k_{1\perp}][d^{d'}k_{2\perp}]}{\vec{k}_{1\perp}^2 \vec{k}_{2\perp}^2 (\vec{k}_{1\perp} - \vec{q}_\perp)^2 (\vec{k}_{2\perp} - \vec{q}_\perp)^2 [(\vec{k}_{1\perp} - \vec{k}_{2\perp})^2]^{\eta/2}} = \frac{B_2(\eta/2)}{(4\pi)^{2-2\epsilon}} (\vec{q}_\perp^2)^{-2-2e-\eta/2}. \tag{4.34}$$

To linear order in η, B_2 is given by [113, 118]

$$\begin{aligned} B_2\left(\frac{\eta}{2}\right) &= B(1,1)^2\, e^{2\gamma_E \epsilon} + \frac{\eta}{2}\Bigg(B(1,1)^2\, e^{2\gamma_E \epsilon} \left(\psi^{(0)}(1+2\epsilon) - \psi^{(0)}(-\epsilon)\right) \\ &\quad + \frac{\Gamma(-\epsilon)^2 \Gamma(-1-\epsilon)\Gamma(2\epsilon)}{\Gamma(-1-3\epsilon)}\, {}_3F_2\left(1,1,-2\epsilon; 1-2\epsilon, 2+\epsilon; 1\right)\Bigg) + O(\eta^2), \\ &= B(1,1)^2\, e^{2\gamma_E \epsilon} + \frac{\eta}{2}\left(-\frac{1}{\epsilon^3} + \frac{\zeta(2)}{\epsilon} - \frac{76\zeta(3)}{3} + O(\epsilon)\right) + O(\eta^2). \end{aligned} \tag{4.35}$$

Adding up the cut graphs, we then have

$$\begin{aligned}\text{Cut graphs} =&\mathcal{M}^{(-)(0)}\left(\frac{\pi}{2}\right)\left(\frac{\alpha_s}{4\pi}\right)^2\left(\frac{\mu^2}{-t}\right)^{2\epsilon}\Bigg[-\left(\frac{1}{\eta}+\frac{1}{2}\log\frac{\nu^2}{-t}\right)\left(2\alpha^{(1)}\right)^2+\frac{8C_A^2}{\epsilon^3}-\frac{22C_A^2}{\epsilon^2}\\&+\frac{8C_A\,T_Fn_f}{\epsilon^2}-\frac{134C_A^2}{3\epsilon}+\frac{4C_A^2\zeta(2)}{\epsilon}+\frac{40C_A\,T_fn_f}{3\epsilon}-\frac{808C_A^2}{9}-22C_A^2\zeta(2)\\&+\frac{68C_A^2}{3}\zeta(3)+\frac{224C_A\,T_Fn_f}{9}-8C_A\,T_Fn_f\zeta(2)\Bigg].\end{aligned}\tag{4.36}$$

where $\alpha_1=-\gamma_{(1,1)}\frac{4\pi}{\alpha}$. The cut graphs are rapidity divergent only because we have not included the collinear contributions. Nonetheless the Eq.(4.17) assures us that the LHS of Eq.(4.24) will also be rapidity divergent. From the two loop formula in Eq. (4.24), we then find that the two-loop RAD to be given by

$$\begin{aligned}\gamma^{(2)}_{(1,1)}=&\left(\frac{\alpha_s}{4\pi}\right)^2C_A\left(\frac{\mu^2}{-t}\right)^{2\epsilon}\Bigg[-\frac{11C_A}{3\epsilon^2}+\frac{4n_fT_F}{3\epsilon^2}-\frac{67C_A}{9\epsilon}+\frac{2C_A}{\epsilon}\zeta(2)+\frac{20T_Fn_f}{9\epsilon}\\&-\frac{404C_A}{27}+\frac{11C_A}{3}\zeta(2)+2C_A\zeta(3)+\frac{112T_Fn_f}{27}-\frac{4T_Fn_f}{3}\zeta(2)\Bigg].\end{aligned}\tag{4.37}$$

This agrees with the standard result [87, 85, 86, 37], after accounting for different choices of normalization. As a further check, we can expand our results to $O(\epsilon^2)$ and compare with the results given in [89], where we again find agreement.

4.5.3 The Role of the Collinear Modes

Notice that when we calculated the cut diagrams we did not include collinear contributions we will not show dont contribute to $\gamma^{(2)}_{(1,1)}$. In [143, 93] it was argued that in the planar limit, all collinear functions $J_{\kappa(i)}$ must reduce to something proportional to $\mathcal{M}_1$. That is, there is no convolution and the result must lead to a Regge pole. Intuitively this follows from the collapse rule which tells us that Glaubers come in a burst and can only be connected to one collinear line. As such, the contribution to the collinear function from planar graphs only depends upon the physical transverse momentum exchanges $q_\perp$ and serves to reproduce the iterative term $\mathcal{M}_1^{(-)}\gamma^{(1)}_{(1,1)}$ in Eq.(4.24). We now show how this comes about by way of an

example. Consider the planar double Glauber vertex correction graph:

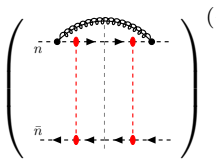

$$= \mathcal{M}_1^{(-)(0)} \frac{C_A}{4}(8\pi\alpha_s) \int \bar{d}^d k\, \bar{d}^d \ell \frac{\mathcal{N}(\ell)}{\vec{k}_\perp^2 (\vec{k}_\perp + \vec{q}_\perp)^2 (\ell+p)^2 (\ell+p+q)^2}$$

$$\times (2\pi)^3 \delta_+(\ell^2)\, \bar{n}\cdot(p+\ell)\, \delta_+\left((p+k+\ell)^2\right)\, n\cdot p'\, \delta_+\left((p'+k)^2\right). \quad (4.38)$$

Here ℓ is the collinear loop momentum, and k is the Glauber loop momentum. $\mathcal{N}(\ell)$ is the numerator, and it is independent of k regardless of whether the collinear projectiles are gluons or quarks. Therefore the only k-dependence in the integrand is in the Glauber propagators and the delta functions, and we can integrate over k to obtain

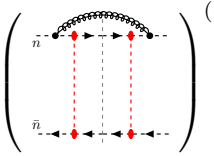

$$= \mathcal{M}_1^{(-)(0)} \frac{C_A}{4}(8\pi\alpha_s) \frac{B(1,1)}{2(4\pi)} \left(\frac{\bar{\mu}^2}{-t}\right)^\epsilon \int \bar{d}^d \ell\, \frac{\mathcal{N}(\ell)\,\theta(-\bar{n}\cdot\ell)\,(2\pi)\delta_+(\ell^2)}{((\ell+p)^2(\ell+p+q)^2}, \quad (4.39)$$

$$= \left[\pi\gamma^{(1)}_{(1,1)}\right] \left(\mathcal{M}_1^{(-)(0)} \int \bar{d}^d \ell\, \frac{\mathcal{N}(\ell)\,\theta(-\bar{n}\cdot\ell)\,(2\pi)\delta_+(\ell^2)}{(\ell+p)^2(\ell+p+q)^2}\right).$$

If we now turn to the one-loop collinear contribution to $\mathcal{M}^{(-)}_{(1)}$, we find

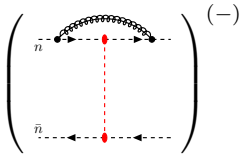

$$= \mathcal{M}_1^{(-)(0)} (-i) \int \bar{d}^d \ell\, \frac{\mathcal{N}(\ell)}{(\ell+p)^2(\ell+p+q)^2 \ell^2}. \quad (4.40)$$

This is almost identical to the term in the round brackets in Eq. (4.39), and indeed they are equal. We can see this by doing the contour integration over $n\cdot\ell$ in Eq. (4.40) Thus we have

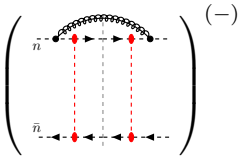

$$= \left[(i\pi)\gamma^{(1)}_{(1,1)}\right] \times$$

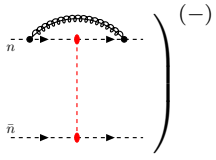

(4.41)

which matches exactly with what we expect for the one-loop iterative terms. An identical set of manipulations work for the other collinear planar graph.

Let us consider the two-loop non-planar collinear cut graphs. These must give a vanishing contribution if we wish to maintain a Regge pole behavior.

These have vanishing contributions to the odd-signature amplitude:

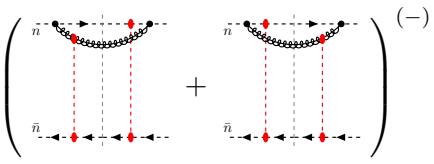

$$= 0. \tag{4.42}$$

4.6 Bootstrapping the Anomalous Dimensions

4.6.1 Determining $\gamma^{(1)}_{(2,2)}$ from $\gamma^{(1)}_{(1,1)}$ in the octet channel

Consider the following form of the master formula at second order in the coupling

$$\begin{aligned}\left(\gamma^{(1)}_{(1,1)}\right)^2 \mathcal{M}_1^{(-)(0)} &= \frac{2}{\pi^2}\left[\left(e^{i\pi\bar{K}_z}-1\right)\mathcal{M}^{(-)}_{\geq 2}\right]^{(2)}, \\ &= \frac{2i}{\pi}\gamma^{(1)}_{(2,2)} \otimes \mathcal{M}^{(-)(0)}_{\geq 2},\end{aligned} \tag{4.43}$$

where the second line is defined as

$$\begin{aligned}\gamma^{(1)}_{(2,2)} \otimes \mathcal{M}^{(-)(0)}_{\geq 2} = \frac{i}{2} J^{(0)(s)A_1A_2}_{\kappa(2)} \otimes \Big(\gamma^{A_1A_2;B_1B_2}_{(2,2)} \otimes S^{(0)(s)B_1B_2;D_1D_2}_{(2,2)} + S^{(0)(s)A_1A_2;C_1C_2}_{(2,2)} \otimes \gamma^{C_1C_2;D_1D_2}_{(2,2)}\Big) \\ \otimes \bar{J}^{(0)(s)D_1D_2}_{\kappa'(2)} - (s \leftrightarrow u).\end{aligned} \tag{4.44}$$

Here we repristinated the color indices as they will play in important role in our analysis. Now we would like to ask what constraints does this equation put on $\gamma_{(2,2)}$? At this order both the soft function and the jet functions are trivially given by (6.17) and (6.19) respectively. In Eq. (4.43) both side of the equation are projected down to the 8_A irrep. due to the minus signature.

Thus Eq. (4.43) is given by

$$\left(\frac{\bar{\mu}^2}{-t}\right)^{2\epsilon} \frac{(C_A\alpha_s)^2}{(4\pi)^2} B[1,1]^2 \mathcal{M}_1^{(-)(0)} = g^4 \frac{2}{\pi}\frac{C_A}{2}\mu^{4\epsilon}\mathcal{M}_0^{(-)}\frac{(q_\perp^2)}{16\pi\alpha_s}\int \frac{[d^{d'}l_\perp]}{l_\perp^2(l_\perp-q_\perp)^2}\frac{[d^{d'}k_\perp]}{k_\perp^2(k_\perp-q_\perp)^2}\gamma^8_{(2,2)}(k_\perp,l_\perp,q_\perp), \tag{4.45}$$

We immediately notice a remarkable simplification. The LHS is proportional to $B[1,1]^2$, which implies that the integral projects out the piece of $\gamma^{8_A}_{(2,2)}$ which is independent of $k_\perp$ and $l_\perp$, since any non-trivial dependence on these variables would necessarily, by dimensional

analysis, lead to terms proportional to $B[1,1+\epsilon]$. So we are left with the relation

$$\begin{aligned}\left(\frac{\bar{\mu}^2}{q_\perp^2}\right)^{2\epsilon}\frac{(\alpha_a C_A)^2}{(4\pi)^2}B[1,1]^2\mathcal{M}_0^{(-)} &= \frac{g^4}{\pi}C_A\mu^{4\epsilon}\frac{(q_\perp^2)}{16\pi\alpha_s}\int\frac{[d^{d'}l_\perp]}{l_\perp^2(l_\perp-q_\perp)^2}\frac{[d^{d'}k_\perp]}{k_\perp^2(k_\perp-q_\perp)^2}\gamma^8_{(2,2)}(q_\perp)\mathcal{M}_0^{(-)} \\ &= \frac{g^4}{\pi}C_A\mu^{4\epsilon}\frac{(q_\perp^2)}{16\pi\alpha_s}((4\pi)^{-1+\epsilon}(q_\perp^{-2-2\epsilon}B[1,1])^2\gamma^8_{(2,2)}(q_\perp)\mathcal{M}_0^{(-)}\end{aligned} \tag{4.46}$$

Therefore

$$\gamma^{8P}_{(2,2)} = C_A\alpha_s q_\perp^2 \tag{4.47}$$

where the P reminds us that in principle there are other terms in $\gamma^8_{(2,2)}$ whose integral yields zero in Eq. (4.46). Note that the fact that the convolutive piece gets projected out implies that there is a power law (Regge pole) solution at NLL in accordance with Eq.(4.1). We can now see how the running up to NLL reproduces the form of (4.1). The RRG equation for $J^{A_1A_2 8_A}$ is given by

$$\begin{aligned}\nu\frac{d}{d\nu}J^{A_1A_2 8_A}(k_\perp) &= \int\frac{[d^{d'}k_\perp]}{k_\perp^2(k_\perp-q_\perp)^2}\gamma_{(2,2)}(k_\perp,q_\perp)J^{A_1A_2 8_A}(k_\perp) \\ &= \gamma_{(1,1)}\ J^{A_1A_2 8_A},\end{aligned} \tag{4.48}$$

which had to be the case if Eq.(4.1) is to hold.

If we want to predict the full $\gamma_{(2,2)}$ we need some additional data, which can be gleaned by recalling that that $J^{A_1A_2 8_A}$ can be factorized into a time ordered product of two O_n^{qB} operators defined in Eq.(2.85)

$$J^{A_1A_2 8_A}(k_\perp) = \int dx_1^\pm dx_2^\pm \langle p \mid T(O_n^{qA_1}(k_\perp,x_1^\pm)O_n^{qA_2}(k_\perp-q_\perp,x_2^\pm)\mid p'\rangle^{8_A}, \tag{4.49}$$

This operator will run due to the anomalous dimensions of the individual $O_n^{qA_1}$, as well as an additional renormalization due to the semi-local nature of the operator. The key distinction between the two types of renormalizations is that the former will not generate any convolution while the ladder will. The anomalous dimensions of $O_n^{qA_1}$ were calculated in [159],

$$\gamma_{O_n^q} = \gamma_{(1,1)} \tag{4.50}$$

which is as we would expect for one Glauber exchange. We will generate such contribution to the anomalous dimensions from each of the Glaubers, the first of which carries momentum $k_\perp$ and the other $k_\perp - q_\perp$. These contributions are shown in the first two diagrams of figure (3).

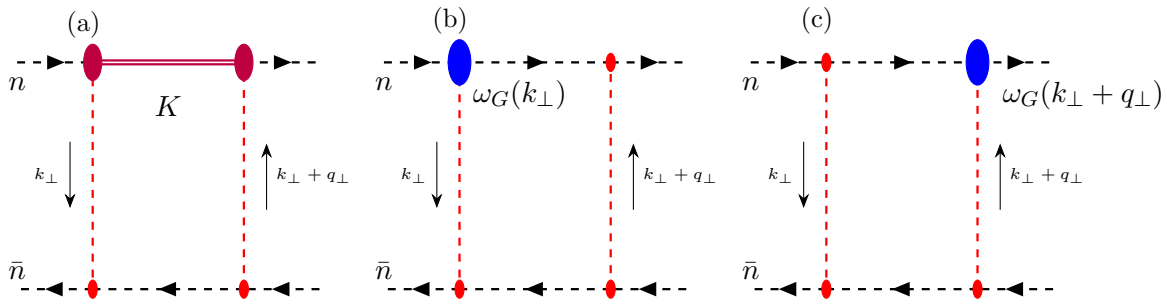

Figure 4.3: A diagramatic representation of $\gamma_{(2,2)}$. In (a), the red line stretching between the two Glauber exchanges represents the convolutive term k of the anomalous dimension, while the blue dots in (b) and (c) represent insertion of the Regge trajectory.

In addition there is another contribution to $\gamma_{(2,2)}$ stemming from diagrams that are of the form of the last diagram in figure (3) which span both exchanges and lead to a non-trivial convolution. Thus we make the following ansatz for the two Glauber jet RRG equation

$$\nu\frac{d}{d\nu}J^{A_1A_2 8_A}(l_\perp) = \int [d^{2-2\epsilon}k]\left[\delta^{2-2\epsilon}\left(k_\perp - l_\perp\right)(\gamma_{(1,1)}(k_\perp) + \gamma_{(1,1)}(k_\perp - q_\perp)\right) + K(l_\perp, k_\perp)\right] J^{A_1A_2 8_A}(k_\perp). \tag{4.51}$$

Now we can fix $K(l_\perp, k_\perp)$ by imposing that Eq.(4.46) be obeyed and find

$$K(l_\perp, k_\perp) = \alpha_s C_A\left[-\frac{l_\perp^2}{k_\perp^2(l_\perp - k_\perp)^2} - \frac{(q_\perp - l_\perp)^2}{k_\perp^2(k_\perp - q_\perp + l_\perp)^2} + \frac{q_\perp^2}{k_\perp^2(q_\perp - k_\perp)^2}\right]. \tag{4.52}$$

which agrees with the explicit calculation performed in [93]. We have thus shown that we can fix the full two Glauber octet anomalous dimension directly from the one Glauber operator. That this had to happen for the integrated anomalous dimension assuming the result in Eq.(4.1), but that the full result could follow from the one Glauber operator is a new result as far as we are aware.

4.6.2 Constraining Other Color Channels from Positive Signature Amplitudes

Let us now explore the information stored in the positive signature amplitude relation Eq.(4.18)

$$\left(e^{i\pi\bar{K}_z} - 1\right)\mathcal{M}^{(+)} = -2\mathrm{Re}[\mathcal{M}^{(+)}]. \tag{4.53}$$

We garner new information from this result since the minus signature is not sensitive to channels other than the octet at the two Glauber level. The plus signature amplitude starts at two Glauber exchange at order α^2 however this contribution if purely imaginary. Thus

the RHS of Eq.(4.18). starts at $O(\alpha^3)$ i.e. two loops.

$$\frac{4i}{\pi}\,\mathrm{Re}[\mathcal{M}]^{(2)(+)} = ((J^{(0)}_{\kappa(2)}\otimes\gamma^{(1)(1,8_S)}_{(2,2)})\otimes S^{(0)}_{(2,2)}\otimes\bar{J}^{(0)}_{\kappa'(2)}+(J^{(0)}_{\kappa(i)}\otimes S^{(0)}_{(2,2)}\otimes(\gamma^{(1)(1,8_S)}_{(2,2)}\otimes\bar{J}^{(0)}_{\kappa'(2)}))+(s\to u), \tag{4.54}$$

Only the 8_S and singlet representation in the decomposition $3\otimes\bar{3}$ contribute for quark states. Extracting the LHS from the full theory calculations [45, 97, 5], and using the known results for $\gamma^{8_S}_{(2,2)}$ (a Regge pole) and singlet (Regge cut)[107] leads to agreement with Eq.(4.54). By calculating the amplitude up to order ϵ^2, we can use the same strategy as in the case of the 8_A to determine the singlet and 8_S as well.

Notice that this method of calculation does not arise from a cut diagram and thus lacks that calculational advantages of the negative signature case. But it does lead to significant simplification relative to the canonical method of calculating the anomalous dimensions from the $1/\eta$ pole in that there is no need for a rapidity regulator since one can simply use the full theory result. Of course the full theory result involves many more diagrams than the EFT which can isolate the sources of the rapidity divergence.

We may generate other sum rules at higher order as well. At three loops $O(\alpha^4)$ the RRGE involves mixing between different $\mathcal{M}_{(i,j)}$, so to facilitate this we introduce the notation

$$\gamma_{(i,j)}\otimes\mathcal{M}^{(+)}_{(i,j)} = \frac{1}{2}J^{(s)}_{\kappa(i)}\otimes\left(S_{(i,k)}\otimes\gamma_{(k,j)}+\gamma_{(i,k)}\otimes S_{(k,j)}\right)\otimes\bar{J}^{(s)}_{\kappa'(j)}+(s\leftrightarrow u).$$

Then the two loop even signature formula at NLO is given by

$$\begin{aligned}-2\,\mathrm{Re}[\mathcal{M}]^{(3)} =& i\pi\Big[\gamma^{(2)}_{(2,2)}\otimes\mathcal{M}^{(+)(0)}_{(2,2)}+\gamma^{(1)}_{(3,3)}\otimes\mathcal{M}^{(0)}_{(3,3)}+\gamma^{(1)}_{(2,3)}\otimes\mathcal{M}^{(+)(0)}_{(2,3)}\\ &+\gamma^{(1)}_{(2,2)}\otimes\mathcal{M}^{(+)(1)}_{(2,2)}+\frac{i\pi}{2!}\gamma^{(1)}_{(2,2)}\otimes\gamma^{(1)}_{(2,2)}\otimes\mathcal{M}^{(+)(0)}_{(2,2)}\Big].\end{aligned} \tag{4.55}$$

We can generate two constraints by considering the real and imaginary parts since the anomalous dimension are purely real and the Glauber loops are are purely imaginary,

$$\gamma^{(2)}_{(2,2)}\otimes\mathcal{M}^{(+)(0)}_{(2,2)}+\gamma^{(1)}_{(2,2)}\otimes\mathcal{M}^{(+)(1)}_{(2,2)} = \frac{2i}{\pi}\,\mathrm{Re}[\mathcal{M}]^{(3)} \tag{4.56}$$

$$\gamma^{(1)}_{(3,3)}\otimes\mathcal{M}^{(0)}_{(3,3)}+\gamma^{(1)}_{(2,3)}\otimes\mathcal{M}^{(+)(0)}_{(2,3)}+\frac{i\pi}{2!}\gamma^{(1)}_{(2,2)}\otimes\gamma^{(1)}_{(2,2)}\otimes\mathcal{M}^{(+)(0)}_{(2,2)} = 0. \tag{4.57}$$

Note that $\mathcal{M}_{(2,3)}$ is purely real as it contains two Glauber loops. Here both formulas provide non-trivial relations about the various anomalous dimensions. In particular, Eq. (4.57) provides an interesting relation between the one-loop anomalous dimensions that appear at this order, while Eq. (4.56) contains the information for the two loop $\gamma_{(2,2)}$. Notably, Eq.

(4.57) constrains terms with different numbers of convolution integrals. However, unlike the lower order relation, in this case there are many color channels (multiple singlets and octets) which will mix.

4.7 Discussion

In this paper, we have uncovered further structure in the two to two scattering amplitude in the Regge limit. This has been accomplished by working with the EFT for near forward scattering in a double expansion in α and t/s which allows us always work with well defined gauge invariant matrix elements. We have demonstrated that anomalous dimensions can be extracted via cut diagrams thus effectively reducing the loop order. Our result (4.17) generalizes the result in [143] in that it works at all orders and for all color channels. We have also shown that the two Glauber rapidity anomalous dimensions can be bootstrapped from the one Glauber case. These results follow from a combination of factorization, unitarity and crossing symmetry. We have given generalized relations between amplitude and anomalous dimension for both the positive and negative signature amplitudes, each of which generates a separate set of constraints on the anomalous dimension. The positive signature constraint allowed us to simply extract the 8_A channel two Glauber anomalous dimensions and our result agree with those in [107, 93].

It would be interesting to use this formalism to compute the three loop Regge trajectory. Progress in this direction has been made within the context of Reggeon field theory [89]. It seems reasonable to believe that our results genearted in the context of an EFT of QCD could also yield insights into the Reggeon approach. In the EFT approach using our formalism should help significantly reduce the complexity of the calculation, reducing most of the work to computing $\mathcal{M}_1^{(-)}$ through two loops. In fact, the full three loop QCD amplitude is known, and so in principle one could avoid computing the cut by simply extracting the imaginary part.

Another avenue worth pursuing is to explore the even signature formula. In principle, one could use this for a very clean derivation of the leading order BFKL equation, and as a useful probe of the mixing between different Glauber operators at next to leading order and beyond. At three loops, one has matrix elements that are both imaginary, such as $S_{(2,2)}$, and real, such as $S_{(3,3)}$, and so one may be able to find interesting relations between anomalous dimensions that appear at different orders through iterative terms.

Chapter 5

SCET Gravity and Graviton Glauber Operators

We now turn our attention from QCD to gravity. In this chapter, we describe the extension of SCET to gravity. First, we give an overview of the SCET gravity building blocks, after which we give the construction and matching of the SCET gravity Glauber Lagrangian. This chapter is based on the appendices of [155].

5.1 The EFT and Gauge Symmetry

We are interested in constructing SCET for a massless real scalar minimally coupled to the graviton. The full theory action for this is given by

$$S = S_{\text{Scalar}} + S_{\text{EH}}, \tag{5.1}$$

where the scalar action is given as

$$S_{\text{Scalar}} = \frac{1}{2}\int d^d x\sqrt{-g}\frac{1}{2}g^{\mu\nu}\partial_\mu\phi\partial_\nu\phi, \tag{5.2}$$

and the graviton action is the usual Einstein Hilbert action,

$$S_{\text{EH}} = 2M_{\text{Pl}}^d\int d^4x\sqrt{-g}R, \tag{5.3}$$

with R being the Ricci scalar. The EFT we construct will be an expansion in the small parameter $\lambda^2 = -t/s$, just as in QCD. To control the loop expansion, we take $\alpha_Q = -\kappa^2 t \sim \lambda^0$, where $\kappa^2 = 16\pi G = 1/2M_{\text{Pl}}^2$. $\alpha_Q \ll 1$ plays the same role as α_s in QCD. We will save a more thorough discussion of the power-counting for the next section, and proceed with

these as given.

We will always be considering the active point of view of gauge transformations where we consider the coordinate system fixed, and the map moves points, along with the geometric structures, to other points on the manifold, leaving a physically equivalent state of the system. While the coordinates are left invariant, fields transform are not, such that, e.g. for a scalar $\phi(x)$, the diffeomorphism f acts

$$f : \phi(x) \to \phi'(f(x)), \tag{5.4}$$

or

$$\phi'(x) = \phi(f^{-1}(x)). \tag{5.5}$$

In this picture the fields are unchanged under a coordinate transformation. We use the term "diff. covariant" for such transformations.

In this picture the invariance of the Einstein-Hilbert action follows by first acting with the diffeomorphism such that the action transforms as

$$\int d^d x \sqrt{-g(x)} R(x) \to \int d^d x \sqrt{-g'(f(x))} R'(f(x)) \tag{5.6}$$

The invariance of the action then follows by changing coordinate from x to $f(x)$. We repeat this elementary definition because we will consider three types of gauge symmetries which, when we have operators connecting various sectors, necessitates careful treatment.

In the EFT each sector, soft, collinear and anti-collinear has its own diffeomorphism invariance, each of which is a subset of the full invariance group. Given a map in a fixed coordinate system $x^\mu \to x^\mu + \epsilon^\mu(x)$ the scalings of the derivatives of ϵ is restricted by the scalings of the associated components of the metric which can be either read off from the form of the two point function in a covariant gauge [1], or by imposing consistency with the Ward identity [149] such that for the collinear sectors we have the scaling

$$g_n^{\mu\nu} \sim \frac{p_n^\mu p_n^\nu}{\lambda}. \tag{5.7}$$

Imposing that the gauge transformation does not destroy this scaling imposes constraints on the momentum support of the gauge parameters $\epsilon^\mu(x)$ such that

$$\partial^\nu \epsilon_n^\mu + \partial^\mu \epsilon_n^\nu \sim \frac{p_n^\mu p_n^\nu}{\lambda}. \tag{5.8}$$

[1] Power counting in the case of non-covariant gauge fixings complicated power counting. A classic example of this arise in HQET where if one naively chooses the gauge $v \cdot A = 0$, then one might conclude that the heavy quark does not interact[133].

The gauge transformation should furthermore not push the mode outside its range of momentum support so

$$\partial^\mu \epsilon^\nu \sim p_n^\mu \epsilon^\nu. \tag{5.9}$$

so that we may further conclude that

$$\epsilon_n^\mu \sim \frac{p_n^\mu}{\lambda}. \tag{5.10}$$

It's important to keep in mind that these $\sim$ relations are only meant to equate scalings in λ. For soft gauge transformations all of the components of the gauge field scale as λ so that we have the constraint

$$\partial_\mu \epsilon_s^\nu \sim p_\mu^s \epsilon_s \sim \lambda. \tag{5.11}$$

and $\epsilon_s \sim \lambda^0$.

5.2 Gauge Invariant Building Blocks

5.2.1 The Collinear Sector

In this section we discuss the gauge invariant operator building blocks for scalar and graviton collinear operators starting with a scalar field. This is accomplished (see [75]) by considering a (codimension one null hypersurface) "platform" at minus null infinity (where diffs are no longer gauge redundancies) and shooting out a geodesic in a direction $\mu = \kappa$ orthogonal to the hypersurface which is coordinatized by $\tilde{x}^\mu$. We assumed that the point x and $\tilde{x}$ are in the same convex neighborhood such that there is unique geodesic which connects the two point. One then labels the points in the bulk as

$$x^\mu = \tilde{x}^\mu + \hat{x}^\kappa s + X^\mu(s). \tag{5.12}$$

where $X^\mu(-\infty) = 0$. $\hat{x}^\kappa$ is the unit vector orthogonal to the platform. The end-point of the geodesic in the bulk is taken at $s = 0$. In flat space $X^\mu(0) = 0$, i.e. we choose the point to be at $x^\kappa = 0$. This allows us to define a gauge invariant (geometric) quantity

$$\chi(x^\mu - X^\mu(0)). \tag{5.13}$$

Taking the point of interest (the argument of the field) to be at $s = 0$, we see that $X_n^\mu(0)$ is the change in the value of the coordinate in going to our genearalized coordinate system and is found by integrating the geodesic equation which we do order by order in the metric fluctuation. Thus we will building up gauge invariance order by order.

At second order X_n^μ is given by

$$X_n^\mu = -\frac{1}{-\bar{n}\cdot\mathcal{P}^2}\Gamma^{(1)\mu}_{++} - \frac{1}{-\bar{n}\cdot\mathcal{P}^2}\Gamma^{(2)\mu}_{++} - \frac{1}{-\bar{n}\cdot\mathcal{P}^2}\left(2\Gamma^{(1)\mu}_{\nu+}\frac{1}{-i\bar{n}\cdot\mathcal{P}}\Gamma^{(1)\nu}_{++} + \left(\mathcal{D}^n_\nu\Gamma^{\mu(1)}_{++}\right)\frac{1}{-\bar{n}\cdot\mathcal{P}^2}\Gamma^{(1)\nu}_{++}\right) + O(h_n^3). \tag{5.14}$$

In the above, $\Gamma^{(1)}$ and $\Gamma^{(2)}$ are the one and two graviton terms in the Christoffel symbols. $\mathcal{D}^n_\mu$ is the operator [2]

$$\mathcal{D}^n_\mu = -i\frac{n_\mu}{2}\bar{n}\cdot\mathcal{P} - i\mathcal{P}^\perp_\mu + \frac{\bar{n}_\mu}{2}n\cdot\partial, \tag{5.15}$$

and $\mathcal{D}^{\bar{n}}_\mu$ is defined analogously.

We then define the translation operator V_n^{-1} via

$$V_n^{-1} = 1 + X_n^\mu\mathcal{D}^n_\mu + \frac{1}{2}X_n^\mu X_n^\nu\mathcal{D}^n_\mu\mathcal{D}^n_\nu + ..., \tag{5.16}$$

Then

$$\chi_n = \left[V_n^{-1}\phi_n\right], \tag{5.17}$$

is diff. invariant order by order in metric perturbations. To leading order in the metric,

$$\chi_n = \phi_n + \frac{\kappa}{2}\left[\frac{1}{-i\bar{n}\cdot\mathcal{P}}\left(h_{n+\mu} - \frac{\mathcal{D}^n_\mu h_{n++}}{-2i\bar{n}\cdot\mathcal{P}}\right)\right]\mathcal{D}^{n\mu}\phi_n + O(\kappa^2). \tag{5.18}$$

The operators $\mathcal{P}$ only act within the brackets. Notice that we are solving the geodesic equation in an expansion in G, thus the action will only be invariant under diffs where

For a tensor field we need to additionally include a tensor to counter-act the transformation. [115], which is defined with W_n as the gravitational Wilson line, which acts on tensors T as

$$\left[W_n^{-1}T\right]^{A_1\ldots A_n}_{B_1\ldots B_m} = W_{n\,\mu'_1}{}^{A_1}\ldots W_{n\,\mu'_n}{}^{A_n}W_n{}^{\nu'_1}_{\ B_1}\ldots W_n{}^{\nu'_m}_{\ B_m}\left(V_n^{-1}T^{\mu'_1\ldots\mu'_n}_{\nu'_1\ldots\nu'_m}\right). \tag{5.19}$$

where we have defined

$$W_{n\,\nu}{}^A = \mathcal{D}^n_\nu(X_n)^A. \tag{5.20}$$

Here we have introduced some new notation, namely indices with capital Roman letters are active diffeomorphism singlets. Thus under the diff. $x^\mu \to x^\mu + \epsilon^\mu$, W_n transforms according to

$$W_n^\nu{}_B \to W_n^\nu{}_B + \partial_B\epsilon^\nu + ... \tag{5.21}$$

[2]The label operator which acts on the $O(\lambda^0)$ momentum obeys the following equivalence $\mathcal{P} = i\partial$.

In this way a vector the vector $W_{n\ B}^{\ \nu} V_\mu(\tilde{x})$ is invariant under diffs. The inverse is defied as

$$(W_n)_\nu{}^A (W_n^{-1})^\nu{}_B = \delta^A_B. \tag{5.22}$$

Let us now consider building blocks for the metric. QCD is pure connection theory where the natural building block is

$$\mathcal{B}^n_\mu = W_n^{-1} D_\mu W_n. \tag{5.23}$$

where D is in the adjoint representation. Since the Wilson line obeys $\bar{n}\cdot D W_n = 0$, only $\mathcal{B}^n_{\mu\perp}$ and $n\cdot\mathcal{B}$ are non-zero. Furthermore, using the gluon equations of motion the latter can be written in terms of the former and the matter current. For the gravitational case we can do something similar. Define the **in**variant derivative $W_n^{-1}\nabla_\mu W_n$, acting on a vector

$$\begin{aligned} W_n^{-1}\nabla_\mu W_n f_A &= W_n^{-1}\nabla_\mu (V W^A_\beta f_A) = W_n^{-1}(\partial_\mu (V W^A_{n\beta} f_A) - \Gamma^\alpha_{\mu\beta}(V W^A_{n\alpha} f_A)) \\ &= \partial_C f_B + W^{-1\beta}_{nB} W^{-1\mu}_{nC} (\partial_\mu W^A_\beta) f_A - W^{-1\mu}_{nB} W^{-1\beta}_{nC} \Gamma^\alpha_{\mu\beta}(\tilde{x}) W^A_{n\alpha} f_A \end{aligned} \tag{5.24}$$

We then defined the diff. invariant connection

$$\mathfrak{B}^A_{BC} = W^{-1\beta}_{nB} W^{-1\mu}_{nC} (\partial_\mu W^A_\beta) - W^{-1\mu}_{nB} W^{-1\beta}_{nC} W^A_{n\alpha} \Gamma^\alpha_{\mu\beta}(\tilde{x}) \tag{5.25}$$

Just as with the standard Levi-Civita connection, we may write the gauge-invariant connection in terms of gauge-invariant metrics, via

$$\mathfrak{B}^A_{BC} = \frac{1}{2}(\mathfrak{g}^{-1})^{AD}\left(\mathcal{D}_B \mathfrak{g}_{DC} + \mathcal{D}_C \mathfrak{g}_{DB} - \mathcal{D}_D \mathfrak{g}_{BC}\right). \tag{5.26}$$

The gauge-invariant metrics (and associated metric perturbations) are given as

$$\mathfrak{g}_{AB} \equiv \eta_{AB} + \frac{\kappa}{2}\mathfrak{h}_{nAB} = \left[W_n^{-1} g_n\right]_{AB}, \tag{5.27}$$

where $g_{n\mu\nu} = \eta_{\mu\nu} + \frac{\kappa}{2} h_{n\mu\nu}$ is the collinear metric. It turns out that this metric satisfies the lightcone-gauge condition [23], analagous to the QCD gluon building block.

At linearized order we have

$$\mathfrak{h}^{\perp\perp}_{nAB} = \delta^{\mu_\perp}_A \delta^{\nu_\perp}_B \left(h_{n\mu\nu} - \frac{\mathcal{P}^\perp_\mu}{\bar{n}\cdot\mathcal{P}} h_{n\nu+} - \frac{\mathcal{P}^\perp_\nu}{\bar{n}\cdot\mathcal{P}} h_{n\mu+} + \frac{\mathcal{P}^\perp_\mu \mathcal{P}^\perp_\nu}{\bar{n}\cdot\mathcal{P}^2} h_{n++}\right) + O(\kappa). \tag{5.28}$$

which all comes from the Jacobian factors at this order, as the translational piece is quadratic in the field. The transverse components of the metric have been picked out. In SCET

[19], the other, non-vanishing[3] (non-transverse) components can be eliminated using a field redefinition. In the present case [23] $\mathfrak{h}_{n++} = \mathfrak{h}_{n+\mu} = 0$ due to the tethering of the field to infinity, as may be checked by using eqs. (5.19) and (5.14). Notice that the one graviton term in the graviton building block is proportional to the $+ \perp + \perp$ component of the linearized Riemann tensor, which is manifestly gauge-invariant under small diffs.

In SCET, once the operator building blocks have been fixed, writing down the relevant Glauber operators is relatively simple in that each building blocks scales with a non-zero power of λ, but in gravity this is no longer the case. Every insertion of $\mathfrak{h}_n$ beyond the first is accompaniied by a factor of κ, and since $\kappa^2 t \sim \alpha_Q \lambda^0$ in our power-counting, the combination $\kappa\, \mathfrak{h}_n \sim \alpha_Q^{1/2} \lambda^0$. Thus one can insert an arbitrary number of graviton blocks into an operator without changing the λ scaling or mass-dimension. In other words we may consider any polynomial in $\mathfrak{h}_{nAB}$ as a building block. At first this may not seem like a big concern since, as discussed in the introduction, we can calculate beyond two loops in α_Q before we run into model dependent counter-term contributions of the same size. Nonetheless we might be interested say in calculating in $N = 8$, where it is perhaps true that there are no counter-terms [4], in which case the calculation would remain predictive to all orders in α_Q.

We will in fact show that, constraints from diffeomorphism will fix the functional dependence of operators on $\mathfrak{h}_n$ since in the full theory metric perturbations arise either as a full metric tensor (i.e. $\eta + h$) or inverse metric tensor; therefore, the graviton building blocks can only come in the combinations

$$\begin{aligned} \mathfrak{g}_{nAB} &\equiv \eta_{AB} + \frac{\kappa}{2}\mathfrak{h}_{nAB}, \\ (\mathfrak{g}_n^{-1})^{AB} &\equiv \eta^{AB} - \frac{\kappa}{2}\mathfrak{h}^{AB} + O(\kappa^2). \end{aligned} \tag{5.29}$$

Thus in the absence of counter-terms beyond the Einstein-Hilbert action, we will still maintain predictive power.

We also know that in the full theory we build invariant operators out of covariant derivatives. Thus we expect the effective theory operators to be built from invariant forms of the connection. With this in mind we introduce the function of the building block $\mathfrak{h}_{nAB}$

$$\mathfrak{B}_n{}_B^A = \delta_\mu^A \delta_B^\nu \Big(\frac{2}{\kappa}\frac{\bar{n}^\alpha}{\bar{n}\cdot\mathcal{P}}\left[\frac{1}{2}(\mathfrak{g}_n^{-1})^{\mu\lambda}\left(\mathcal{D}_\alpha \mathfrak{g}_{n\lambda\nu} + \mathcal{D}_\nu \mathfrak{g}_{n\lambda\alpha} - \mathcal{D}_\lambda \mathfrak{g}_{n\alpha\nu}\right)\right]\Big). \tag{5.30}$$

This is the simply the + component of the Levi-Civita symbol built out of gauge-invariant metric building blocks. Using the metric compatibility condition implies we can write this

[3] The analogous field in QCD will be in the light cone gauge as well.

[4] Presently $N = 8$ is known to be finite up to five loops [**Bern˙2018**].

as

$$\mathfrak{B}_{n\,B}^{\;A} = \frac{2}{\kappa}\frac{1}{\bar{n}\cdot\mathcal{P}}(\mathfrak{g}_n^{-1})^{AC}\bar{n}\cdot\mathcal{P}\mathfrak{g}_{nCB}. \tag{5.31}$$

The $\mathfrak{B}_n$'s have the same λ scaling and mass dimension as the $\mathfrak{h}_n$'s, and differ only at $O(\kappa)$. They also inherit the useful properties of the $\mathfrak{h}_n$ building blocks. In particular, $\mathfrak{B}_{n\,A}^{\;+} = 0$ and $\mathfrak{B}_{n+}^{\;\;A} = 0$, which follows from the lightcone gauge condition $\mathfrak{h}_{n+\mu} = 0$. These also have vanishing trace. We will see that this operator (function of $\mathfrak{h}_{nAB}$) will naturally arise in the matching.

5.2.2 The Soft Sector

In the soft sector, we will just see the appearance of soft Wilson lines S_n, which are defined similarly to Eq. (5.19):

$$\left[S_n^{-1}T\right]_{B_1\ldots B_m}^{A_1\ldots A_n} = S_{n\,\mu_1'}^{\;\;A_1}\ldots S_{n\,\mu_n'}^{\;\;A_n}S_{n\;B_1}^{\;\;\nu_1'}\ldots S_{n\;B_m}^{\;\;\nu_m'}\left(Z_n^{-1}T_{\nu_1'\ldots\nu_m'}^{\mu_1'\ldots\mu_n'}\right), \tag{5.32}$$

with

$$\begin{aligned}
Z_n^{-1} &= 1 + X_{Sn}^{\mu}(-i\mathcal{P}_{S\mu}) + \frac{1}{2}X_{Sn}^{\mu}X_{Sn}^{\nu}(-i\mathcal{P}_{S\mu})(-i\mathcal{P}_{S\nu}) + \ldots, \\
S_{n\nu}^{\;\;A} &= (-i\mathcal{P}_{S\nu})(x + X_{Sn})^A, \\
X_{Sn}^{\mu} &= -\frac{1}{-n\cdot\partial_S^2}\Gamma_{--}^{(1)\mu} - \frac{1}{n\cdot\partial_S^2}\Gamma_{--}^{(2)\mu} - \frac{1}{n\cdot\partial_S^2}\left(2\Gamma_{\nu-}^{(1)\mu}\frac{1}{n\cdot\partial_S}\Gamma_{--}^{(1)\nu} + \left(-i\mathcal{P}_{S\nu}\Gamma_{--}^{\mu(1)}\right)\frac{1}{n\cdot\partial_S^2}\Gamma_{--}^{(1)\nu}\right) + O(h_s^3).
\end{aligned} \tag{5.33}$$

The soft label operator $\mathcal{P}_S$ is written as

$$\mathcal{P}_S^{\mu} = \frac{\bar{n}^{\mu}}{2}n\cdot i\partial_S + \frac{n^{\mu}}{2}\bar{n}\cdot i\partial_S + \mathcal{P}_{\perp}^{\mu}, \tag{5.34}$$

where all of the components are $O(\lambda)$. Notice that when acting on collinear fields $\mathcal{P}_S^{\mu}$ will only act upon the transverse momentum.

5.2.3 Useful Wilson Line Identities

Here we list some useful properties of the gravitational Wilson lines that will be utilized in the matching procedure. These are presented in Appendix C of [23], but we reproduce them here for completeness. Firstly, the Wilson lines satisfy a "Product Rule":

$$[W_n\phi_1\phi_2] = [W_n\phi_1][W_n\phi_2], \tag{5.35}$$

where the square brackets denote that the Wilson line operator only acts on the terms enclosed in the square brackets. This result follows from the fact that the Wilson line is a

translation operator and we may consuder the project of two tensors an just a single tensor. Similarly, there is an integration by parts (distributional) identity,

$$[W_n^{-1}T_1]\,T_2 = \det(W_n)\,T_1\,[W_n(T_2)], \tag{5.36}$$

where $\det(W_n)$ is the determinant of the Jacobian matrix. These identities are obeyed by the soft Wilson lines as well. This latter identity will be important for the construction of the soft graviton operator and follows from peforming a change of coordinates. This identity implies a factor of the determinant of the Jacobian always appears with inverse Wilson lines; it is therefore useful to package the determinant together with the Jacobian determinant.

5.3 Matching the Glauber Lagrangian

We begin by presenting the matching of the Glauber operator at tree level. The Glauber operators are constructed by considering the scattering of projectiles in two distinct rapidity sectors of $\{n, \bar{n}, s\}$, and the projectiles may be taken to be either scalars or gravitons.

5.3.1 Collinear Glauber Operators

We start by considering n-$\bar{n}$ scattering, collinear soft scattering will follow in a similar fashion. We perform the matching using the same conventions as [159], where the external lines are chosen to be $\phi(p_2^n) + \phi(p_1^{\bar{n}}) \to \phi(p_3^n) + \phi(p_4^{\bar{n}})$, where the superscript denotes the collinear sector of each momentum. All calculations are in the de Donder gauge, and we write the polarization tensors for $h = \pm 2$ as products of spin-1 polarization vectors on shell

$$\epsilon_\pm^{\mu\nu}(p_i) = \epsilon_\pm^\mu(p_i)\epsilon_\pm^\nu(p_i), \tag{5.37}$$

and we will suppress the $\pm$ label. To simplify notation further, we write $\epsilon^\mu(p_i) \equiv \epsilon_i^\mu$. For the on-shell states we are considering, we also have $\epsilon_i^2 = 0$ and $p_i \cdot \epsilon_i = 0$.

For the chosen kinematics, momentum conservation gives $p_1 + p_2 = p_3 + p_4$. The momentum transfer is given by $q = p_3 - p_2 = p_1 - p_4$. For n-$\bar{n}$ scattering the Glauber momentum scales as $q^\mu \sim (\lambda^2, \lambda^2, \lambda)$. This then implies that the large $\sim \lambda^0$ components of the collinear momenta are conserved, giving $p_2^+ = p_3^+$ and $p_1^- = p_4^-$. We choose to work in a frame where $q^+ = q^- = 0$, which allows us to write the momenta as

$$\begin{aligned} p_1^\mu &= \frac{\bar{n}^\mu}{2}p_1^- + \frac{n^\mu}{2}p_1^+ + \frac{1}{2}q_\perp^\mu, \qquad & p_2^\mu &= \frac{\bar{n}^\mu}{2}p_2^- + \frac{n^\mu}{2}p_2^+ - \frac{1}{2}q_\perp^\mu, \\ p_3^\mu &= \frac{\bar{n}^\mu}{2}p_3^- + \frac{n^\mu}{2}p_2^+ + \frac{1}{2}q_\perp^\mu, \qquad & p_4^\mu &= \frac{\bar{n}^\mu}{2}p_1^- + \frac{n^\mu}{2}p_4^+ - \frac{1}{2}q_\perp^\mu. \end{aligned} \tag{5.38}$$

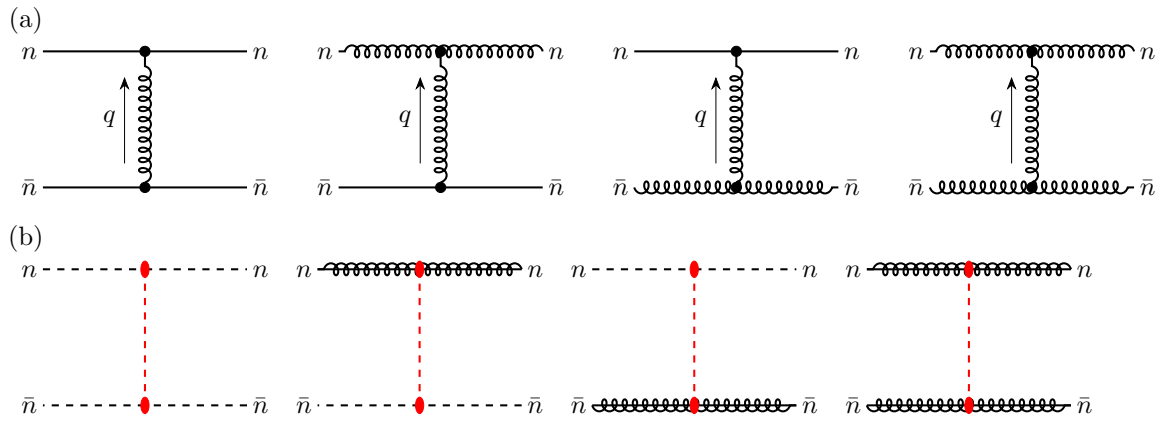

Figure 5.1: Tree level matching for n-$\bar{n}$ Glauber operators. These are the full theory diagrams with a t-channel pole. For scalar-scalar scattering this is sufficient to extract the Glauber operator, but for scalar-graviton scattering, one must also include s- and u-channel graphs, as well as the 4-point contact term. These additional contributions will be automatically accounted for order by order in expansion parameters in the EFT given that we build operators out of gauge invariant building blocks.

The on-shell condition $p_i^2 = 0$ also lets us fix the small $\sim \lambda^2$ component of the momenta, $p_1^+ = p_4^+ = -q_\perp^2/p_1^-$ and $p_2^- = p_3^- = -q_\perp^2/p_2^+$. The Mandelstam variables s and t may then be written in terms of these variables as

$$s = p_1^- p_2^+ + O(\lambda^2), \qquad t = q_\perp^2. \tag{5.39}$$

Note that the expression for s has corrections which are subleading in the power-expansion, whereas t is exact in the chosen frame of $q = q_\perp$. We have $s \sim \lambda^0$ and $t \sim \lambda^2$, and for physical kinematics $s > 0$ and $t < 0$.

We now match the Glauber operators onto the tree-level graphs shown in Fig. (5.1).

We expand each diagram to leading power in λ, and we have

$$\begin{aligned}
iM =& -i\left[\frac{\kappa}{2}\bar{n}\cdot p_2^2\right]\frac{2}{q_\perp^2}\left[\frac{\kappa}{2}n\cdot p_1^2\right], \\
&-i\left[\frac{\kappa}{2}\frac{\left(\bar{n}\cdot p_2^2\,\epsilon_2\cdot\epsilon_3-\bar{n}\cdot p_2\,p_3\cdot\epsilon_2\,\bar{n}\cdot\epsilon_3-\bar{n}\cdot p_2\,p_2\cdot\epsilon_3\,\bar{n}\cdot\epsilon_2+p_2\cdot p_3\,\bar{n}\cdot\epsilon_2\,\bar{n}\cdot\epsilon_3\right)^2}{\bar{n}\cdot p_2^2}\right]\frac{2}{q_\perp^2}\left[\frac{\kappa}{2}n\cdot p_1^2\right], \\
&-i\left[\frac{\kappa}{2}\bar{n}\cdot p_2^2\right]\frac{2}{q_\perp^2}\left[\frac{\kappa}{2}\frac{\left(n\cdot p_1^2\,\epsilon_1\cdot\epsilon_4-n\cdot p_1\,p_4\cdot\epsilon_1\,n\cdot\epsilon_4-n\cdot p_1\,p_1\cdot\epsilon_4\,n\cdot\epsilon_1+p_1\cdot p_4\,n\cdot\epsilon_1\,n\cdot\epsilon_4\right)^2}{n\cdot p_1^2}\right], \\
&-i\left[\frac{\kappa}{2}\frac{\left(\bar{n}\cdot p_2^2\,\epsilon_2\cdot\epsilon_3-\bar{n}\cdot p_2\,p_3\cdot\epsilon_2\,\bar{n}\cdot\epsilon_3-\bar{n}\cdot p_2\,p_2\cdot\epsilon_3\,\bar{n}\cdot\epsilon_2+p_2\cdot p_3\,\bar{n}\cdot\epsilon_2\,\bar{n}\cdot\epsilon_3\right)^2}{\bar{n}\cdot p_2^2}\right]\frac{2}{q_\perp^2} \\
&\qquad\times\left[\frac{\kappa}{2}\frac{\left(n\cdot p_1^2\,\epsilon_1\cdot\epsilon_4-n\cdot p_1\,p_4\cdot\epsilon_1\,n\cdot\epsilon_4-n\cdot p_1\,p_1\cdot\epsilon_4\,n\cdot\epsilon_1+p_1\cdot p_4\,n\cdot\epsilon_1\,n\cdot\epsilon_4\right)^2}{n\cdot p_1^2}\right].
\end{aligned} \tag{5.40}$$

The double copy relation [26] are manifested in the last four lines.

One may then write down the Lagrangian for Glauber operators to match the amplitudes

$$\mathcal{L}_G^{ns\bar{n}}=\sum_{n,\bar{n}}\sum_{i,j}\mathcal{O}_n^i\frac{1}{\mathcal{P}_\perp^2}\mathcal{O}_S\frac{1}{\mathcal{P}_\perp^2}\mathcal{O}_{\bar{n}}^j. \tag{5.41}$$

Here i and j run over the particle species of the projectiles, which in this case is just scalars and gravitons. To match onto the full-theory diagrams in Eq. (5.40), where there are no soft-graviton emissions. We find the collinear operators to be

$$\begin{aligned}
\mathcal{O}_n^\phi &= \frac{\kappa}{2}\chi_n^\dagger\left[\frac{\bar{n}}{2}\cdot\left(\mathcal{P}+\mathcal{P}^\dagger\right)\right]^2\chi_n(1+F[\mathfrak{h}_n,\mathfrak{B}_n]), \\
\mathcal{O}_n^h &= \frac{\kappa}{2}\left[\left((\bar{n}\cdot\mathcal{P}(\mathfrak{B}_n,\mathfrak{h}_n)_B^A\right)^2+A\left((\bar{n}\cdot\mathcal{P}(\mathfrak{B}_n,\mathfrak{h}_n)_A^A\right)^2\right]+O[\mathfrak{h}_n^3]...
\end{aligned} \tag{5.42}$$

with $\mathcal{O}_{\bar{n}}^i$ given by swapping $n\leftrightarrow\bar{n}$. With this choice of normalizations the soft operators reduces to $\mathcal{O}_S=2\mathcal{P}_\perp^2$. A is an unknown constant that can be fixed by going to higher orders in the metric. This trace term vanishes on shell at leading order in $\mathfrak{h}$ so was not detected in the on shell matching result (5.40). Notice that for the operators we have written $(\mathfrak{B}_n,\mathfrak{h}_n)$, this is because we have only matched at quadratic order in the field and at this order this is no distinction between $\mathfrak{h}_n$ and $\mathfrak{B}_n$. In the next section we will show that constraints from the full theory will fix the field to be $\mathfrak{B}_n$, that $A=-1, F=0$ and that there are no powers of the $\mathfrak{h}$ beyond quadratic.

The Glauber Lagrangian exactly reproduces the full-theory diagrams to leading power in the λ-expansion. Since $\chi_n\sim(\mathfrak{B}_n,\mathfrak{h}_n)\sim\lambda$, $\bar{n}\cdot\mathcal{P}\sim\lambda^0$, the collinear operators scale as

$\mathcal{O}_n^i \sim \kappa\lambda^2$ while for the soft operator $\mathcal{O}_S = 2\mathcal{P}_\perp^2 \sim \lambda^2$ for zero soft graviton emissions, and thus $\mathcal{L}_G^{ns\bar{n}} \sim \kappa^2\lambda^2$. Given that the measure scales as $1/\lambda^2$ we see that $S_G \sim s^2/M_{pl}^2 \sim \frac{\alpha_Q}{\lambda^2}$. The matching and construction of the full soft operator is more involved, and will be discussed in the next section.

It is interesting to see how the Ward indentities are satsified in the EFT given that when we matched we did not bother with the contact interactions that in the full theory are required to ensure they are satisified. The terms which would arise from contact terms in the full theory, arise in the EFT Ward identity from the last term in 5.28 which end up killing the factor of $1/q_\perp^2$ in the ampltiude.

5.3.2 Soft-Collinear Glauber Operators

We can perform analogous matching calculations for n-s and $\bar{n} - s$ scattering. We focus here on n-s scattering, as the results for $\bar{n}s$ scattering are given simply by replacing $n \leftrightarrow \bar{n}$. We take the n-s scattering to be given by $\phi(p_2^n) + \phi(p_1^s) \to \phi(p_3^n) + \phi(p_4^s)$. The momentum transfer q is defined identically as $q = p_3 - p_2 = p_1 - p_4$, but q now has scaling $q \sim (\lambda, \lambda^2, \lambda)$. Expanding the full-theory diagrams in these kinematics, the result is identical to eq.(5.1). For the Glauber operators, we may write the Glauber Lagrangian as

$$\mathcal{L}^{ns} = \sum_n \sum_{i,j} \mathcal{O}_n^i \frac{1}{\mathcal{P}_\perp^2} \mathcal{O}_{Sn}^j. \tag{5.43}$$

The collinear operators in $\mathcal{L}^{ns}$ are identical to those in $\mathcal{L}^{ns\bar{n}}$. The soft operators meanwhile are identical to the collinear case with the replacement of collinear fields with soft fields $\chi_{Sn}, \mathfrak{B}_{Sn}$ and $\mathfrak{h}_{Sn}$.

The soft fields $\chi_{Sn}, \mathfrak{B}_{Sn}$ and $\mathfrak{h}_{Sn}$ scale as $\sim \lambda$, while the soft momenta scale as $i\partial_S \sim \lambda$. The soft operators $\mathcal{O}_{Sn}$ then scale as $\sim \kappa\lambda^4$. Since $O_n^i \sim \kappa\lambda^2$, we find the n-s Glauber Lagrangian scales as $\sim \kappa^2\lambda^4$. The scaling of the measure $d^4x \sim \lambda^{-3}$ for the soft Glauber operator since the soft momenta are all order λ. Therefore, the Glauber actions will scale as

$$\mathcal{S}_G^{ns\bar{n}} = \int d^4x \mathcal{L}_G^{ns\bar{n}} \sim \alpha_Q \lambda^{-2}, \tag{5.44}$$

$$\mathcal{S}_G^{ns} = \int d^4x \mathcal{L}_G^{ns} \sim \alpha_Q \lambda^{-1}. \tag{5.45}$$

Given that the actions for the kinetic terms in the soft and collinear Lagrangians are normalized to scale as $\sim \lambda^0$, we can clearly see that the Glauber operators are enhanced, as discussed in the main body of the text. We also see that the action for n-s Glaubers is down by λ compared to the n-$\bar{n}$ action. However, time-ordered products of n-s and $\bar{n}$-s Glaubers

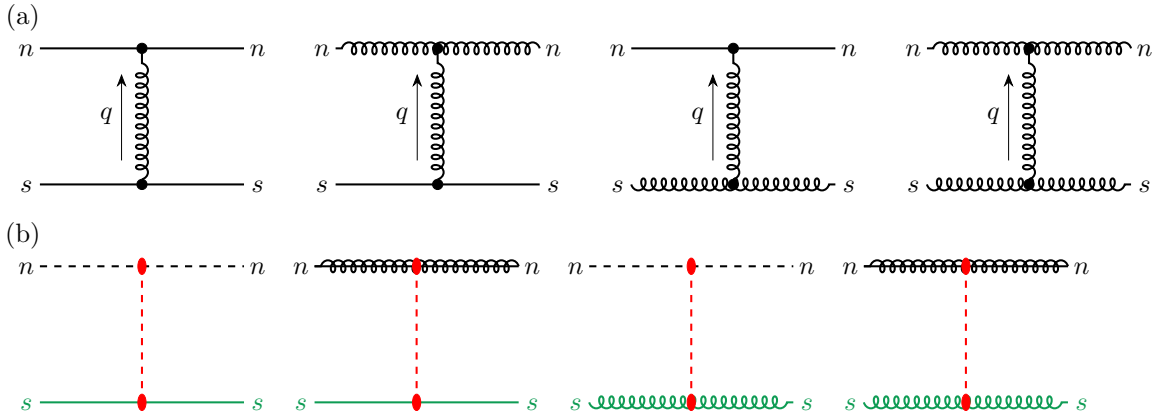

Figure 5.2: Tree level matching for n-s Glauber operators. These are the full theory diagrams with a t-channel pole. We can obtain the matching for $\bar{n}$-s scattering by taking $n \leftrightarrow \bar{n}$.

have the same enhancement as n-$\bar{n}$ Glaubers.

5.3.3 Collinear Operators to All Orders

We recall that the n-collinear sector is equivalent to full GR in the absence of soft or $\bar{n}$-collinear particles. Thus we may match by building operators in the full theory that are diff. scalars, i.e. not invariants, and then lift them to their diff. invariant form in the EFT. We also restrict the form of the operators by using two symmetries. The first is the shift symmetry on the scalar field inheretid from the full theory and the other is RPI-III [134] which is the symmetry of the EFT under the rescaling $\bar{n} \to \alpha\bar{n}$ and $n \to 1/\alpha n$. From the tree-matching, we can see that each collinear operator transforms as $\mathcal{O}_n \to \alpha^2 \mathcal{O}_n^i$, and so each collinear operator must have two lightcone vectors $\bar{n}$ contracted with it. Finally the operators must start off bilinear in the fields. With all this, we may write down the most general form of the collinear operator [5]

$$\mathcal{O}_n^i = \left[\left(W_n^{-1}\right)_{AB}^{\rho\sigma} f_{\rho\sigma}^i(g_n, \boldsymbol{\nabla}_n, \mathcal{D}_\mu \phi_n)\right] \bar{n}^A \bar{n}^B, \tag{5.46}$$

where $f_{\rho\sigma}^i$ has mass-dimension 3 and transforms covariantly under diffeomorphisms. Note that only the combination of $\mathcal{D}_\mu \phi_n$ can appear, as a scalar minimally coupled to gravity has an additional shift symmetry $\phi_n \to \phi_n + c$ for constant c. For scalars, there is only one possibility for f which we can write down:

$$f_{\rho\sigma}^\phi = \frac{\kappa}{2} \mathcal{D}_\rho \phi_n^\dagger \mathcal{D}_\sigma \phi_n. \tag{5.47}$$

[5] $\bar{n}^\nu$ is a diff. scalar so we write it as $\bar{n}^A$.

Using Wilson line identity (5.35), we find the operator is given by

$$\mathcal{O}_n^\phi = \frac{\kappa}{2} \mid \bar{n}\cdot \mathcal{P}\chi_n \mid^2, \tag{5.48}$$

which is equivalent to to the scalar operator given in Eq. (5.42), with $F = 0$. For the gravitons, there are two operators which we can write down:

$$f^h_{1,\rho\sigma} = \frac{2}{\kappa} g^n_{\rho\sigma}(\boldsymbol{\nabla}^n)^2, \qquad f^h_{2,\rho\sigma} = \frac{2}{\kappa}\boldsymbol{\nabla}^n_\rho \boldsymbol{\nabla}^n_\sigma. \tag{5.49}$$

The factor of $2/\kappa$ is needed **by dimensional analysis** and since we need the term quadratic in the metric perturbation to be linear κ. We note that since $f_{\rho\sigma}$ is symmetric, only the symmetric piece of $\boldsymbol{\nabla}^n_\rho \boldsymbol{\nabla}^n_\sigma$ will contribute. f^h_1 vanishes when plugged into Eq. (5.46), as we have

$$\bar{n}^A \bar{n}^B \left[\left(W_n^{-1}\right)^{\rho\sigma}_{AB} g^n_{\rho\sigma} \right] = \bar{n}^A \bar{n}^B (\eta_{AB} + \mathfrak{h}^n_{AB}) = 0, \tag{5.50}$$

where we have used the lightcone-gauge condition for $\mathfrak{h}^n$, $\mathfrak{h}^n_{++} = 0$ and assumed metric compatibility. Thus the only non-vanishing operator we can construct is f^g_2. It takes some work to see that this is equivalent to the graviton operator in Eq. (5.41). Writing out the covariant derivatives in terms of the connection, we may write the graviton operator as

$$\begin{aligned} \frac{2}{\kappa}\left[\left(W_n^{-1}\right)^{\rho\sigma}_{AB} \boldsymbol{\nabla}^n_\rho \boldsymbol{\nabla}^n_\sigma \right] \bar{n}^A \bar{n}^B &= \frac{2}{\kappa}\left(\bar{n}\cdot\mathcal{P} + \frac{\kappa}{2}\bar{n}\cdot\mathcal{P}\mathfrak{B}_{n}{}^{A}_{A} \right)\left(\bar{n}\cdot\mathcal{P} + \frac{\kappa}{2}\bar{n}\cdot\mathcal{P}\mathfrak{B}_{n}{}^{A}_{A} \right), \\ &= \bar{n}\cdot\mathcal{P}^2 \mathfrak{B}_{n}{}^{A}_{A} + \frac{\kappa}{2}\left(\bar{n}\cdot\mathcal{P}\mathfrak{B}_{n}{}^{A}_{A} \right)^2, \end{aligned} \tag{5.51}$$

where in the first line we have used $\mathfrak{B}_{n}{}^{\mu}_{+} = 0$ and in the second line we have used the fact that $\bar{n}\cdot\mathcal{P} = 0$ when not acting on collinear operators. From here we must now invoke the equations of motion for collinear gravitons. By acting with a Wilson line and restricting to the $++$ component, the equations of motion become

$$\bar{n}\cdot\mathcal{P}^2 \mathfrak{B}_{n}{}^{A}_{A} + \frac{\kappa}{2}\left(\bar{n}\cdot\mathcal{P}\mathfrak{B}_{n}{}^{A}_{B} \right)^2 = -\kappa(\bar{n}\cdot\mathcal{P}\chi_n)^2. \tag{5.52}$$

Using this, we may remove the term in Eq. (5.51) linear in $\mathfrak{B}_n$, and we obtain

$$\frac{2}{\kappa}\left[\left(W_n^{-1}\right)^{\rho\sigma}_{AB} \boldsymbol{\nabla}^n_\rho \boldsymbol{\nabla}^n_\sigma \right] \bar{n}^A \bar{n}^B \;=\; -\frac{\kappa}{2}\left[\left(\bar{n}\cdot\mathcal{P}\mathfrak{B}_{n}{}^{A}_{B} \right)^2 - \left(\bar{n}\cdot\mathcal{P}\mathfrak{B}_{n}{}^{A}_{A} \right)^2 \right] - 2\mathcal{O}^\phi_n. \tag{5.53}$$

Despite the fact that the equations of motion introduce scalar fields, we see that this is the same scalar operator that we have already introduced. Therefore, the graviton and collinear

operators are uniquely determined to be, up to overall numerical factors,

$$\mathcal{O}_n^\phi = \frac{\kappa}{2}(\bar{n}\cdot\mathcal{P}\chi_n)^2, \qquad \mathcal{O}_n^g = \frac{\kappa}{2}\left[\left((\bar{n}\cdot\mathcal{P}\mathfrak{B}_{nB}^A)\right)^2 - \left((\bar{n}\cdot\mathcal{P}\mathfrak{B}_{nA}^A)\right)^2\right], \tag{5.54}$$

supports the conclusion reached after Eq. (5.41). A similar procedure gives the $\bar{n}$-collinear as well as the S_n and $S_{\bar{n}}$ operators as well.

Lastly, in principle we could attempt to circumvent the power-counting and mass-dimension constraints by adding additional factors of $(\kappa\boldsymbol{\nabla})^m$. However, such operators can only appear when matching to higher-derivative terms in the full graviton action, such as R^3, etc. This follows from the fact that Einstein-Hilbert action is normalized such that powers of κ only arise multiplying the graviton.

5.4 The Graviton Soft Operator to All Orders

In this section, we shall describe the construction and matching of the gravitational mid-rapidity Glauber soft operator. Using the observations made in the previous section, we shall show that the operator basis has a finite number of terms, and that the matching can be performed at the level of a single soft graviton emission.

5.4.1 Soft Gauge Symmetry in Soft-Collinear Gravity

As mentioned in section 5.6 there is a fly in the ointment when it comes to soft gauge invariance. For hard scattering operators collinear fields can not transform under soft transformations, as they would throw the lines off shell. However, care must be taken when applying this argument to collinear bilinears. To understand why utilize the power of the label formalism whereby the large momenta are explicitly removed from the field by rephasing. For instance, for a collinear field we would write

$$\phi_n(x) = \sum_{n\cdot p} e^{in\cdot p\bar{n}\cdot x}\phi_{n\cdot p}(0, n\cdot x, x_\perp) \tag{5.55}$$

such that $\phi_{n\cdot p}(x)$ carry no large momenta. In this was a collinear composite operator $\phi_n^\dagger\phi_n$ carries no large label. As such it produces quanta with momentum scaling as $(\lambda, \lambda^2, \lambda)$ with invariant mass of order λ^2. A soft gauge transformation will not change this scaling. As such, we should think of the collinear forward bilinear as carrying gauge charge. The same is true in QCD, and in fact this line of reasoning is consistent with the placement of Wilson lines in the soft operators in section 6.3 of [159].

The notion of soft gauge-invariance in gravity is much more subtle in gravity that in QCD. In QCD, one is able to construct soft operators which are completely gauge invariant

at the level of the Lagrangian. In gravity meanwhile, this approach appears to work in the linearized theory, but it tends to break down once nonlinearities are included[6]. The solution, which can be found by performing explicit matching calculations, is that operators need to be soft diffeomorphism scalars, rather than diffeomorphism invariants. In particular, under an infinitesimal soft gauge transformation $g_{s\mu\nu} \to g_{s\mu\nu} + \partial_\mu \xi_\nu + \partial_\nu \xi_\mu$, the operator needs to transform as a total derivative,

$$\mathcal{O} \to \mathcal{O} + \boldsymbol{\nabla}_{s\mu} \left(\xi^\mu \mathcal{O} \right). \tag{5.56}$$

Then the action $S = \int d^d x \, \mathcal{O}$ will be gauge invariant up to boundary terms. This is the approach taken in [23] for constructing interactions between collinear fields and ultra-soft gravitons in an SCET_I context.

For constructing the Glauber operators, we can implement this as follows. By acting on collinear operators with inverse soft Wilson lines, we end up with objects that transform covariantly under soft diffeomorphisms. More explicitly, we may take the gauge-invariant combination of operators appearing in the Glauber Lagrangian,

$$\frac{1}{\mathcal{P}_\perp^2} \mathcal{O}_{\bar{n}}, \tag{5.57}$$

and we may convert this into a soft diffeomorphism scalar by acting with an inverse Wilson line:

$$\frac{1}{\mathcal{P}_\perp^2} \mathcal{O}_{\bar{n}} \to \left[S_{\bar{n}} \frac{1}{\mathcal{P}_\perp^2} \mathcal{O}_{\bar{n}} \right]. \tag{5.58}$$

The action of the soft Wilson line is to translate the collinear operator from a point x to the point $Y_{S\bar{n}}(x)$, where $Y_{S\bar{n}}(x)$ is related to $X_{S\bar{n}}$ by

$$X_{S\bar{n}} \left(Y_{S\bar{n}}(x) \right) = Y_{S\bar{n}} \left(X_{S\bar{n}}(x) \right) = x. \tag{5.59}$$

The operator evaluated at $Y_{S\bar{n}}$ then transforms as a scalar under soft diffeomorphisms.

Schematically, we may then decompose the soft operator as

$$\mathcal{O}_S = \sum_i f_i(\mathcal{P}_S) S_n^T C_i \sqrt{-g_S} O_i S_{\bar{n}} g_i(\mathcal{P}_S). \tag{5.60}$$

In the above, the operators O_i are soft diffeomorphism scalars built out of covariant derivatives and soft fields, the C_i are some numerical coefficients, and the functions f_i and g_i are scalar functions of the soft label operators. We have also included an explicit factor of the determinant of the metric, which is required by gauge-invariance. The Wilson line S_n^T

[6] See [91] for a recent example of this.

denotes the transpose, in the sense that S_n acts on fields to the left, while $S_{\bar{n}}$ acts on fields to the right. In the next section, we will discuss constraints on the functions f_i, g_i, and the operators O_i.

5.4.2 The Basis of Soft Graviton Operators

We now describe the construction of the soft operator basis. These operators must have mass dimension 2 and scale as $\sim \lambda^2$, and must be consistent with soft diffeomorphism symmetry. To make operators which are consistent with gauge invariance in the sense discussed in the previous section, every term must contain one n inverse Wilson line S_n and one $\bar{n}$ inverse Wilson line, as well as a factor of the soft metric determinant, $\sqrt{-g_s}$. We then build our operators out of soft label operators $\mathcal{P}_\mu^S$ and soft covariant derivatives $\boldsymbol{\nabla}_{S\mu}$. The soft label operators do not transform under soft diffeomorphisms, and so they can only appear outside the Wilson line pair; similarly, the soft covariant derivatives can only appear between the two Wilson lines.

Constraints from reparameterization invariance are crucial here. Since the light-cone vectors n and $\bar{n}$ are soft diffeomorphism invariant, they must appear entirely outside the Wilson line pair. As can be seen from their definitions in Eq. (5.41), the collinear operators each have RPI weight 2 in their respective direction. Thus to make the Glauber operator RPI-III invariant, we are forced to write the Glauber operator as

$$\mathcal{O}_{ns\bar{n}} = \mathcal{O}_n \frac{1}{\mathcal{P}_\perp^2} \frac{n^\mu n^\nu}{(n\cdot\bar{n})^2} \mathcal{O}_S^{\mu\nu,\,\rho\sigma} \frac{\bar{n}^\rho \bar{n}^\sigma}{(n\cdot\bar{n})^2} \frac{1}{\mathcal{P}_\perp^2} \mathcal{O}_{\bar{n}}, \tag{5.61}$$

where we have written

$$\mathcal{O}_S = \frac{n^\mu n^\nu}{(n\cdot\bar{n})^2} \mathcal{O}_S^{\mu\nu,\,\rho\sigma} \frac{\bar{n}^\rho \bar{n}^\sigma}{(n\cdot\bar{n})^2}. \tag{5.62}$$

We have left the factors of n and $\bar{n}$ to make the RPI invariance as explicit as possible. The form of the soft operator in Eq. (5.61) then completely fixes all dependence on the light-cone vectors, once the Wilson lines are taken into account, as the soft sector otherwise has no explicit preferred direction dependence, unlike the collinear operators.

Next, we have constraints from the hermiticity of the full Glauber operator. As described in Section 6.3 of [159], equality of $\mathcal{L}_G$ and $(\mathcal{L}_G)^\dagger$ requires the soft operator to satisfy

$$(\mathcal{O}_S)^\dagger = \mathcal{O}_S|_{n\leftrightarrow\bar{n}}\,. \tag{5.63}$$

This is a slight variation on the statement that there is a symmetry between the n and $\bar{n}$ sectors, given that swapping n and $\bar{n}$ is equivalent to taking an adjoint. In the context of the full Glauber operator, this reduces to the usual symmetry under exchanging n and $\bar{n}$. An additional constraint is that the total label momentum flowing through each term in

the Glauber Lagrangian is conserved. Therefore we have equality between $\mathcal{P}_S$ and $\mathcal{P}_S^\dagger$, and we may interchange them freely.

We find it useful then to introduce the notation

$$(S_n)^{\mu_1\ldots\mu_n}_{\nu_1\ldots\nu_n} \equiv \det\left[\left(S_n^{-1}\right)^\mu_\nu\right] Z_n S_n{}^{\mu_1}{}_{\nu_1}\ldots S_n{}^{\mu_2}{}_{\nu_2}, \tag{5.64}$$

$$(S_n^T)^{\mu_1\ldots\mu_n}_{\nu_1\ldots\nu_n} \equiv S_n{}^{\mu_1}{}_{\nu_1}\ldots S_n{}^{\mu_2}{}_{\nu_2} Z_n^T \det\left[\left(S_n^{-1}\right)^\mu_\nu\right]. \tag{5.65}$$

In the above, Z_n acts on all fields to the right, including the Jacobian factors, and similarly Z_n^T acts on all fields to the left. $(S_n)^{\mu_1\ldots\mu_n}_{\nu_1\ldots\nu_n}$ is then an inverse Wilson line in the sense of Eq. (5.36), as it satisfies

$$\left[S_n^{-1}T\right]^{\mu_1\ldots\mu_n}\phi_1 = T^{\nu_1\ldots\nu_n}\left[(S_n)^{\mu_1\ldots\mu_n}_{\nu_1\ldots\nu_n}\phi\right]. \tag{5.66}$$

Lastly, there are two useful identities which will be used to simplify the operator basis. The first follows from the properties of the gauge invariant metric building blocks $\mathfrak{h}^{S_n}$, which is defined analogously to the collinear metric building blocks in Eq. (5.27). Using $\mathfrak{h}^{S_n}_{-\mu} = 0$, we have

$$n^{\nu_1}n^{\nu_2}(S_n^T)^{\mu_1\mu_2,\alpha_1\ldots\alpha_n}_{\nu_1\nu_2,\beta_1\ldots\beta_n} g_{\mu_1\mu 2} = n^\mu n^\nu(\eta_{\mu\nu} + \mathfrak{h}^{S_n}_{\mu\nu})\,(S_n^T)^{\alpha_1\ldots\alpha_n}_{\beta_1\ldots\beta_n} = 0. \tag{5.67}$$

Similarly, replacing a light cone vector n with a derivative also leads to a vanishing operator,

$$\mathcal{P}_S^{\nu_1}n^{\nu_2}(S_n^T)^{\mu_1\mu_2,\alpha_1\ldots\alpha_n}_{\nu_1\nu_2,\beta_1\ldots\beta_n} g_{\mu_1\mu 2} = \mathcal{P}_S^\mu n^\nu(\eta_{\mu\nu} + \mathfrak{h}^{S_n}_{\mu\nu})\,(S_n^T)^{\alpha_1\ldots\alpha_n}_{\beta_1\ldots\beta_n} = 0, \tag{5.68}$$

where in the final equality we have used $n\cdot\mathcal{P}_S = 0$ when acting to the left of the Wilson lines, as soft $n\cdot k$ momenta cannot flow into $\mathcal{O}_n^i$.

With these constraints, we can now write down a list of all possible operators that satisfy them. There are eight such operators:

$$\begin{aligned}
O_1 &= \mathcal{P}_S^2(S_n^T)^{\mu\nu}_{--}g_{\mu\rho}g_{\nu\sigma}(S_{\bar n})^{\rho\sigma}_{++} + (S_n^T)^{\mu\nu}_{--}g_{\mu\rho}g_{\nu\sigma}(S_{\bar n})^{\rho\sigma}_{++}\mathcal{P}_S^2,\\
O_2 &= (S_n^T)^{\mu\nu}_{--}g_{\mu\rho}g_{\nu\sigma}g^{\alpha\beta}\boldsymbol{\nabla}_{S\alpha}\boldsymbol{\nabla}_{S\beta}(S_{\bar n})^{\rho\sigma}_{++},\\
O_3 &= (S_n^T)^{\mu\nu}_{--}R^S_{\mu\rho\nu\sigma}(S_{\bar n})^{\rho\sigma}_{++},\\
O_4 &= \mathcal{P}_S^\alpha(S_n^T)^{\mu\,\nu\,\beta}_{--\alpha}g_{\beta\rho}g_{\nu\sigma}g_{\mu\lambda}(S_{\bar n})^{\rho\,\sigma\,\lambda}_{++\gamma}\mathcal{P}_S^\gamma,\\
O_5 &= \mathcal{P}_S^\alpha(S_n^T)^{\mu\,\nu\,\beta}_{--\alpha}g_{\mu\rho}g_{\beta\lambda}g_{\nu\sigma}(S_{\bar n})^{\rho\,\sigma\,\lambda}_{++\gamma}\mathcal{P}_S^\gamma,\\
O_6 &= \mathcal{P}_S^\alpha\mathcal{P}_S^\beta(S_n^T)^{\mu\,\nu\,\gamma\lambda}_{--\alpha\beta}g_{\gamma\lambda}g_{\mu\rho}g_{\nu\sigma}(S_{\bar n})^{\rho\sigma}_{++} + (S_n^T)^{\mu\nu}_{--}g_{\mu\rho}g_{\nu\sigma}g_{\gamma\lambda}(S_{\bar n})^{\rho\,\sigma\,\gamma\lambda}_{++\alpha\beta}\mathcal{P}_S^\alpha\mathcal{P}_S^\beta,\\
O_7 &= \mathcal{P}_S^\alpha(S_n^T)^{\mu\,\nu\,\beta}_{--\alpha}g_{\mu\rho}g_{\nu\sigma}i\boldsymbol{\nabla}_{S\beta}(S_{\bar n})^{\rho\sigma}_{++} + (S_n^T)^{\mu\nu}_{--}g_{\mu\rho}g_{\nu\sigma}i\boldsymbol{\nabla}_{S\beta}(S_{\bar n})^{\rho\,\sigma\,\beta}_{++\alpha}\mathcal{P}_S^\alpha,\\
O_8 &= \mathcal{P}_S^\alpha(S_n^T)^{\mu\,\nu\,\beta}_{--\alpha}g_{\beta\rho}g_{\nu\sigma}i\boldsymbol{\nabla}_{S\mu}(S_{\bar n})^{\rho\sigma}_{++} + (S_n^T)^{\mu\nu}_{--}g_{\mu\beta}g_{\nu\sigma}i\boldsymbol{\nabla}_{S\rho}(S_{\bar n})^{\rho\,\sigma\,\beta}_{++\alpha}\mathcal{P}_S^\alpha.
\end{aligned} \tag{5.69}$$

In the above, we are implicitly assuming the Lorentz indices are contracted with lightcone

vectors as in Eq. (5.62). Not making this assumption can lead to several more allowed operators, as identities such as Eqs. (5.67) would no longer apply. This could be an important consideration when trying to construct the operator basis to subleading level, but for the current purposes it is enough to consider those in Eq. (5.69).

5.4.3 Matching

We now perform the matching of the Wilson coefficients for the soft operator. It will be sufficient to match at 0, 1, or 2 soft graviton emissions. Moreover, we may perform this matching taking the external collinear projectiles to be scalars. We can in principle replace one or both of the scalars by collinear gravitons, but we will obtain the same result for the soft operator. This is due to the universal nature of the coupling of Glauber gravitons to either soft or collinear particles, as well as the universal eikonal coupling of soft particles.

At zero soft graviton emissions, the Glauber operator must reproduce the tree scalar-scalar amplitude given in Eq. (5.40). The soft operator in this case must reduce to $\mathcal{O}_S = 2\mathcal{P}_\perp^2$. From their definitions in Eq. (5.33), the soft Wilson lines simply become the identity, the covariant derivative becomes $\mathcal{P}_S$, and $\mathcal{P}_S^2 = \mathcal{P}_\perp^2$ since no soft $k^\pm$ flows through the operator. This then places the constraint of

$$2 = 2C_1 - C_2 + C_5 + 2C_6 + 2C_7. \tag{5.70}$$

At one soft graviton emission, we have 7 full theory diagrams which contribute. We calculate on-shell, with arbitrary graviton polarization tensors, and soft graviton momentum k. Using momentum conservation to write $k = q' - q$, the amplitude contains several momentum structures which generate matching conditions. Several of the momentum structures generate degenerate matching conditions, and in the end the one graviton matching yields 5 constraints:

$$\begin{aligned}
2 &= C_1 - C_5 + 2C_6 - C_7, \\
0 &= C_1 - C_2 + C_7, \\
0 &= 4C_1 - 4C_2 + C_4 + 2C_5 - 4C_6 - 4C_7 + C_8, \\
8 &= 4C_1 + C_4 - 2C_5 + 4C_6 + C_8, \\
4 &= C_4 - C_3.
\end{aligned} \tag{5.71}$$

Combining this with the constraint from zero graviton emissions, we are able to fix 6 of the eight coefficients:

$$C_1 = 2, \quad C_4 = 4 + C_3, \quad C_5 = 0, \quad C_6 = 1 - C_2/2, \quad C_7 = 0, \quad C_8 = -2C_2 - C_3. \tag{5.72}$$

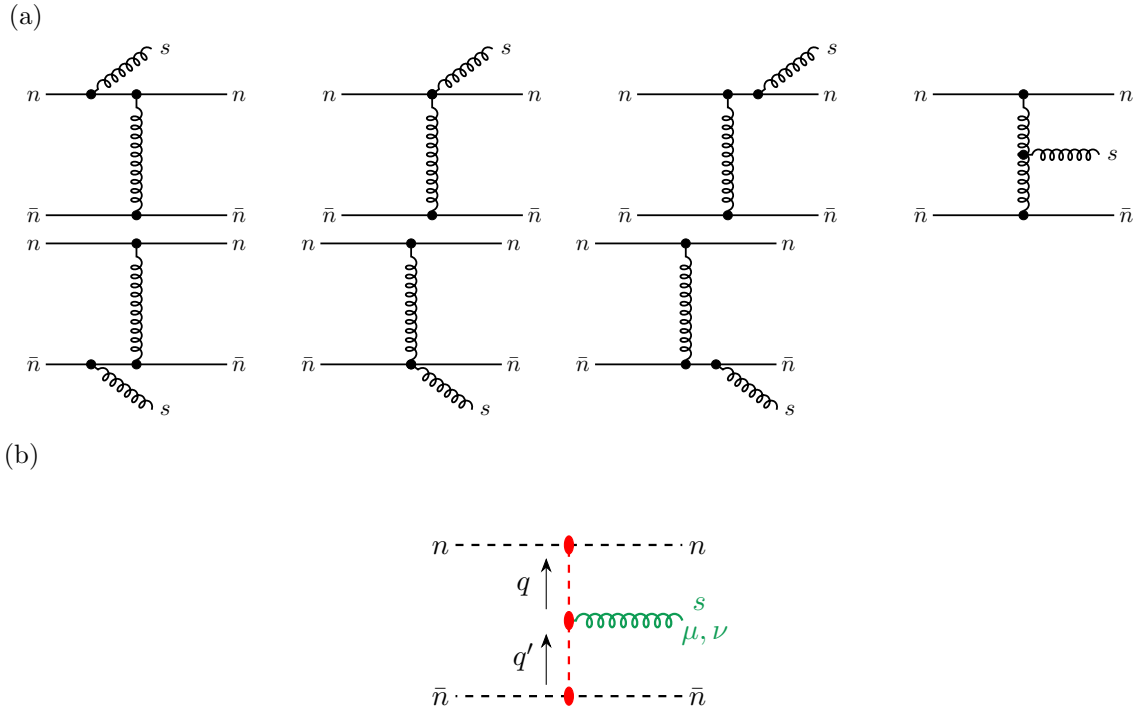

Figure 5.3: The matching for one soft graviton emission. In (a), we show the 7 full-theory diagrams which can contribute. In (b), we have the lone SCET diagram, which reproduces the gravitational Lipatov vertex.

At two soft graviton emissions, there are 40 full-theory Feynman diagrams which contribute. We calculate all such diagrams directly, using Feyncalc [138, 166, 165, 164] to streamline the computation. We performed the calculation using harmonic gauge, and we used the Feynman rules for the three and four graviton vertices [69]. The calculation may be streamlined using other choices of gauge-fixing or choice of interpolating fields [52], but given that the soft operator is gauge-invariant by construction, we would expect the result to be identical (up to field redefinitions). As a non-trivial cross-check of the calculation, we verified that the result for the full amplitude satisfies the graviton Ward identity in both external graviton polarization tensors.

In the EFT, we have 3 contributions to the amplitude; one from the two-graviton contribution in the soft operator, and two involving T-products of EFT operators, including the one-graviton emission in a T-product with a Lagrangian insertion. Because we used the graviton equations of motion to simplify the basis of soft operators, the first two rows of full-theory diagrams do not exactly match the contribution from the single soft graviton emission from the EFT. However, we do cancel the non-local graviton propagator generated by the T-product. Similarly, the full soft propagator in the remaining diagrams on the

second row and those on the third match the soft propagator in the EFT T-product of the n-s and $\bar{n}S$ Glauber operators. The difference between the full amplitude and the EFT T-product contributions is then local, containing only Glauber $\perp$ propagators and eikonal $1/n\cdot k$ and $1/\bar{n}\cdot k$ terms.

It is then enough to match to the eikonal propagators. From the $1/n\cdot(k_1+k_2)^2$ terms we are able to fix $C_2 = 2$, and the remaining eikonal contributions of the form $1/n\cdot k_1^2$ sets the remaining coefficient $C_3 = -4$. Thus we have the full set of coefficients for the operator basis in Eq. (5.69):

$$\boxed{C_1 = 2, \quad C_2 = 2, \quad C_3 = -4, \quad C_4 = 0, \quad C_5 = 0, \quad C_6 = 0, \quad C_7 = 0, \quad C_8 = 0.} \tag{5.73}$$

This gives the full soft operator of

$$\begin{aligned}\mathcal{O}_S =& 2\mathcal{P}_S^2 (S_n^T)^{\mu\nu}_{--} g_{\mu\rho} g_{\nu\sigma} (S_{\bar{n}})^{\rho\sigma}_{++} + (S_n^T)^{\mu\nu}_{--} g_{\mu\rho} g_{\nu\sigma} (S_{\bar{n}})^{\rho\sigma}_{++} \mathcal{P}_S^2 + 2(S_n^T)^{\mu\nu}_{--} g_{\mu\rho} g_{\nu\sigma} \Box_S (S_{\bar{n}})^{\rho\sigma}_{++} \\ & - 4(S_n^T)^{\mu\nu}_{--} R^S_{\mu\rho\nu\sigma} (S_{\bar{n}})^{\rho\sigma}_{++}. \end{aligned} \tag{5.74}$$

There are a few interesting points worth mentioning about this soft operator. Firstly, the only operators with non-zero Wilson coefficients all have Wilson lines with only two Lorentz indices; all operators O_{4-8} have at least one Wilson line with three or more indices in each term. One way to potentially understand this is that only Wilson lines which have the same transformation under diffeomorphisms as the metric are allowed in the soft operator (i.e. traceless symmetric rank-2 tensors). This is motivated by the QCD soft operator, only soft Wilson lines in the adjoint representation appear. The soft graviton operator also shows striking parallels to the QCD soft operator, which can be written as

$$\mathcal{O}^{BC}_{S,\,\mathrm{QCD}} = 4\pi\alpha_s n^\mu \bar{n}^\nu \left\{ \mathcal{P}_S^2 \eta_{\mu\nu} \mathcal{S}_n^T \mathcal{S}_{\bar{n}} + \mathcal{S}_n^T \mathcal{S}_{\bar{n}} \eta_{\mu\nu} \mathcal{P}_S^2 + \mathcal{S}_n^T g_{\mu\nu} (iD_S)^2 \mathcal{S}_{\bar{n}} - 2\mathcal{S}_n^T ig\tilde{G}_{S\,\mu\nu} \mathcal{S}_{\bar{n}} \right\}^{BC}, \tag{5.75}$$

where in the above $\mathcal{S}_n$ and $\mathcal{S}_{\bar{n}}$ are soft gluon Wilson lines, D_S is the soft gluon covariant derivative, and $\tilde{G}$ is the gluon field strength tensor in the adjoint representation. Comparing the soft graviton operator with the soft gluon operator, we can see that term-by-term we can obtain the soft graviton operator by replacing gluon Wilson lines with graviton Wilson lines, gluon field strength with the Riemann tensor, and adjoint color indices with Lorentz indices, contracted with an external n and $\bar{n}$ vectors. Some similarity might have been expected simply from double copy considerations, but it is somewhat surprising that this manifests at the level of the operators. It could be interesting to explore this correspondence further in the future.

5.4.4 Matching the Scalar Soft Function

We now match the soft scalar terms in the soft operator. Here, in constructing the operator basis, we are aided by an additional symmetry of mass scalars, that is a symmetry of shifting by an additive constant,

$$\phi \to \phi + c. \tag{5.76}$$

The EFT of course must also respect this symmetry. This then requires that all scalars must come with a derivative in the combinations $\boldsymbol{\nabla}_\mu \phi$. This then fixes the derivatives in the soft operator, leaving only the distinct ways indices can be contracted between the Wilson lines and the derivatives. Thus, there are only two scalar operators one can write down:

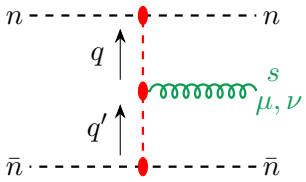

$$\begin{aligned}
&= i\left[\frac{\kappa}{2}\bar{n}\cdot p_2^2\right]\left[\frac{\kappa}{2}n\cdot p_1^2\right]\left(\frac{\kappa}{\sqrt{2}q_\perp^2 q_\perp'^2}\right)\Bigg(2\frac{\bar{n}^\mu\bar{n}^\nu}{\bar{n}\cdot q^2}q_\perp'^2 q\cdot(q'-q)+2\frac{n^\mu n^\nu}{n\cdot q^2}q_\perp^2 q'\cdot(q-q') \\
&\quad - 2q_\perp'^2\frac{n\cdot q'\bar{n}^\mu\bar{n}^\nu-\bar{n}^\mu q^\nu-\bar{n}^\nu q^\mu}{\bar{n}\cdot q} - 2q_\perp^2\frac{\bar{n}\cdot q\, n^\mu n^\nu - n^\mu q'^\nu - n^\nu q'^\mu}{n\cdot q'} \\
&\quad + 2(q^\mu q'^\nu + q^\nu q'^\mu) - (q^\mu+q'^\mu)(n\cdot q'\bar{n}^\nu+\bar{n}\cdot q\, n^\nu) - (q^\nu+q'^\nu)(n\cdot q'\bar{n}^\mu+\bar{n}\cdot q\, n^\mu) \\
&\quad + (n\cdot q'\bar{n}^\mu+\bar{n}\cdot q\, n^\mu)(n\cdot q'\bar{n}^\nu+\bar{n}\cdot q\, n^\nu) - (q_\perp^2+q_\perp'^2)(n^\mu\bar{n}^\nu+n^\nu\bar{n}^\mu) - 2q\cdot q'\eta^{\mu\nu}\Bigg).
\end{aligned}$$

We can then match the coefficients of these operators by considering the scalar-scalar forward scattering with the emission of two additional soft scalars. In the EFT there are three contributions, one which is a time-ordered product involving the gravitational Lipatov vertex, two from a time-ordered product of an n-s and an $\bar{n}s$ scalar-scalar Glauber operator, and one from the soft scalar operator. Meanwhile in the full theory there are 9 diagrams. We are able to straightforwardly perform the calculations, and we find the Wilson coefficients to be

$$\boxed{C_1^\phi = 0, \qquad C_2^\phi = -2.} \tag{5.77}$$

This completes the matching of the soft function for the specified matter fields. In general, we can expect additional soft operator contributions for matter fields of different spins and different couplings to gravity. Note that this does include a soft fermion emission operator. In gravity, each additional matter field comes with a factor of κ, which reduce the mass dimension of the field by one; therefore two fermion fields come with a mass dimension of 1, and can satisfy the mass dimension constraint. This with QCD, where a soft fermion bilinear has mass dimension 3 and is thus ruled out. Finally note that, as pointed out in the context of NRQCD [158], an advantage of building operators with gauge invariant

interpolating fields is that we we do not need to consider operators with ghosts on external legs.

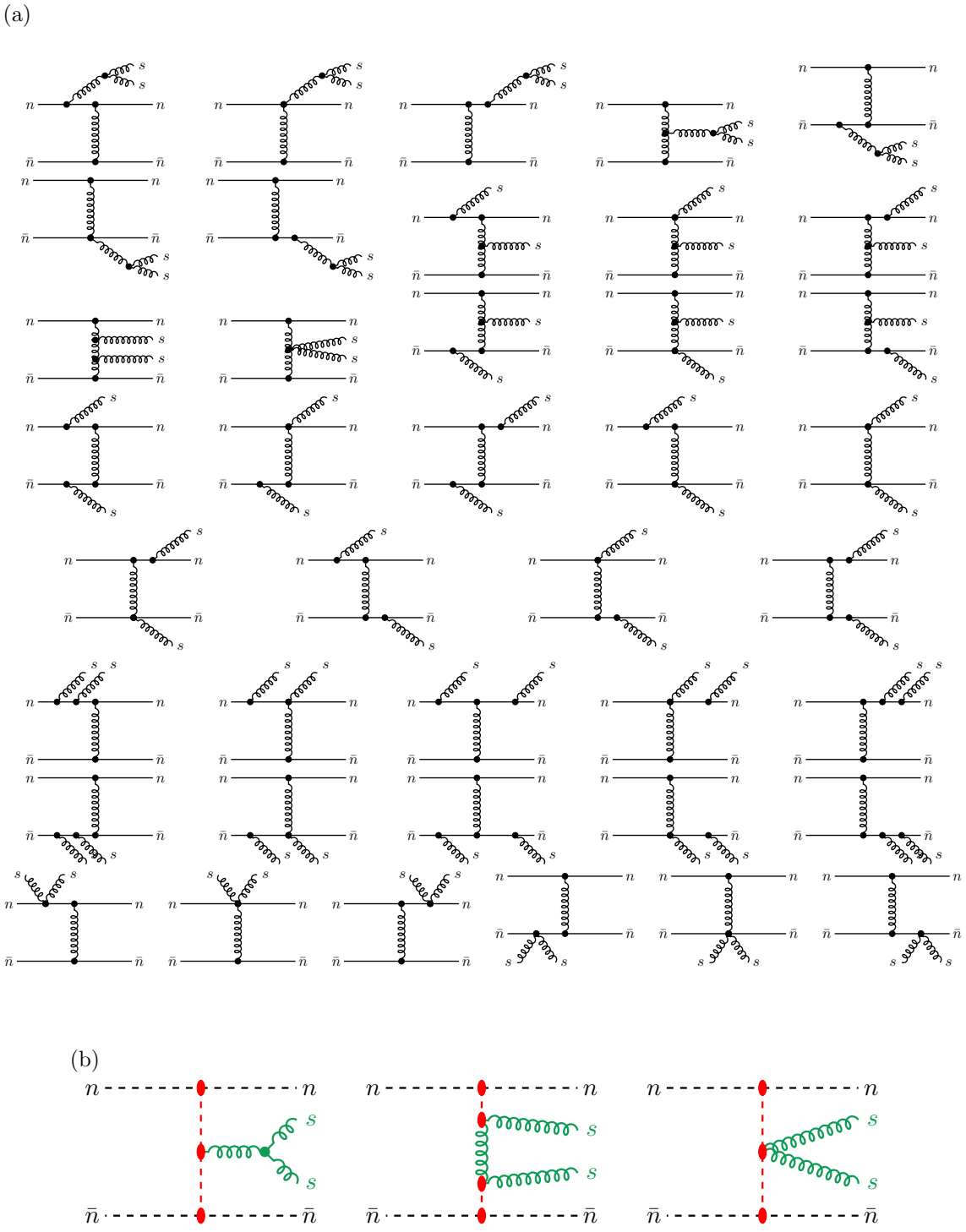

Figure 5.4: Diagrams for matching two soft graviton emissions. In (a) we show the 40 full-theory diagrams. In (b) we have the SCET diagrams. The first two are time-ordered products of known EFT operators, while the third is an insertion of the two-graviton term in the soft operator.

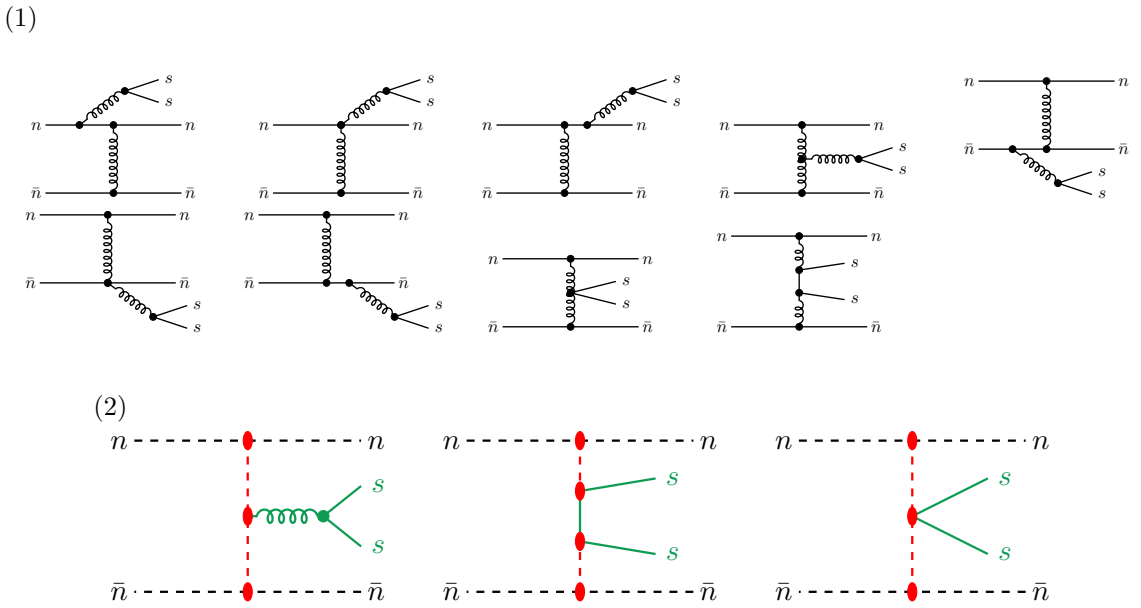

Figure 5.5: Matching for two soft scalar emissions. In (a), we show the 9 full-theory diagrams. In (b), we show the EFT contributions. The first two involve time-ordered products of EFT operators, while the third is an insertion of the two scalar term of the soft operator.

Chapter 6

Forward Scattering in Gravity

6.1 Introduction

Quantum gravity as an effective field theory, at least formally, is well understood[76] as long as all invariants are sufficiently small compared to the fundamental scale M_{pl}. In this regime the non-renormalizability of gravity is tamed save for the fact that as we aspire to higher accuracy we introduce more unknown UV parameters that must be fixed from experiment, or matched from some UV completion. The renormalization group flow into the IR is not terribly interesting since all logs are power suppressed and there is no limit in which a resummation can be done systematically.

However, we know this can not be the only kinematic regime for which we can maintain calculational control as, after all, we certainly can predict astronomical orbits with high accuracy. This super-Planckian scattering, corresponding to the limit $s \gg t$, i.e. the so-called "Regge" regime, must be within our calculational reach even though the graviton coupling scales as s/M_{pl}^2 and t/M_{pl}^2 when the emission occurs off of energetic/soft partons. Note that even if we work in the regime $s \gg M_{pl}^2 \gg t$, we are immediately faced with a severe power counting challenge given the growth of coupling in the super-Planckian limit. In fact, matters are made worse by the existence of large ("Regge") logs of the ratio s/t, and, more importantly, this regime of forward scattering is enhanced due to the t-channel graviton exchange by a factor of $1/t$.

The super-Planckian limit is a double edged sword. On the one hand, the growth of the cross section in s, at fixed t, leads to, at least naively, a violation of unitarity, but also pushes the process into the semi-classical (eikonal) regime (for an extensive review of progress using the eikonal approximation see [72]) over which we would expect to have calculational control. In the case of massless particle scattering, the classical picture of the initial state consists of two Aichelburg-Sexl shock wave metrics, and for impact parameter

$b \sim 1/t$ large compared to the effective Schwarzchild radius $R_S = 2G\sqrt{s}$, is tractable by classical GR[81]. As the impact parameter diminishes we reach the regime of black hole production and a thermal final state, as per Hawkings' result. Thus it seems that, at least for $t < R_S$, super Planckian scattering is dominated by IR physics. We might glibly conclude that we may maintain calculational control by simply working at large impact parameter such that only-non local interactions will contribute, since contact interactions will be suppressed for localized incoming wave packets. However, this is premature as it is possible for local operators to mix with non-local operators via soft exchanges of gauge bosons. In fact this occurs in NRQCD [50, 128, 39], the theory of non-relativistic bound states. But as we shall discuss gravity does not allow for this mixing to happen for the class of observables which are of relevant to this work.

The goal of this chapter is to build a Lagrangian formalism which allows one to calculate systematically in a double expansion in $\alpha_Q \equiv t/M_{pl}^2$ and $\alpha_C \equiv st/M_{pl}^4$. These ratios control quantum and classical corrections respectively. In addition we will be working to leading order in $\lambda = \sqrt{t/s}$. Our motivating factors for generating this formalism are: Formally, we would like define, in a gauge invariant operator formalism, the notion of a Regge trajectory and a BFKL equation for gravity, and to search for commonalities between QCD and gravity that go beyond what is known in the double copy relations [35, 34]. Practically, to show that this a Lagrangian effective field theory formalism can greatly simplify calcuations of the Regge trajectory, as well as higher order corrections in the PM expansion.

Significant effort has been put into the calculation of higher order PM corrections to the classical scattering angle for the purposes of increasing the accuracy of parameter extractions for binary inspirals. While the PM expansion is not a systematic expansion in either the relativistic or non-relativistic regimes, it does resum a subset of relativistic corrections and is believed to increase the accuracy of models which interpolate between the PN and relativistic parts of the inspiral such as the effective one body model [44]. There are various ways of approaching these corrections, including using the classical world line approach [98] in the PM expansion [74], the QFT world line approach [140, 77], and the S-matrix approach [148, 36, 33]. All of these calculations utilize the physical limit, $s \sim m$, and since we will be considering light-like scattering, our results will only agree with a subset of the contributions[1]. The massive and massless eikonal theories are not continuosly connected, and thus the mass effects must arise from distinct theory, only to be touched upon below, from the massless case.

As concrete calculations in this chapter we will show a simple way to extract the, mass independent, classical log at 3PM, as well as the leading order Regge trajectory for which

[1]The soft loops, are insensitive to the existence of a mass.

the two calculations in the literature [15, 137] seems to disagree[2]. It is our hope that by illuminating the all orders structure of the series we may be able to perform suitable resummations.

The technical details of our calculations will be couched in terms of EFT language. However, in an effort to make the physics accessible to a more general audience, we have relegated most of the EFT details to appendices. The EFT is the scaffolding that allows for all orders proofs of factorization of the leading order in t/s contribution to forward scattering. That is, the amplitude can be written as a convolution of soft and collinear functions

$$\langle O \rangle = \langle O_n \rangle \langle O_s \rangle \langle O_{\bar{n}} \rangle, \tag{6.1}$$

Readers interested in generating fixed order results can do so using the full theory and using the method of regions [167, 21, 168] to find the appropriate integrands dictated by the EFT. However, the resummations are based upon operator rapidity anomalous dimensions which are defined within the EFT.

There are several existing approaches in the literature to studying the super-Planckian limit. Early work tended to focus on obtaining the leading classical Eikonal phase through a variety of approaches [1, 170, 145]. Amati, Ciafaloni, and Veneziano (ACV) expanded string amplitudes in the semi-classical limit[11, 7, 9, 10], which allowed them to extract the two loop contribution to the classical phase. More recent approaches involve Wilson lines [137, 129] and double copy considerations [162, 163, 6, 161, 146, 153, 151, 152]. Lipatov [126] introduced "effective actions" for high energy scattering which involved "Reggeon fields", which is quite distinct from our approach; several other effective actions approaches closely related to Reggeon fields have also appeared in the literature [114, 8, 12, 123]. Recently the authors of [93], have given a nice explanation of the differences between Reggeon fields, in the context of QCD, and the theory formulated in [159], upon which our theory is based.

6.2 Lessons from YM Theory

To gain insight into gravity in the Regge limit it behooves us to consider the case of YM theory which is, in some ways, simpler than gravity, since the coupling is dimensionless so power counting is almost trivial, but in other ways more complicated due to the color structures that arise as we increase the orders of our calculations. However, as we shall see, the structure of the gravitational theory is considerably simpler than QCD once we know how to tame the seemingly non-perturbative coupling behavior, as will be discussed in the

[2]The Regge trajectory is IR divergent and thus the local pieces are regulator dependent. However, the results in [15, 137] also disagree in their $\log(t)$ dependence of the trajectory which should be independent of the regulator.

next section.

YM theory has the nice property that hard processes are power suppressed [3], as a consequence of the fact that it is classically conformal. Let us first consider the case of a generic hard scattering process away from the forward limit, where we integrate out the hard modes and match onto a theory of light-like scatterers. The systematics of this theory are based on a double expansion in α_s and Λ/Q, where $Q \sim s \sim t$ is the hard scattering scale and Λ is the appropriate IR scale for the observable of interest. The amplitude will contain large (double) logs of the ratio Q/Λ^2 whose resummation can be achieved by working in the EFT called SCET, (Soft-Collinear Effective theory) [17, 16, 18]. Some of these logs are due to loops or large virtuality ("hard loops") which can be resummed using renormalization group techniques, while other logs, of the ratio s/t are actually due to the large ratio of rapidities which can be resummed using rapidity renormalization group (RRG) methods[57, 54].

Once we consider the Regge limit the power counting changes drastically, as the higher dimensional near forward scattering operator which arises from the exchange of a so-called "Glauber gluon", becomes order one. This is not to say that there are no near forward interactions in a hard scattering event (all invariants being large), however, it can be proven [61][4], that for sufficiently inclusive observables these interactions cancel up to corrections which are suppressed by the hard scattering scale. Thus in the Regge regime (no hard scattering) the forward scattering interaction dominates and amplitude. The interactions are characterized by the exchange of a Glauber gluon with light-cone momentum scalings $p^\mu \sim \sqrt{s}(\lambda^2, \lambda^2, \lambda)$, which are off-shell ($p_+ p_- \ll p_\perp^2$) and can be integrated out, leading to an interaction which is non-local in the transverse direction. Theses gluons are called "Glauber modes" as the analagous mode in QED is relevant for quantum optics. The canonical definition of SCET does not include these modes, which lead to a generalized version of SCET, GSCET, [159]. The resummation of these Glauber exchanges leads to the eikonal phase characteristic of the semi-classical nature of the near forward scattering process.

Let us consider the form of the one loop amplitude

$$M \sim \frac{\alpha_s}{t}(1 + i\pi C_1 \alpha_s \Gamma[\epsilon] \left(\frac{t}{\mu^2}\right) + C_2 \alpha_s \log\left(\frac{s}{-t}\right) + ... \tag{6.2}$$

Here we have ignored color which leads to complex structure at higher orders. It is important to note that there are *no hard loop* correction to any order for forward scattering kinematics, as such contributions are all power suppressed by factors of t/s [159]. The imaginary term

[3] For on-shell operators. i.e. those which only contain physical polarizations.

[4] All factorization proofs for hard scattering observables in SCET, to date, assume that Glaubers do not contribute.

in Eq.(6.2) is the avatar of the classical phase and the large $\log\left(\frac{s}{-t}\right)$, which needs to be resummed to regain calculational control in the asymptotic limit, leads to the "Regge trajectory"[5]. There is storied history of the resummation of these logs that goes under the name of "Reggeization". Gribov's original approach [99] to the problem has led to a number of perspectives including the classic work of Balitsky, Fadin, Kuraev and Lipatov [88], Lipatov's effective action [124], and more modern approaches in terms of Wilson lines[13, 46, 47, 171, 90]. For an historical review see [66]. In some instances, e.g. in the anti-symmetric octet color channel, the resummations of these logs leads to so-called Regge form of the amplitude where the amplitude can be written as [6]

$$M \sim C(\alpha_s) \left(\frac{s}{t}\right)^{\alpha(t)} . \tag{6.3}$$

$\alpha(t)$ is the, infrared divergent, Regge trajectory. This form of the amplitude holds up to next-to leading log in general [78] and to all orders in the planar limit [120]. Amplitudes of this form have "Regge pole" behavior since they arise when there is a pole in complex angular momentum plane. This is as opposed to the case where cuts arise and the amplitude takes on a more complicated form. Recent progress has shown that there are relations between $\alpha(t)$ and the series in α_s that defines C [65, 144]. In addition, it has been shown that, by considering ampltiudes with definate crossing symmetry, that unitarity implies that there are relations between the Regge trajectory and the eikonal phase [157], as well as between various anomalous dimensions.

6.3 The Gravitational Case

Now let us return to the gravitational case. We would expect the amplitude in the gravitational case to take a form identical to (6.3). However, as discussed in the introduction the hard scattering S-channel operators are enhanced by powers of s/M_{pl}^2. For instance, for scalar scattering the tree level s-channel graviton exchange will generate a local operator with a Wilson coefficient that scales as s/M_{pl}^2.

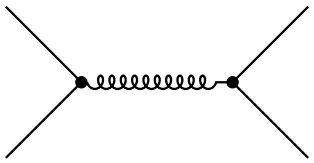

[5]The Regge trajectory is defined at the running of the octet operator.

[6]In momentum space the eikonal phase is not manifest, but instead the series C includes both classical (eikonal) and quantum contributions.

Any observable sensitive to this operator will not be under calculational control. In fact, we could insert higher dimensional operators with unknown Wilson coefficients at the vertices, and they too would be super-leading. Notice that simply specifying the kinematics as being Regge does not eliminate the contributions from such operators. However, if we consider a set of observables (O) as being those for which the incoming wave packets have a compact region of support and are separated in the transverse direction by an amount greater than Schwarzchild radius, then operators which interpolate for a fixed number of partial waves wont contribute. It is interesting to note that this is NOT the end of story, as soft emissions can mix local and non-local operators. In fact, this is exactly what happens in the case of non-relativistic bound states [169, 131], such a quarkonium where the annihilation diagram generates a local color octet $T^a \otimes T^a \delta(x)$ potential that gets corrected by a soft exchance as in this diagram [7]

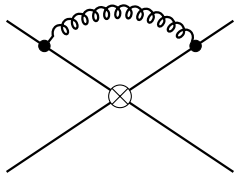

that generates a counter term for a non-local potential $V(x) \sim \frac{1}{r^3}$ which would contribute to the set of observables O. Physically we can imagine two widely separated partons one of which emits a soft quanta which shifts its momenta, leading to a head on annihilation after which the quantum is reabsorbed and the final state is again well separated. In NRQCD this poses no challenge to the power counting since the annihilation graph is down by $\alpha_s \sim v^8$.

We may worry that something similar can happen in the gravitational case and indeed it would, however only if the the matter propagator assumes the dispersion relation $E = \frac{p^2}{2m}$, that is the soft exchange would cause the source line to recoil and thus the matter lines are not eikonal, and must behave quantum mechanically which, in turn, implies $mv \sim 1/r$ or $L \sim 1$, which is outside the set O. This argument applied to massive partons, whereas here we are interested in the massless case. However, the same conclusion can be reached in the massless case as the diagrams with the exchange of a soft graviton will be insensitive to $q_\perp \sim \sqrt{t}$ for observables within O. Had this not been the case it would have meant that the matching from the UV completion of gravity to Einstein-Hilbert gravity would have to exponentially suppress all of the dangerous operators.

Finally, one may worry that the exclusion of the s-channel operators will pose a challenge to the Ward identity once we put gravitons on external states. In the EFT the Ward identity must be satisfied order by order in each of the expansion parameters. As we shall see, by

[7] In the EFT NRQCD [50, 128, 39], this gluon is called "Ultra-Soft" because all of its momentum components scale as mv^2, where v is the relative velocity in the bound state.

[8] In the bound state the power counting is such that $\alpha \sim v$.

building operators using explicitly gauge invariant building blocks we are assured that that the Ward identities will be satisfied and the contribution from local interactions (s-channel processes) will automatically be included [9].

6.4 Glauber Gravitational SCET

6.4.1 Power Counting

There are multiple kinematic scenarios of interest depending upon whether or not the scatterers are massive or not. In this chapter we will consider massless case. As mentioned in the introduction the EFT will be valid when the following hierarchy is satisfied

$$s \gg M_{pl} \gg t. \tag{6.4}$$

As in the case of QCD we will be working to leading order in the parameter $\lambda = \sqrt{t/s}$. However, we will be working to all order in the parameters

$$\alpha_Q \equiv \frac{t}{M_{pl}^2} < 1 \qquad \alpha_C \equiv \frac{st}{M_{pl}^4} < 1, \tag{6.5}$$

which control the quantum and classical loop corrections. $\alpha_C \equiv \frac{st}{M_{pl}^4} < 1$ implies that classical non-linearities are sub-leading such that we are not in the regime where black hole formation occurs[10]. However, we can study the approach to black hole formation as a function of α_C.

As opposed to QCD, the gravitational Glauber interaction is power *enhanced*, i.e. $1/\lambda$. Such a state of affairs is usually a death knell for any EFT since power counting forces us to rescale the action such that the superleading interaction scales as unity, which would make the kinetic pieces sub-leading, and the theory would have no propagating degrees of freedom. However, since the Regge limit is a semi-classical in nature the amplitude has sufficient structure that calculational control can be maintained. To see this note that the semi-classical nature of the process ensures that the amplitude can be written in impact parameter space [72] in the form

$$M(b,s) \sim \left((1 + [\sum_{i=0} \alpha_Q^i C_i(bs)]) e^{i\delta_{\rm C1}^{(0)} \sum_{j=0} (\alpha_C^j D_j(bs))} - 1 \right), \tag{6.6}$$

[9] This may seem strange from the point of view that local interactions are suppressed. However, unphysical polarizations on external lines can lead to leading order local contributions which will automatically be accounted for in the EFT operators.

[10] Here t is the typical momentum in one graviton (Glauber) exchange, which is called $t_{individual}$ in [9, 10], and should not be confused with the physical t which results from a coherent field of Glaubers which constitutes the shock wave.

where $\delta_{\rm Cl}^{(0)}$ is the Fourier transform of the leading order Glauber result

$$\delta_{\rm Cl}^{(0)} = Gs\pi^{\epsilon}(\bar{\mu}^2 b^2)^{\epsilon}\Gamma(-\epsilon). \tag{6.7}$$

The function $D(bs)$ is a series of logs.

Given this form of the amplitude we may treat the kinetic term as being as the same order as the Glauber interaction. Furthermore this form of the amplitude allows us to cleanly separate the classical from the quantum [11] . This need not have been the case given that we have three dimensionful parameters (s, t, M_{pl}^2), the dimensionless couplings λ, α_Q and α_C are not independent ($\frac{\alpha_Q^2}{\lambda^2} = \alpha_C$). This would not be a problem save for the fact that the theory contains (Glauber) operators which scale as inverse powers of λ which complicates the power counting. At the diagrammatic level we may distinguish classical and quantum corrections when considering soft gravitons as any soft loop that does not involve an eikonal line will be quantum mechanical. In the massless case, as we consider here, we run into the complications

Notice that a direct calculation of terms which scale as powers of α_C would not suffice to extract the classical piece since, as we can see from the form of the amplitude, the expansion of the exponent will yield powers of α_C (from the leading term) that will hit quantum terms in the prefactor and generate classical scaling contributions ($\frac{s}{t}\alpha_Q^2 = \alpha_C$). Figure one shows the general structure of the series. We see that the classical contribution skips orders in the PM expansion since we need an extra Glauber exchange to get a factor of s/M_{pl}^2 to accompany a quantum suppression of t/M_{pl}^2. The RRG sums all the logs along the green lines, as each step to the right generates another log, whereas vertical motion does not. The bottom green line generates the leading order Regge trajectory. These logs can arise from either soft or collinear emissions. As we will discuss below in the EFT all diagrams get contributions from soft and collinear partons. In the soft sector it is easy to determine which diagrams are classical and which are quantum, as any loop which does not involve an eikonal line is necessarily quantum. The RRG running of the soft function sums diagrams which involve adding rungs between Glauber lines will include both quantum as well a classical piece. It also sums soft eye graphs which are purely quantum mechanical. In the collinear sector the massless parton can split [12] and the existence of a collinear propagator in every loop is no longer sufficient to ensure classicality. Nevertheless, if one is only interested in logs one can calculate solely in the soft sector since the logs are all fixed by the anomalous dimensions which can be calculated by choosing to work either in the soft sector or the

[11] In the massive case there is an alternative path one can take by working in an EFT of potentials. Then the super classical terms that show up in iterations are canceled when matching onto the EFT [**Neill:2013ws**].

[12] When working in the limit where $s \sim m^2$, collinear emissions are no longer relevant and the source always behaves classically, and can be treated as in NRGR [98].

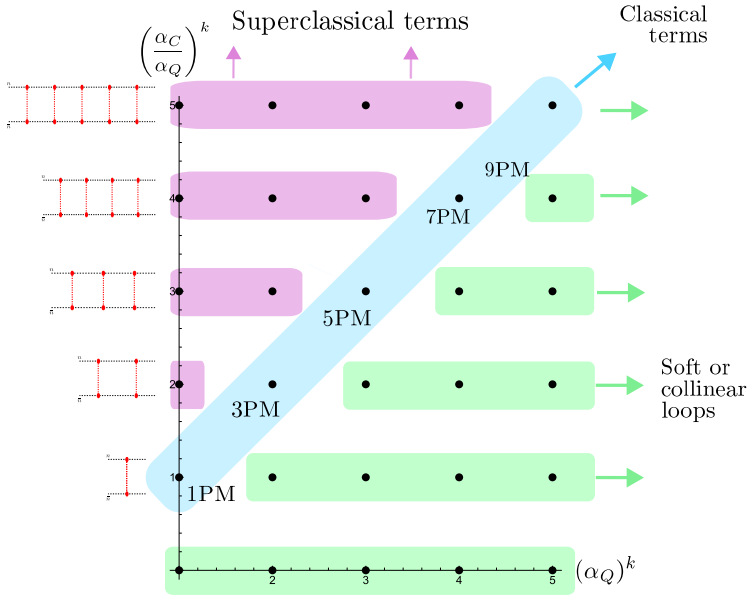

Figure 6.1: The structure of the perturbative series. The blue circles correspond to classical contributions in the Post-Minkowskian expansion. The pink circles are super classical (box diagrams) while the greens lines indicate quantum corrections from soft and collinear loops. The classical contributions occur at odd orders in the PM expansion. Each soft/collinear loop generates a log while Glauber loops generate $i\pi$.

collinear sectors [13], as will be discussed below. As one goes to higher orders in the quantum expansion one must include power corrected Glauber operators which can be lifted up by subsequent Glauber exchange. In this chapter we will not be working to sufficiently high order for this to be an issue.

If one wishes to power count by diagrams instead of operators, it is simple to read off the scaling of a given diagram. Each matter vertex gives as factor of s, while each matter line gives a factor of $1/\sqrt{s}$. All vertices give a power of $1/M_{pl}$ and given that the amplitude for scalars is scaleless the remaining units are made by powers of t with a minimum exponent of -1. Note that each operator scales homogeneously with λ but not in α_Q, or α_C, thus even though those couplings are ratios of scales we should think of them in the same as we would α_S in YM theory. Also all amplitudes are analytic in s since there are no hard momenta flowing through the loops. This seems to fly in the face of the Regge logs, but in the EFT the s dependence only shows up as a boundary value for the solution to the RRGE. Counting using operator insertion is simpler, since each Glauber exchange generates a factor of $\frac{s}{M_{pl}^2}$ while each soft vertex generates a factor of $\sqrt{\alpha_Q}$. There is additional overall

[13] In the EFT the full amplitude has no rapidity divergences which cancel between the collinear and soft sectors.

factor of $\frac{s}{t}$ in the matrix element. Thus the soft eye graph, e.g., in figure (6.28) which in this case arises due to the time ordered product of two collinear soft Glauber operators is of order $\left(\frac{s}{t}\frac{s}{M_{pl}^2}\right)$ where the quantity in the brackets is the scaling of the leading order Glauber exchange.

6.4.2 The Action

As mentioned in the introduction, the scaffolding of our calculations will be Glauber SCET, and here will will quickly review this topic in preparation for the introduction of the crucial factorization theorem (6.12) upon which our analysis hinges. For the case of hard scattering a version of SCET for gravity was developed in [24, 149]. Here we will be considering the complementary case which describes the Regge region. Some of atomistic gauge invariant objects upon which we build our theory can be ported over from the EFT for gravity for the case of hard scattering in [24, 149]. The EFT for near forward scattering in gravity is structurally very similar to the case of YM theory [159]. The starting point for building the EFT is to determine the modes necessary to reproduce the IR physics of the full theory. The relevant modes are fixed by determining, given the relevant kinematics, the kinematic regions for which IR singularities arise. There is no distinction between the modal analysis in gravity and in YM theory, though the power counting of the modes fields components are different (see below). For high energy scattering the relevant modes [14] correspond to soft (s), collinear (n) and anti-colinear ($\bar{n}$) where the light cone momentum scale as $p_s^\mu \sim (\lambda, \lambda, \lambda)$, $p_n^\mu \sim (1, \lambda^2, \lambda)$ and $p_{\bar{n}}^\mu \sim (\lambda^2, 1, \lambda)$, respectively. Here $\lambda \sim \sqrt{t}/\sqrt{s}$ is the power counting parameter. Any prediction will be made in the context of a triple expansion in λ, α_C and α_Q, though we will only work to leading order in λ. Both soft and collinear scalar modes exist in the theory and both fields scale as $\sqrt{\lambda}$. The scalar soft mode loops will not generate rapidity logs and wont play a role at the order we will be working. In the de Donder gauge the polarization of the collinear graviton field will scale as (in the $(+, -, \perp)$) basis

$$h_{\mu\nu}^n \sim \frac{p_\mu^n p_\nu^n}{\lambda} \tag{6.8}$$

and the soft graviton scales as λ.

The total Lagrangian is written as

$$\mathcal{L} = \mathcal{L}_n + \mathcal{L}_{\bar{n}} + \mathcal{L}_s + \mathcal{L}_{\mathcal{G}}. \tag{6.9}$$

where $\mathcal{L}_n + \mathcal{L}_{\bar{n}} + \mathcal{L}_s$ correspond to the Lagrangian for soft and collinear modes while $\mathcal{L}_{\mathcal{G}}$

[14] This corresponds to what is known as SCETII. There is also an SCETI where where the Ultra soft modes replaces the soft mode and has $p \sim \lambda^2$. The choice of observables determines which of the two theories should be applied.

accounts for the factorization violating interactions, i.e they connect modes in different sectors, that take place due to Glauber exchange. The theory has three distinct gauge symmetries (diffeomorphism invariances), collinear, anti-collinear and soft, and one can build the action from gauge invariant operator building blocks. It is because the leading order action can be factored in this way that is it relatively simple to write down factorization theorems when the Glauber mode is included, as it is the only mode which has the ability to connect various sectors. Here we are only interested in bosonic scattering so the collinear partons will be labelled ϕ and h for the scalar and graviton respectively. Glauber exchanges will generate the following set of non-local (in the transverse plane) gauge invariant operators

$$
\begin{aligned}
O^{\phi\phi}_{ns\bar{n}} &= \mathcal{O}^{\phi}_{n}\frac{1}{\mathcal{P}^2_\perp}\mathcal{O}_s\frac{1}{\mathcal{P}^2_\perp}\mathcal{O}^{\phi}_{\bar{n}} & O^{h\phi}_{ns\bar{n}} &= \mathcal{O}^{\phi}_{n}\frac{1}{\mathcal{P}^2_\perp}\mathcal{O}_s\frac{1}{\mathcal{P}^2_\perp}\mathcal{O}^{h}_{\bar{n}}\,, \\
O^{\phi h}_{ns\bar{n}} &= \mathcal{O}^{\phi}_{n}\frac{1}{\mathcal{P}^2_\perp}\mathcal{O}_s\frac{1}{\mathcal{P}^2_\perp}\mathcal{O}^{h}_{\bar{n}}\,, & O^{hh}_{ns\bar{n}} &= \mathcal{O}^{h}_{n}\frac{1}{\mathcal{P}^2_\perp}\mathcal{O}_s\frac{1}{\mathcal{P}^2_\perp}\mathcal{O}^{h}_{\bar{n}}\,.
\end{aligned}
\tag{6.10}
$$

On the left-hand side the subscripts indicate that these operators involve three sectors $\{n, s, \bar{n}\}$, while the first and second superscript determine whether we take a (scalar) quark or graviton operator in the n-collinear or $\bar{n}$-collinear sectors.

6.4.3 The Need for Power Suppressed Operators

If we are interested in higher order corrections we will need to include operators suppressed by powers of λ. This is due to the superleading λ-scaling of the leading power Glauber Lagrangian, which scales as $\mathcal{O}^{ij}_{ns\bar{n}} \sim \frac{s}{M^2_{pl}} \sim \frac{1}{\lambda^2}\alpha_Q$. As we can see in Fig. 6.1, we may add leading power Glaubers to obtain power enhancements. A power suppressed operator O_k which scales as $O_k \sim \lambda^{2k}$, $k > 0$ may then be inserted into a diagram with $k+1$ Glaubers to have the same λ scaling as the tree amplitude, and more Glauber insertions then served to further raise the enhancement. Sub-leading operators represent quantum corrections and thus if we are interested in classical pieces one would think that they can be ignored at the outset. In general this is true, as the interference like terms between super classical and quantum will not contribute to the classical phase in Eq. (6.6). However, there are exceptions, as there are power corrections to the Glauber operators that lead to classical corrections that must be included in the classical phase. The need for power-suppressed operators is not unique to the SCET approach to forward scattering in gravity presented here. In the Heavy Particle Effective Theory (HEFT) formalism for example, power suppressed, or quantum, operators are known to be necessary for higher order classical results [63, 40, 41, 103].

6.4.4 Factorization of the Amplitude from Glauber SCET for YM

Using this action we can write down a factorized form for the amplitude that looks effectively two dimensional. To include effects of the Glaubers within the EFT following [159, 144, 93] we start with the time evolution operator

$$U(a,b;T) = \lim_{T\to\infty(1-i0)} \int \left[\mathcal{D}\phi\right] \exp\left[i\int_{-T}^{T} d^4x \left(\mathcal{L}^{(0)}_{n\bar{n}s}(x) + \mathcal{L}^{\mathrm{II}(0)}_{G}(x)\right)\right], \tag{6.11}$$

one then expands in the number of Glauber potential insertions attaching to the n and $\bar{n}$ projectiles, given by i and j respectively, so that

$$\exp\left[i\int_{-T}^{T} d^4x \left(\mathcal{L}^{\mathrm{II}(0)}_{G}(x)\right)\right] = 1 + \sum_{i=1}^{\infty}\sum_{j=1}^{\infty} U_{(i,j)}. \tag{6.12}$$

For any number of Glauber potential insertions, one can then factorize the soft and collinear operators to give a factorized expression for the amplitude for scattering of projectile κ with κ' is

$$M^{\kappa\kappa'} = i\sum_{MN}\int\int_{\perp(N,M)} J_{\kappa N}(\{l_{\perp i}\},\epsilon,\eta) S_{(N,M)}(\{l_{\perp i}\};\{l'_{\perp i}\},\epsilon,\eta)\bar{J}_{\kappa' M}(\{l'_{\perp i}\},\epsilon,\eta) \tag{6.13}$$

where, following the notation in [93], we defined

$$\int\int_{\perp(N,M)} = \frac{(-i)^{N+M}}{N!M!}\int\prod_{i=1}^{N}\prod_{j=1}^{M}\frac{[d^{d'}l_{i\perp}]}{l^2_{i\perp}}\frac{[d^{d'}l'_{j\perp}]}{l'^2_{j\perp}}\bar{\delta}^{d'}(\sum l_{i\perp} - q_\perp)\bar{\delta}^{d'}(\sum {l'}_{j\perp} - q_\perp), \tag{6.14}$$

κ and κ' label the external states, i.e. scalars or gravitons. Note that in Eq.(6.13) all of the Glauber light cone momentum integrals have been performed, as have all of the soft and collinear loops, that is why J, S depend upon the regulators ϵ and η. All of the Glauber loops correspond to box integrals [15] which are rapidity finite and give a result independent of the perp momenta, since the Glauber light-cone momenta are dropped in the soft function. After performing the Glauber energy integral by contours we then use the result for the rapidity regulated k_z integration

$$\int \frac{[dk_z]}{-2k_z + A + i\epsilon} \mid \frac{2k_z}{\nu} \mid^{-\eta} = -\frac{1}{4}. \tag{6.15}$$

[15] Cross box integrals vanish with this regulator.

More generally it was shown in [159] that the n-Glauber box diagram generates a factor of $\frac{i^n}{n!}$ which is necessary to form the semi-classical phase. This explains why the amplitude is defined with the factorial prefactors in Eq.(6.14).

The jet function are defined as time ordered products, e.g. at the one and two Glauber gluon level

$$\begin{aligned} J(k_\perp) &= \int dx_1^\pm \langle p \mid T((O_n^\phi + O_n^h)(k_\perp, x_1^\pm) \mid p' \rangle \\ J(k_\perp, k'_\perp) &= \int dx_1^\pm dx_2^\pm \langle p \mid T((O_n^\phi + O_n^h)(k_\perp, x_2^\pm)(O_n^\phi + O_n^h)(k_\perp, x_1^\pm) \mid p' \rangle, \end{aligned} \quad (6.16)$$

The jets are written in this way because the combination $(O_n^\phi + O_n^h)$, see equation (5.42) for the definition, is an eigen-vector of $\nu \frac{d}{d\nu}$. At tree level the individual jet functions for n Glauber exchange

$$\begin{aligned} J_{\phi n}^{(0)} &= (n \cdot p)^{n+1} \left(\frac{\kappa}{2}\right)^n \\ J_{hn}^{(0)} &= (b_{\mu\nu} \epsilon^\mu \epsilon^\nu)^2 (n \cdot p)^{n+1} (\frac{\kappa}{2})^n \end{aligned} \quad (6.17)$$

where

$$b_{\mu\nu} = \bar{n} \cdot p_1 g_\perp^{\mu\nu} - \bar{n}^\mu p_{1\perp}^\nu - \bar{n}^\nu p_{4\perp}^\nu + \frac{p_{1\perp} \cdot p_{4\perp} \bar{n}^\mu \bar{n}^\nu}{\bar{n} \cdot p_2}. \quad (6.18)$$

For p_1/p_4 the incoming and out going momenta respectively. The tree level soft function for (i, j) is given by

$$S_{(i,j)}^{(0)}(l_{i\perp}; l'_{i\perp}) = 2\delta_{ij} i^j j! \prod_{a=1}^{j} l'^2_{i\perp} \prod_{n=1}^{j-1} \tilde{\delta}^{d'}(l_{n\perp} - l'_{n\perp}) \quad (6.19)$$

Note that $S_{(1,1)}^{(0)} = 2il_\perp^2$ and $J_1^{(0)} = (n \cdot p)^2 \frac{\kappa}{2}$, such that the leading order, one Glauber, tree level exchange gives

$$M_0 = -s^2 \frac{\kappa^2}{2t}. \quad (6.20)$$

We will need the form of the tree level results for the purposes of renormalization.

6.4.5 Summing the Logs using the Rapidity Renormalization Group (RRG)

While the amplitude is free of rapidity divergences, the individual components are not, and they obey the RRG equations

$$\begin{aligned}
\nu\frac{\partial}{\partial\nu}J_{\kappa(i)} &= \sum_{j=1}^{\infty} J_{\kappa(j)} \otimes \gamma^{J}_{(j,i)}, \\
\nu\frac{\partial}{\partial\nu}S_{(i,j)} &= -\sum_{k=1}^{\infty} \gamma^{S}_{(i,k)} \otimes S_{(k,j)} - \sum_{k=1}^{\infty} S_{(i,k)} \otimes \gamma^{S}_{(k,j)}, \\
\nu\frac{\partial}{\partial\nu}\bar{J}_{\kappa'(i)} &= \sum_{j=1}^{\infty} \gamma^{\bar{J}}_{(i,j)} \otimes \bar{J}_{\kappa'(j)}.
\end{aligned} \tag{6.21}$$

$\gamma_{(i,j)}$ are the rapidity anomalous dimensions, which will be defined below.

In Yang-Mills theory Each J_i and $S_{(i,j)}$ is decomposed into irreducible representations of the $SU(N)$ gauge symmetry and operators with different numbers of Glaubers, but in the same irrep, can mix (for a discussion of the general structure see [93]). This is one complication that will obviously not arise in the case of gravity which will present a different set of challenges. Another significant simplification that arises in the gravitational case is that $S_{M,N} \propto \delta_{MN}$ due to RPI invariance which is the invariance of the physics under small deformations of the choice of light cone directions for the partons [134]. Which is to say that, in the EFT we must choose a large light cone momentum around which to expand and there is arbitrariness in that choice. Technically this correponds to invariance under a shifts of the light cone directions n and $\bar{n}$ that leave the inner products $n\cdot n = \bar{n}\cdot\bar{n} = 0$ and $n\cdot\bar{n} = 2$ invariant. In the case at hand we will utilize the fact that RPI implies that every amplitude scales as $n^a\bar{n}^b$ with $a = b$[16]. Any amplitude can only depend upon the product of the two large incoming (conserved) light cone momenta $n\cdot p\bar{n}\cdot p$. Each insertion of a Glauber graviton generates a factor of $(n\cdot p^{-1}, \bar{n}\cdot p^{-1})$ from the associated collinear and anti-collinear propagator to which they connect i.e. if the collinear/Glauber momenta are p/k then

$$\frac{1}{(p-k)^2} \approx \frac{1}{n\cdot p(\bar{n}\cdot k - \frac{k_\perp^2}{n\cdot p})}. \tag{6.22}$$

Thus the number of insertions of Glaubers on the top and the bottom must be the same. This is a significant simplification from QCD where diagrams such as the "tennis court" diagram arise at three loops which vanish in gravity. This result holds independent of the type of collinear parton being considered. In QCD we lose this constraint because the numerators cancel out these additional powers of the light cone momenta. Operationally,

[16] This is called RPIII in the language of [134].

the vanishing of diagrams with a different number of Glauber connections on the top and bottom of the diagram arises due to the vanishing of the tensor integrals. It might seem curious that we can find a diagram which is not RPI invariant given that the action is RPI invariant. But one must recall that J and $\bar{J}$ are composed of time ordered products of non-RPI invariant operators. Thus if we wrote the amplitude in the form $J \otimes S \otimes \bar{J}$, we will only get a non-vanishing (RPI invariant) result if J and $\bar{J}$ have the same number of Glaubers attached to them.

Now that we know that S is diagonal this simplifies the RRG equations considerably. In addition it allows us to write down the following simple constraint

$$J_{(i)} \otimes \gamma^{J}_{(i)} + \gamma^{\bar{J}}_{(i)} \otimes \bar{J}_{(i)} - \gamma^{S}_{(i)} \otimes S_{(i)} - S_{(i)} \otimes \gamma^{S}_{(i)} = 0, \tag{6.23}$$

which follows from the fact that the full result must be independent of the ν. Note that since S is diagonal we have simplified its index structure.

With this simplification we have

$$\begin{aligned} J_i(\{l_{\perp i}\}, \epsilon, \eta, \nu) &= \int_{\perp(i)} J_i(k_{\perp i}, \epsilon, \nu) Z^J_i(\{k_{\perp i}\}; \{l_{\perp i}\}, \epsilon, \eta, \nu) \\ S_i(\{l_{\perp i}\}; \{l'_{\perp i}\}, \eta, \nu, \epsilon) &= \int_{\perp(i)} \int_{\perp(i)} Z^S_i[\{l_{\perp i}\}; \{k_{\perp i}\}, \epsilon, \eta, \nu] S_i[\{k_{\perp i}\}; \{k'_{\perp i}\}, \nu] Z^S_i[\{k'_{\perp i}\}; \{l'_{\perp i}\}) \epsilon, \eta, \nu]. \end{aligned} \tag{6.24}$$

where the left hand sides are bare quantities which have poles in η. Note that there is ϵ dependence in the renormalized quantities because these objects are not IR safe. The integrations are defined by

$$\int_{\perp(A)} \equiv \frac{(-i)^A}{A!} \int \prod_{a=1,A} \frac{[d^{d'} k^a_\perp]}{(k^a_\perp)^2} \bar{\delta}^{d'}(\sum_{a=1,A} k^a_\perp - q_\perp). \tag{6.25}$$

The anomalous dimensions are defined by imposing

$$\nu \frac{d}{d\nu} J_i(\{l_{\perp i}\}, \epsilon, \eta, \nu) = 0, \tag{6.26}$$

and are then given by

$$\gamma^{(i)}_J = -(\nu \frac{d}{d\nu} \mathbf{Z}^J_i)(\mathbf{Z}^J_i)^{-1}, \tag{6.27}$$

where the bold faced lettering denotes the convolutional nature of the equation. Due to our choice of normalization in the convolution eq.(6.14), the Z factor has units of plus two.

6.5 The Rapidity Renormalization Group and the Regge Trajectory

Let us calculate the leading order running of the $S_{(1,1)}$, which will yield the Regge trajectory. This correction is down by a factor of α_Q relative to the Glauber contribution. There is only one diagram to calculate in the EFT, the so-called "eye-graph", which if opened up into the full theory would correspond to the soft graph topologies corresponding to vacuum bubble, box and cross box graphs. The flower graph also contributes at this order but does not contain any rapidity divergences. The same can be said for the scalar vacuum bubble. To calculate the anomalous dimensions we are only interested in the rapidity divergent term which is given by

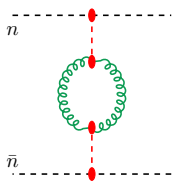

$$\begin{aligned} &= -i\frac{\kappa^4 s^2\, w^2}{8\pi\eta}(3-2\epsilon)q_\perp^2 \int \frac{[d^{d'}k_\perp]}{k_\perp^2(k_\perp - q_\perp)^2} \\ &= i\frac{\kappa^4 s^2\, w^2}{32\pi^2\eta}(3-2\epsilon)B[1,1]\left(\frac{-t}{\bar{\mu}^2}\right)^{-\epsilon}. \end{aligned} \tag{6.28}$$

Since there is only one Glauber exchanged the renormalization is multiplicative, as opposed to convolutive. We then can write

$$S^B_{(1,1)} = \tilde{Z}^S_{(1,1)} S^R_{1,1}, \tag{6.29}$$

Here we have introduced $\tilde{Z}$ as the multiplicative renormaliation factor. The anomalous dimension in this case will also be written as $\tilde{\gamma}_{(1,1)}$, since the RRG is multiplicative.

Recalling that that at leading order $S_{(1,1)} = 2it$, and that two factors of $\kappa s/2$ get absorbed into the J's we find

$$\tilde{Z}^S_{(1,1)} = \frac{\kappa^2 t\, w^2}{16\pi^2\eta}(3-2\epsilon)B[1,1]\left(\frac{-t}{\bar{\mu}^2}\right)^{-\epsilon}. \tag{6.30}$$

which leads to the RRG equation

$$\nu\frac{dS^R_{(1,1)}}{d\nu} = -\tilde{\gamma}^S_{(1,1)}(t) S_R, \tag{6.31}$$

with $\tilde{\gamma}^S_{(1,1)}$ being given by

$$\tilde{\gamma}^S_{(1,1)} = -\frac{\kappa^2 t}{16\pi^2}(3-2\epsilon)B[1,1]\left(\frac{-t}{\bar{\mu}^2}\right)^{-\epsilon}. \tag{6.32}$$

We way then identify $\omega_G(t) = -\frac{1}{2}\tilde{\gamma}^S_{(1,1)}(t)$ as the graviton Regge trajectory [17]

$$\omega_G(t) = \frac{\kappa^2 t}{32\pi^2}(3-2\epsilon)B[1,1]\left(\frac{-t}{\bar{\mu}^2}\right)^{-\epsilon} = \frac{\kappa^2 t}{16\pi^2}\left(-\frac{3}{\epsilon} + 3\log\frac{-t}{\mu^2} + 2 + O(\epsilon)\right). \tag{6.33}$$

We can compare is this leading order Regge trajectory found in the literature. Our results agree with those given in [15], for the physical non-local piece. The only other result that we are aware of for the Regge trajectory was given in [137]. The $\log(t)$ coefficient seems to disagree with ours result, but the result in [137] has dependence on both t as well as an impact parameter z (the transverse separation between the Wilson lines), so it's not clear how to compare.

6.5.1 The Systematics of the Regge Trajectory

The Regge trajectory is defined as the IR divergent anomalous dimensions of $S_{(1,1)}$ which is not physical. Nonetheless, it is of considerable theoretical interest. In this chapter we have calculated the leading order trajectory which sums terms of the form $\frac{t}{M_{pl}^2}\log\left(\frac{s}{-t}\right)$. For this to be a sysematic resummation we would need $\frac{t}{M_{pl}^2}\log\left(\frac{s}{-t}\right) \sim 1$, at least for Einstein Gravity, since the existence of counter-terms starting at order $(\frac{t}{M_{pl}^2})^6$ will dominate higher order terms in the re-summation if the criteria above is not met. The same conclusion applies to the running of higher dimension soft operators (or collinear for that matter), and their subsequent BFKL type of equations. There is evidence that $N = 8$ supergravity is finite, having the same UV behavior as $N = 4$ SYM theory [27]. If this were indeed the case then resummation program for $N = 8$ [162, 163] would indeed be systematic. However, even that conclusion would be model dependent, as the lack of divergences, while compelling, does not necessarily imply that the counter-terms, the existence of which are still being debated [111], don't contribute to the amplitude. If the theory were truly UV complete then these contributions would vanish and resummation would be systematic.

6.6 The Gravitational BFKL Equation

In this section we derive the gravitational BFKL equation, which was first given for the total cross section in [127]. As shown in [93], the BFKL equation is derived in the EFT through

[17] Note that there is an additional factor of 1/2 because the trajectory is defined as $M \sim (s/-t)^{\omega}$.

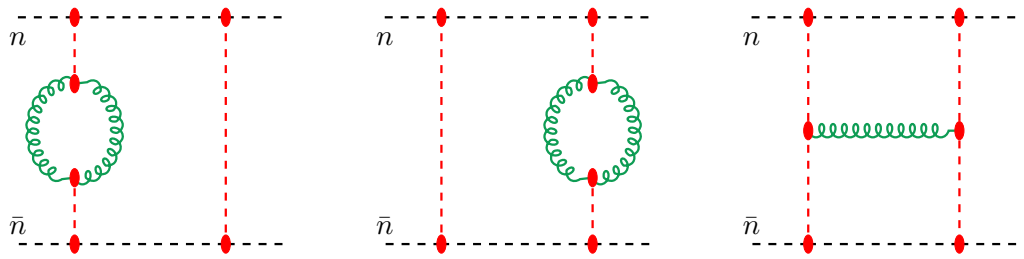

Figure 6.2: Diagrams needed for the renormalization of $S_{(2,2)}$. The first two diagrams are soft eye insertions into a Glauber rung, while the third diagrams is H graph.

the renormalization of $S_{(2,2)}$. We perform this renormalization, and then we generalize this result and renormalize $S_{(N,N)}$ for arbitrary N. It is worth emphasizing that there is nothing special about $N = 2$ other than the fact that this is the first soft operator which obeys convolutional running. There are also BFKL like equations for higher N. The caveats about the systematics in the previous discussion of the Regge trajectory apply here as well.

6.6.1 Renormalizing $S_{(2,2)}$

There are only two loop topologies which renormalize $S_{(2,2)}$ corresponding the H graphs and eye graphs as shown in figure (6.2). Graphs such as those involving scalar contributions to the Glauber polarization have no rapidity divergences. The H-graph, shown on the right hand side of figure (6.2) with no additional Glauber rungs, is calculated using the Feynman rule for the Lipatov vertex in Fig. (5.3b), and is given by

$$i\mathcal{M}_H = \frac{i\kappa^6 s^3}{8}\int \frac{[d^d k_n][d^d k_{\bar{n}}]\, w'^4 \left|\frac{k_n^- - k_{\bar{n}}^+}{\nu'}\right|^{-2\eta'} \mathcal{N}(k_n, k_{\bar{n}})}{((k_n - k_{\bar{n}})^2 + i\epsilon)\left(p_1^+ + k_{\bar{n}}^+ + \frac{(k_{\bar{n}\perp}+q_\perp/2)^2}{p_1^-} + i\epsilon\right)\left(p_2^- - k_n^- + \frac{(k_{n\perp}+q_\perp/2)^2}{p_2^+} + i\epsilon\right) D_G}, \tag{6.34}$$

where we have defined

$$\begin{aligned}
D_G &= d_1\, d_2\, d_3\, d_4,\\
\mathcal{N}(k_n, k_{\bar{n}}) &= \Big(q_\perp^2((k_n - k_{\bar{n}})^2 + q_\perp^2) - (d_1 + d_4)(d_2 + d_3) - \frac{1}{k_n^+ k_{\bar{n}}}(d_1 d_4 + d_2 d_3)(d_1 + d_2 + d_3 + d_4 - 2q_\perp^2)\\
&\quad - \frac{1}{(k_n^+ k_{\bar{n}})^2}\big[(d_1 - d_3)(d_2 - d_4)(d_1 d_4 + d_2 d_3) + d_5(d_1 d_4 - d_2 d_3)(d_1 - d_2 - d_3 + d_4)\\
&\quad - d_5^2(d_1 d_4 + d_2 d_3)\big]\Big) w^2 \left|\frac{k_n^+ + k_{\bar{n}}^-}{\nu}\right|^{-\eta}, \qquad (6.35)\\
d_1 &= k_{n\perp^2}, \qquad d_2 = (k_{n\perp} + q_\perp)^2, \qquad d_3 = k_{\bar{n}\perp}^2, \qquad d_4 = (k_{\bar{n}\perp} + q_\perp)^2, \qquad d_5 = (k_{n\perp} - k_{\bar{n}\perp})^2.
\end{aligned}$$

To compute the H-graph we must be sure to handle the η regulators properly, as discussed in [93], by integrating over the $O(\lambda^2)$ Glauber k_n^- and $k_{\bar{n}}^+$ components of momenta, expanding in η' and taking $w' \to 1$. In principle we must make a choice of $\pm i\epsilon$ in the eikonal factors of $(k_n^+ \pm i\epsilon)$ and $(k_{\bar{n}}^- \pm i\epsilon)$, but as discussed in [159, 93], any additional contributions are removed by zero-bin subtractions [132](which vanish), and so the result for the integral is independent of the choice. Changing variables to $k_n^+ - k_{\bar{n}}^- = k^0$ and $k_n^+ + k_{\bar{n}}^- = k^3$, we can perform the k^0 integral by contours and integrate over k^3 to obtain the divergent piece of the graph

$$i\mathcal{M}_H = -\frac{\kappa^6 s^3 w^2}{2^6 \pi \eta} \int \frac{[d^{d'}k_\perp][d^{d'}l_\perp]}{d_1\, d_2\, d_3\, d_4} \left(q_\perp^4 - 2\frac{(d_1 d_4 + d_2 d_3) q_\perp^2}{d_5} + \frac{d_1^2 d_4^2 + d_2^2 d_3^2}{d_5^2} \right), \tag{6.36}$$

where for notational clarity we have relabelled $k_{n\perp}$ and $k_{\bar{n}\perp}$ by $k_\perp$ and $l_\perp$ respectively. Note that there is no corresponding ghost graph. The reason is that collinear soft operator is composed of gauge invariant building blocks. Something similar happens in NRQCD [158] as well as Glauber SCET [159]. This is not to say that ghosts dont show up at higher orders. Indeed, if we were to include a vacuum polarization in the soft or collinear sectors themselves, we would require ghost loops to keep the theory unitary.

The other relevant topolgy is the double box with an soft eye subgraph. These topologies will never contribute to any classical observable as they corresponds to cross terms between the classical exponent and the quantum corrections in (6.6). These diagrams are simply the one loop soft eye diagram convoluted with the Glauber box diagram in $\perp$-momenta. This is because the soft loop is insensitive to the Glauber $k^\pm \sim \lambda^2$, while soft $l^\pm \sim \lambda$. Given the soft eye has been computed already in Eq. (6.28), we may write down the divergent result for the sum of the two soft eye boxes as

$$i\mathcal{M}_{SEB} = -\frac{\kappa^6 s^3 w^2}{32\pi\eta} \int \frac{[d^{d'}k_\perp][d^{d'}\ell_\perp]\,(k_\perp + q_\perp)^2(3-2\epsilon)}{k_\perp^2\, \ell_\perp^2\, (k_\perp + \ell_\perp + q_\perp)^2} \tag{6.37}$$

In the above, we have already performed the small Glauber $k^\pm \sim \lambda^2$ integrals.

The factorized $O(\alpha_Q)$ matrix elements is then written as

$$i\mathcal{M}_H + i\mathcal{M}_{SEB} = J_{(2)}^{(0)} \otimes S_{(2,2)}^{(1)} \otimes \bar{J}_{(2)}^{(0)}. \tag{6.38}$$

Expanding out the convolutions, the amplitude becomes

$$J_{(2)}^{(0)} \otimes S_{(2,2)}^{(1)} \otimes \bar{J}_{(2)}^{(0)} = \frac{1}{4} \int \frac{[d^{d'}k_\perp][d^{d'}\ell_\perp]}{k_\perp^2 (k_\perp + q_\perp)^2 \ell_\perp^2 (\ell_\perp + q_\perp)^2} J_{(2)}^{(0)}(k_\perp) S_{(2,2)}^{(1)}(k_\perp, \ell_\perp) \bar{J}_{(2)}^{(0)}(\ell_\perp). \tag{6.39}$$

Since $J_{(2)}^{(0)}$ and $J_{(2)}^{(0)}$ are independent of the transverse momentum (from their definition in

Eq.(6.17), we can extract $S^{(1)}_{(2,2)}$ from the amplitudes in Eqs. (6.36) and (6.37). The bare [18] one loop soft function then given by

$$S^{(1)}_{(2,2)}(k_\perp,\ell_\perp) = \frac{-8w^2}{\eta}\left[\frac{\kappa^2}{8\pi}K_{\rm GR}(k_\perp,\ell_\perp) + \tilde{\delta}^{d-2}(k_\perp-\ell_\perp)\ell_\perp^2(\ell_\perp+q_\perp)^2(\omega_G(k_\perp)+\omega_G(k_\perp+q_\perp))\right], \tag{6.40}$$

where ω_G is the Regge trajectory given in Eq. (6.33), and K_{GR} is the convolutional kernel

$$K_{\rm GR}(k_\perp,\ell_\perp) = \left(q_\perp^4 - 2q_\perp^2\frac{(k_\perp^2(\ell_\perp-q_\perp)^2+(k_\perp-q_\perp)^2\ell_\perp^2)}{(k_\perp-\ell_\perp)^2} + \frac{(k_\perp^4(\ell_\perp-q_\perp)^4+(k_\perp-q_\perp)^4\ell_\perp^4}{(k_\perp-\ell_\perp)^4}\right). \tag{6.41}$$

The leading RRGE is then given by

$$\nu\frac{\partial}{\partial\nu}S_{(2,2)}(k_\perp,\ell_\perp) = \frac{1}{2}\int\frac{[d^{d'}p_\perp]}{p_\perp^2(p_\perp-q_\perp)^2}\left(\gamma^{(1)}_{(2,2)}(k_\perp,p_\perp)S_{(2,2)}(p_\perp,\ell_\perp) + S_{(2,2)}(k_\perp,p_\perp)\gamma_{(2,2)}(p_\perp,\ell_\perp)\right). \tag{6.42}$$

Using the result of Eq. (6.19) for $S^{(1)}_{(2,2)}$, we can then extract the anomalous dimension $\gamma_{(2,2)}$:

$$\gamma_{(2,2)}(k_\perp,p_\perp) = \frac{\kappa^2}{4\pi}K_{\rm GR}(k_\perp,p_\perp) + 2\tilde{\delta}^{d-2}(k_\perp-p_\perp)p_\perp^2(p_\perp-q_\perp)^2(\omega_G(p_\perp)+\omega_G(p_\perp-q_\perp)). \tag{6.43}$$

This rapidity RGE reproduces the gravitational analogue of the BFKL equation, given by Lipatov [127], in his Eq. (80). It is interesting to compare this anomalous dimension to the one computed in QCD. There, one has[93]

$$\begin{aligned}\gamma^{A_1A_2;B_1B_2}_{(2,2),\rm YM} =& 4\alpha_s f^{A_1B_1C}f^{A_2B_2C}K_{\rm YM}(k_\perp,\ell_\perp) \\ &+ 2\delta^{A_1B_1}\delta^{A_2B_2}\tilde{\delta}^{d-2}(k_\perp-\ell_\perp)\ell_\perp^2(\ell_\perp-q_\perp)^2(\alpha_R(\ell_\perp)+\alpha_R(\ell_\perp-q_\perp)),\end{aligned} \tag{6.44}$$

where α_R is the gluon Regge trajectory, and the QCD kernel is given by

$$K_{\rm YM}(k_\perp,\ell_\perp) = q_\perp^2 + \frac{\ell_\perp^2(q_\perp-k_\perp)^2+k_\perp^2(\ell_\perp-q_\perp)^2}{(\ell_\perp-k_\perp)^2} \tag{6.45}$$

The QCD and gravity anomalous dimensions have obvious structural similarities, in that they are both the sums of a kernel representing a gluon/graviton exchange and a Reggeization term on each Glauber exchange. Quite remarkably, there is also a relation between the convolutional kernels. Specifically, one has

$$K_{\rm GR}(k_\perp,\ell_\perp) = (K_{\rm YM}(k_\perp,\ell_\perp))^2 + \text{scaleless}, \tag{6.46}$$

[18] We will drop the B superscript from here on. Bare objects depedence upon ϵ and η will be made explicit.

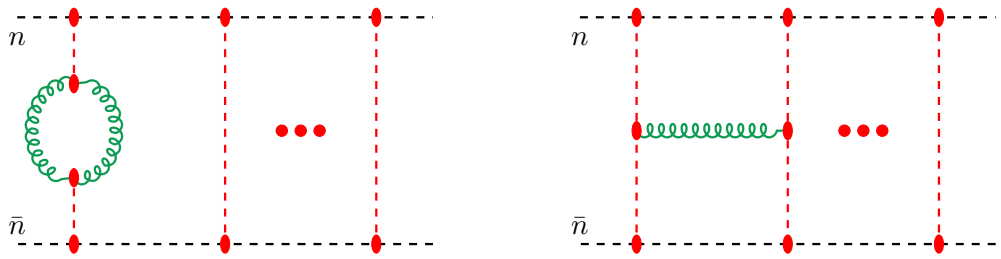

Figure 6.3: Prototypical diagrams needed to renormalize $S_{(N+1,N+1)}$. The diagram on the left is the $N+1$-rung Glauber box with a soft eye insertion, and the diagram on the right is the multi-rung H diagram. The soft graviton exchange can be between any two Glauber rungs, and the soft eye can similarly be inserted into any individual rung. The H graph contribution fo $S_{(2,2)}$ has no additional Glauber rungs.

where the "+ scaleless" means terms which lead to scaleless integrals in the convolutions and thus vanish. It has long been appreciated that there exists a double copy relation between the QCD and gravitational Lipatov vertices [127, 125, 161], so it is perhaps not too surprising that this extends to the emission piece of the anomalous dimension. The authors are unaware of any previous mentions of this squaring relation in the literature, although it could have been noticed as early as [127].

6.6.2 The BFKL Equation for all Soft Functions

We now extract the one loop anomalous dimensions of $S_{(N+1,N+1)}$ for arbitrary N. There is a very limited class of diagrams which can contribute: N-Glauber boxes with a soft eye insertion on one rung, or N-Glauber boxes with a graviton exchanged between two rungs, i.e. the H diagram with additional Glauber rungs. We may write the contribution of the amplitude then as

$$\sum_{j>k} i\mathcal{M}_H^{jk} + \sum_j i\mathcal{M}_{SEB}^j = J_{(N+1)}^{(0)} \otimes S_{(N+1,N+1)}^{(1)} \otimes \bar{J}_{(N+1)}^{(0)}, \tag{6.47}$$

where $\mathcal{M}_H^{jk}$ denotes a graviton exchange between Glauber rungs j and k, and $\mathcal{M}_{SEB}^j$ denotes an insertion of the soft eye on rung j. Adding additional Glauber rungs does not complicate the calculation of the diagrams, since, as discussed above, the soft loops are insensitive to the Glauber $k^\pm$. Each additional Glauber loop, beyond the first, adds a factor of $(-i)i^2\kappa^2\frac{s}{2}[d^{d'}k_{i\perp}]/k_{i\perp}{}^2$, as well an additional factor that arises, from performing the

Glauber lightcone integrals, of $(-1/2)^N/(N+1)!$. The result for $\mathcal{M}^j_{SEB}$ is then

$$i\mathcal{M}^j_{SEB} = \frac{(-i)^{N+1}\kappa^{4+2N}s^{2+N}w^2}{2^{2N+3}\pi\,\eta(N+1)!}\int\left(\prod_{m=1}^{N+1}\frac{[d^{d'}k_{m\perp}]}{k^2_{m\perp}}\right)\delta^{d'}\left(\sum_{m=1}^{N+1}k_{m\perp}-q_\perp\right) \times\int\frac{d^{d'}\ell_\perp\,k^4_{j\perp}(3-2\epsilon)}{\ell^2_\perp\,(k_{j\perp}-\ell_\perp)^2}. \tag{6.48}$$

The multi-rung H graph may similarly be computed as

$$i\mathcal{M}^{jk}_H = \frac{(-i)^{N+1}\kappa^{4+2N}s^{2+N}w^2}{2^{3+2N}\pi\eta\,(N+1)!}\int\left(\prod_{m=1}^{N+1}\frac{[d^{d'}k_{m\perp}]}{k^2_{m\perp}}\right)\delta^{d'}\left(\sum_{m=1}^{N+1}k_{m\perp}-q_\perp\right) \times\int\frac{[d^{d'}\ell_\perp]}{\ell^2_\perp(\ell_\perp-k_{j\perp}-k_{k\perp})^2}K(k_{j\perp},k_{k\perp};\ell_\perp,\ell_\perp-k_{j\perp}-k_{k\perp}), \tag{6.49}$$

where K is given by

$$K(k_1,k_2;\ell_1,\ell_2)=\left((k_1+k_2)^4-2(k_1+k_2)^2\frac{(k_1^2\ell_2^2+k_2^2\ell_1^2)}{(k_1-\ell_1)^2}+\frac{(k_1^4\ell_2^4+k_2^4\ell_1^4)}{(k_1-\ell_1)^4}\right). \tag{6.50}$$

The amplitude in terms of the convolutions is given by

$$J^{(0)}_{(N+1)}\otimes S^{(1)}_{(N+1,N+1)}\otimes\bar{J}^{(0)}_{(N+1)} = (-1)^{N+1}\frac{\kappa^{2N+2}s^{N+2}}{2^{2+2N}(N+1)!^2}\int\left(\prod_{m=1}^{N+1}\frac{[d^{d'}k_{m\perp}]}{k^2_{m\perp}}\right)\left(\prod_{n=1}^{N+1}\frac{[d^{d'}\ell_{n\perp}]}{\ell^2_{n\perp}}\right) \times S^{(1)}_{(N+1,N+1)}(\{k_{m\perp}\};\{\ell_{n\perp}\})\delta^{d'}\left(\sum_m k_{m\perp}-q_\perp\right)\delta^{d'}\left(\sum_n l_{n\perp}-q_\perp\right). \tag{6.51}$$

Comparing the sum of Eqs. (6.48) and (6.49), we can obtain $S^{(1)}_{(N+1,N+1)}$:

$$S^{(1)}_{(N+1,N+1)} = \frac{4i^{N+1}(N+1)!w^2}{\eta}\Bigg[\sum_{i<j}\frac{\kappa^2}{8\pi}K(k_{i\perp},k_{j\perp};\ell_{i\perp},\ell_{j\perp})\prod_{p\neq i,j}\ell^2_{p\perp}\delta^{d'}(\ell_{p\perp}-k_{p\perp} +\sum_j\ell^2_{j\perp}\omega_G(\ell_j)\prod_{p\neq j}\ell^2_{p\perp}\delta^{d'}(\ell_{p\perp}-k_{p\perp})\Bigg]. \tag{6.52}$$

The leading RRGE is then given by

$$\nu\frac{\partial}{\partial\nu}S_{(N+1,N+1)}(\{k_{i\perp}\},\{\ell_{\perp_i}\}) = -\int_{\perp(N+1)}\Big(\gamma^{(1)}_{(N+1,N+1)}(\{k_{i\perp}\};\{\ell'_{j\perp}\})S_{(N+1,N+1)}(\{\ell'_{i\perp}\};\{\ell_{j\perp}\}) \tag{6.53}$$
$$+ S_{(N+1,N+1)}(\{k_{i\perp}\};\{\ell'_{j\perp}\})\gamma_{(N+1,N+1)}(\{\ell'_{i\perp}\};\{\ell_{j\perp}\})\Big)..$$

Recalling the definition of $S^{(0)}_{(N+1,N+1)}$

$$S^{(0)A_1\ldots A_i;B_1\ldots B_j}_{(i,j)}(l_{i\perp};l'_{i\perp}) = 2\delta_{ij}i^j j!\prod_{a=1}^{j} l'^2_{i\perp}\prod_{n=1}^{j-1}\bar{\delta}^{d'}(l_{n\perp}-l'_{n\perp}) \tag{6.54}$$

we find the anomalous dimension is given by

$$\gamma_{(N+1,N+1)} = -i^{N+1}(N+1)!\Big[\sum_{i<j}\frac{\kappa^2}{8\pi}K(k_{i\perp},k_{j\perp};\ell_{i\perp},\ell_{j\perp})\prod_{m\neq i,j}\ell^2_{m\perp}\bar{\delta}^{d-2}(\ell_{m\perp}-k_{m\perp}) \tag{6.55}$$
$$+\sum_j\omega_G(\ell_j)\prod_{m\neq j}\ell^2_{m\perp}\bar{\delta}^{d-2}(\ell_{m\perp}-k_{m\perp})\Big].$$

A few comments are in order. Firstly, we note that although it appears that the anomalous dimension might be imaginary for even N, this is somewhat illusory, as the factor of i^{N+1} drops out in the convolution. This is also the case with the overall factor of $(N+1)!$. Secondly, we note that this does return $\gamma_{(2,2)}$ in Eq. (6.43) when setting $N=1$. To see this, we apply $\perp$ momentum conservation to set $k_2 = q-k_1$ and $\ell_2 = q-\ell_1$. This also reproduces $\gamma_{(1,1)}$ after setting $N=0$. We simply drop the terms involving K since there is no convolution at the one Glauber level, and we have

$$\gamma_{(1,1)} = iq^2_\perp\omega_G(q_\perp). \tag{6.56}$$

The reason for the discrepancy of a factor of $iq^2_\perp$ between this anomalous dimension and the Regge trajectory computed in Section 6.5 is that this factor comes from the convolution for $S_{(1,1)}$, and in Section 6.5 this factor has been absorbed into the anomalous dimension, as the convolution is trivial. For $N\geq 2$, this cannot be consistently done, and so the factor from the convolution has been pulled out. Lastly, we mention that the anomalous dimension is symmetric under $k_{i\perp}\leftrightarrow\ell_{i\perp}$. This is not obvious given the definition of the kernel K in Eq. (6.50). Under the support of the $\perp$ delta-functions in the convolutions, one can see that $\gamma_{(N,N)}$ is indeed symmetric.

6.7 Extracting the Classical Logs

6.7.1 The 3PM Classical Log

As per our power counting discussion the first classical logs that can appear are at 3PM (two loop) order since we are looking for contributions that scale as $\alpha_C = G^2 st$ relative to the leading order Glauber exchange which starts at $O(G)$. The relevant logs can be extracted from the classical piece of the anomalous dimensions of the soft function. At each PM order there will be one classical log. We could equally as well calculate them from the collinear piece. By working in the EFT we can considerably reduce the amount of effort it takes to extract the log since we only need to calculate the $1/\eta$ pole, moreover to get the log (at any PM order) we never need to calculate more than a one loop diagrams. The price to be paid is the need to iteratively solve the RRG equations to the necessary order. At $(2n+1)$ order we need to iterate the $n-1$ times, so that there is no need to solve the RRG at all at 3PM.

The eikonal form of the amplitude is given explicitly by

$$(1 + i\Delta_Q)\, e^{i\delta_{\rm Cl}} - 1 = i\tilde{\mathcal{M}}(s,b), \tag{6.57}$$

where $\tilde{\mathcal{M}}(s,b)$ is the Fourier transform of the amplitude,

$$\tilde{\mathcal{M}}(s,b) = \int \bar{d}^{d-2} q_\perp \frac{\mathcal{M}(s,q_\perp^2)}{2s} e^{iq_\perp \cdot b}. \tag{6.58}$$

As prevsiously mentioned there exist terms in the series expansion of $\tilde{\mathcal{M}}(s,b)$ that scale classically which arise from mixing between quantum and super-classical terms. However, these terms are easily discarded at the beginning of the calculation as they are guaranteed not to contribute to the classical phase. To see this explicitly we may consider a graph with quantum loops with any number of Glauber enhancements that contributes to the amplitude at the classical level. Its Fourier transfrom will be equal to the product of the Fourier transform of the purely quantum piece and of (possibly iterated) Glauber box with a symmetry factor. This term will cancel with the aforemention mixed terms in eq(6.58). For example, consider a purely quantum contribution which is down by a factor of $(\frac{t}{M_{pl}^2})^n$ $I(k)$. To bring it up to classical scaling we need n Glaubers. Peforming the light cone integrals generates a factor of $1/(n+1)!$ and the Fourier transform then just leads to the products $\frac{1}{(n+1)!} I(b)\delta_0(b)^n$. We compare this to the cotribution which arises from expanding out the exponential to order $\delta_0(b)^n$. The difference in the combinatorial factors $1/(n+1)$ is compensated for by the fact that in the diagram we may insert $I(k)$ in any of $n+1$ places. The general rule that we need not worry about enhanced quantum corrections is violated

by any quantum insertion which gives non-trivial dependence on the Glauber light cone momentum, as this spoils the factorization in impact parameter space. As an example of this are the power suppressed operators, mentioned in section 6.4.3.

Thus to get the 3PM log we need only calculate the H graph rapidity divergent contribution which is given at one loop by

$$i\mathcal{M}_H^{(\log)} = -\log\left(\frac{\nu^2}{-t}\right) 2G^3 s^3 \left(\frac{\bar{\mu}^2}{-t}\right)^{2\epsilon} \left(-\frac{6-4\epsilon}{3} B(1,1)B(1,1+\epsilon) + B(1,1)^2\right), \quad (6.59)$$

which leaves for the 3PM classical log in impact parameter space

$$\begin{aligned}\delta_{\rm Cl}^{(2,\log)} &= i\log\left(\frac{\nu^2}{-t}\right) \frac{G^3 s^2}{b^2} \frac{\left(\bar{\mu}^2 b^2\right)^{3\epsilon}}{\pi^{1-\epsilon} 2^{4\epsilon}} \frac{\Gamma(1-3\epsilon)\Gamma(-\epsilon)^3}{3\Gamma(2\epsilon)} \left(\frac{3\Gamma(-\epsilon)\Gamma(1+\epsilon)^2}{\Gamma(-2\epsilon)^2} - 2\frac{(3-2\epsilon)\Gamma(1+2\epsilon)}{\Gamma(-3\epsilon)}\right), \\ &= i\log(s)\frac{4G^3 s^2}{b^2}\left(-\frac{1}{\epsilon}+2\right)\frac{\left(\bar{\mu}^2 b^2\right)^{3\epsilon}}{\pi^{1-\epsilon}2^{4\epsilon}} + O(\epsilon). \end{aligned} \quad (6.60)$$

This reproduces the result [73, 71]. As a cross-check, this also reproduces the $O(\epsilon^3)$ of the eikonal phase given in [102, 38, 70] for $N = 8$ supergravity. However, our result at order ϵ^4 seems to disagree with the "possible guess" made for this term. Note the $Log(s)$ comes from the fact that to eliminate all of the large logs from the collinear sector, and push them into the soft sector we choose $\nu^2 = s$.

The phase is imaginary indicating that it is a consequence of real radiation. At next order (5PM) the leading log will be real since it will arise from $S_{(3,3)}$ which has an additional Glauber, each of which generates a factor of i. This process will continue as N is increased.

6.7.2 Extracting Classical Logs to any PM Order

This procedure may be generalized to extract classical logarithms at any PM order by solving the rapidity RGEs for higher Glauber soft functions. To see this consider the $(2N+1)$PM term. This contribution to the amplitude will scale as

$$\mathcal{M}^{(2N+1)\rm PM} \sim \frac{Gs^2}{t}\alpha_{\rm C}^N \sim \frac{Gs^2}{t}(Gs)^N \alpha_Q^N. \quad (6.61)$$

Since each Glauber loop generates an enhancement of $\sim s/M_{pl}^2$, a classical term will generally involve N Glauber loops and N soft loops. To obtain the $(2N+1)$PM term, we then need to calculate the N-loop correction to $S_{(N+1,N+1)}$, as this is the only operator in the EFT that has the appropriate number of s/M_{pl} enhancements. That is, only need to consider one of the soft operators at each order in the PM expansion. As a concrete example, we have already computed the one loop correction to $S_{(2,2)}$, which gave the 3PM correction to the amplitude. To calculate the log at 5PM, it seems that we need the two loop correction

to $S_{(3,3)}$. However we can get that log indirectly via the RRG. By computing the one soft loop correction to $S_{(N+1,N+1)}$, we can extract the lowest-order anomalous dimension and write down the leading RRGE. The solution of this equation generates a series of logs in powers of $\alpha_Q \log(s)$, and so by picking out the Nth order term in the series, we have selected the classical log generated by the RRG. Moreover, this tells us that the $(2N+1)$PM contribution will generically contain $\log^N(s)$. At 3PM, we see this with the single $\log(s)$, and at 5PM we can expect the logarithmic term to be a $\log^2(s)$. These logs predicted by the one loop RRG's will also be the leading logs at each PM order. Rapidity anomalous dimensions are independent of ν and therefore of $\log(s)$, so the RRG can only generate a single power of $\log(s)$ at each order. An m-loop diagram can then at best generate an α_Q^m correction to the anomalous dimension; any $\alpha_Q^m \log^m(s)$ terms must then be predicted by the one loop RRG. We may then predict the classical $\alpha_Q^N \log^N(s)$ contribution to $S_{(N+1,N+1)}$ just through solving the one loop RRGE. To get sub-leading logs at a given order we need to calculate the two loop anomalous dimension but the order of necessary iterations is one less. To avoid having to subtract out quantum interference terms we simply only include the classical contribution to the anomalous dimensions as we did in the case of $3PM$. However, at higher orders we would expect to have to include sub-leading Glauber operators (as discussed in section 6.4.3) to reproduce the subleading logs.

We should mention that if we are interested in the classical problem of scattering objects with typical size r, then this scale introduces a new set of logarithms of the ratio r/b. In our theory, the scale r fits into the hierarchy as follows

$$s \gg M_{pl}^2 \gg 1/r^2 \gg t. \tag{6.62}$$

This scale shows up as a matching scales in the problem, the relevant log will be an RG and not an RRG log. The associated counter-term will correspond to a higher dimensional operator of the form $\phi^\star \phi (E, B)^n$, where (E, B) are the electric and magnetic pieces of the Weyl curvature [53, 31, 101, 4, 108, 109].

6.8 Conclusions and Future Directions

We have presented an effective field theory which is valid for massless particles in the (super-Planckian) Regge regime. To avoid sensitivity to the UV completion of GR we restrict ourselves to observables which get no contributions from, uncontrolled, local interactions. By utilizing a factorization theorem we have shown how to systematically resum large rapidity logs for the scattering of massless particles. We have calculated the one loop graviton Regge trajectory, the BFKL equation as well as the classical rapidity log at 3PM that is a consequence of radiation losses. The factorization theorem makes manifest the

all orders form of the series. At $2N+1$ order in the PM expansion one generates a series of Logs starting at $\log^{N-1}$ down to $\log N$. The logs have complex/real coefficients for N even/odd. This is a consequence of the fact that each Glauber loop gives an additional factor of i. The leading classical Log at each order can be calculated by utilizing the one loop anomalous dimensions shown in Eq.(6.55) and by iterating the RRGE $N-1$ times. The next to leading logs will follow from the two loop anomalous dimensions and so on.

While in this chapter we have only considered massless particles, the leading logs we have calculated will also apply to the case of massive particles, as the log follows from the soft function which is insensitive to the partonic masses. As discussed in the in Chapter 5, the couplings of soft gravitons to collinear particles is universal, and therefore the soft sector is independent of the particle species being scattered. Furthermore, any logs computed via the RRGE will then be universal as well. This can be seen explicitly via the equality of the 3PM eikonal phase in the high-energy limit computed in various gravitational theories with both massive and massless scalars and various degrees of supersymmetry [9, 73, 71] (see also [150]). In a future publication we will extend the formalism to the case of massive partons with $s \gg m \gg M_{pl}$. We expect that other simplifications will arise once one accounts for unitarity constraints. In QCD is has been shown that unitarity imposes very strong constraints on the structure of the anomalous dimensions [156]. In particular, by considering amplitudes of definite signature it was shown that anomalous dimensions (including Regge trajectories) are related to cut amplitudes. Moreover, the full anomalous dimensions (including both the Regge pole and cut pieces) of the two Glauber operator anti-symmetric octet operator, can be determined from the anomalous dimension of the single Glauber exchange operator[157]. We expect similar simplifications to arise in gravity.

Appendix A

Conventions and Notation

Here, we list the conventions and notation used through this thesis.

We use the mostly minus metric $\eta_{\mu\nu} = Diag(1, -1, -1, -1)$ for all contexts, including the gravitational scattering considered here, and define the usual $\overline{\text{MS}}$ factor

$$\bar{\mu}^{2\epsilon} = \mu^{2\epsilon}(4\pi)^{-\epsilon}e^{\epsilon\gamma_E}, \tag{A.1}$$

where we use $d = 4 - 2\epsilon$ and

$$[d^d k] = \frac{d^d k}{(2\pi)^d}. \tag{A.2}$$

For transverse momentum integration, we will use the notation $d' = 2 - 2\epsilon$.

For the light cone coordinates we define two null vectors $n/\bar{n}^\mu = (1, 0, 0, \pm 1)$ and decompose four vectors as follows

$$p^\mu = n\cdot p\frac{\bar{n}^\mu}{2} + \bar{n}\cdot p\frac{n^\mu}{2} + p_\perp^\mu \equiv (n\cdot p,\, \bar{n}\cdot p,\, p_\perp^\mu), \tag{A.3}$$

such that

$$p^- = n\cdot p, \quad p^+ = \bar{n}\cdot p. \tag{A.4}$$

We use the super/subscript $\perp$ to denote indices which are transverse to the lightcone vectors. In particular, the transverse part of the metric is

$$\eta_\perp^{\mu\nu} = \eta^{\mu\nu} - \frac{1}{2}n^\mu\bar{n}^\nu - \frac{1}{2}n^\nu\bar{n}^\mu = \text{Diag}(0, 0, -1, -1). \tag{A.5}$$

We often use the notation $(p\cdot k)_\perp = p_\mu\eta_\perp^{\mu\nu}k_\nu$ to denote products between the transverse components of momenta. We may also Euclideanize the components to write $p_\perp\cdot k_\perp = -\vec{p}_\perp\cdot\vec{k}_\perp$.

The phase space on shell delta function will be written as

$$\delta_+(p^2 - m^2) = (2\pi)\delta(p^2 - m^2)\bar{\theta}(\bar{n}\cdot p + n\cdot p). \tag{A.6}$$

We also use the notation

$$\bar{\delta}^d(k) \equiv (2\pi)^d \delta^d(k). \tag{A.7}$$

We focus on 2-to-2 scattering in the limit of $s >> |t|$, $s > 0$, $t < 0$, which in the s-channel we take to be $(p_1, p_2 \to p_3, p_4)$,

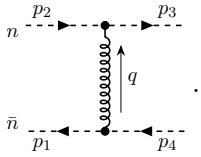

We work in a frame such that $q = q_\perp$ and

$$p_1 = (n\cdot p_1, \bar{n}\cdot p_1, \vec{q}_\perp/2), \qquad p_2 = (n\cdot p_2, \bar{n}\cdot p_2, -\vec{q}_\perp/2), \tag{A.8}$$

with $p_3 = p_2 + q$ and $p_4 = p_1 - q$. We then have Mandelstams $t = q_\perp^2$ and $s = n\cdot p_1 \bar{n}\cdot p_2 + O(t)$. We will also need the u-channel process, which we can take to be $(p_1, \bar{p}_3) \to \bar{p}_2, p_4)$, which diagrammatically is

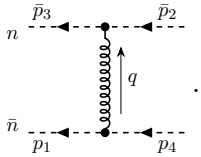

We perform all calculations involving gluons in Feynman gauge, so that the propagator is given by

$$\mu \underbrace{\qquad\qquad p \qquad\qquad} \nu \;= \frac{-ig_{\mu\nu}}{p^2 + i\epsilon} \tag{A.9}$$

Similarly, we use de Donder gauge for all graviton calculations, where the graviton propagator is given in d-dimensions as

$$\mu,\nu \underbrace{\qquad\qquad p \qquad\qquad} \rho,\sigma \;= \frac{i}{p^2 + i\epsilon}\frac{1}{2}\left(\eta^{\mu\rho}\eta^{\nu\sigma} + \eta^{\mu\sigma}\eta^{\nu\rho} - \frac{2}{d-2}\eta^{\mu\nu}\eta^{\rho\sigma}\right). \tag{A.10}$$

Note that we use the same curly line for both gluons and gravitons, though it should be clear from context which is being represented.

For the coupling constants we use $\alpha_s = g_s^2/(4\pi)$ for the gauge theory case, where g_s

is the Yang-Mills coupling constant, and $\kappa^2 = 16\pi G = 1/2M_{\rm Pl}^2$, with G being Newton's constant and $M_{\rm Pl}$ being the Planck mass.

Appendix B

Feynman Rules

Here we list all of the SCET Feynman rules used in calculations performed in this thesis. For all calculations involving gluons, we use Feynman gauge, and for all calculations involving gravitons, we use de Donder gauge. We just list the non-standard Feynman rules within the EFT; any Feynman rule not listed here are equivalent to their full-theory counterparts, e.g. the soft quark propagator is given by the full QCD quark propagator.

B.1 Collinear Quark and Gluon Feynman Rules

- Collinear quark propagator

$$n \xrightarrow{\quad p \quad} = \frac{\bar{n}\!\!\!/}{2} \frac{i\bar{n}\cdot p}{\bar{n}\cdot p\, n\cdot p + p_\perp^2 + i\epsilon} \tag{B.1}$$

- Collinear gluon propagator

$$n \overset{\mu}{\sim\!\sim\!\sim} \overset{p}{\sim\!\sim\!\sim} \overset{\nu}{\sim\!\sim\!\sim} = \frac{-i\eta_{\mu\nu}}{\bar{n}\cdot p\, n\cdot p + p_\perp^2 + i\epsilon} \tag{B.2}$$

- Collinear quark-collinear gluon vertex

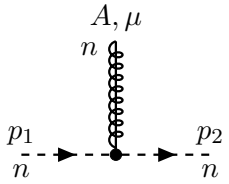

$$= igT^A \frac{\bar{n}\!\!\!/}{2} \left[n_\mu + \frac{\gamma_\mu^\perp p\!\!\!/_{1\perp}}{\bar{n}\cdot p_1} + \frac{p\!\!\!/_{2\perp}\gamma_\mu^\perp}{\bar{n}\cdot p_2} - \frac{p\!\!\!/_{2\perp} p\!\!\!/_{1\perp}}{\bar{n}\cdot p_1\, \bar{n}\cdot p_2} \bar{n}_\mu \right] \tag{B.3}$$

B.2 QCD Glauber Operators

- Collinear-collinear quark-antiquark Glauber

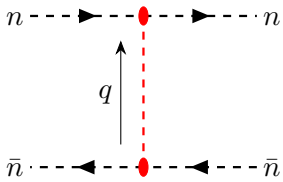

$$= \frac{8\pi i\alpha_s}{q_\perp^2}\left[\frac{\bar{n}\!\!\!/}{2}T^A\right]\otimes\left[\frac{n\!\!\!/}{2}\bar{T}^A\right] \tag{B.4}$$

- Collinear-collinear gluon-antiquark Glauber

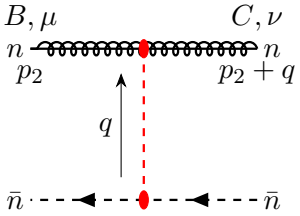

$$= \frac{8\pi\alpha_s f^{ABC}}{q_\perp^2}\left[\bar{n}\cdot p_2\,\eta_\perp^{\mu\nu} - \bar{n}^\mu p_{3\perp}^\nu - \bar{n}^\nu p_{2\perp}^\mu + \frac{p_{2\perp}\cdot p_{3\perp}\bar{n}^\mu\bar{n}^\nu}{\bar{n}\cdot p_2}\right]\left[\frac{n\!\!\!/}{2}\bar{T}^A\right] \tag{B.5}$$

- Soft-collinear quark-quark Glauber

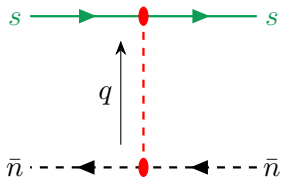

$$= \frac{8\pi i\alpha_s}{q_\perp^2}\left[\frac{\bar{n}\!\!\!/}{2}T^A\right]\otimes\left[\frac{n\!\!\!/}{2}\bar{T}^A\right] \tag{B.6}$$

- Soft-collinear gluon-quark Glauber

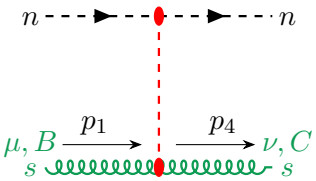

$$= \frac{8\pi\alpha_s f^{ABC}}{(p_1-p_4)_\perp^2}\left[\frac{\bar{n}\!\!\!/}{2}T^A\right]\left[n\cdot k\,\eta_\perp^{\mu\nu} - n^\mu\ell_\perp^\mu - n^\nu k_\perp^\nu + \frac{\ell_\perp\cdot k_\perp\, n^\mu n^\nu}{n\cdot k}\right] \tag{B.7}$$

- Collinear-collinear quark-quark Glauber with soft emission

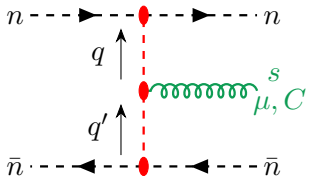

$$= i\frac{8\pi\alpha_s}{\vec{q}_\perp^{\,2}\vec{q}_\perp^{\,\prime 2}} igf^{ABC}\left(q_\perp^\mu + q'_\perp\mu - n\cdot q'\frac{\bar{n}^\mu}{2} - \bar{n}\cdot q\frac{n^\mu}{2} - \frac{n^\mu\vec{q}_\perp^{\,2}}{n\cdot q'} - \frac{\bar{n}^\mu\vec{q}_\perp^{\,\prime 2}}{\bar{n}\cdot q}\right)$$

$$\times\left[\frac{\bar{n}\!\!\!/}{2}T^A\right]\otimes\left[\frac{n\!\!\!/}{2}T^A\right] \tag{B.8}$$

B.3 Gravity Glauber Operators

- Collinear-collinear scalar-scalar Glauber

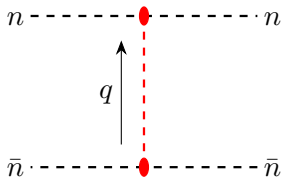

$$= -i\left[\frac{\kappa}{2}\bar{n}\cdot p_2^2\right]\frac{2}{q_\perp^2}\left[\frac{\kappa}{2}n\cdot p_1^2\right] \tag{B.9}$$

- Soft-collinear graviton-scalar Glauber

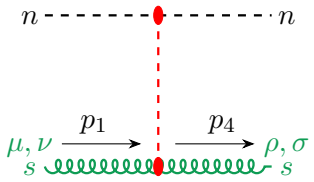

$$= -i\left[\frac{\kappa}{2}\bar{n}\cdot p_2^2\right]\frac{2}{q_\perp^2}\frac{\kappa}{2}\left[\frac{n\cdot p_1}{2}\eta^{\mu(\alpha}\eta^{\beta)\nu} - \frac{1}{2}p_1^{(\alpha}\eta^{\beta)(\nu}n^{\mu)} + \frac{p_1^\alpha p_1^\beta n^\mu n^\nu}{n\cdot p_1}\right]$$

$$\times\left[\frac{n\cdot p_1}{2}\eta^{\rho(\alpha}\eta^{\beta)\sigma} - \frac{1}{2}p_4^{(\alpha}\eta^{\beta)(\sigma}n^{\rho)} + \frac{p_4^\alpha p_4^\beta n^\rho n^\sigma}{n\cdot p_1}\right], \tag{B.10}$$

with $T^{(ab)} = T^{ab} + T^{ba}$.

- Collinear-collinear scalar-scalar Glauber with soft emission

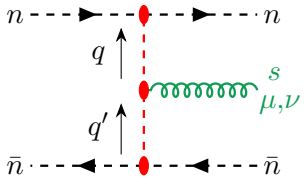

$$= i\left[\frac{\kappa}{2}\bar{n}\cdot p_2^2\right]\left[\frac{\kappa}{2}n\cdot p_1^2\right]\left(\frac{\kappa}{\sqrt{2}q_\perp^2 q_\perp'^2}\right)\Bigg(2\frac{\bar{n}^\mu\bar{n}^\nu}{\bar{n}\cdot q^2}q_\perp'^2 q\cdot(q'-q)$$

$$+2\frac{n^\mu n^\nu}{n\cdot q^2}q_\perp^2 q'\cdot(q-q')-2q_\perp'^2\frac{n\cdot q'\bar{n}^\mu\bar{n}^\nu-\bar{n}^\mu q^\nu-\bar{n}^\nu q^\mu}{\bar{n}\cdot q}$$

$$-2q_\perp^2\frac{\bar{n}\cdot q\, n^\mu n^\nu-n^\mu q'^\nu-n^\nu q'^\mu}{n\cdot q'}+2(q^\mu q'^\nu+q^\nu q'^\mu)$$

$$-(q^\mu+q'^\mu)(n\cdot q'\bar{n}^\nu+\bar{n}\cdot q\, n^\nu)-(q^\nu+q'^\nu)(n\cdot q'\bar{n}^\mu+\bar{n}\cdot q\, n^\mu)$$

$$+(n\cdot q'\bar{n}^\mu+\bar{n}\cdot q\, n^\mu)(n\cdot q'\bar{n}^\nu+\bar{n}\cdot q\, n^\nu)$$

$$-(q_\perp^2+q_\perp'^2)(n^\mu\bar{n}^\nu+n^\nu\bar{n}^\mu)-2q\cdot q'\eta^{\mu\nu}\Bigg) \qquad \text{(B.11)}$$

Bibliography

[1] Gerard 't Hooft. "Graviton Dominance in Ultrahigh-Energy Scattering". In: *Phys. Lett. B* 198 (1987), pp. 61–63. DOI: 10.1016/0370-2693(87)90159-6.

[2] B. P. Abbott et al. "Observation of Gravitational Waves from a Binary Black Hole Merger". In: *Phys. Rev. Lett.* 116 (6 Feb. 2016), p. 061102. DOI: 10.1103/PhysRevLett.116.061102. URL: https://link.aps.org/doi/10.1103/PhysRevLett.116.061102.

[3] B. P. *et al* Abbott et al. "GW170817: Observation of Gravitational Waves from a Binary Neutron Star Inspiral". In: *Phys. Rev. Lett.* 119 (16 Oct. 2017), p. 161101. DOI: 10.1103/PhysRevLett.119.161101. URL: https://link.aps.org/doi/10.1103/PhysRevLett.119.161101.

[4] Manuel Accettulli Huber et al. "From amplitudes to gravitational radiation with cubic interactions and tidal effects". In: *Phys. Rev. D* 103.4 (2021), p. 045015. DOI: 10.1103/PhysRevD.103.045015. arXiv: 2012.06548 [hep-th].

[5] Taushif Ahmed, Johannes Henn, and Bernhard Mistlberger. "Four-particle scattering amplitudes in QCD at NNLO to higher orders in the dimensional regulator". In: *JHEP* 12 (2019), p. 177. DOI: 10.1007/JHEP12(2019)177. arXiv: 1910.06684 [hep-ph].

[6] Ratindranath Akhoury, Ryo Saotome, and George Sterman. "Collinear and Soft Divergences in Perturbative Quantum Gravity". In: *Phys. Rev. D* 84 (2011), p. 104040. DOI: 10.1103/PhysRevD.84.104040. arXiv: 1109.0270 [hep-th].

[7] D. Amati, M. Ciafaloni, and G. Veneziano. "Classical and Quantum Gravity Effects from Planckian Energy Superstring Collisions". In: *Int. J. Mod. Phys. A* 3 (1988), pp. 1615–1661. DOI: 10.1142/S0217751X88000710.

[8] D. Amati, M. Ciafaloni, and G. Veneziano. "Effective action and all order gravitational eikonal at Planckian energies". In: *Nucl. Phys. B* 403 (1993), pp. 707–724. DOI: 10.1016/0550-3213(93)90367-X.

[9] D. Amati, M. Ciafaloni, and G. Veneziano. "Higher Order Gravitational Deflection and Soft Bremsstrahlung in Planckian Energy Superstring Collisions". In: *Nucl. Phys. B* 347 (1990), pp. 550–580. DOI: 10.1016/0550-3213(90)90375-N.

[10] D. Amati, M. Ciafaloni, and G. Veneziano. "Planckian scattering beyond the semiclassical approximation". In: *Phys. Lett. B* 289 (1992), pp. 87–91. DOI: 10.1016/0370-2693(92)91366-H.

[11] D. Amati, M. Ciafaloni, and G. Veneziano. "Superstring Collisions at Planckian Energies". In: *Phys. Lett. B* 197 (1987), p. 81. DOI: 10.1016/0370-2693(87)90346-7.

[12] D. Amati, M. Ciafaloni, and G. Veneziano. "Towards an S-matrix description of gravitational collapse". In: *JHEP* 02 (2008), p. 049. DOI: 10.1088/1126-6708/2008/02/049. arXiv: 0712.1209 [hep-th].

[13] I. Balitsky. "Operator expansion for high-energy scattering". In: *Nucl. Phys. B* 463 (1996), pp. 99–160. DOI: 10.1016/0550-3213(95)00638-9. arXiv: hep-ph/9509348.

[14] I. I. Balitsky and L. N. Lipatov. "The Pomeranchuk Singularity in Quantum Chromodynamics". In: *Sov. J. Nucl. Phys.* 28 (1978), pp. 822–829.

[15] Jochen Bartels, Lev N. Lipatov, and Agustín Sabio Vera. "Double-logarithms in Einstein-Hilbert gravity and supergravity". In: *JHEP* 07 (2014), p. 056. DOI: 10.1007/JHEP07(2014)056. arXiv: 1208.3423 [hep-th].

[16] Christian W. Bauer, Sean Fleming, and Michael E. Luke. "Summing Sudakov logarithms in $B \to X_s\gamma$in effective field theory." In: *Phys. Rev. D* 63 (2000), p. 014006. DOI: 10.1103/PhysRevD.63.014006. arXiv: hep-ph/0005275.

[17] Christian W. Bauer, Dan Pirjol, and Iain W. Stewart. "A Proof of factorization for B —> D pi". In: *Phys. Rev. Lett.* 87 (2001), p. 201806. DOI: 10.1103/PhysRevLett.87.201806. arXiv: hep-ph/0107002.

[18] Christian W. Bauer, Dan Pirjol, and Iain W. Stewart. "Soft collinear factorization in effective field theory". In: *Phys. Rev. D* 65 (2002), p. 054022. DOI: 10.1103/PhysRevD.65.054022. arXiv: hep-ph/0109045.

[19] Christian W. Bauer and Iain W. Stewart. "Invariant Operators in Collinear Effective Theory". In: *Physics Letters B* 516 (2001), pp. 134–142. DOI: 10.1016/S0370-2693(01)00902-9.

[20] Christian W. Bauer et al. "Hard scattering factorization from effective field theory". In: *Phys. Rev. D* 66 (2002), p. 014017. DOI: 10.1103/PhysRevD.66.014017. arXiv: hep-ph/0202088.

[21] M. Beneke and V. A. Smirnov. "Asymptotic Expansion of Feynman Integrals Near Thresholds". In: *Nucl. Phys. B* 522 (1998), pp. 321–344. DOI: 10.1016/S0550-3213(98)00138-2. arXiv: hep-ph/9711391 [hep-ph].

[22] Martin Beneke, Patrick Hager, and Robert Szafron. "Soft-Collinear Gravity and Soft Theorems". In: 2023. DOI: 10.1007/978-981-19-3079-9_4-1. arXiv: 2210.09336 [hep-th].

[23] Martin Beneke, Patrick Hager, and Robert Szafron. "Soft-collinear gravity beyond the leading power". In: *JHEP* 03 (2022). [Erratum: JHEP 04, 141 (2024)], p. 080. DOI: 10.1007/JHEP03(2022)080. arXiv: 2112.04983 [hep-ph].

[24] Martin Beneke and Grisha Kirilin. "Soft-collinear gravity". In: *JHEP* 09 (2012), p. 066. DOI: 10.1007/JHEP09(2012)066. arXiv: 1207.4926 [hep-ph].

[25] Z. Bern, J. J. M. Carrasco, and Henrik Johansson. "New Relations for Gauge-Theory Amplitudes". In: *Phys. Rev. D* 78 (2008), p. 085011. DOI: 10.1103/PhysRevD.78.085011. arXiv: 0805.3993 [hep-ph].

[26] Zvi Bern, John Joseph M. Carrasco, and Henrik Johansson. "Perturbative Quantum Gravity as a Double Copy of Gauge Theory". In: *Phys. Rev. Lett.* 105 (2010), p. 061602. DOI: 10.1103/PhysRevLett.105.061602. arXiv: 1004.0476 [hep-th].

[27] Zvi Bern, Lance J. Dixon, and Radu Roiban. "Is N = 8 supergravity ultraviolet finite?" In: *Phys. Lett. B* 644 (2007), pp. 265–271. DOI: 10.1016/j.physletb.2006.11.030. arXiv: hep-th/0611086.

[28] Zvi Bern, Lance J. Dixon, and Vladimir A. Smirnov. "Iteration of planar amplitudes in maximally supersymmetric Yang-Mills theory at three loops and beyond". In: *Phys. Rev. D* 72 (2005), p. 085001. DOI: 10.1103/PhysRevD.72.085001. arXiv: hep-th/0505205.

[29] Zvi Bern, Julio Parra-Martinez, and Eric Sawyer. "Structure of two-loop SMEFT anomalous dimensions via on-shell methods". In: *Journal of High Energy Physics* 2020.10 (Oct. 2020), p. 211. ISSN: 1029-8479. DOI: 10.1007/JHEP10(2020)211. URL: http://link.springer.com/10.1007/JHEP10(2020)211.

[30] Zvi Bern et al. "Amplitudes, supersymmetric black hole scattering at $\mathcal{O}\left(G^5\right)$, and loop integration". In: *JHEP* 10 (2024), p. 023. DOI: 10.1007/JHEP10(2024)023. arXiv: 2406.01554 [hep-th].

[31] Zvi Bern et al. "Leading Nonlinear Tidal Effects and Scattering Amplitudes". In: *JHEP* 05 (2021), p. 188. DOI: 10.1007/JHEP05(2021)188. arXiv: 2010.08559 [hep-th].

[32] Zvi Bern et al. "One loop n point gauge theory amplitudes, unitarity and collinear limits". In: *Nucl. Phys. B* 425 (1994), pp. 217–260. DOI: 10.1016/0550-3213(94)90179-1. arXiv: hep-ph/9403226.

[33] Zvi Bern et al. "Scattering Amplitudes and Conservative Binary Dynamics at $\mathcal{O}(G^4)$". In: *Phys. Rev. Lett.* 126.17 (2021), p. 171601. DOI: 10.1103/PhysRevLett.126.171601. arXiv: 2101.07254 [hep-th].

[34] Zvi Bern et al. "Snowmass White Paper: the Double Copy and its Applications". In: (2022). arXiv: 2204.06547 [hep-th].

[35] Zvi Bern et al. "The Duality Between Color and Kinematics and its Applications". In: *J. Phys. A* 52 (2019), p. 44. DOI: 10.1088/1751-8121/ab7c8c. arXiv: 1909.01358 [hep-th].

[36] N. E. J. Bjerrum-Bohr, John F. Donoghue, and Pierre Vanhove. "On-shell Techniques and Universal Results in Quantum Gravity". In: *JHEP* 02 (2014), p. 111. DOI: 10.1007/JHEP02(2014)111. arXiv: 1309.0804 [hep-th].

[37] J. Blumlein, V. Ravindran, and W. L. van Neerven. "On the gluon Regge trajectory in O alpha-s**2". In: *Phys. Rev. D* 58 (1998), p. 091502. DOI: 10.1103/PhysRevD.58.091502. arXiv: hep-ph/9806357.

[38] C. Boucher-Veronneau and L. J. Dixon. "N >- 4 Supergravity Amplitudes from Gauge Theory at Two Loops". In: *JHEP* 12 (2011), p. 046. DOI: 10.1007/JHEP12(2011)046. arXiv: 1110.1132 [hep-th].

[39] Nora Brambilla et al. "Potential NRQCD: An Effective theory for heavy quarkonium". In: *Nucl. Phys. B* 566 (2000), p. 275. DOI: 10.1016/S0550-3213(99)00693-8. arXiv: hep-ph/9907240.

[40] Andreas Brandhuber et al. "A new gauge-invariant double copy for heavy-mass effective theory". In: *JHEP* 07 (2021), p. 047. DOI: 10.1007/JHEP07(2021)047. arXiv: 2104.11206 [hep-th].

[41] Andreas Brandhuber et al. "Classical gravitational scattering from a gauge-invariant double copy". In: *JHEP* 10 (2021), p. 118. DOI: 10.1007/JHEP10(2021)118. arXiv: 2108.04216 [hep-th].

[42] Ruth Britto, Freddy Cachazo, and Bo Feng. "New recursion relations for tree amplitudes of gluons". In: *Nucl. Phys. B* 715 (2005), pp. 499–522. DOI: 10.1016/j.nuclphysb.2005.02.030. arXiv: hep-th/0412308.

[43] Ruth Britto et al. "Direct proof of tree-level recursion relation in Yang-Mills theory". In: *Phys. Rev. Lett.* 94 (2005), p. 181602. DOI: 10.1103/PhysRevLett.94.181602. arXiv: hep-th/0501052.

[44] A. Buonanno and T. Damour. "Effective one-body approach to general relativistic two-body dynamics". In: *Phys. Rev. D* 59 (1999), p. 084006. DOI: 10.1103/PhysRevD.59.084006. arXiv: gr-qc/9811091.

[45] Fabrizio Caola et al. "Three-loop helicity amplitudes for quark-gluon scattering in QCD". In: *JHEP* 12 (2022), p. 082. DOI: 10.1007/JHEP12(2022)082. arXiv: 2207.03503 [hep-ph].

[46] Simon Caron-Huot. "When does the gluon reggeize?" In: *JHEP* 05 (2015), p. 093. DOI: 10.1007/JHEP05(2015)093. arXiv: 1309.6521 [hep-th].

[47] Simon Caron-Huot, Einan Gardi, and Leonardo Vernazza. "Two-parton scattering in the high-energy limit". In: *JHEP* 06 (2017), p. 016. DOI: 10.1007/JHEP06(2017)016. arXiv: 1701.05241 [hep-ph].

[48] Simon Caron-Huot, Einan Gardi, and Leonardo Vernazza. "Two-parton scattering in the high-energy limit". In: *Journal of High Energy Physics* 2017.6 (June 2017), p. 16. ISSN: 1029-8479. DOI: 10.1007/JHEP06(2017)016. URL: http://link.springer.com/10.1007/JHEP06(2017)016.

[49] Simon Caron-Huot and Matthias Wilhelm. "Renormalization group coefficients and the S-matrix". In: (July 2016). DOI: 10.1007/JHEP12(2016)010. URL: http://dx.doi.org/10.1007/JHEP12(2016)010.

[50] W. E. Caswell and G. P. Lepage. "Effective Lagrangians for Bound State Problems in QED, QCD, and Other Field Theories". In: *Phys. Lett. B* 167 (1986), pp. 437–442. DOI: 10.1016/0370-2693(86)91297-9.

[51] K. G. Chetyrkin, Bernd A. Kniehl, and M. Steinhauser. "Decoupling relations to O (alpha-s**3) and their connection to low-energy theorems". In: *Nucl. Phys. B* 510 (1998), pp. 61–87. DOI: 10.1016/S0550-3213(97)00649-4. arXiv: hep-ph/9708255.

[52] Clifford Cheung and Grant N. Remmen. "Hidden Simplicity of the Gravity Action". In: *JHEP* 09 (2017), p. 002. DOI: 10.1007/JHEP09(2017)002. arXiv: 1705.00626 [hep-th].

[53] Clifford Cheung and Mikhail P. Solon. "Tidal Effects in the Post-Minkowskian Expansion". In: *Phys. Rev. Lett.* 125.19 (2020), p. 191601. DOI: 10.1103/PhysRevLett.125.191601. arXiv: 2006.06665 [hep-th].

[54] Jui-Yu Chiu et al. "A formalism for the systematic treatment of rapidity logarithms in Quantum Field Theory". In: *Journal of High Energy Physics* 2012.5 (May 2012), p. 84. ISSN: 1029-8479. DOI: 10.1007/JHEP05(2012)084. URL: http://link.springer.com/10.1007/JHEP05(2012)084.

[55] Jui-yu Chiu et al. "Electroweak Corrections in High Energy Processes using Effective Field Theory". In: *Phys. Rev. D* 77 (2008), p. 053004. DOI: 10.1103/PhysRevD.77.053004. arXiv: 0712.0396 [hep-ph].

[56] Jui-yu Chiu et al. "Electroweak Sudakov corrections using effective field theory". In: *Phys. Rev. Lett.* 100 (2008), p. 021802. DOI: 10.1103/PhysRevLett.100.021802. arXiv: 0709.2377 [hep-ph].

[57] Jui-yu Chiu et al. "The Rapidity Renormalization Group". In: *Phys. Rev. Lett.* 108 (2012), p. 151601. DOI: 10.1103/PhysRevLett.108.151601. arXiv: 1104.0881 [hep-ph].

[58] John Collins. *Foundations of perturbative QCD*. Vol. 32. Cambridge University Press, Nov. 2013. ISBN: 978-1-00-940184-5. DOI: 10.1017/9781009401845.

[59] John C. Collins and Davison E. Soper. "Back-To-Back Jets in QCD". In: *Nucl. Phys. B* 193 (1981). [Erratum: Nucl.Phys.B 213, 545 (1983)], p. 381. DOI: 10.1016/0550-3213(81)90339-4.

[60] John C. Collins, Davison E. Soper, and George F. Sterman. "Soft Gluons and Factorization". In: *Nucl. Phys. B* 308 (1988), pp. 833–856. DOI: 10.1016/0550-3213(88)90130-7.

[61] John C. Collins, Davison E. Soper, and George F. Sterman. "Transverse Momentum Distribution in Drell-Yan Pair and W and Z Boson Production". In: *Nucl. Phys. B* 250 (1985), pp. 199–224. DOI: 10.1016/0550-3213(85)90479-1.

[62] P. D. B. Collins. *An Introduction to Regge Theory and High Energy Physics*. Cambridge University Press, 1977. ISBN: 978-1-009-40326-9, 978-1-009-40329-0, 978-1-009-40328-3, 978-0-521-11035-8. DOI: 10.1017/9781009403269.

[63] Poul H. Damgaard, Kays Haddad, and Andreas Helset. "Heavy Black Hole Effective Theory". In: *JHEP* 11 (2019), p. 070. DOI: 10.1007/JHEP11(2019)070. arXiv: 1908.10308 [hep-ph].

[64] Thibault Damour. "High-energy gravitational scattering and the general relativistic two-body problem". In: *Phys. Rev. D* 97.4 (2018), p. 044038. DOI: 10.1103/PhysRevD.97.044038. arXiv: 1710.10599 [gr-qc].

[65] Vittorio Del Duca. "Iterating QCD scattering amplitudes in the high-energy limit". In: *Journal of High Energy Physics* 2018.2 (Feb. 2018). ISSN: 1029-8479. DOI: 10.1007/jhep02(2018)112. URL: http://dx.doi.org/10.1007/JHEP02(2018)112.

[66] Vittorio Del Duca and Lorenzo Magnea. "The long road from Regge poles to the LHC". In: Dec. 2018. arXiv: 1812.05829 [hep-ph].

[67] Vittorio Del Duca et al. "An infrared approach to Reggeization". In: *Phys. Rev. D* 85 (2012), p. 071104. DOI: 10.1103/PhysRevD.85.071104. arXiv: 1108.5947 [hep-ph].

[68] Vittorio Del Duca et al. "The Infrared structure of gauge theory amplitudes in the high-energy limit". In: *JHEP* 12 (2011), p. 021. DOI: 10.1007/JHEP12(2011)021. arXiv: 1109.3581 [hep-ph].

[69] Bryce S. DeWitt. "Quantum Theory of Gravity. 3. Applications of the Covariant Theory". In: *Phys. Rev.* 162 (1967). Ed. by Jong-Ping Hsu and D. Fine, pp. 1239–1256. DOI: 10.1103/PhysRev.162.1239.

[70] Paolo Di Vecchia et al. "A tale of two exponentiations in $\mathcal{N} = 8$ supergravity at subleading level". In: *JHEP* 03 (2020), p. 173. DOI: 10.1007/JHEP03(2020)173. arXiv: 1911.11716 [hep-th].

[71] Paolo Di Vecchia et al. "The eikonal approach to gravitational scattering and radiation at $\mathcal{O}(G^3)$". In: *JHEP* 07 (2021), p. 169. DOI: 10.1007/JHEP07(2021)169. arXiv: 2104.03256 [hep-th].

[72] Paolo Di Vecchia et al. "The gravitational eikonal: From particle, string and brane collisions to black-hole encounters". In: *Phys. Rept.* 1083 (2024), pp. 1–169. DOI: 10.1016/j.physrep.2024.06.002. arXiv: 2306.16488 [hep-th].

[73] Paolo Di Vecchia et al. "Universality of ultra-relativistic gravitational scattering". In: *Phys. Lett. B* 811 (2020), p. 135924. DOI: 10.1016/j.physletb.2020.135924. arXiv: 2008.12743 [hep-th].

[74] Christoph Dlapa et al. "Dynamics of binary systems to fourth Post-Minkowskian order from the effective field theory approach". In: *Phys. Lett. B* 831 (2022), p. 137203. DOI: 10.1016/j.physletb.2022.137203. arXiv: 2106.08276 [hep-th].

[75] William Donnelly and Steven B. Giddings. "Diffeomorphism-invariant observables and their nonlocal algebra". In: *Phys. Rev. D* 93.2 (2016). [Erratum: Phys.Rev.D 94, 029903 (2016)], p. 024030. DOI: 10.1103/PhysRevD.93.024030. arXiv: 1507.07921 [hep-th].

[76] John F. Donoghue. "Introduction to the effective field theory description of gravity". In: *Advanced School on Effective Theories*. June 1995. arXiv: gr-qc/9512024.

[77] Mathias Driesse et al. "Conservative Black Hole Scattering at Fifth Post-Minkowskian and First Self-Force Order". In: *Phys. Rev. Lett.* 132.24 (2024), p. 241402. DOI: 10.1103/PhysRevLett.132.241402. arXiv: 2403.07781 [hep-th].

[78] Vittorio Del Duca and E.W. Nigel Glover. "The high energy limit of QCD at two loops". In: *Journal of High Energy Physics* 2001.10 (Oct. 2001), pp. 035–035. ISSN: 1029-8479. DOI: 10.1088/1126-6708/2001/10/035. URL: http://dx.doi.org/10.1088/1126-6708/2001/10/035.

[79] Claude Duhr, Bernhard Mistlberger, and Gherardo Vita. "Four-Loop Rapidity Anomalous Dimension and Event Shapes to Fourth Logarithmic Order". In: *Phys. Rev. Lett.* 129.16 (2022), p. 162001. DOI: 10.1103/PhysRevLett.129.162001. arXiv: 2205.02242 [hep-ph].

[80] Claude Duhr, Bernhard Mistlberger, and Gherardo Vita. "Four-Loop Rapidity Anomalous Dimension and Event Shapes to Fourth Logarithmic Order". In: *Phys. Rev. Lett.* 129.16 (2022), p. 162001. DOI: 10.1103/PhysRevLett.129.162001. arXiv: 2205.02242 [hep-ph].

[81] Douglas M. Eardley and Steven B. Giddings. "Classical black hole production in high-energy collisions". In: *Phys. Rev. D* 66 (2002), p. 044011. DOI: 10.1103/PhysRevD.66.044011. arXiv: gr-qc/0201034.

[82] Miguel G. Echevarria, Ahmad Idilbi, and Ignazio Scimemi. "Factorization Theorem For Drell-Yan At Low q_T And Transverse Momentum Distributions On-The-Light-Cone". In: *JHEP* 07 (2012), p. 002. DOI: 10.1007/JHEP07(2012)002. arXiv: 1111.4996 [hep-ph].

[83] Miguel G. Echevarria, Ignazio Scimemi, and Alexey Vladimirov. "Universal transverse momentum dependent soft function at NNLO". In: *Physical Review D* 93.5 (Mar. 2016), p. 054004. ISSN: 2470-0010. DOI: 10.1103/PhysRevD.93.054004. URL: https://link.aps.org/doi/10.1103/PhysRevD.93.054004.

[84] Joan Elias Miró, James Ingoldby, and Marc Riembau. "EFT anomalous dimensions from the S-matrix". In: *JHEP* 09 (2020), p. 163. DOI: 10.1007/JHEP09(2020)163. arXiv: 2005.06983 [hep-ph].

[85] Victor S. Fadin, R. Fiore, and M. I. Kotsky. "Gluon Regge trajectory in the two loop approximation". In: *Phys. Lett. B* 387 (1996), pp. 593–602. DOI: 10.1016/0370-2693(96)01054-4. arXiv: hep-ph/9605357.

[86] Victor S. Fadin, R. Fiore, and A. Quartarolo. "Reggeization of quark quark scattering amplitude in QCD". In: *Phys. Rev. D* 53 (1996), pp. 2729–2741. DOI: 10.1103/PhysRevD.53.2729. arXiv: hep-ph/9506432.

[87] Victor S. Fadin, M. I. Kotsky, and R. Fiore. "Gluon Reggeization in QCD in the next-to-leading order". In: *Phys. Lett. B* 359 (1995), pp. 181–188. DOI: 10.1016/0370-2693(95)01016-J.

[88] Victor S. Fadin, E. A. Kuraev, and L. N. Lipatov. "On the Pomeranchuk Singularity in Asymptotically Free Theories". In: *Phys. Lett. B* 60 (1975), pp. 50–52. DOI: 10.1016/0370-2693(75)90524-9.

[89] Giulio Falcioni et al. "Disentangling the Regge Cut and Regge Pole in Perturbative QCD". In: *Phys. Rev. Lett.* 128.13 (2022), p. 132001. DOI: 10.1103/PhysRevLett.128.132001. arXiv: 2112.11098 [hep-ph].

[90] Giulio Falcioni et al. "Scattering amplitudes in the Regge limit and the soft anomalous dimension through four loops". In: *JHEP* 03 (2022), p. 053. DOI: 10.1007/JHEP03(2022)053. arXiv: 2111.10664 [hep-ph].

[91] Karan Fernandes and Feng-Li Lin. "Next-to-eikonal corrected double graviton dressing and gravitational wave observables at $\mathcal{O}\left(G^2\right)$". In: *JHEP* 06 (2024), p. 015. DOI: 10.1007/JHEP06(2024)015. arXiv: 2401.03900 [hep-th].

[92] Sean Fleming et al. "Jets from massive unstable particles: Top-mass determination". In: *Phys. Rev. D* 77 (2008), p. 074010. DOI: 10.1103/PhysRevD.77.074010. arXiv: hep-ph/0703207.

[93] Anjie Gao et al. "A collinear perspective on the Regge limit". In: *JHEP* 05 (2024), p. 328. DOI: 10.1007/JHEP05(2024)328. arXiv: 2401.00931 [hep-ph].

[94] Miguel Garcia-Echevarria, Ahmad Idilbi, and Ignazio Scimemi. "SCET, Light-Cone Gauge and the T-Wilson Lines". In: *Phys. Rev. D* 84 (2011), p. 011502. DOI: 10.1103/PhysRevD.84.011502. arXiv: 1104.0686 [hep-ph].

[95] Einan Gardi, Jennifer M. Smillie, and Chris D. White. "The non-Abelian exponentiation theorem for multiple Wilson lines". In: *Journal of High Energy Physics* 2013.6 (2013). ISSN: 10298479. DOI: 10.1007/JHEP06(2013)088.

[96] Einan Gardi et al. "Webs in multiparton scattering using the replica trick". In: *Journal of High Energy Physics* 2010.11 (2010). ISSN: 10298479. DOI: 10.1007/jhep11(2010)155.

[97] E. W. Nigel Glover. "Two loop QCD helicity amplitudes for massless quark quark scattering". In: *JHEP* 04 (2004), p. 021. DOI: 10.1088/1126-6708/2004/04/021. arXiv: hep-ph/0401119.

[98] Walter D. Goldberger and Ira Z. Rothstein. "An Effective field theory of gravity for extended objects". In: *Phys. Rev. D* 73 (2006), p. 104029. DOI: 10.1103/PhysRevD.73.104029. arXiv: hep-th/0409156.

[99] V. N. Gribov. "A REGGEON DIAGRAM TECHNIQUE". In: *Zh. Eksp. Teor. Fiz.* 53 (1967), pp. 654–672.

[100] Benjamin Grinstein and Ira Z. Rothstein. "Effective field theory and matching in nonrelativistic gauge theories". In: *Phys. Rev. D* 57 (1998), pp. 78–82. DOI: 10.1103/PhysRevD.57.78. arXiv: hep-ph/9703298.

[101] Kays Haddad and Andreas Helset. "Tidal effects in quantum field theory". In: *JHEP* 12 (2020), p. 024. DOI: 10.1007/JHEP12(2020)024. arXiv: 2008.04920 [hep-th].

[102] Johannes M. Henn and Bernhard Mistlberger. "Four-graviton scattering to three loops in $\mathcal{N} = 8$ supergravity". In: *JHEP* 05 (2019), p. 023. DOI: 10.1007/JHEP05(2019)023. arXiv: 1902.07221 [hep-th].

[103] Aidan Herderschee, Radu Roiban, and Fei Teng. "The sub-leading scattering waveform from amplitudes". In: *JHEP* 06 (2023), p. 004. DOI: 10.1007/JHEP06(2023)004. arXiv: 2303.06112 [hep-th].

[104] André H. Hoang et al. "Hard matching for boosted tops at two loops". In: *Journal of High Energy Physics* 2015.12 (Dec. 2015), pp. 1–36. ISSN: 1029-8479. DOI: 10.1007/JHEP12(2015)059. URL: http://link.springer.com/10.1007/JHEP12(2015)059.

[105] Edmond Iancu, Andrei Leonidov, and Larry D. McLerran. "Nonlinear gluon evolution in the color glass condensate. 1." In: *Nucl. Phys. A* 692 (2001), pp. 583–645. DOI: 10.1016/S0375-9474(01)00642-X. arXiv: hep-ph/0011241.

[106] Ahmad Idilbi and Ignazio Scimemi. "Singular and Regular Gauges in Soft Collinear Effective Theory: The Introduction of the New Wilson Line T". In: *Phys. Lett. B* 695 (2011), pp. 463–468. DOI: 10.1016/j.physletb.2010.11.060. arXiv: 1009.2776 [hep-ph].

[107] Boris Lazarevich Ioffe, Victor Sergeevich Fadin, and Lev Nikolaevich Lipatov. *Quantum chromodynamics: Perturbative and nonperturbative aspects*. Cambridge Univ. Press, 2010. ISBN: 978-1-107-42475-3, 978-0-521-63148-8, 978-0-511-71744-4. DOI: 10.1017/CBO9780511711817.

[108] Mikhail M. Ivanov and Zihan Zhou. "Vanishing of Black Hole Tidal Love Numbers from Scattering Amplitudes". In: *Phys. Rev. Lett.* 130.9 (2023), p. 091403. DOI: 10.1103/PhysRevLett.130.091403. arXiv: 2209.14324 [hep-th].

[109] Gustav Uhre Jakobsen et al. "Tidal effects and renormalization at fourth post-Minkowskian order". In: *Phys. Rev. D* 109.4 (2024), p. L041504. DOI: 10.1103/PhysRevD.109.L041504. arXiv: 2312.00719 [hep-th].

[110] Jamal Jalilian-Marian et al. "The BFKL equation from the Wilson renormalization group". In: *Nucl. Phys. B* 504 (1997), pp. 415–431. DOI: 10.1016/S0550-3213(97)00440-9. arXiv: hep-ph/9701284.

[111] Renata Kallosh. "An Update on Perturbative N=8 Supergravity". In: (Dec. 2014). arXiv: 1412.7117 [hep-th].

[112] H. Kawai, D. C. Lewellen, and S. H. H. Tye. "A Relation Between Tree Amplitudes of Closed and Open Strings". In: *Nucl. Phys. B* 269 (1986), pp. 1–23. DOI: 10.1016/0550-3213(86)90362-7.

[113] D. I. Kazakov. "Multiloop Calculations: Method of Uniqueness and Functional Equations". In: *Teor. Mat. Fiz.* 62 (1984), pp. 127–135. DOI: 10.1007/BF01034829.

[114] R. Kirschner and L. Szymanowski. "Effective action for high-energy scattering in gravity". In: *Phys. Rev. D* 52 (1995), pp. 2333–2340. DOI: 10.1103/PhysRevD.52.2333. arXiv: hep-th/9412087.

[115] Arthur Komar. "Construction of a Complete Set of Independent Observables in the General Theory of Relativity". In: *Phys. Rev.* 111.4 (1958), p. 1182. DOI: 10.1103/PhysRev.111.1182.

[116] I. A. Korchemskaya and G. P. Korchemsky. "Evolution equation for gluon Regge trajectory". In: *Phys. Lett. B* 387 (1996), pp. 346–354. DOI: 10.1016/0370-2693(96)01016-7. arXiv: hep-ph/9607229.

[117] I. A. Korchemskaya and G. P. Korchemsky. "High-energy scattering in QCD and cross singularities of Wilson loops". In: *Nucl. Phys. B* 437 (1995), pp. 127–162. DOI: 10.1016/0550-3213(94)00553-Q. arXiv: hep-ph/9409446.

[118] A. V. Kotikov and S. Teber. "Multi-loop techniques for massless Feynman diagram calculations". In: *Phys. Part. Nucl.* 50.1 (2019), pp. 1–41. DOI: 10.1134/S1063779619010039. arXiv: 1805.05109 [hep-th].

[119] Yuri V. Kovchegov and Eugene Levin. *Quantum Chromodynamics at High Energy*. Vol. 33. Oxford University Press, 2013. ISBN: 978-1-009-29144-6, 978-1-009-29141-5, 978-1-009-29142-2, 978-0-521-11257-4, 978-1-139-55768-9. DOI: 10.1017/9781009291446.

[120] E. A. Kuraev, L. N. Lipatov, and Victor S. Fadin. "Multi - Reggeon Processes in the Yang-Mills Theory". In: *Sov. Phys. JETP* 44 (1976), pp. 443–450.

[121] E. A. Kuraev, L. N. Lipatov, and Victor S. Fadin. "The Pomeranchuk Singularity in Nonabelian Gauge Theories". In: *Sov. Phys. JETP* 45 (1977), pp. 199–204.

[122] Roman N. Lee et al. "Quark and Gluon Form Factors in Four-Loop QCD". In: *Phys. Rev. Lett.* 128.21 (2022), p. 212002. DOI: 10.1103/PhysRevLett.128.212002. arXiv: 2202.04660 [hep-ph].

[123] L. N. Lipatov. "Effective action for the Regge processes in gravity". In: *Phys. Part. Nucl.* 44 (2013), pp. 391–413. DOI: 10.1134/S1063779613020214. arXiv: 1105.3127 [hep-th].

[124] L. N. Lipatov. "Gauge invariant effective action for high-energy processes in QCD". In: *Nucl. Phys. B* 452 (1995), pp. 369–400. DOI: 10.1016/0550-3213(95)00390-E. arXiv: hep-ph/9502308.

[125] L. N. Lipatov. "GRAVITON REGGEIZATION". In: *Phys. Lett. B* 116 (1982), pp. 411–413. DOI: 10.1016/0370-2693(82)90156-3.

[126] L. N. Lipatov. "High-energy scattering in QCD and in quantum gravity and two-dimensional field theories". In: *Nucl. Phys. B* 365 (1991), pp. 614–632. DOI: 10.1016/0550-3213(91)90512-V.

[127] L. N. Lipatov. "Multi - Regge Processes in Gravitation". In: *Sov. Phys. JETP* 55 (1982), pp. 582–590.

[128] Michael E. Luke, Aneesh V. Manohar, and Ira Z. Rothstein. "Renormalization group scaling in nonrelativistic QCD". In: *Phys. Rev. D* 61 (2000), p. 074025. DOI: 10.1103/PhysRevD.61.074025. arXiv: hep-ph/9910209.

[129] A. Luna et al. "Next-to-soft corrections to high energy scattering in QCD and gravity". In: *JHEP* 01 (2017), p. 052. DOI: 10.1007/JHEP01(2017)052. arXiv: 1611.02172 [hep-th].

[130] Sucheta Majumdar. "Residual gauge symmetry in light-cone electromagnetism". In: *JHEP* 02 (2023), p. 215. DOI: 10.1007/JHEP02(2023)215. arXiv: 2212.10637 [hep-th].

[131] Aneesh V. Manohar and Iain W. Stewart. "The QCD heavy quark potential to order v**2: One loop matching conditions". In: *Phys. Rev. D* 62 (2000), p. 074015. DOI: 10.1103/PhysRevD.62.074015. arXiv: hep-ph/0003032.

[132] Aneesh V. Manohar and Iain W. Stewart. "The Zero-Bin and Mode Factorization in Quantum Field Theory". In: *Phys. Rev. D* 76 (2007), p. 074002. DOI: 10.1103/PhysRevD.76.074002. arXiv: hep-ph/0605001.

[133] Aneesh V. Manohar and Mark B. Wise. *Heavy quark physics*. Vol. 10. 2000. ISBN: 978-0-521-03757-0, 978-1-009-40212-5. DOI: 10.1017/9781009402125.

[134] Aneesh V. Manohar et al. "Reparameterization invariance for collinear operators". In: *Phys. Lett. B* 539 (2002), pp. 59–66. DOI: 10.1016/S0370-2693(02)02029-4. arXiv: hep-ph/0204229.

[135] Claudio Marcantonini and Iain W. Stewart. "Reparameterization Invariant Collinear Operators". In: *Phys. Rev. D* 79 (2009), p. 065028. DOI: 10.1103/PhysRevD.79.065028. arXiv: 0809.1093 [hep-ph].

[136] B. M. McCoy and Tai Tsun Wu. "Theory of Fermion Exchange in Massive Quantum Electrodynamics at High-Energy. 1." In: *Phys. Rev. D* 13 (1976), pp. 369–378. DOI: 10.1103/PhysRevD.13.369.

[137] S. Melville et al. "Wilson line approach to gravity in the high energy limit". In: *Phys. Rev. D* 89.2 (2014), p. 025009. DOI: 10.1103/PhysRevD.89.025009. arXiv: 1306.6019 [hep-th].

[138] R. Mertig, M. Bohm, and Ansgar Denner. "FEYN CALC: Computer algebraic calculation of Feynman amplitudes". In: *Comput. Phys. Commun.* 64 (1991), pp. 345–359. DOI: 10.1016/0010-4655(91)90130-D.

[139] Alexander Mitov, George Sterman, and Ilmo Sung. "Diagrammatic exponentiation for products of Wilson lines". In: *Phys. Rev. D* 82 (9 Nov. 2010), p. 096010. DOI: 10.1103/PhysRevD.82.096010. URL: https://link.aps.org/doi/10.1103/PhysRevD.82.096010.

[140] Gustav Mogull, Jan Plefka, and Jan Steinhoff. "Classical black hole scattering from a worldline quantum field theory". In: *JHEP* 02 (2021), p. 048. DOI: 10.1007/JHEP02(2021)048. arXiv: 2010.02865 [hep-th].

[141] Ian Moult, Hua Xing Zhu, and Yu Jiao Zhu. "The four loop QCD rapidity anomalous dimension". In: *JHEP* 08 (2022), p. 280. DOI: 10.1007/JHEP08(2022)280. arXiv: 2205.02249 [hep-ph].

[142] Ian Moult, Hua Xing Zhu, and Yu Jiao Zhu. "The four loop QCD rapidity anomalous dimension". In: *JHEP* 08 (2022), p. 280. DOI: 10.1007/JHEP08(2022)280. arXiv: 2205.02249 [hep-ph].

[143] Ian Moult et al. "Anomalous dimensions from soft Regge constants". In: *JHEP* 05 (2023), p. 025. DOI: 10.1007/JHEP05(2023)025. arXiv: 2207.02859 [hep-ph].

[144] Ian Moult et al. "Anomalous dimensions from soft Regge constants". In: *JHEP* 05 (2023), p. 025. DOI: 10.1007/JHEP05(2023)025. arXiv: 2207.02859 [hep-ph].

[145] I. J. Muzinich and M. Soldate. "High-Energy Unitarity of Gravitation and Strings". In: *Phys. Rev. D* 37 (1988), p. 359. DOI: 10.1103/PhysRevD.37.359.

[146] Stephen G. Naculich. "All-loop-orders relation between Regge limits of $\mathcal{N} = 4$ SYM and $\mathcal{N} = 8$ supergravity four-point amplitudes". In: *JHEP* 02 (2021), p. 044. DOI: 10.1007/JHEP02(2021)044. arXiv: 2012.00030 [hep-th].

[147] Stephen G. Naculich and Howard J. Schnitzer. "Regge behavior of gluon scattering amplitudes in N=4 SYM theory". In: *Nucl. Phys. B* 794 (2008), pp. 189–194. DOI: 10.1016/j.nuclphysb.2007.10.026. arXiv: 0708.3069 [hep-th].

[148] Duff Neill and Ira Z. Rothstein. "Classical Space-Times from the S Matrix". In: *Nucl. Phys. B* 877 (2013), pp. 177–189. DOI: 10.1016/j.nuclphysb.2013.09.007. arXiv: 1304.7263 [hep-th].

[149] Takemichi Okui and Arash Yunesi. "Soft collinear effective theory for gravity". In: *Phys. Rev. D* 97.6 (2018), p. 066011. DOI: 10.1103/PhysRevD.97.066011. arXiv: 1710.07685 [hep-th].

[150] Julio Parra-Martinez, Michael S. Ruf, and Mao Zeng. "Extremal black hole scattering at $\mathcal{O}(G^3)$: graviton dominance, eikonal exponentiation, and differential equations". In: *JHEP* 11 (2020), p. 023. DOI: 10.1007/JHEP11(2020)023. arXiv: 2005.04236 [hep-th].

[151] Himanshu Raj and Raju Venugopalan. "Gravitational wave double copy of radiation from gluon shockwave collisions". In: *Phys. Lett. B* 853 (2024), p. 138669. DOI: 10.1016/j.physletb.2024.138669. arXiv: 2312.03507 [hep-th].

[152] Himanshu Raj and Raju Venugopalan. "QCD-gravity double-copy in the Regge regime: Shock wave propagators". In: *Phys. Rev. D* 110.5 (2024), p. 056010. DOI: 10.1103/PhysRevD.110.056010. arXiv: 2406.10483 [hep-th].

[153] Himanshu Raj and Raju Venugopalan. "Universal features of 2→N scattering in QCD and gravity from shockwave collisions". In: *Phys. Rev. D* 109.4 (2024), p. 044064. DOI: 10.1103/PhysRevD.109.044064. arXiv: 2311.03463 [hep-th].

[154] Ira Rothstein and Michael Saavedra. "In preparation". In: ().

[155] Ira Z. Rothstein and Michael Saavedra. "A Systematic Lagrangian Formulation for Quantum and Classical Gravity at High Energies". In: (Dec. 2024). arXiv: 2412.04428 [hep-th].

[156] Ira Z. Rothstein and Michael Saavedra. "Extracting the asymptotic behavior of S-matrix elements from their phases". In: *JHEP* 11 (2024), p. 155. DOI: 10.1007/JHEP11(2024)155. arXiv: 2312.03676 [hep-th].

[157] Ira Z. Rothstein and Michael Saavedra. "Relations Between Anomalous Dimensions in the Regge Limit". In: (Oct. 2024). arXiv: 2410.06283 [hep-ph].

[158] Ira Z. Rothstein, Prashant Shrivastava, and Iain W. Stewart. "Manifestly Soft Gauge Invariant Formulation of vNRQCD". In: *Nucl. Phys. B* 939 (2019), pp. 405–428. DOI: 10.1016/j.nuclphysb.2018.12.027. arXiv: 1806.07398 [hep-ph].

[159] Ira Z. Rothstein and Iain W. Stewart. "An Effective Field Theory for Forward Scattering and Factorization Violation". In: *JHEP* 08 (2016), p. 025. DOI: 10.1007/JHEP08(2016)025. arXiv: 1601.04695 [hep-ph].

[160] Ira Z. Rothstein and Iain W. Stewart. "An Effective Field Theory for Forward Scattering and Factorization Violation". In: *JHEP* 08 (2016), p. 025. DOI: 10.1007/JHEP08(2016)025. arXiv: 1601.04695 [hep-ph].

[161] Agustin Sabio Vera, Eduardo Serna Campillo, and Miguel A. Vazquez-Mozo. "Graviton emission in Einstein-Hilbert gravity". In: *JHEP* 03 (2012), p. 005. DOI: 10.1007/JHEP03(2012)005. arXiv: 1112.4494 [hep-th].

[162] Howard J. Schnitzer. "Reggeization of N=8 supergravity and N=4 Yang-Mills theory". In: (Jan. 2007). arXiv: hep-th/0701217.

[163] Howard J. Schnitzer. "Reggeization of N=8 supergravity and N=4 Yang-Mills theory. II." In: (June 2007). arXiv: 0706.0917 [hep-th].

[164] Vladyslav Shtabovenko, Rolf Mertig, and Frederik Orellana. "FeynCalc 10: Do multiloop integrals dream of computer codes?" In: *Comput. Phys. Commun.* 306 (2025), p. 109357. DOI: 10.1016/j.cpc.2024.109357. arXiv: 2312.14089 [hep-ph].

[165] Vladyslav Shtabovenko, Rolf Mertig, and Frederik Orellana. "FeynCalc 9.3: New features and improvements". In: *Comput. Phys. Commun.* 256 (2020), p. 107478. DOI: 10.1016/j.cpc.2020.107478. arXiv: 2001.04407 [hep-ph].

[166] Vladyslav Shtabovenko, Rolf Mertig, and Frederik Orellana. "New Developments in FeynCalc 9.0". In: *Comput. Phys. Commun.* 207 (2016), pp. 432–444. DOI: 10.1016/j.cpc.2016.06.008. arXiv: 1601.01167 [hep-ph].

[167] V. A. Smirnov. "Asymptotic Expansions of Feynman Diagrams in the Sudakov Limit". In: *Theor. Math. Phys.* 84 (1990), pp. 1072–1082. DOI: 10.1007/BF01028251.

[168] Vladimir A. Smirnov. "Applied asymptotic expansions in momenta and masses". In: *Springer Tracts Mod. Phys.* 177 (2002), pp. 1–262.

[169] S. Titard and F. J. Yndurain. "Rigorous QCD evaluation of spectrum and ground state properties of heavy q anti-q systems: With a precision determination of m(b) M(eta(b))". In: *Phys. Rev. D* 49 (1994), pp. 6007–6025. DOI: 10.1103/PhysRevD.49.6007. arXiv: hep-ph/9310236.

[170] Herman L. Verlinde and Erik P. Verlinde. "Scattering at Planckian energies". In: *Nucl. Phys. B* 371 (1992), pp. 246–268. DOI: 10.1016/0550-3213(92)90236-5. arXiv: hep-th/9110017.

[171] Leonardo Vernazza et al. "The Regge Limit and infrared singularities of QCD scattering amplitudes to all orders". In: *PoS* LL2018 (2018), p. 038. DOI: 10.22323/1.303.0038.

[172] Alexey A. Vladimirov. "Soft-/rapidity- anomalous dimensions correspondence". In: *Physical Review Letters* 118.6 (Oct. 2016), p. 062001. ISSN: 0031-9007. DOI: 10.1103/PhysRevLett.118.062001. URL: http://arxiv.org/abs/1610.05791%20http://dx.doi.org/10.1103/PhysRevLett.118.062001.

[173] Stefan Weinzierl. *Feynman Integrals. A Comprehensive Treatment for Students and Researchers*. UNITEXT for Physics. Springer, 2022. ISBN: 978-3-030-99557-7, 978-3-030-99560-7, 978-3-030-99558-4. DOI: 10.1007/978-3-030-99558-4. arXiv: 2201.03593 [hep-th].